CHARLES UNIVERSITY IN PRAGUE

Faculty of Science

Study program: Molecular and Cell Biology, Genetics and Virology

Mgr. Ondřej Černý

Signalizační působení adenylát-cyklázového toxinu na fagocyty

Signaling effects of adenylate cyclase toxin action on phagocytes

Dissertation

Supervisor: prof. Ing. Peter Šebo, CSc.

MBÚ

Prague, 2014

Statement of originality

The work contained in this thesis has not been previously submitted for a degree or diploma at any other higher education institution. To the best of my knowledge and belief, the thesis is the product of my own work and contains no material previously published or written by another person, except where due references are made.

Prague,

Signature

I would like to thank my supervisor prof. Peter Sebo for introducing me to science, for giving me the opportunity to perform this work, and for taking me to outstanding scientific meetings and wonderful collaborations. Moreover, I would like to acknowledge him for his enthusiasm, readiness to help, and for his trust in my work.

I am also grateful to the members of the Laboratory of Molecular Biology of Bacterial Pathogens at the Institute of Microbiology for creative teamwork and scientific environment. My special thanks go to Drs. Jana Kamanova and Jiri Masin. I would also like to thank Hana Lukeova, Sona Kozubova, and Iva Marsikova for their excellent technical assistance.

I appreciated very much the collaborations with Dr. Phill Hawkins and Dr. Karen Anderson at the Babraham Institute in Cambridge, as well as with Dr. Maria Eugenia Rodriguez and Dr. Yanina Lamberti at CINDEFI in La Plata.

Last but not least, I would like to thank my family for their endless support.

1. Abstract

The adenylate cyclase toxin (CyaA) plays a key role in the virulence of *Bordetella pertussis*. CyaA penetrates CR3-expressing phagocytes and catalyzes the uncontrolled conversion of cytosolic ATP to the key second messenger molecule cAMP. This paralyzes the capacity of neutrophils and macrophages to kill bacteria by oxidative burst and opsonophagocytic mechanisms. Here we show that CyaA suppresses the production of bactericidal reactive oxygen and nitrogen species in neutrophils and macrophages, respectively.

The inhibition of reactive oxygen species (ROS) production is most-likely achieved by the combined PKA-dependent inhibition of PLC and Epac-dependent dysregulation of NADPH oxidase assembly. Activation of PKA or Epac interfered with fMLP-induced ROS production and the inhibition of PKA partially reversed the CyaA-mediated inhibition of ROS production. CyaA/cAMP signaling then inhibited DAG formation, while the PIP3 formation was not influenced. These results suggest that cAMP produced by CyaA influences the composition of target membranes.

We further show here that cAMP signaling through the PKA pathway activates the tyrosine phosphatase SHP-1 and suppresses the production of reactive nitrogen species (RNS) in macrophages. Selective activation of PKA interfered with LPS-induced iNOS expression in macrophages, while the inhibition of PKA largely restored the production of iNOS in CyaA-treated murine macrophages. CyaA/cAMP signaling induced SHP phosphatase-dependent dephosphorylation of the c-Fos subunit of the transcription factor AP-1 and thereby inhibited the TLR4-triggered induction of iNOS gene expression. Selective siRNA knockdown of the phosphatase SHP-1 then rescued the production of TLR-inducible RNS in toxin-treated cells. Finally, the inhibition of SHP phosphatase abrogated *B. pertussis* survival inside murine macrophages. These results reveal that an as yet unknown cAMP-activated signaling pathway controls SHP-1 phosphatase activity and may regulate numerous receptor signaling pathways in leukocytes. The hijacking of SHP-1 by CyaA action then enables *B. pertussis* to evade RNS-mediated killing inside macrophages.

In conclusion, we propose a model of CyaA-provoked signaling which allows *Bordetella pertussis* to evade killing by the sentinel cells of the host immune system.

2. Abstrakt

Adenylát-cyklázový toxin (CyaA) je klíčovým faktorem virulence bakterie *Bordetella pertussis*. CyaA se váže na fagocyty produkující komplementový receptor 3 (CR3) a následně katalyzuje přeměnu vnitrobuněčného ATP na významného „druhého posla“ cAMP. Tímto paralyzuje schopnost neutrofilů a makrofágů zabíjet bakterie pomocí oxidativního vzplanutí a mechanismů závislých na fagocytóze. V této práci analyzujeme mechanismus, kterým CyaA blokuje produkci baktericidních reaktivních kyslíkových a dusíkových radikálů neutrofily a makrofágy.

CyaA potlačuje produkci reaktivních kyslíkových radikálů (ROS, z angl. „reactive oxygen species“) jednak prostřednictvím inhibice PLC přes PKA a dále nejspíše ovlivněním skládání komplexu NADPH oxidázy prostřednictvím aktivace proteinu Epac. Selektivní aktivace PKA nebo Epac blokovala produkci ROS indukovanou fMLP. Inhibice PKA pomocí specifických inhibitorů navíc vedla jen k částečnému obnovení produkce ROS u neutrofilů vystavených CyaA. Signalizace CyaA/cAMP následně omezila tvorbu DAG, zatímco tvorba PIP3 zůstala neovlivněna. Tyto výsledky naznačují, že působení CyaA může ovlivnit lipidické složení membrány fagocytů.

Dále jsme ukázali, že aktivace PKA pomocí cAMP vyvolává aktivaci tyrozínové fosfatázy SHP-1. To v makrofázích způsobí potlačení produkce reaktivních dusíkových radikálů (RNS, z angl. „reactive nitrogen species“). Selektivní aktivace PKA pomocí 6-Bnz-cAMP utlumila v makrofázích expresi iNOS stimulovanou LPS. Účinek toxinu byl pak zablokován po inhibici PKA. Signalizace CyaA/cAMP dále vyvolala defosforylaci c-Fos podjednotky transkripčního faktoru AP-1 v závislosti na aktivaci SHP-1, což vedlo ke zrušení exprese iNOS vyvolané signalizací TLR4. Snížení hladiny SHP-1 pomocí siRNA vedlo k obnovení produkce RNS v makrofázích aktivovaných TLR4 ligandy. Inhibice SHP fosfatáz nakonec snížila přežívání *B. pertussis* v makrofázích. Tyto výsledky odhalují novou signální dráhu, kterou cAMP aktivuje fosfatázu SHP-1 prostřednictvím aktivace signalizace PKA. SHP-1 pak může v leukocytech regulovat aktivitu celé řady receptorů. Působení CyaA tak prostřednictvím aktivace SHP-1 umožňuje *B. pertussis* uniknout před zabitím makrofágy produkujícími RNS.

Na základě získaných mechanismů jsme navrhli model signalizace vyvolané CyaA, kterou bakterie *B. pertussis* používá k potlačení baktericidní aktivity fagocytů hostitele.

3. Contents

4. Introduction

Despite the high rates of pertussis vaccine intake, whooping cough is a reemerging disease in developed countries. This respiratory illness is caused by a Gram-negative coccobacilus *Bordetella pertussis* that inhibits host immune functions by production of a whole range of virulence factors. These can be roughly divided into three classes: complement resistance factors, adhesins, and toxins. The main complement resistance factors are autotransporters *Bordetella* resistance to killing A (BrkA) and Vag8. Among the adhesins, filamentous hemagglutinin, pertactin, fimbriae, and tracheal colonization factor are the most important. Of the known toxins of *B. pertussis*, the pertussis toxin, tracheal cytotoxin, dermonecrotic toxin, and adenylate cyclase toxin (CyaA) appear to play a prominent role in virulence. In this thesis, we focused on the role of CyaA that was shown to be an essential virulence factor of *B. pertussis*.

CyaA belongs to the RTX (Repeat in ToXin) protein family and binds the complement receptor 3 (CD11b/CD18 integrin) and thus targets the phagocytic cells of the innate immune system. After binding to the receptor, CyaA either permeabilizes cellular membrane by a cation-selective pore or delivers its adenylate cyclase (AC) domain into the cytosol of target cells. After translocation, AC domain converts cellular ATP into the second messenger cAMP. The production of cAMP by CyaA was repeatedly shown to block phagocytosis, superoxide production, neutrophil extracellular trap (NET) formation, as well as dendritic cell maturation and antigen presentation. In addition, both CyaA-mediated cAMP production and pore-formation were shown to contribute to CyaA-provoked cytotoxicity.

In this thesis, the impact of CyaA toxin action on the most important bactericidal activities of phagocytes, such as the production of reactive oxygen and nitrogen species, and on dendritic cells activation of the adaptive immune system, is characterized. A description of the signaling pathways involved in the CyaA-provoked inhibition of the immune response to *B. pertussis* is also provided.

5. Current State of Knowledge

5.1. Myeloid phagocytic cells and bactericidal functions of the innate immune system

For successful colonization of the host organism, bacteria must overcome several bactericidal mechanisms of the immune system. The first line of defense of the host consists of factors in extracellular fluids, such as complement or antibacterial peptides and enzymes (*e.g.* lysozyme). In the second phase, colonizing bacteria are bound and engulfed by myeloid phagocytic cells, mainly neutrophils, monocytes, macrophages, or dendritic cells (Kaufmann, 2008). These cells are closely related myeloid cells that cooperate in the clearance of bacteria and in some cases can also clear inflammatory sites without the contribution of the adaptive immune system (Soehnlein and Lindbom, 2010). These professional phagocytic cells originate in bone marrow, where a cell called granulocyte/macrophage colony-forming unit (GM-CFU) develops from a stem cell. GM-CFU is the last common precursor for granulocytes and monocytes, from which either a granulocyte colony-forming unit (G-CFU), or macrophage colony-forming unit (M-CFU) can develop (Akashi et al., 2000). While G-CFU is a direct precursor for neutrophils, M-CFU develops first into a monoblast, which subsequently turns into a monocyte, from which a macrophage or a dendritic cell (DC) can differentiate (Geissmann et al., 2003). The development of neutrophils, macrophages, and dendritic cells is summarized in Fig. 1. (Gordon and Taylor, 2005). Finally, while mature neutrophils are short-lived cells recruited to the inflammatory site from the blood stream, macrophages and dendritic cells may reside in tissues for several years.

Monocytes, and subsequently also macrophages can be classified into at least two distinct phenotypic and functional forms – classical (M1) and non-classical or alternative (M2) macrophages. Classical macrophages initiate inflammation, whereas alternative macrophages are more potent at antigen presentation, immunoregulatory cytokine secretion, and tissue remodeling (Zhao et al., 2009). In addition to the M1/M2 phenotypic groups, other macrophage populations were identified in response to distinct physiological stimuli (Italiani and Boraschi, 2014).

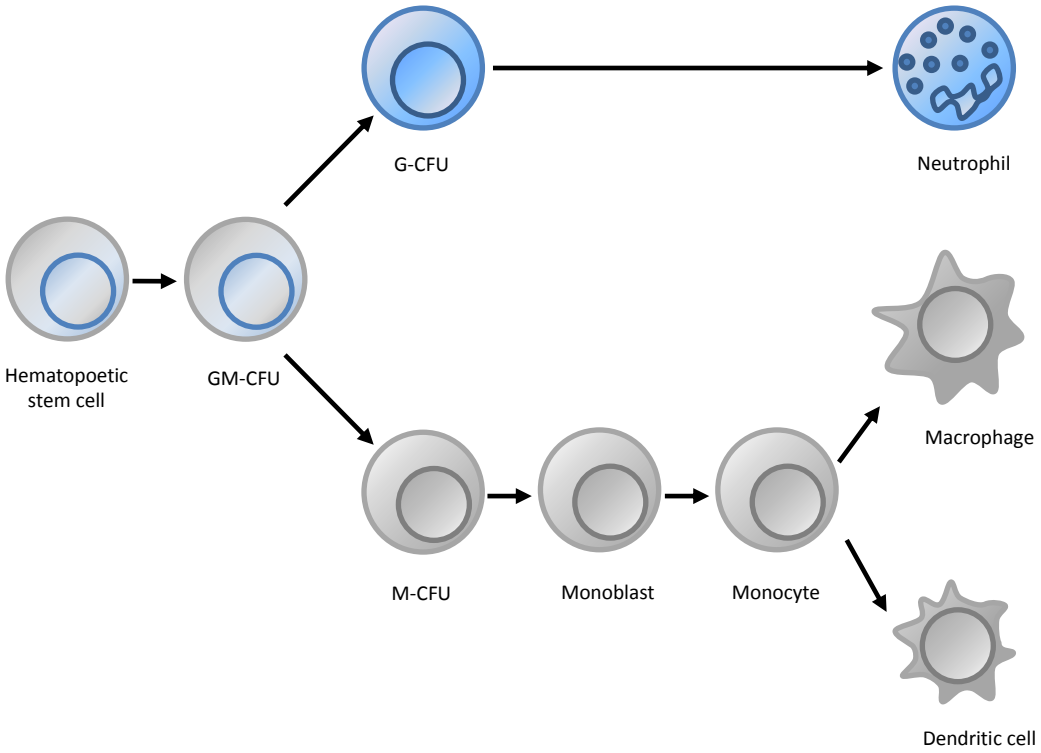

Fig. 1: Schematic representation of the maturation of cells in the myeloid lineage. Neutrophils, dendritic cells, and macrophages develop from a common hematopoietic stem cell. Their development diverges in the phase of granulocyte/macrophage colony-forming unit (GM-CFU), from which granulocyte colony-forming unit (G-CFU), or macrophage colony-forming units (M-CFU) arise. From an M-CFU, a monoblast and subsequently a monocyte develop. Monocytes are then the precursors for macrophages and dendritic cells.

Both neutrophils and M1 macrophages possess potent bactericidal capacities. Neutrophils are equipped with a high number of granules filled with a broad range of antimicrobial peptides and easily produce reactive oxygen species (ROS). While macrophages also produce ROS, they do so in smaller amounts than neutrophils. Moreover, macrophages express also an inducible nitric oxide synthase (iNOS). Thus neutrophils and macrophages are not redundant and rather complement each other's actions (Soehnlein and Lindbom, 2010).

The bactericidal activities of M1 macrophages and of neutrophils can be further increased by the priming of mature cells with low doses of pro-inflammatory cytokines, such as IFNγ or TNFα. Both are used to achieve phagocytic cell priming *in vitro*. The same cytokines also serve to potentiate bactericidal capacities of myeloid phagocytes *in vivo*.

After maturation or priming in the target tissue, phagocytes can take up particles labeled with pathogen-/danger-associated molecular patterns (PAMPs/DAMPs) or opsonized by complement or antibodies. After phagocytosis,

the engulfed bacteria are sequestered into a vesicle called a phagosome, which can fuse with lysosome to form a phagolysosome. Upon phagosome-lysosome fusion, the pH of the bacterial surrounding decreases and bacteria are killed by antimicrobial peptides present in lysosomes, or released from fusing granules of neutrophils (*e.g.* defensisns). At any time after recognition by a phagocytic cell, the bacteria can be killed by oxidative agents produced by specialized enzymatic complexes – the NADPH oxidase producing ROS, or the inducible nitric oxide synthase (iNOS) producing reactive nitrogen species (RNS). Both ROS and RNS are small polarized molecules able to diffuse through membranes and thus can also kill extracellular bacteria (Fig. 2). In this thesis, special emphasis is placed on the capacity of *Bordetella pertussis* adenylate cyclase toxin to block the ability of phagocytes to produce ROS and RNS.

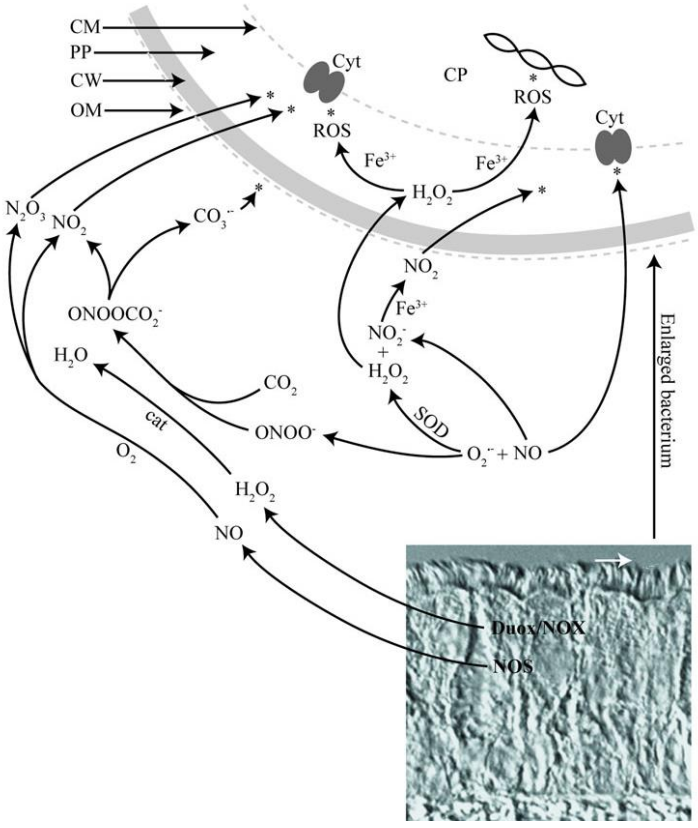

Fig. 2: ROS and RNS as antimicrobial agents in the airway mucosa. Differential interference contrast microscopy photography shows pseudostratified airway epithelium with ciliated cells, which is the natural niche for *Bordetellae*. The production of and interaction between ROS and RNS is depicted. The main targets of ROS and RNS in bacteria are marked with asterisks (*). Reprinted from (Omsland et al., 2008).

5.1.1. Reactive oxygen species production

The term "Reactive oxygen species" denominates a group of several highly reactive radicals and compounds, like superoxide anion (O_2^-), hydroxyl anion (OH^-),

or hydrogen peroxide (H_2O_2). These short-living agents often react with Cl^- or RNS to create even more reactive (and thus toxic) substances. Although ROS can be produced by most cells of the innate immune system, neutrophils are considered to be the primary source of bactericidal ROS (Mittal et al., 2014). Superoxide anion is formed by NADPH oxidase complexes in the membranes of myeloid phagocytes. There exist at least seven different NADPH oxidase complexes. Among them NOX1, NOX3, NOX4, NOX5, DUOX1, and DUOX2 are expressed in non-phagocytic cells and ROS produced by these cells serve mainly as signaling molecules. In contrast, NOX2 complex is expressed by phagocytic cells, mainly by neutrophils and macrophages (Bedard and Krause, 2007); and is responsible for production of bactericidal ROS. The NOX2 complex consists of six proteins: heme containing $gp91^{PHOX}$ (Nox2) and $p22^{PHOX}$ form together the flavocytochrome b_{558}, $p67^{PHOX}$, $p47^{PHOX}$, $p40^{PHOX}$, and Rac1/2. A schematic composition of the NOX2 complex is shown in Fig. 3.

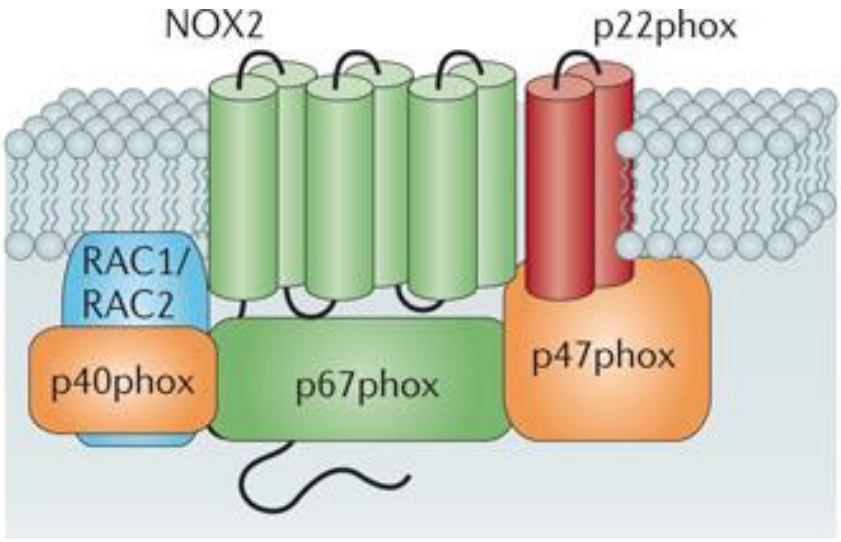

Fig. 3: Subunit composition of the NOX2 complex. The catalytic core subunits of the enzyme complex is shown in green; NOX maturation and stabilization partner $p22^{phox}$ is shown in red; cytosolic organizers $p40^{phox}$ and $p47^{phox}$ are shown in orange; cytosolic activator $p67^{phox}$ is shown in green; and small GTPases (RAC1 and RAC2) are shown in blue. Reprinted from (Drummond et al., 2011)

In resting cells, the NOX2 complex is inactive and its components are separated into different cellular compartments. The cytosolic parts of inactive NOX2 complex can be co-immunoprecipitated in the form of a heterotetramer of a not yet precisely defined stoichiometry (Iyer et al., 1994; Park et al., 1994; Park et al., 1992). This heterotetramer contains at least one molecule of $p67^{PHOX}$ and $p40^{PHOX}$. The $p67^{PHOX}$ was found to be associated with the Triton X-100 insoluble cytoskeletal

fraction and binds the $p40^{PHOX}$ subunit stably (Tsunawaki and Yoshikawa, 2000). The interaction of $p67^{PHOX}$ with the cytoskeleton is crucial for the delivery of cytosolic components to the membraneous components of NOX2. In contrast, $p47^{PHOX}$ is a cytosolic protein and does not bind to the cytoskeleton until the cells are activated (El Benna et al., 1999). The membraneous part of NOX2 complex forms a heterodimer of integral membrane proteins $gp91^{PHOX}$ and $p22^{PHOX}$, which serve as a docking site for other components of the NOX2 complex (de Mendez et al., 1996). Depending on the membrane where $gp91^{PHOX}$ and $p22^{PHOX}$ are located, the final NOX2 is assembled at the phagosomal or plasma membrane.

NOX2 assembly and activation can be initiated by signaling of soluble or particulate factors. To the soluble factors comprise the complement factor C5a (Daniel et al., 2006), fMLP (Condliffe et al., 2005), platelet activating factor (PAF) (Chen et al., 2006), or leukotriene B4 (LTB4) (Batra et al., 2012). Any object, either opsonized and detected by Fc receptors or complement receptors, or unopsonized and recognized by mannose-binding lectin, or scavenger receptors, and thereby targeted for phagocytosis, can serve as a particulate stimulus (Anderson et al., 2010).

Both soluble and particulate stimuli trigger activation and assembly of NOX2 by a similar mechanism. Binding to products of phosphoinositide 3 kinase (PI3K) and phosphorylation-induced structural changes appear to play a crucial role in NOX2 assembly. The main target for phosphorylation was identified to be the $p47^{PHOX}$, which can be phosphorylated on several residues inside its polybasic motif (Hoyal et al., 2003; Inanami et al., 1998; Johnson et al., 1998). Upon phosphorylation, the polybasic motif of $p47^{PHOX}$ binds the SH3 domain of $p67^{PHOX}$ and thus forms a heterotrimeric complex $p67^{PHOX}/p40^{PHOX}/p47^{PHOX}$ (Lapouge et al., 2002; Massenet et al., 2005). $p67^{PHOX}$ undergoes several phosphorylations, mainly by mitogen-activated protein kinases (MAPKs) (Benna et al., 1997; Dang et al., 2003; Dusi and Rossi, 1993; Forbes et al., 1999a; Forbes et al., 1999b), but the role of these phosphorylations remains unclear. Similarly, $p40^{PHOX}$ can be phosphorylated probably by protein kinase C (PKC) (Bouin et al., 1998; Fuchs et al., 1997; Someya et al., 1999) and this phosphorylation seems to be required for full NOX2 activation (Chessa et al., 2010). The ternary complex $p67^{PHOX}/p40^{PHOX}/p47^{PHOX}$ migrates towards the target membrane, where the *phox* homology (PX) domains of $p40^{PHOX}$

and $p47^{PHOX}$ bind phosphatidylinositol 3-phosphate (PI3P) (Ago et al., 2001; Ellson et al., 2001; Kanai et al., 2001; Karathanassis et al., 2002; Perisic et al., 2004). This constitutes another physiological signal for NOX2 activation (Ellson et al., 2006). Once localized at the membrane, the $p67^{PHOX}$/$p40^{PHOX}$/$p47^{PHOX}$ complex interacts with $gp91^{PHOX}$/$p22^{PHOX}$ heterodimer and binds GTP-loaded Rac (Meijles et al., 2014).

The information needed for NOX2 assembly is transmitted by several signaling pathways from the plasma membrane to the *phox* proteins. Some proteins may mediate crosstalk between these signaling pathways, which makes the establishment of the hierarchy of signaling events in the process of NOX2 assembly rather problematic (Bourdonnay et al., 2012). The most important signaling pathways for the induction of NOX2 assembly are depicted on Fig. 4.

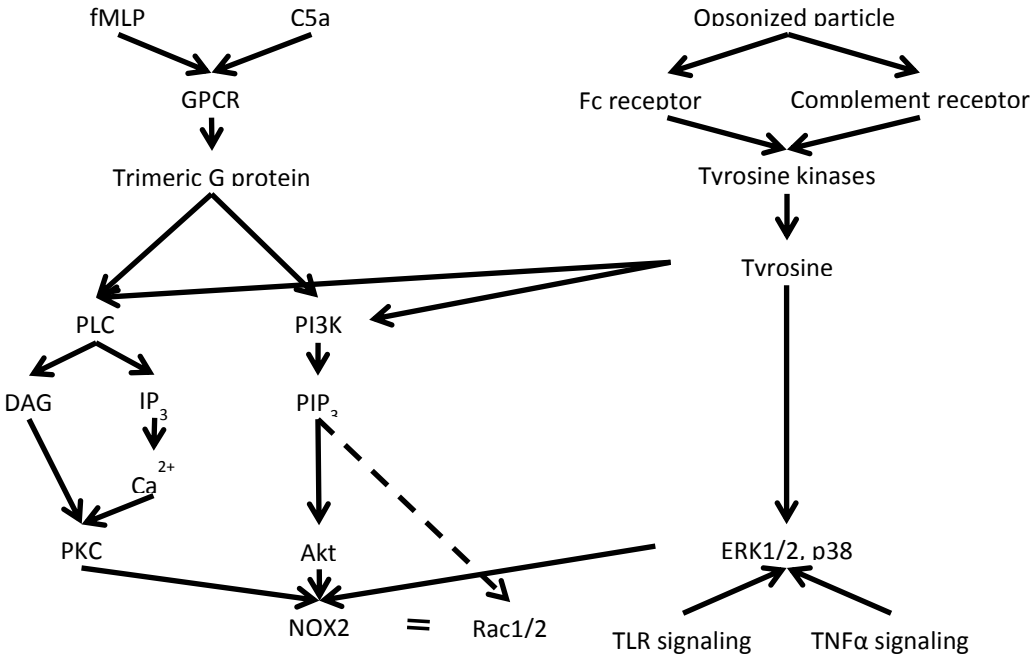

Fig. 4: Schematic representation of signaling pathways leading to the assembly of NOX2 complex and ROS production in neutrophils.

When the ROS production is not needed any more, it can be terminated in several ways. The first is the dephosphorylation of NOX2 complex subunits due to the activation of phosphatases, or by the inhibition of kinases maintaining the appropriate phosphorylation status of the complex. For instance, the general inhibitors of the PKC family, such as staurosporine or H-7, rapidly abrogate PMA-stimulated NADPH oxidase activity (Heyworth and Badwey, 1990). This leads to

disassembly of the NOX2 complex (Curnutte et al., 1994). In addition, pretreatment of cells with inhibitors of protein phosphatase 1 (PP1) and 2A (PP2A) reverses the action of PKC inhibition (Ding and Badwey, 1992). Similarly, inhibition of PP2A by ocadaic acids prolongs fMLP stimulated ROS production (Ding and Badwey, 1992; Garcia et al., 1992; Harbecke et al., 1997; Harbecke et al., 1996; Lu et al., 1992). This suggests that phosphorylation of NOX2 complex subunits is a steady-state process, which is ongoing even throughout ROS production.

The second mode for termination of ROS production is the removal of Rac from the NOX2 complex. This is achieved by GTP to GDP hydrolysis, leading to the disruption of interaction between Rac and $p67^{phox}$ and ultimately to the disassembly of the oxidase complex (Moskwa et al., 2002; Scheffzek et al., 1997; Vetter and Wittinghofer, 2001). Thus all processes used for NOX2 assembly serve also for their disassembly and for the termination of ROS production.

5.1.2. Reactive nitrogen species production

Reactive nitrogen radicals are created by the reaction of nitric oxide (NO) with ROS or O_2. Besides NO itself, the most important radical is probably the peroxynitrate ($OONO^-$). The list of commonly found ROS and RNS is presented in Table 1.

Table. 1: List of commonly found reactive oxygen and nitrogen species. Adapted from (Mugoni and Santoro, 2013).

Reactive Oxygen Species (ROS)	Symbol	Reactive Nitrogen Species (RNS)	Symbol
Hydroxyl	$OH^{\cdot}$	Nitrous oxide	$NO^{\cdot}$
Superoxide	$O_2^{\cdot -}$	Peroxynitrite	$OONO^-$
Nitric oxide	$NO^{\cdot}$	Peroxynitrous acid	ONOOH
Peroxyl	$RO_2^{\cdot}$	Nitroxyl anion	NO^-
Lipid peroxyl	$LOO^{\cdot}$	Nitrogen dioxide	$NO^{\cdot}{}_2$
Peroxynitrate	$ONOO^-$	Dinitrogen trioxide	N_2O_3
Hydrogen peroxide	H_2O_2	Nitrous acid	HNO_2
Singlet oxygen	$^{-1}O_2$	Nitril chloride	NO_2Cl
Hypochloric acid	HOCl	Nitrosyl cation	NO^+

Nitric oxide, serving as an input for RNS generation, is produced by the inducible nitric oxide synthase (iNOS, NOS2). In contrast, neuronal nitric oxide synthase (nNOS, NOS1) and endothelial nitric oxide synthase (eNOS, NOS3) do not

produce bactericidal amounts of NO. All the three NOS enzymes are catalytically active when dimerized and use two substrates, L-arginine and molecular oxygen. NO synthesis requires as co-factors nicotinamide-adenine- dinucleotide phosphate (NADPH), flavin adenine dinucleotide (FAD), flavin mononucleotide (FMN), and (6R)5,6,7,8-tetrahydro-l-biopterin (BH4) (Forstermann and Sessa, 2012). In contrast to nNOS and eNOS, the iNOS is a highly active and Ca^{2+}-independent enzyme. While nNOS and eNOS produce a small amount of NO, which is usually considered to be the signaling messenger, iNOS is a high output enzyme that produces toxic amounts of NO and plays an important role in host's defense against pathogens (MacMicking et al., 1997).

The expression of iNOS can be induced in cells of the innate immune system such as macrophages, as well as in cells of epithelial origin (Lane et al., 2004; Xie et al., 1993). The expression pattern of iNOS can, however, differ according to the host species (Pautz et al., 2010). In mice, the expression of iNOS is induced easily by individual proinflammatory factors such as LPS or IFNγ (Xie et al., 1993). In humans, in contrast, a combination of LPS, IFNγ, TNFα, and IL-1β is required for robust iNOS expression (Fang and Vazquez-Torres, 2002). Based on the complexity of input stimuli, human cells are usually not used as a model for studying iNOS expression, and mouse cells are used for deciphering of the effects on particular signaling pathways regulating iNOS expression and NO production (Chang et al., 2013; Koide et al., 2003; Tsukamoto et al., 2008).

In mouse macrophages, the induction of iNOS expression is regulated by several signaling pathways. Upon the activation of cells by IFNγ, the transcription factor Signal Transducer and Activator of Transcription (Stat1) is activated and triggers the expression of another transcription factor, the Interferon Regulatory Factor 1 (IRF1). Both transcription factors subsequently collaborate with additional transcription factors: the Nuclear Factor κB (NF-κB) and the Activator Protein 1 (AP1). In contrast, the activation of macrophages by LPS primarily leads to the activation of NF-κB and to MAPK-dependent activation of AP1, although the activation of Stat1 by LPS was also described (Rhee et al., 2003). The cooperation of all four transcription factors is then crucial for iNOS gene expression (Kleinert et al.,

2003; Pautz et al., 2010). The signaling pathways leading to iNOS expression are illustrated in Fig. 5.

The expression of iNOS is also regulated post-transcriptionally on the level of mRNA stability. The 3'-UTR of iNOS mRNA was found to interact with the KH-type Splicing Regulatory Protein (KSRP), which is a key mediator of mRNA decay. The overexpression of KSRP markedly decreased cytokine-induced iNOS expression in epithelial cells (Linker et al., 2005). In contrast, iNOS mRNA is bound by the HuR protein upon cytokine-mediated induction of iNOS expression and this leads to mRNA stabilization by blocking KSRP-mediated mRNA decay (Linker et al., 2005). Similarly, the potentiating effect of IFNγ on LPS-induced iNOS expression was found to depend on mRNA stabilization (Lorsbach et al., 1993; Weisz et al., 1994). In contrast to the interaction of iNOS mRNA with proteins regulating its stability, no significant interaction of iNOS mRNA and non-coding RNAs was found (Pautz et al., 2010).

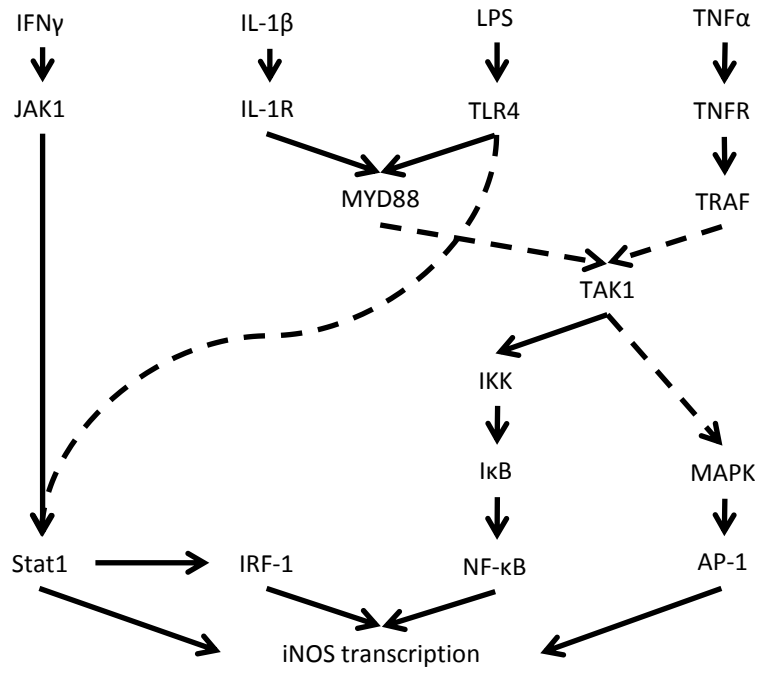

Fig. 5: Schematic representation of signaling pathways leading to iNOS expression and NO production in macrophages.

The iNOS protein was shown to be degraded by proteasome (Musial and Eissa, 2001), where proteasomal degradation of iNOS is mediated by caveolin-1 binding and subsequent aggregation (Felley-Bosco et al., 2002; Felley-Bosco et al., 2000). iNOS is also targeted for degradation after its phosphorylation by Src tyrosine

kinase (Hausel et al., 2006). The degradation of iNOS is the main way of the termination of the NO production, in contrast to ROS production.

In addition to iNOS expression regulation, NO production by iNOS can be influenced by substrate accessibility. iNOS competes for its substrate above all with arginases (Gotoh and Mori, 1999; Chang et al., 1998). Arginases consume L-arginine and produce urea. This serves as a paracrine messenger that inhibits the innate immune response (Satriano, 2004).

Regulation of iNOS by cAMP-provoked signaling is a crucial physiological process. The effects of cAMP on iNOS expression were previously reviewed by Galea *et al.* (Galea and Feinstein, 1999) and cAMP was found to induce iNOS expression in most cell types. In myeloid cells, however, cAMP was shown to inhibit iNOS expression by a so far uncharacterized mechanism. Recently, cAMP was shown to both inhibit iNOS gene transcription (Koide et al., 2003; Pang and Hoult, 1997) and to induce iNOS protein degradation (Chang et al., 2013). These sharp differences in cAMP effects on iNOS protein expression and stability prompted us to analyze in detail the impact of CyaA action on NO production in macrophages.

5.2. Regulation of innate immunity by cAMP

The cyclic nucleotide 3'-5'-cyclic adenosine monophosphate (cAMP), the first described second messenger, was discovered already in 1968 by Dr. Earl W. Sutherland. Biological processes mediated by this second messenger include memory, metabolism, gene regulation, and immune function (Beavo and Brunton, 2002).

In eukaryotes, cAMP is produced by Adenylyl Cyclase enzymes (AC; EC 4.6.1.1) after stimulation of the G Protein-Coupled Receptor (GPCR). Ligand binding to GPCRs provokes exchange of GDP to GTP in the heterotrimeric G proteins, which leads to dissociation of Gα subunit from the rest of the complex. The free Gα subunit stimulates AC to catalyze the cyclization of ATP to yield cAMP and release of pyrophosphate (Kamenetsky et al., 2006). The reaction yielding cAMP production by AC is shown in Fig. 6*A*. Ten isoforms of AC enzymes were described in eukaryotes up to now. Nine of them are anchored into the plasma membrane by transmembrane helices, while the last isoform is soluble in the cytoplasm and may bind to cytoplasmic vesicles or mitochondria through interaction with the scaffolding proteins (Valsecchi et al., 2014).

The action of AC is opposed by phosphodiesterases (PDE) that degrade intracellular cAMP as shown in Fig. 6*B*. There are 11 distinct PDE families, whose expression is tissue-specific. Moreover, ACs and PDEs can be localized to different spatial compartments within the cell, so that the presence of cAMP can be further regulated at a subcellular level (Baillie et al., 2005).

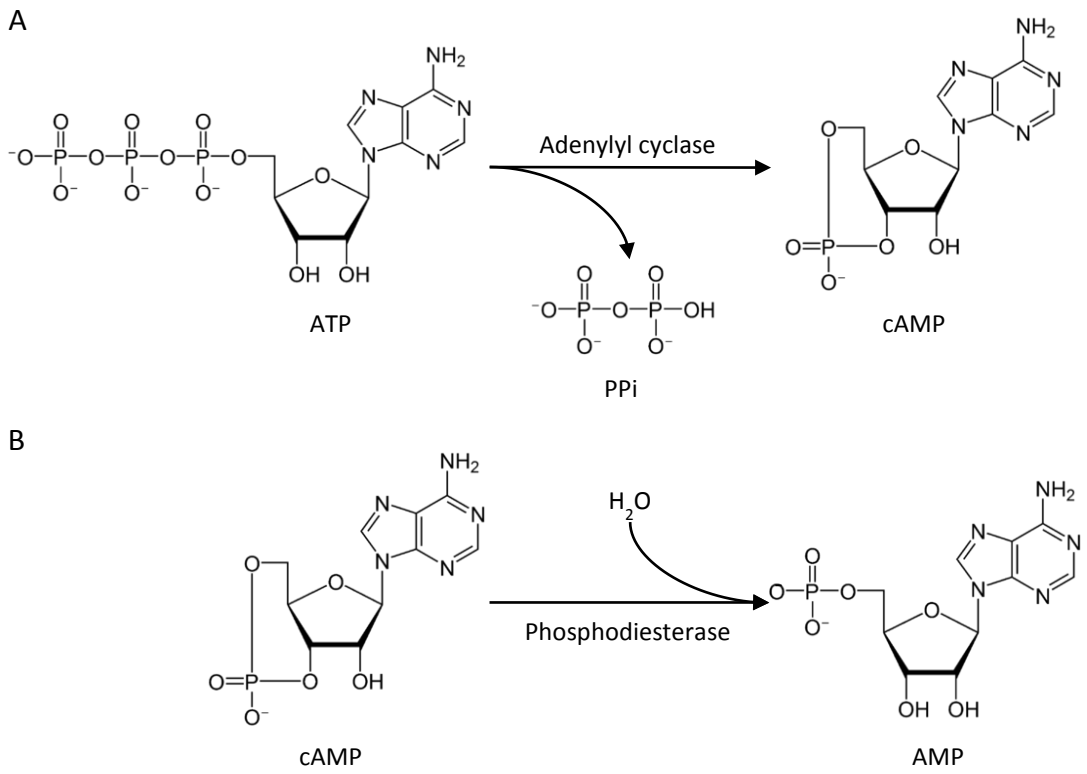

Fig. 6: Schematic representation of cAMP production and degradation. *A.* Adenylyl Cyclase enzymes (AC) catalyze the cyclization of adenosine triphosphate (ATP) into 3'-5'-cyclic adenosine monophosphate (cAMP). Pyrophosphate (PPi) is created as a side product of this reaction. *B.* On the other hand, cAMP is hydrolyzed in the reaction catalyzed by phosphodiesterases.

Another level of complexity and regulation is obtained by diverse cAMP effector molecules. Binding of cAMP to regulatory subunits of PKA leads to dissociation of the catalytic subunit, which is then free to phosphorylate serine and threonine residues in its target consensus sequence (-RRXS/T- where X stands for any amino acid). The transcription factor cAMP response element-binding protein (CREB) often serves as an example of a PKA-targeted protein. The spatial specificity of PKA signaling is achieved by its binding to the A-kinase-anchoring proteins (AKAPs) at various subcellular locations. AKAPs were also shown to bind PDEs, as well as other cAMP effectors (McConnachie et al., 2006), thereby enabling formation of discrete subcellular pools of cAMP and of its effectors within a cell. Alternative (PKA-independent) cAMP effectors, including cyclic nucleotide-gated channels and the exchange protein directly activated by cAMP (Epac), have also been identified (Kopperud et al., 2003). Their roles in mediating a variety of cellular functions are still emerging. The only direct effector of Epac seems to be the small GTPase Rap1. The PKA and Epac proteins may have redundant, independent, or even opposing effects within the same cell. The cyclic nucleotide-gated channels were not described

in human myeloid phagocytes yet (www.proteinatlas.org). The general structure of cAMP signaling pathway is shown in Fig. 7.

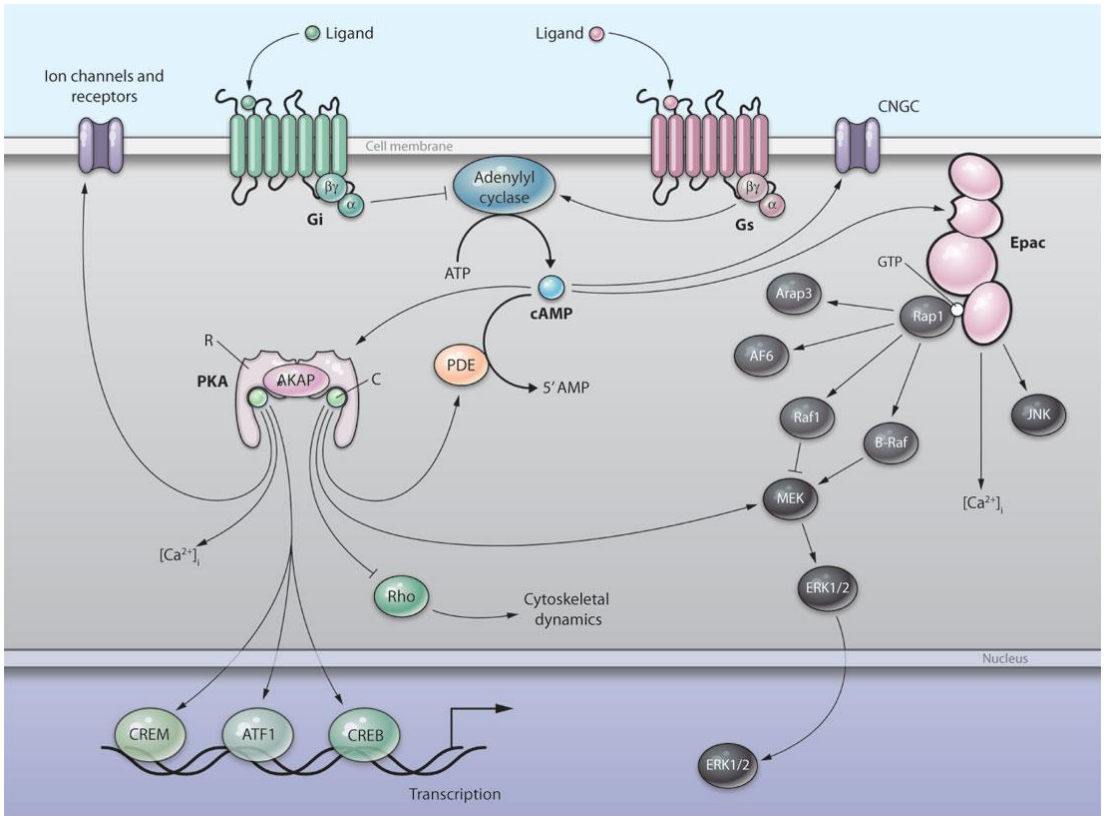

Fig. 7: General structure of the cAMP signaling pathway. cAMP is produced from ATP by AC enzymes and is degraded by phosphodiesterases a shown earlier in Fig. 6. Activity of AC is driven by heterotrimeric G proteins after their stimulation by GPCR. cAMP acts directly on three targets: PKA, Epac, and CNGCs, which are, however, not expressed by myeloid cells. PKA and Epac in turn regulate various cellular processes both directly and through intermediaries. For clarity, only limited number of pathways mediated by PKA and Epac are depicted in this figure. ATF1, activating transcription factor 1; C, protein kinase A catalytic subunit; CNGC, cyclic nucleotide–gated ion channel; CREB, cAMP response element–binding protein; CREM, cAMP response element modulator; ERK1/2, extracellular signal–related kinase 1/2; JNK, Jun N-terminal kinase; PDE, phosphodiesterases; PKA, protein kinase A; R, protein kinase A regulatory subunit. Reprinted from (Murray, 2008).

Increased cAMP concentration inhibits killing capacities of myeloid phagocytic cells towards bacteria (Aronoff et al., 2005; O'Dorisio et al., 1979; Serezani et al., 2007), viruses (Nokta and Pollard, 1992), fungi (Fulop et al., 1985), and eukaryotic parasites (Wirth and Kierszenbaum, 1984). This includes the blocking of ROS and RNS production as well as the blocking of phagosomal acidification. The PKA as well as Epac activation was shown to inhibit production of ROS due to the blocking

of NADPH complex assembly by an as yet undefined mechanism (Bengis-Garber and Gruener, 1996; Wang et al., 2014). Inhibition of production of RNS by a cAMP-dependent mechanism was also observed in myeloid cells but the mechanism has not been elucidated (Koide et al., 1993; Messmer and Brune, 1994; Pang and Hoult, 1997). This seems to be specifically due to PKA (Galea and Feinstein, 1999). The fine-tuned balance between PKA, Epac and PDE4 also appears to regulate the phagosomal acidification and maturation (Brock et al., 2008; Kalamidas et al., 2006; Pryzwansky et al., 1998). Indeed, increased cAMP concentration was also shown to inhibit phagocytosis. Elevation of intracellular cAMP level suppresses CR-, FcR-, and scavenger receptor–mediated phagocytosis. This seems to be due to a combination of PKA and Epac signaling (Atkinson et al., 1977; Makranz et al., 2006; Nambu et al., 1989). The role of Epac in inhibition of phagocytosis could consist in the activation of phosphatases, such as PP2A and PTEN (Canetti et al., 2007; Hong et al., 2008). Several examples of modulation of antimicrobial actions by bacterial toxins are shown in Fig. 8.

Increased cAMP concentration was also shown to inhibit expression of TNFα, IL-1α and -1β (Aronoff et al., 2006), interleukin-12 (van der Pouw Kraan et al., 1995), and the pro-inflammatory lipid mediator leukotriene B_4 (Luo et al., 2004). In contrast, cAMP was shown to enhance production of anti-inflammatory IL-10 (Aronoff et al., 2006) and stimulates expression of the Suppressor Of Cytokine Signaling (SOCS) 3 transcription factor (Gasperini et al., 2002). The exact mechanism of how cAMP modulates production of cytokines remains unknown. It, however, seems likely that both PKA and Epac are involved (Aronoff et al., 2006; Xu et al., 2008).

Finally, the immunosubversive effects of cAMP are widely used in the clinical practice. For example, GPCR ligands stimulating cAMP production are used in the treatment of pulmonary arterial hypertension. In contrast, the nonsteroidal anti-inflammatory drugs were shown to inhibit PKA (Zentella de Pina et al., 2007), which may explain their beneficial effects on the microbial clearance (Aronoff et al., 2004; Rangel Moreno et al., 2002; Serezani et al., 2008).

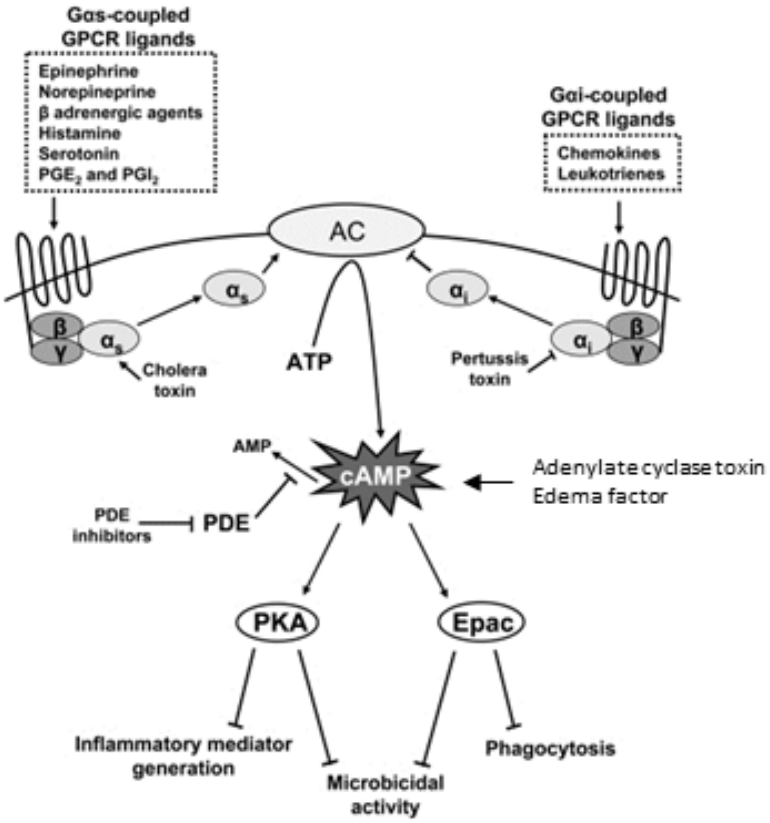

Fig. 8: The regulation of cyclic AMP (cAMP) levels by bacterial toxins. In addition to regulation of AC enzymes by heterotrimeric G protein, the production of cAMP is also regulated by microbial pathogens. Pertussis toxin and cholera toxin cause elevated cAMP levels through ADP-ribosylation of either the Gαi subunit to prevent its inhibition of AC or of the Gαs subunit to constitutively activate AC, respectively. On the other hand, adenylate cyclase toxin and edema factor are AC produced by bacteria and delivered into the eukaryotic cells. Phosphodiesterases (PDEs), which degrade cAMP to AMP, are another regulator of intracellular cAMP levels. PDE inhibitors [such as 3-isobutyl-1-methylxanthine (IBMX)] prevent such degradation, resulting in accumulation of intracellular cAMP. The downstream signaling of cAMP is mediated by its interactions with effector molecules, protein kinase A (PKA) or exchange proteins directly activated by cAMP (Epac). Both PKA and Epac have been shown to modulate phagocyte functions. Depicted here is a pattern demonstrated for alveolar macrophages in which specific antimicrobial functions are differentially regulated by particular cAMP effectors. Adapted from (Serezani et al., 2008).

5.3. Whooping cough disease

Whooping cough, also known as pertussis, is a highly contagious respiratory disease affecting especially young children and non-vaccinated newborns and infants. Adolescents and adults are often serving as carriers and thus as a reservoir for cyclic outbreaks of the disease (Birkebaek et al., 1999; Rocha et al., 2015). The disease is caused by Gram-negative bacteria from the genus *Bordetellae* (Mattoo and Cherry, 2005). In humans, the most severe form of pertussis is caused by the strict human pathogen *B. pertussis*, whereas *B. parapertussis* and *B. bronchiseptica* cause a milder disease. In animals, the disease is caused mainly by *B. bronchiseptica*, although sheep-specific *B. parapertussis* was also identified (Porter et al., 1994).

In the year 2013, about 16 million pertussis cases occurred worldwide, accounting for about 195,000 deaths of children per year. Despite the generally very high intake of pediatric pertussis vaccines, pertussis is ranked among the 10 leading causes of childhood mortality (http://www.cdc.gov/pertussis/countries.html; http://www.who.int/immunization_monitoring/diseases/pertussis/en/).

B. pertussis can be transmitted by aerosol, without any need for direct physical contact between infected and naïve host (Warfel et al., 2012a; Warfel et al., 2012b). In the course of the incubation period of 9–10 days, the causative agent of whooping cough colonizes the ciliated epithelium of nasopharynx and trachea. Patients develop catarrhal symptoms including a cough and other flu-like symptoms typically without any rise in body temperature. This is called the catarrhal phase. About 1 to 2 weeks post infection, coughing paroxysms ending in the characteristic whoop may occur, indicating the beginning of the paroxysmal phase. The paroxysmal coughing is associated with tenacious mucus, but the production of purulent sputum does not occur. Beyond the paroxysmal cough, several systemic symptoms can occur such as posttussive vomiting, causing dehydration and malnutrition; lymphocytosis; alteration of neurologic functions (confusion and loss of consciousness); and dysregulated secretion of insulin. Interestingly, between paroxysms the patient may appear normal without any respiratory distress. The paroxysmal stage lasts for 2 to 8 weeks and sometimes longer. The transition to the convalescent stage is gradual and is associated with an initial decrease in the frequency of the paroxysms and subsequently a decrease in the severity of the events as well (Mattoo and Cherry, 2005). During the convalescent phase, the paroxysmal cough can last for a number of

weeks after the infection has been cleared. The infection is typically well localized and only rarely disseminates from the respiratory tract.

In severe cases, the disease results in pediatric intensive care unit admission or death. This is called as a "critical pertussis" and occurs typically in early infancy prior any vaccination (Berger et al., 2013). These children often develop bronchopneumonia connected with intractable pulmonary hypertension (while having systemic hypotension) and respiratory failure, which responds inadequately to advanced ventilation maneuvers (Paddock et al., 2008). During the initial stages, infiltration of the mucosa by lymphocytes and polymorphonuclear leukocytes occurs, suggesting that the initial pulmonary lesion in pertussis is a lymphoid hyperplasia of peribronchial and tracheobronchial lymph nodes. Children with white blood cell count greater than $50{,}000 \times 10^9$/l had nearly a ten times higher risk of death (Berger et al., 2013). In line with this finding, it was shown that 80% (four of five) of patients with critical pertussis, pulmonary hypertension, and leukocytosis survived, when treated with leukoreduction therapy (Rowlands et al., 2010). In contrast, this therapy did not offer a clear therapeutic advantage in a study on large cohort of patients (Berger et al., 2013).

The lung infiltration by leukocytes is followed by a necrotizing process that affects the midzonal and basilar layers of the bronchial epithelium (Mattoo and Cherry, 2005). The necrotizing process is, together with the leukocytosis, the cause of pulmonary hypertension (Paddock et al., 2008), which may result in right-sided heart failure or fatal cardiac arrhythmias (Rocha et al., 2015). In addition, encephalopathy associated with pertussis infection occurs in 0.5–1% of all cases (Hiraiwa-Sofue et al., 2012). However, the aetiology of central nervous system complications is not fully understood. The mortality rate of all infant pertussis infection is about 1%, with more than half of the deaths occurring in infants below two months of age (Haberling et al., 2009). Infants who are younger than six weeks have the worst prognosis (83.6% case fatality rate) (Rocha et al., 2015).

The pulmonary histopathologic examination of the samples obtained from dead infants with confirmed *B. pertussis* pneumonia revealed an abundant presence of extracellular bacteria in cilia of the trachea, bronchi, and bronchioles, as well as intracellular bacteria and antigens in alveolar macrophages and ciliated epithelium

(Paddock et al., 2008). Histopathologic features of necrotizing bronchiolitis, bronchopneumonia, pulmonary hemorrhage and edema were also observed (Sawal et al., 2009). Most samples showed damaged tracheal mucosa with extensive loss of cilia, denuded and attenuated epithelium, and moderate-to-marked squamous metaplasia (Paddock et al., 2008).

The reader is further referred for more details to several reviews discussing whooping cough pathogenesis, virulence factors, and vaccination strategies (Hewlett et al., 2014; Mattoo and Cherry, 2005; Melvin et al., 2014; Sebo et al., 2014).

5.4. Bordetella pertussis

The Gram-negative, aerobic coccobacillus *Bordetella pertussis* is one of nine species of the genus *Bordetella*. Besides *B. pertussis*, the *B. parapertussis* and *B bronchiseptica* species are of great medical and economical interest as well. *B. pertussis* was originally isolated by Bordet and Gengou in 1906.

According to phylogenetic analyzes, *B. pertussis* and *B. parapertussis* evolved independently from a *B. bronchiseptica*-like ancestor (Diavatopoulos et al., 2005; Gerlach et al., 2001; Park et al., 2012). The process of speciation of *B. pertussis* and *B. parapertussis* to the human-restricted niche was accompanied by large-scale gene loss, the accumulation of pseudogenes and of insertion elements (Parkhill et al., 2003). In line with this, the genome of *B. pertussis* encodes only 11 species-specific genes (Cummings et al., 2004). A schematic representation of the phylogenetic relationships within the *B. bronchiseptica* cluster is depicted in the Fig. 9.

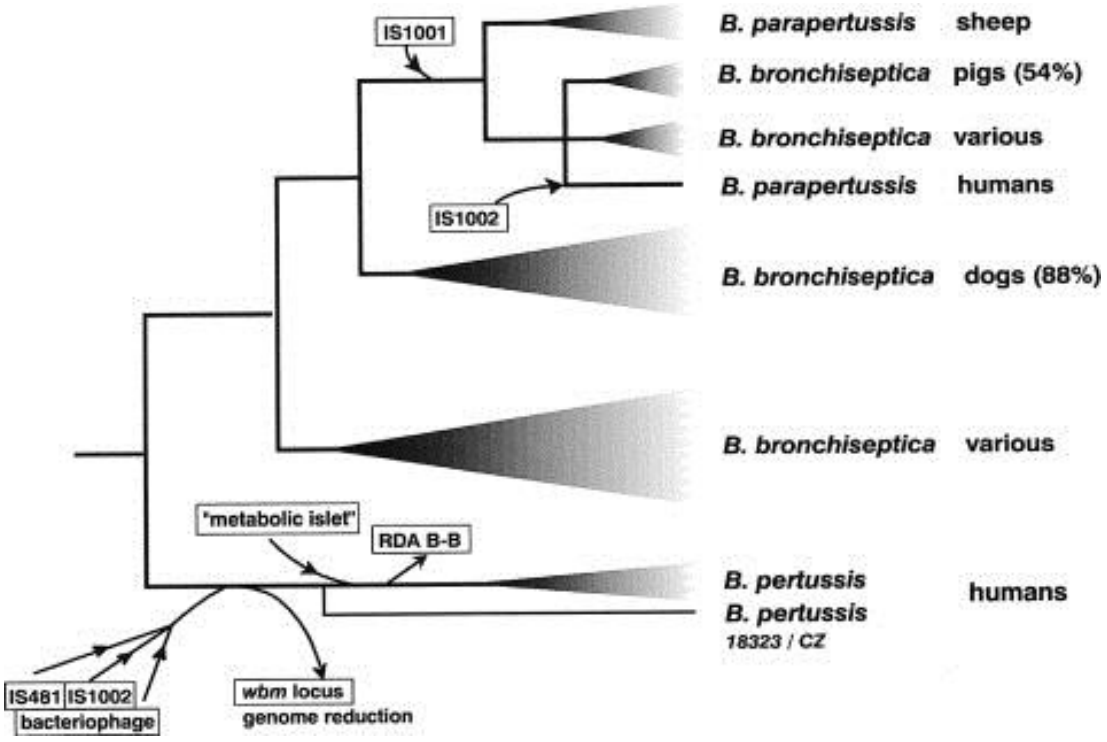

Fig. 9: Schematic representation of phylogenetic relationships within the *B. bronchiseptica* cluster. The cluster was devised based on the distribution of insertion elements and MLEE described previously by van der Zee and co-workers (van der Zee et al., 1997). In some lineages the frequency of isolation from particular host species is indicated. The acquisition and loss of genetic elements in different lineages is marked by arrows. Reprinted from (Gerlach et al., 2001).

5.4.1. Virulence regulation

The genes required for the virulence of *Bordetellae* are mainly regulated by a two component BvgAS system. Their expression defines the virulent phase of

Bordetellae, while it was shown that the nonvirulent phase is needed for the survival of nutrition limitation in *B. bronchiseptica* (Porter et al., 1991). The existence of a similar phase in the lifestyle of *B. pertussis* is a matter of discussion (Byrd et al., 2013; Mattoo and Cherry, 2005; Veal-Carr and Stibitz, 2005). The nonvirulent phase (Bvg^-) is characterized by the expression of virulence repressed genes (*vrgs*), such as those needed for flagella synthesis and motility in *B. bronchiseptica*. In *B. pertussis*, the Bvg^- phase can be induced by physical and chemical modulators. Virulence is repressed upon cultivation at temperatures below 25°C. The presence of high sulfate concentrations (5 – 50 mM) or of nicotinic acid serves as an example of chemical modulators. In contrast, the shift in temperature to 37°C induces the virulent phase (Bvg^+), at which the *vrgs* are not expressed and the expression of virulence activated genes (*vags*) starts. During the shift from nonvirulent to the fully virulent phase, the intermediary phase (Bvg^i) is characterized by the expression of early response genes, such as BipA or genes involved in the adhesion to host cells (filamentous hemagglutinin and fimbriae).

The two-component regulatory system BvgAS transfers the signal from the periplasmic space sensor domain of BvgS to the DNA binding regulator BvgA (Decker et al., 2012). The transmembrane sensor kinase BvgS undergoes autophosphorylation on H729 upon sensing the activation signal (Uhl and Miller, 1994). The phosphate group is subsequently transferred to D1023 and H1172 (Uhl and Miller, 1996). Finally, the phosphate group is transferred from BvgS to the D54 residue in the receiver domain of the response regulator protein BvgA (Boulanger et al., 2013). Phosphorylation of BvgA leads to its dimerization and increased binding to sites upstream of *bvg*-activated promoters (Boucher et al., 1994).

Beside temperature, the natural signals sensed by the BvgAS regulatory system remain unknown. It is plausible to hypothesize, however, that the sensing of sulfate released from mucus during bacterial presence may be used by *Bordetellae* to fine-tune the production of virulence factors. A schematic representation of the BvgAS function is depicted in Fig. 10.

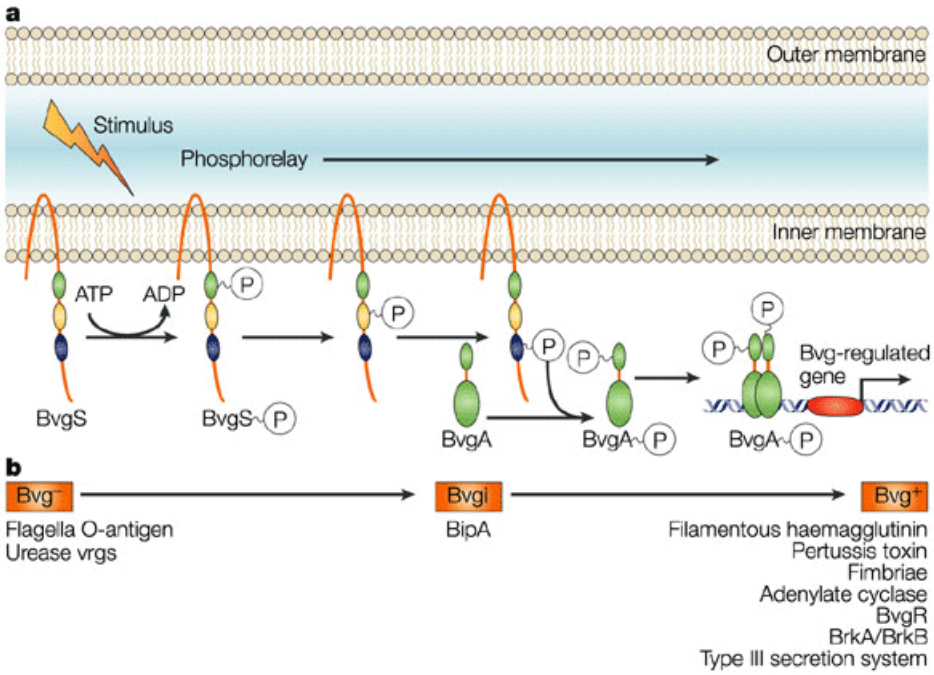

Fig. 10: Schematic representation of phosphorelay in the BvgAS two-component system. *A.* Upon the detection of the periplasmic stimulus, BvgS undergoes autophosphorylation. The phosphate group is subsequently relayed along the BvgS molecule and finally to BvgA. Phosphorylated BvgA then activates transcription of a number of genes. This Bvg-active state is referred to as the Bvg^+ phase. *B.* Without stimulation of BvgS phosphorylation, the bacteria are in the so called Bvg^- phase and express a set of Bvg^- phase-specific genes. With low BvgA activation, an intermediate phase (Bvg^i) was observed. With increasing BvgA activity, the bacteria shift into a Bvg^+ phase. The figure lists examples of factors that are expressed at each Bvg phase. Vrg, vir-repressed genes. (Preston et al., 2004)

Additional regulatory systems were identified to play a role in the expression of some virulence factors of *B. pertussis*. Among these systems, regulation by iron availability (Brickman et al., 2011) and a CO_2 sensory systems (Hester et al., 2012) were identified, but not yet fully described. Additional regulatory circuits are likely to be yet discovered.

5.4.2. Virulence factors

B. pertussis produces a broad spectrum of virulence factors, which can by roughly divided into three groups: complement resistance factors, adhesins, and toxins. The main complement resistance factors are autotransporters *Bordetella* resistance to killing A (BrkA) and Vag8. Among adhesins, filamentous hemagglutinin (FHA), pertactin (PRN), tracheal colonization factor (Tcf), and fimbriae are the most studied. Among the characterized toxins are dermonecrotic toxin (DNT), tracheal cytotoxin (TCT), pertussis toxin (PTX), and above all

adenylate cyclase toxin (CyaA, ACT). The schematic representation of *B. pertussis* and its virulence factors is shown in Fig. 11.

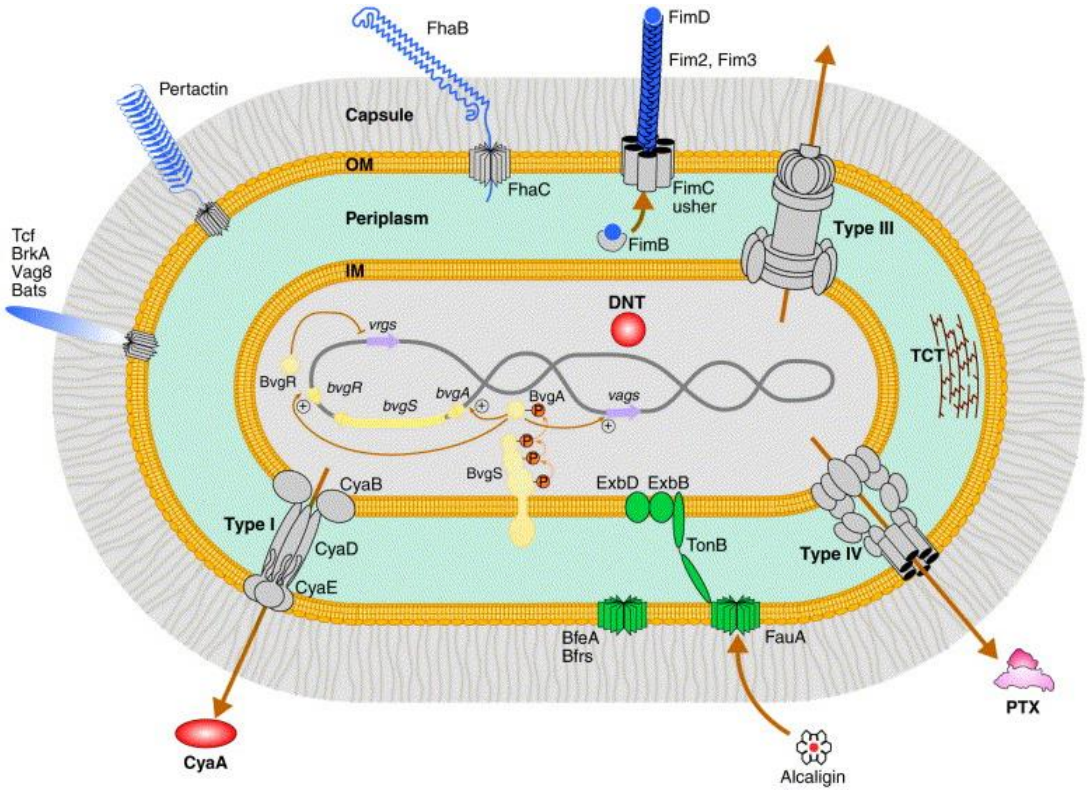

Fig. 11: Virulence factors of *Bordetella pertussis*. *B. pertussis* is depicted as a Gram-negative organism with inner and outer membranes (IM and OM), a periplasm and a capsule. The adhesins Fim, FhaB, pertactin, Tcf, BrkA, Vag8 and Bats are shown in blue; the toxins PTX, CyaA and DNT are in red; the accessory proteins FhaC, FimB, FimC, Type III, Type IV and Type I are in grey; the iron uptake systems ExbB/ExbD, TonB, FauA, BfeA and Bfrs are in green; and the regulatory systems BvgA, BvgS and BvgR are in beige. The large brown arrows represent the orientation of export and import of virulence factors and siderophores, respectively. The thinner brown arrows show the phosphorelay and the regulation circuit. Reprinted from (Locht et al., 2001).

Complement resistance factors

- BrkA reduces C4 and C3 deposition on the bacterial surface and, subsequently, the formation of membrane attack complex, thus inhibiting the classical pathway of complement activation (Barnes and Weiss, 2001). This autotransporter also mediates bacterial attachment to host cells and thus serves as an adhesin (Fernandez and Weiss, 1994).
- Vag8 was identified as a C1 Esterase Inhibitor (C1-inh) binding protein. C1-inh binding by *B. pertussis* inhibits its targeting by classical and lectin complement pathways (Marr et al., 2011). The expression of Vag8 was shown to be under the control of BvgAS (Marr et al., 2007).

- *B. pertussis* was also shown to bind the C4b-binding protein, an inhibitor of the classical complement pathway, through its interaction with FHA (Berggard et al., 1997). This, however, does not protect *B. pertussis* from complement-mediated killing (Fernandez and Weiss, 1998).
- *B. pertussis* also binds the proteins of the factor H (fH) family of negative regulators of alternative complement pathway. This contributes to bacterial resistance to complement-mediated killing (Amdahl et al., 2011) that, however, is not due to the fH-mediated inhibition of C3b (Meri et al., 2013).
- *B. pertussis* further produces the Bps exopolysaccharide belonging to the family of β-(1-6)-linked polymeric-N-acetylglucosamine polysaccharides. Bps was shown to participate in biofilm formation in respiratory tract of infected mice (Sloan et al., 2007) and to be essential for the early phases of colonization of the respiratory tract of mice (Conover et al., 2010; Geurtsen et al., 2014). Although the role of Bps in human infection is not clear, Bps production was shown to inhibit the deposition of complement proteins during the colonization of mice (Ganguly et al., 2014).

Adhesins

- Filamentous hemagglutinin belongs to be the main adhesins of *Bordetellae*. This large rode-shaped protein was shown to mediate the adhesion of *B. pertussis* to several non-ciliated eukaryotic cell types *in vitro* (Alonso et al., 2001; Inatsuka et al., 2005). FHA was proposed to bind several integrins, such as the very late antigen V (VLA-5, CD49e/CD29, $\alpha_5\beta_1$) and the complement receptor 3 (CR3, CD11b/CD18, Mac-1, $\alpha M\beta_2$) were identified. These integrins interact with the RGD (Arg-Gly-Asp) motif of FHA (Van Strijp et al., 1993). The exact role of FHA and its interaction partners *in vivo* remains, however, to be elucidated and was recently questioned (Villarino Romero et al., 2014).
- Tracheal colonization factor harbors an RGD motif (Finn and Stevens, 1995) suggesting a similar role in adhesion as is for FHA.
- Pertactin is a member of the classical autotransporter family of the outer membrane proteins (Henderson et al., 2004). Its expression was shown to be regulated by a CO_2 response element (Hester et al., 2012). PRN protein also completely disappeared from *B. bronchiseptica* after deletion of gene for

protein BspR, which is involved in the iron-responsive regulation of *Bordetella* virulence (Kurushima et al., 2012). Although PRN was shown to mediate the bacterial adherence to ciliated epithelial cells in the model of rabbit tracheal rings (Edwards et al., 2005), no conclusive results on the target were obtained in the mouse model of infection (Khelef et al., 1994). In recent years, *B. pertussis* strains not expressing PRN were frequently isolated from patients (Pawloski et al., 2014) suggesting that PRN is not essential for infection *in vivo*.

- Fimbriae expressed by *B. pertussis* are type I pili. Fimbriae consist of Fim2 or Fim3 proteins, the expression of which can undergo phase variation (Willems et al., 1990). FimX, FimY, and FimN, other structural fimbrial proteins, were identified and are homologues to Fim 2 and Fim3 (Kania et al., 2000; Mooi et al., 1992; Pedroni et al., 1988). The tip adhesin protein FimD was described later (Willems et al., 1992). Fimbriae were shown to mediate the adherence of *Bordetellae* to ciliated epithelium in the rabbit tracheal ring model (Edwards et al., 2005; Funnell and Robinson, 1993) and in the mouse respiratory tract (Geuijen et al., 1997; Mattoo et al., 2000).

Toxins

- Dermonecrotic toxin activity was described using a subcutaneous injection of purified protein that yields the necrotic lesions in a mouse model (Cowell et al., 1979). DNT exhibits a transglutaminase activity that can activate small GTPases from the Rho family (Horiguchi et al., 1995; Schmidt et al., 1999). DNT is, however, not secreted from bacteria in culture, and would be released by lysing cells (Cowell et al., 1979; Nakai et al., 1985).
- Tracheal cytotoxin is released during bacterial cell wall remodeling as a disaccharide-tetrapeptide monomer of peptidoglycan (Cookson et al., 1989). It stimulates, synergistically with bacterial lipooligosaccharide (LOS), the secretion of proinflammatory cytokines (TNFα, IL-1β, and IL-6) and the expression of inducible nitric oxide synthase (iNOS). Subsequent NO production would damage ciliated cells in an infected trachea (Flak and Goldman, 1999; Heiss et al., 1993). In mice, TCT is recognized by NOD1. However, TCT is efficiently recognized only by rodent NOD1 and not by human NOD1 (Magalhaes et al., 2005). There are only a few histology

specimens from infected humans available, but their examination indicated that the epithelial layer in these samples appear to be intact despite the presence of a biofilm of *B. pertussis*. This supports the possibility that TCT does not play a role in human pertussis.

- The pertussis toxin is an ADP-rybosilating toxin of the AB_5 toxin family (Stein et al., 1994a). Due to mutations accumulated in the promoter region in *B. parapertussis* and *B. bronchiseptica*, PTX is expressed only in *B. pertussis* (Arico and Rappuoli, 1987). The catalytic subunit A and five receptor-binding subunits B form a complex in the bacterial periplasmic space and, subsequently, are secreted using the type 4 secretion system (Kotob et al., 1995). PTX binds to sialic acid-containing glycoproteins (Locht et al., 2011; Stein et al., 1994b) and is endocytosed. It follows the retrograde transport pathway to the endoplasmic reticulum (el Baya et al., 1999). From the endoplasmic reticulum, the catalytic subdomain translocates into the cytoplasm (Worthington and Carbonetti, 2007), where the A (S1) subunit of PTX catalyzes ADP-ribosylation of the α-subunit of trimeric G proteins. This leads to the accumulation of cAMP in the target cell upon receptor stimulation by exogenous stimulus (Graf et al., 1992). PTX can enter the blood flow and acts systematically. It probably accounts for the hyperleukocytosis characteristic for malignant pertussis (Morse and Morse, 1976). PTX action inhibits migration of neutrophils and lymphocytes *in vitro* (Spangrude et al., 1985), as well as chemokine production by macrophages (Andreasen and Carbonetti, 2008). PTX also inhibits phagocytosis by human monocytic cells (Schaeffer and Weiss, 2001). The primary targets for PTX in human infection thus probably are airway macrophages (Carbonetti et al., 2007).

During natural infection, *B. pertussis* also expresses the type 3 secretion system (T3SS) (Fennelly et al., 2008). T3SS enables bacterial pathogens to inject their effectors directly into the target cell across plasma membrane. The general schematic structure and mode of action of T3SS is shown in Fig. 12.

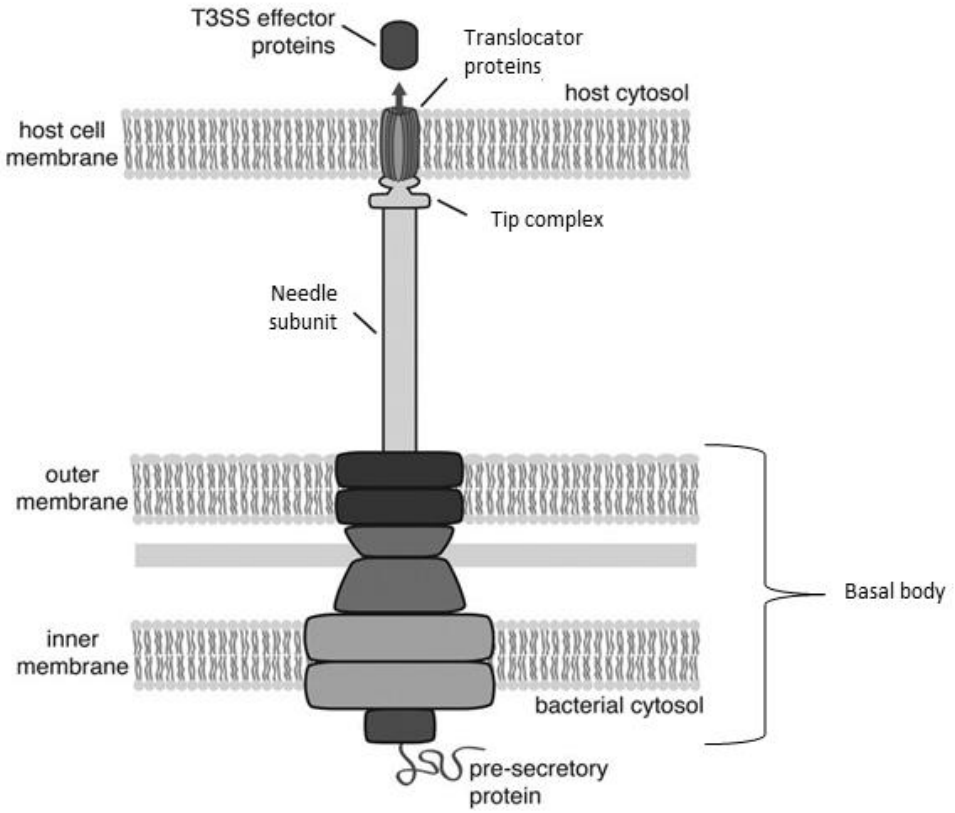

Fig. 12: Schematic representation of type III secretion system structure and function. The T3SS is composed of a basal body, a needle structure, and a needle tip complex. The basal body spans the bacterial inner and outer membranes. Once the basal body is assembled, it becomes a functional secretion system. The needle subunit is then targeted for secretion through the basal body, and forms a hollow extracellular appendage extending up to 60 nm from the bacterial outer membrane. The needle tip protein is secreted next and assembles at the apex of the needle. Upon host cell contact, the hydrophobic translocator proteins are secreted through the T3SS. The tip complex is then thought to insert the translocator proteins into the host membrane, forming a pore. Finally, partially unfolded effector proteins are translocated through the fully assembled T3SS into the cytoplasm of host cell, where they interfere with host defense mechanisms. Adapted from (Duncan et al., 2012)

Five genes potentially encoding proteins secreted by T3SS were identified in the genome of *B. pertussis* – BopN, BopB, BopD, BopC, and Bsp22 (Fennelly et al., 2008). Bsp22 forms the tip of the complex. This protein is massively produced and is highly immunogenic in the course of mouse infection by *B. bronchiseptica* (Medhekar et al., 2009). We have, however, not found anti-Bsp22 antibodies in the sera of human patients infected by *B. pertussis*. Similarly, despite the induction of high anti-Bsp22 antibody titers, Bsp22 did not serve as a protective antigen in the mouse model of *B. pertussis* infection (Villarino Romero et al., 2013). BopB and BopD are translocator proteins and assemble into a pore in the plasma membrane of the target cell. BopC (also called as BteA) and BopN are effector proteins:

- BopC is an effector of T3SS in *B. bronchiseptica*, which is cytotoxic on a broad range of host cell types (French et al., 2009). Although BopC is a monomeric protein, the N-terminal domain enables BopC to form oligomers at higher protein concentrations (Guttman et al., 2013). The sequence of BopC is highly conserved among *B. pertussis, B. parapertussis, and B. bronchiseptica*, which suggest the same mode of action in infection by these bacteria (French et al., 2009).
- BopN modulates the nuclear translocation of NF-κB. During the inhibition of the translocation of the p65 subunit, the translocation of p50 NF-κB subunit is activated by BopN. Moreover, BopN is itself also able to translocate to the nucleus of the target cell, where it induces the expression of IL-10. In this way BopN would manipulate the immune system of a host (Nagamatsu et al., 2009).

5.5. Adenylate cyclase toxin and its interaction with host immune functions

In the year 1976, a multifunctional adenylate cyclase toxin-hemolysin of *Bordetellae* was discovered by E. L. Hewlett (Hewlett et al., 1976). Since then, it has been shown to be a crucial virulence factor of *Bordetella pertussis*. The toxin binds the Complement Receptor 3 (also known as the integrin CD11b/CD18, as $\alpha_M\beta_2$, or Mac-1) expressed by the myeloid cells of the innate immune system, such as monocytes, macrophages, dendritic cells, or neutrophils (Guermonprez et al., 2001).

The importance of CyaA for whooping cough pathogenesis was first recognized by Goodwin *et al.*, who showed that *B. pertussis* mutants lacking CyaA were cleared rapidly from the respiratory tract of infected mice (Goodwin and Weiss, 1990).

5.5.1. From gene to CyaA secretion

Production of the toxin is encoded in the *cyaA* locus. The adenylate cyclase toxin-hemolysin gene *cyaA* is transcribed as the first gene of the *cyaABDE* operon, where the *cyaB, D* and *E* genes encode components of type 1 secretion system responsible for CyaA secretion. The promoter for the *cyaA* gene was mapped in the position 115 nucleotides upstream of the *cyaA* start codon. Another promoter was identified upstream of the *cyaB* gene (Laoide and Ullmann, 1990). The importance of the second promoter is highlighted by the fact that most transcripts from the *cyaA* promoter are terminated in the intergenic region between *cyaA* and *cyaB* genes, thereby leading to monocistronic transcripts. In contrast to the *cyaA* promoter, regulated by BvgAS two-component system, the *cyaBDE* promoter seems to display a low but constitutive activity (Laoide and Ullmann, 1990). The fifth gene of the *cyaA* locus, *cyaC*, is located upstream to *cyaA* and is transcribed in the opposite orientation to the *cyaA* gene, from the second DNA strand. The *cyaC* gene encodes an acyl transferase enzyme that is necessary for the posttranslational activation of CyaA (Barry et al., 1991). The *cyaA* and the *cyaC* genes are expressed from different promoters (Fig. 13).

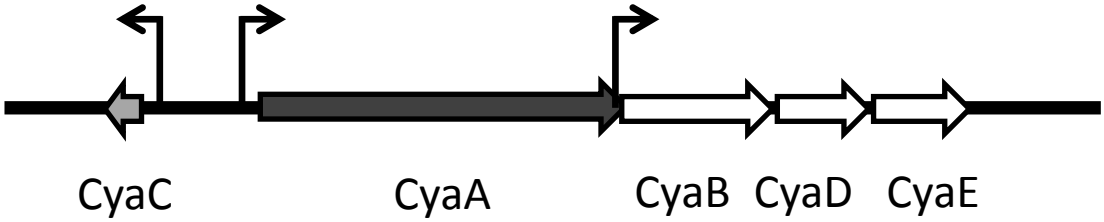

Fig. 13: Schematic structure of CyaA locus. *cyaA*, *cyaB*, *cyaD*, and *cyaE* genes are transcribed in the same direction and in part from the same promoter. Another promoter allows separate transcription of *cyaB, cyaD, cyaE* genes encoding the secretion machinery. The gene for toxin-activating acyltransferase *cyaC* is transcribed from a separate promoter in the opposite direction to the other genes of the locus. Arrows represent the promoters and the direction of transcription.

The main regulator of CyaA expression is the two-component system BvgAS. Transcription of the *cyaA* gene has, however, been found to be regulated to some extent also by a CO_2 responding element unrelated to BvgAS (Hester et al.). Phosphorylated BvgA binds to several sites in the region between base pairs -137 and -51 upstream of the *cyaA* transcriptional starting site (Karimova et al., 1996). The major BvgA-P binding site is then located between nucleotides -100 and -80, providing subsequent cooperative binding of other BvgA molecules to the neighboring low-affinity binding sites (Karimova and Ullmann, 1997). Despite the cooperative binding, BvgA-P has still a rather low affinity to the *cyaA* promoter as compared to promoters of other *Bordetella* virulence genes. As a result, other virulence factors are expressed earlier after *Bordetella* infection and *cyaA* is thus among the so called "late-response" genes.

In addition to the known BvgAS-mediated regulation on the transcriptional level, regulation of CyaA expression by sRNA in the presence of the RNA chaperon Hfq has recently been described in our laboratory. Although there is the same amount of *cyaA* mRNA transcribed in a *Δhfq* mutant as in the wild-type bacteria, the amount of CyaA protein is lower in the *Δhfq* mutant. This suggests a regulation of CyaA expression on the level of mRNA stabilization (Bibova et al.; 2013).

After the translation of CyaA and its posttranslational acylation by CyaC, the CyaA toxin molecule is secreted by the Type 1 Secretion System (T1SS). T1SS is composed of three components, comprising an ABC (ATP-binding cassette) transporter incorporated as a polytopic protein into the inner bacterial membrane (called CyaB in *Bordetellae*); a membrane fusion protein (MFP) extending from the inner membrane into periplasm (called CyaD in *Bordetellae*); and a protein of the

TolC family (OMP) that spans into periplasm from the outer membrane (called CyaE in *Bordetellae*) (Delepelaire, 2004; Holland et al., 2005; Thomas et al., 2014). The secretion signal of CyaA (as well as in case of other T1SS substrates) is located at the C-terminal part of the toxin molecule and remains unprocessed after secretion (Mackman et al., 1987; Masure et al., 1990; Sebo and Ladant, 1993). The interaction of the secreted protein with the ABC transporter of T1SS triggers hydrolysis of ATP and provokes a power stroke that enables insertion of the secreted protein into the T1SS conduit (Koronakis et al., 2000; Letoffe et al., 1996; Thanabalu et al., 1998). This is followed by a series of events that lead to reorganization of the periplasmic domain of the MFP and conformational changes within the transmembrane domain of the ABC transporter, so as to yield recruitment of the trimeric OMP component of the T1SS translocator. Once the C-terminus of the translocated polypeptide emerges from the outer opening of the T1SS conduit on the bacterial surface, a folding nucleus (amino acid residues 1636 to 1642) would form a structure that initiates and scaffolds Ca^{2+}-ion binding-dependent folding of the extruded RTX repeat block segment into a β-roll structure (Bumba *et al.*, under revision). In parallel, the total proton motive force was shown to be required at an early but not at late stage of RTX proteins (Koronakis et al., 1991).

At conditions of limited Ca^{2+} concentration, most of secreted CyaA molecules remain associated with the filamentous hemagglutinin on the bacterial surface after secretion, and exhibit no toxin activity. They also exhibit no capacity to penetrate target cells. For this reason it appears that only the newly secreted toxin can target and penetrate cells acting as a "contact weapon" under such conditions (Gray et al., 2004; Zaretzky et al., 2002). In contrast, at 2 mM Ca^{2+} concentration typical for body fluids, CyaA appears to be efficiently exported and quantitatively released into the culture supernatant (Bumba *et al.*, under revision).

5.5.2. CyaA structure

In the course of secretion from the bacterium, CyaA binds numerous Ca^{2+} ions, which enables the proper folding and activity of the toxin molecule (Rhodes et al., 2001; Rose et al., 1995). The folding starts from the carboxy-terminus concomitantly with toxin secretion (Bumba et al., under revision).

The completely secreted and folded 1706 aa long CyaA molecule consists of two structurally and functionally independent domains (Glaser et al., 1988; Sakamoto et al., 1992). The N-terminally located adenylate cyclase (AC) domain (~400 aa long) is linked to the ~1,300 aa long RTX (Repeat in ToXin) moiety, where the hydrophobic pore-forming domain, activation domain, calcium-binding RTX domain, and the secretion signal for T1SS are located, respectively (Sakamoto et al., 1992). The organization of the CyaA molecule is schematically depicted in Fig. 14.

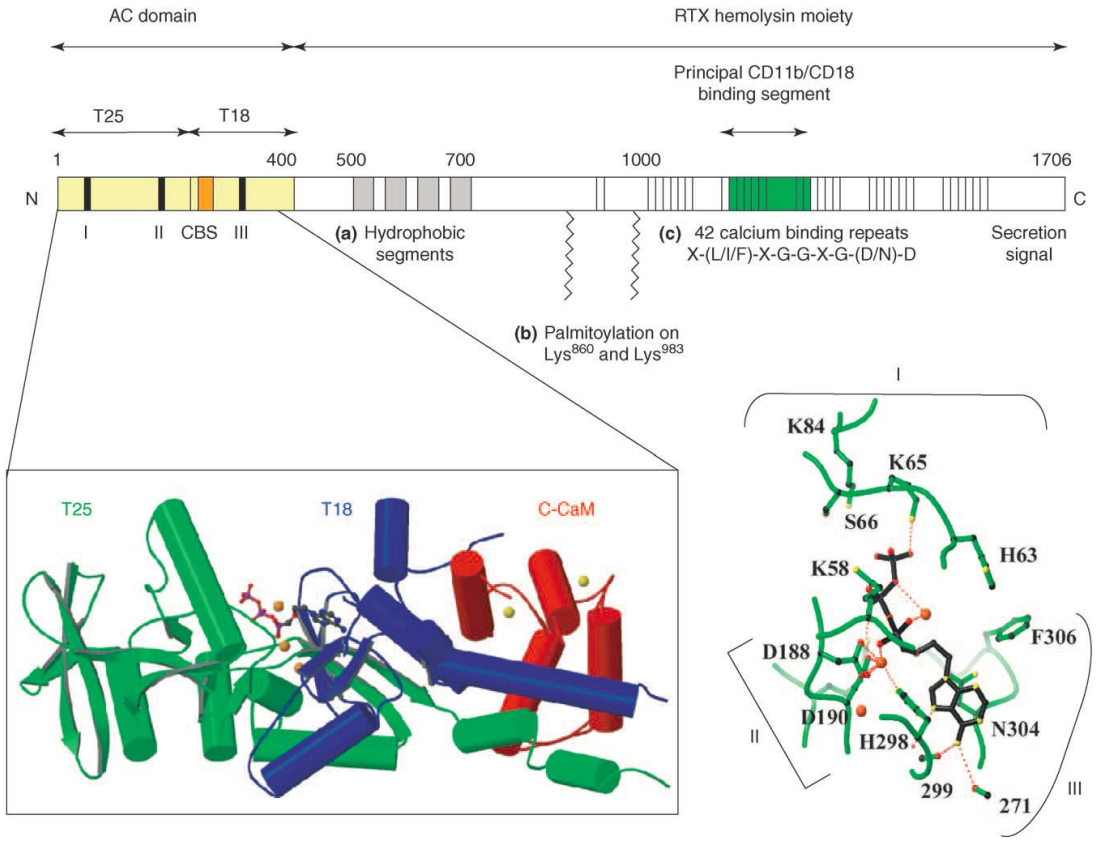

Fig. 14: Structural organization of the 1706 residue-long *Bordetella pertussis* adenylate cyclase (CyaA) toxin molecule. The N-terminal catalytic domain of ~400 residues is a cell-invasive and calmodulin-activated adenylate cyclase (AC) enzyme; T25 and T18 correspond to subdomains of AC, CBS represents the main calmodulin-binding site, and boxes I, II and III highlight the AC segments involved in catalysis. The catalytic domain is enlarged to show the recently solved three-dimensional structure of the ternary complex of AC with the C-terminal fragment of calmodulin and adefovir diphosphate, a metabolite of an anti-viral drug that tightly binds into the catalytic site of CyaA thereby mimicking the binding of ATP (Guo et al., 2005). The structure of the catalytic site with bound adefovir diphosphate (black structure) is shown in a further close-up (right). It shows that aspartates 188 and 190 (D188 and D190), as well as histidine 298 (H298) of AC, are crucial for the binding of the catalytic Mg^{2+} metal ions (red balls), and asparagine 304 (N304) is involved in the positioning of ribose, arginine 37, and three lysine residues, K58, K65 and K84 are involved in binding the triphosphate of the ATP substrate of AC. Deprotonation of 3' OH of ATP is accomplished by histidine 63 (H63), the central catalytic residue of AC. The last ~1,300 residues represent an RTX hemolysin moiety (Hly) of CyaA. This harbors the hydrophobic domain forming cation-selective membrane pores (a), the acylated domain (b), where post-translational activation of the pro-toxin is

accomplished through CyaC-mediated covalent fatty-acylation of either of ε-amino groups of Lys860 and Lys983 (Masin et al., 2005) and the RTX repeat blocks (c) binding calcium ions (~40 Ca^{2+} per CyaA molecule) and allowing the interaction of toxin with its β_2 integrin receptor CD11b/CD18 on myeloid phagocytic cells (El-Azami-El-Idrissi et al., 2003; Guermonprez et al., 2001). The concerted action of these segments allows toxin interaction with and the translocation of the AC domain across target cell membranes. Reprinted from (Vojtova et al., 2006).

Adenylate cyclase domain

The adenylate cyclase (AC) domain consists of 385 amino acid residues (~40 kDa) and its enzymatic activity is activated by the binding of eukaryotic calmodulin inside the host cell cytosol (Berkowitz et al., 1980; Guo et al., 2005). In this respect, CyaA belongs to the family of bacterial toxins activated by host calmodulin, just as the edema factor of *Bacillus anthracis*. Other bacterial toxins harboring the adenylate cyclase activity were also described: ExoY of *Pseudomonas aeruginosa*, extracellular adenylate cyclase of *Yersinia pestis*, and *Vibrio vulnificus* biotype 3 multifunctional autoprocessing RTX toxin (Ahuja et al., 2004; Ziolo et al., 2014).

Calmodulin binding to CyaA leads to the activation of AC enzyme activity by more than 1,000-fold, thus reaching the catalytic activity $k_{cat} \sim 2{,}000\ s^{-1}$ (Ladant and Ullmann, 1999). The specific catalytic activity of the calmodulin-activated AC domain is about 3 orders of magnitude higher than the specific catalytic activity of host adenylate cyclases (Glaser et al., 1989; Ladant, 1988). Calmodulin binds to the four distinct regions of the CyaA AC domain, as shown by the crystal structure of the complex of the AC domain (A7 to A364) bound to the C-terminal fragment of calmodulin (T79 to A147) (Guo et al., 2005). All these four binding sites contribute to calmodulin-induced conformational change that is crucial for AC catalytic activity (Bouhss et al., 1993; Glaser et al., 1989; Ladant et al., 1989). Results obtained by limited proteolysis revealed two separate subdomains of the AC domain - T18 and T25 (Ladant, 1988). Although the T18 subdomain (A236 to E399) is responsible for calmodulin binding, the N-terminal T25 subdomain (M1 to T223) harbors the catalytic site of the AC enzyme (Glaser et al., 1989). The binding of calmodulin to the T18 subdomain leads to the assembly of a stable ternary complex with full catalytic activity. Amino acid substitution of W242 in T18 subdomain leads to a reduced affinity for calmodulin, while the catalytic activity remains fully preserved (Glaser et al., 1989; Ladant et al., 1989).

The catalytic mechanism of the AC domain activity would be deduced from its crystal structure in complex with adefovir diphosphate (Guo et al., 2005). Two aspartates (D188 and D190) and one histidine (H298) of the AC domain are crucial for the binding of Mg^{2+} ions, while asparagine (N304) plays a role in the positioning of ribose, and one arginine (R37) and three lysine residues (K58, K65, and K84) are required for the binding of the triphosphate of ATP. Deprotonation of 3'OH of the ATP substrate is accomplished by histidine (H63), the key catalytic residue of the AC enzyme, which is further involved in the reaction mechanism of adenylyl cyclization (Munier et al., 1992). The knowledge of the catalytic mechanism can now be used in development of inhibitors of the AC enzyme (Geduhn et al., 2011; Gentile et al., 1988; Gille and Seifert, 2003; Shen et al., 2004; Schuler et al., 2012; Smidkova et al., 2014; Soelaiman et al., 2003).

In addition to the conversion of ATP into cAMP, the AC domain was also recently shown to catalyze the formation of cCMP and cUMP, and all these activities come from a single catalytic site (Gottle et al., 2010). Thus, cCMP and cUMP formation may cooperate with cAMP formation in the modulation of the immune responses (Anderson, 1982).

Pore-forming domain

The pore-forming domain of CyaA, comprised of amino acid residues 500 to 700, accounts for the formation of cation-selective pores in the plasma membrane of target cells. The pore-forming domain is composed of several hydrophobic segments and potentially amphipathic and hydrophobic α-helical structures (Basler et al., 2007; Bellalou et al., 1990; Osickova et al., 1999) that form an oligomeric pore of approximately 0.6 to 0.8 nm in diameter (Ehrmann et al., 1991; Vojtova-Vodolanova et al., 2009).

The permeabilization of target membrane for small cations by CyaA (Benz et al., 1994; Gray et al., 1998; Szabo et al., 1994) can result in colloid-osmotic lysis of erythrocytes, accounting for the hemolytic halo surrounding *B. pertussis* colonies on the blood Bordet-Gengou agar plates (Weiss et al., 1984). The specific hemolytic activity of CyaA is, however, relatively low in comparison with the canonical pore-forming toxins such as the α-hemolysin of *E. coli* (Benz et al., 1994; Ehrmann et al., 1991; Masin et al., 2013). The main role of the RTX moiety is thus the support of the

AC domain delivery, rather than cell permeabilization *per se* (Fiser et al., 2012; Rogel and Hanski, 1992; Rogel et al., 1991).

The pore-forming capacity of CyaA is highly dependent on loading of the RTX domain by calcium. The minimal stimulatory Ca^{2+} concentration ranges between 0.6 and 0.8 mM, while the half-maximal pore-forming activity was observed at 2 to 4 mM Ca^{2+} (Knapp et al., 2003). Similarly, pore formation by CyaA is dependent on the membrane potential (Knapp et al., 2008). The pore-forming capacity of CyaA could be increased by deletion of 489 N-terminal amino acid residues (Gray et al., 2001; Masin et al., 2013). This suggests that the deletion of the catalytic domain, along with the additional amino acids distal to it, elicits a conformation of the toxin molecule that is more favorable for pore formation (Gray et al., 2001). Permeabilization of cells by CyaA pores elicits potassium efflux from cells (Osickova et al., 2010; Wald et al., 2014) and can cause lysis of target cells, thereby contributing to the overall cytotoxicity of CyaA (Basler et al., 2006; Hewlett et al., 2006; Osickova et al., 2010).

Activation domain

To acquire its biological activity, CyaA requires post-translational activation by CyaC in the so called activation domain of CyaA (Barry et al., 1991). In this domain, the ε-amino group of the K983 residue is palmitoylated by CyaC (Hackett et al., 1994). Palmitoylation of K983 was shown to be necessary and sufficient for cell-invasive activity of CyaA on erythrocytes (Basar et al., 2001). In addition, a second lysine residue (K860) was found to be palmitoylated when the toxin is co-expressed with CyaC in *E. coli* (Hackett et al., 1995). This second palmitoylation was also later identified in CyaA expressed in recombinant *B. pertussis* (Havlicek et al., 2001). The replacement of K860 residue by an arginine (K860R) leads to decreased insertion of toxin into the target membrane of erythrocytes (Basar et al., 1999). Independently of its acylation status, lysine 860 itself appears to play a crucial structural role in membrane insertion and translocation of the toxin into sheep erythrocytes that do not possess the CD11b receptor (Basar et al., 1999). The acylation of K860 is also sufficient for tight CD11b/CD18 receptor binding and partial toxin activity of CyaA on murine macrophage-like cells. Besides of being the essential acylation residue, the K983 residue plays a structural role in determining the cation selectivity of CyaA

channels, and its acylation controls the pore-forming propensity of CyaA (Masin et al., 2005).

Intriguingly, the non acylated pro-toxin (pro-CyaA) is still able to form pores in lipid bilayers. Although pro-CyaA creates pores with lower efficiency, the formed pores have the same properties as pores created by fully active CyaA (Masin et al., 2005). Non-acylated toxin is also able to penetrate membranes of liposomes (Masin et al., 2004). In contrast, pores created by monoacylated K983R toxin mutant show a reduced selectivity for cations, when compared with the pores formed by wild-type CyaA (Masin et al., 2005). This supports the hypothesis that the K983 residue plays an important role in toxin structure.

RTX domain and secretion signal

The crucial structural part of CyaA is the RTX (Repeat in ToXin) domain consisting of the last approximately 700 amino acyl residues. The RTX domain encompasses five distinct repeat blocks (I to V) consisting of repetitive nonapeptides separated by linkers of variable length (23 to 49 amino acyl residues). Models of RTX domain structure were proposed based on the homology of RTX blocks with a similar domain of metalloproteases and lipases from *Pseudomonas aeruginosa* and *Serratia* spp., for which the structures were solved by X-ray crystallography (Baumann, 1994; Baumann et al., 1993; Hamada et al., 1996). According to these models, the nonapeptide repeats fold into parallel β-rolls connected by loops with Ca^{2+} atoms coordinated by the conserved aspartic residues and protein-backbone carbonyl groups. Stacking of the parallel β-rolls then builds up a right-handed helix. The crystal structure of the RTX block V was recently solved in our laboratory (Fig. 15; Bumba *et al.*, under revision).

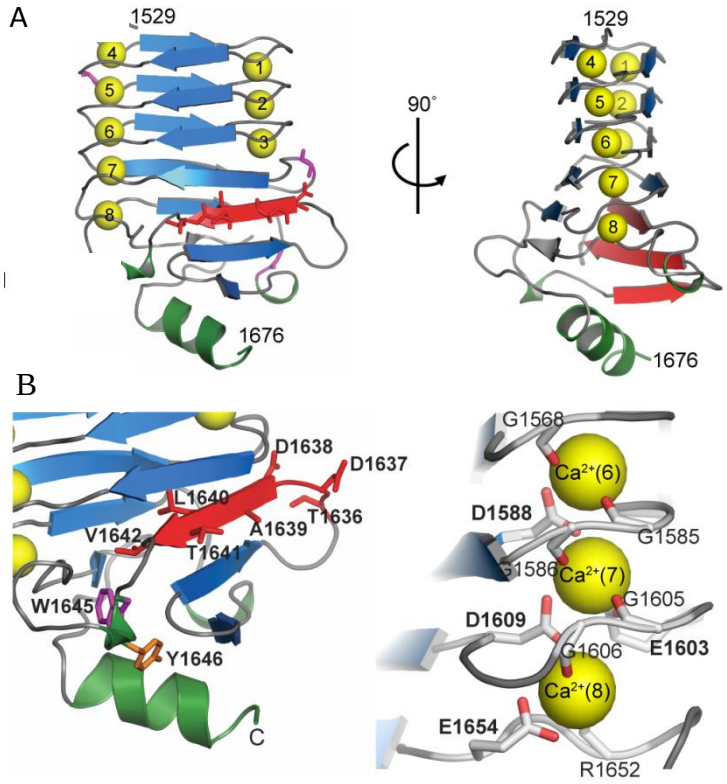

Fig. 15: The X-ray structure of CyaA1529-1681. *A.* The N-terminal consecutive nonapeptide tandem repeats (GGxGxDxxx) are arranged in a regular right-handed helix of parallel β-strands (β-roll). The first six residues of the RTX motif (GGxGxD) constitute a turn with bound calcium ion (yellow ball), while the last three non-conserved residues (xxx) form a short β-strand. Calcium ions are numbered for clarity. Residues 1636 to 1642 constituting the 'folding nucleus' are labeled in red. *B.* Close-up view of the CyaA1529-1681 structure. Left panel: the tertiary structure of the scaffold structure is formed by hydrogen bonding between the backbone chains of three antiparallel β-strands (not shown) that surround a hydrophobic core of the scaffold constituted by hydrophobic side chains of Trp1645 (magenta), Tyr1646 (orange), and Leu1640-Val1642 (red) residues. Right panel: the detailed view of calcium-binding sites within the C-terminal segment of CyaA1529-1681. Ca^{2+}(6) and Ca^{2+}(7) are completely buried within the turns and regularly coordinated by the side chains of Asp residues in position 6 (Asp1588 and Asp1609) and backbone carbonyl groups of Gly residues of the GGxGxDxxx motif, respectively. Ca^{2+}(8) is more exposed to the solvent and is coordinated by side chains of Asp1609 and Glu1654 along with backbone carbonyls of Gly1606 and Arg1652 and two water molecules. The carbon and oxygen atoms are represented in grey and red color, respectively. Reprinted from Bumba *et al.* (under revision).

The calcium-loaded structure of the RTX domain is required for efficient toxin binding to target cells (Rose et al., 1995). Several parts of the RTX domain were shown to be crucial for proper toxin function. Deletions of two nonapeptide repeats at the beginning of the block III (residues 1245 to 1273) or insertion of hexa- or nonapeptides into a specific position (1166, 1281, 1416, 1548) strongly impaired toxin binding to and penetration into cells (Osicka et al., 2000). Moreover, the residues 1166 and 1281 within the block II and III were identified as the major receptor binding site (El-Azami-El-Idrissi et al., 2003). Binding of CyaA to the

receptor could be blocked by antibodies elicited by the immunization of mice with the RTX domain (Betsou et al., 1995; Wang and Maynard, 2014). Furthermore, the integrity of the last repeat block V (1523 to 1638) seems to be essential for toxin activity (Bejerano et al., 1999; Iwaki et al., 1995; Bumba *et al.*, under revision).

The secretion signal is located C-terminally to the RTX domain, in the last 74 amino acid residues (1633 to 1706) (Sebo and Ladant, 1993). Deletion of this portion, or of the last nonapeptide repeat, or the insertion of the FLAG epitope into the position 1623, all resulted in the complete loss of toxin activity (Bejerano et al., 1999; El-Azami-El-Idrissi et al., 2003; Iwaki et al., 1995). This is probably due to the inability of such mutants to adopt a proper conformation. This hypothesis is further supported by the finding that residues 1632 to 1650 are crucial for calcium-dependent folding of the isolated $CyaA_{1530-1680}$ segment (Chenal et al., 2010). Calcium-provoked toxin folding is a highly cooperative process (Knapp et al., 2003; Rose et al., 1995).

5.5.3. Interaction with target membrane

CyaA binds to and penetrates a broad range of eukaryotic cells of various origins. The interaction of CyaA with almost all cell types can be detected due to the extremely high specific enzymatic activity of CyaA. This enables to demonstrate the toxin penetration into cells as production of cAMP in the cytosol. It was shown that CyaA binds to sheep erythrocytes and Jurkat cells in a nonsaturable manner (Gray et al., 1999; Ladant and Ullmann, 1999; Rogel and Hanski, 1992), suggesting that no specific CyaA receptor is present on these cell types. CyaA binding to such target cells as well as CyaA-mediated cAMP production could be blocked by the pre-incubation of the toxin with gangliosides (Gordon et al., 1989). In mouse respiratory infection with *Bordetella*, CyaA specifically destroys leukocytes without having any significant effect on epithelial cells (Gueirard et al., 1998; Harvill et al., 1999). An effect of CyaA on epithelial cells was, however, described later *in vitro* (Eby et al., 2010). In 2001, the complement receptor 3 (CR3, CD11b/CD18, $\alpha_M\beta_2$, Mac-1) was finally identified as the receptor for CyaA on myeloid phagocytes (Guermonprez et al., 2001). The interaction of CyaA with a β_2 integrin corresponds with the observed interaction of other RTX family members with other β_2 integrins (Ambagala et al., 1999; Jeyaseelan et al., 2000; Lally et al., 1997; Li et al., 1999). The binding to CD11b/CD18 is a prerequisite for the efficient insertion of CyaA into the cellular

membrane of phagocytes and the subsequent delivery of the AC domain into cell cytosol or pore formation. The toxin activities can be blocked by competition for receptor binding with the anti-CD11b specific antibodies (Guermonprez et al., 2001). Despite the recent demonstration that CyaA also binds to some extent to CD11a/CD18 when used in high concentrations (Paccani et al., 2011), it is widely accepted that CD11b/CD18 is the only physiologically relevant receptor for the CyaA toxin. By binding to CD11b/CD18, CyaA is targeted to sentinel cells of the innate immune system, such as monocytes/macrophages, neutrophils, and dendritic cells (Guermonprez et al., 2001). Paralysis of phagocytes due to CyaA activity explains the major role played by CyaA in the early phases of *Bordetella* infection (Gueirard et al., 1998; Harvill et al., 1999; Khelef et al., 1993).

The first step of CyaA interaction with a target cell seems to be the recognition of N-linked oligosaccharides on the CD11b/CD18 integrin (Morova et al., 2008). These oligosaccharide chains have a similar structure as the saccharide chains of gangliosides. This offers an explanation of the residual interaction of CyaA with cells lacking the CD11b/CD18 integrin (Gordon et al., 1989). The removal of N-linked oligosaccharides from cellular surface using PNGase F, or the block of N-glycosylation using tunicamycin, both led to the complete loss of CyaA binding to CD11b/CD18-expressing cells. Moreover, CyaA binding to CD11b/CD18 was efficiently inhibited in the presence of soluble saccharides that are found in the N-linked oligosaccharide chains of CD11b/CD18 (Morova et al., 2008). It appears that several N-linked oligosaccharide chains of CD11b/CD18 integrin cooperate in toxin binding, suggesting a multivalent CyaA-oligosaccharide interaction (Hasan et al., 2014).

The binding of CyaA to CD11b/CD18 strongly depends on the toxin loading by Ca^{2+} ions. On the other hand, the binding of CyaA to CR3 is Mg^{2+}-independent. Thus, CyaA appears be the first known Mg^{2+}-independent interaction partner of CD11b/CD18 (Guermonprez et al., 2001). Guermonprez *et al.* also suggested that CyaA may bind the CR3 outside the I domain, which is known to bind all other natural ligands of the β_2 integrin. This hypothesis was recently confirmed by our group that mapped the toxin binding site to the hinge region of CD11b (Osicka *et al.*, manuscript in preparation).

The integrin-binding site of CyaA was previously localized between amino acid residues 1166 and 1281 of the RTX domain (El-Azami-El-Idrissi et al., 2003), which contains several aspartate/glutamate rich regions. The negative charge of the RTX domain is neutralized by the binding of approximately 40 positively charged Ca^{2+} ions. This may facilitate the interaction of CyaA with the negatively charged sialic acid on the CD11b/CD18.

In addition to the toxin interaction with oligosaccharides, the acylation of CyaA plays an important role in the interaction of CyaA with the CD11b/CD18 integrin (El-Azami-El-Idrissi et al., 2003). The nonacylated pro-CyaA exhibits a decreased capacity to bind the integrin and the pro-CyaA can be outcompeted from binding to CD11b/CD18 by acylated CyaA or anti-CD11b mAb. Moreover, the interaction of pro-CyaA with CD11b/CD18 supports penetration of the AC domain into target cells very poorly (El-Azami-El-Idrissi et al., 2003). This is in agreement with the finding that acylation of K983 is necessary and sufficient for full activity of CyaA on CD11b/CD18-expressing J774A.1 monocytes (Masin et al., 2005).

Upon interaction of CyaA with CD11b/CD18, the toxin molecule invades the target membrane. This is a prerequisite for pore formation and AC domain translocation into the target cell, which is coupled with toxin-mediated Ca^{2+} entry into cell cytosol independently of the pore-forming activity of the toxin (Bumba et al., 2010; Fiser et al., 2007). Following Ca^{2+} entry, the CD11b/CD18-CyaA complex relocates to lipid rafts. This is enabled by Ca^{2+} mediated activation of the calpain protease, which cleaves the talin molecule and thus liberates CD11b/CD18 from association with the actin cytoskeleton (Bumba et al., 2010). Moreover, Ca^{2+} entry increases the interaction of the AC domain with host calmodulin that is required for AC toxin activity (Guo et al., 2005; Ladant et al., 1989). The toxin-mediated calcium entry into the target cell is thus crucial for enzymatic and cytotoxic action of CyaA.

After liberation of CD11b/CD18 from the cytoskeleton and the relocation of the toxin-receptor complex into lipid rafts, the AC domain translocation is completed. The translocation appears to be driven by membrane potential (Otero et al., 1995). In addition, the translocation could be dissociated from the formation of the cation selective pores by amino acid substitutions in the predicted membrane segments of CyaA (Basler et al., 2007; Basler et al., 2006; Osickova et al., 2010;

Osickova et al., 1999). The translocation of the AC domain directly across the plasma membrane is supported by the predicted alpha helix 454 to 485, which was shown to possess a lipid bilayer-interacting and membrane-destabilizing capacity (Karst et al., 2012; Subrini et al., 2013). AC domain translocation does not occur via the cation selective pore (Osickova et al., 2010). The exact mechanism of AC domain translocation is, however, still not completely understood.

Similarly, the exact mechanism of pore formation in the target membrane remains to be elucidated. Several studies confirmed the critical role of the hydrophobic pore-forming domain for the penetration of small cations through the target membrane (Benz et al., 1994; Glaser et al., 1988; Osickova et al., 2010; Osickova et al., 1999; Powthongchin and Angsuthanasombat, 2009). While AC domain translocation appears to be a linear function of toxin concentration, the pore formation by CyaA is a higher order function of CyaA concentration, with a Hill cooperativity number ≥ 3. This suggests that CyaA monomers are sufficient for AC domain translocation, whereas toxin oligomerization is involved in pore formation (Betsou et al., 1993; Gray et al., 1998; Osickova et al., 1999; Szabo et al., 1994; Vojtova-Vodolanova et al., 2009). Moreover, pores formed by CyaA in artificial membranes behave as frequently opening and closing membrane channels (with opening life-time approximately 2.8 s), suggesting an equilibrium between non-conducting monomers and conducting oligomers in the membrane (Basler et al., 2007; Benz et al., 1994). Cooperative action between distinct toxin molecules could also be deduced from complementation studies of mutated toxin variants. For example, cytotoxic activity can be partially restored by the *in vitro* complementation of a toxin missing its C-terminal part with the purified C-terminal part of the another toxin molecule (Iwaki et al., 1995). Similarly, Bejerano obtained a highly active toxin complex by a combination of a toxoid lacking a conserved sequence between amino acid residues 1636 and 1650 (block A) with a C-terminal CyaA fragment (1490 to 1706) carrying block A (Bejerano et al., 1999). Moreover, the AC domain translocation across the target membrane may be potentiated by the addition of an excess of CyaA lacking the AC domain (Iwaki et al., 2000). More recently, it was shown that CyaA may form oligomers already prior to insertion into the target membrane (Lee et al., 2005b), although these results are questionable due to the presence of detergent in the experimental procedure.

Although the toxin concentrations needed for the manifestation of its particular activities is known *in vitro*, the exact CyaA concentration in natural infections is still not completely clear. First experimental estimation was recently provided by Eby and coworkers who measured the concentration of CyaA in nasopharyngeal lavages during respiratory infections in the baboon model of pertussis. They found that CyaA concentration could reach 100 ng/ml near target cell surface in the host nasopharynx (Eby et al., 2013).

5.6. Modulation of immune system functions by CyaA

CyaA was shown to be essential for colonization of mice by *B. pertussis*, since bacteria expressing a mutated CyaA were rapidly cleared from mouse airways, when low-dose bacterial cultures were used for challenge experiments (Goodwin and Weiss, 1990). A *B. pertussis* mutant devoid of the adenylate cyclase activity of CyaA showed decreased multiplication during the first 5 days following infection (Khelef et al., 1992). CyaA also contributes to numerous pathological effects in the murine model of *Bordetella* infection, such as recruitment of inflammatory leukocytes and the induction of histopathology lesions in the lung (Gueirard et al., 1998; Khelef et al., 1994; Weiss et al., 1984). In line with that, a *B. pertussis* mutant devoid of adenylate cyclase activity, as well as an avirulent mutant, induced no inflammation in comparison with the parental strain (Khelef et al., 1994). These facts together suggest that CyaA is able, either directly or indirectly, to influence a broad spectrum of processes of both innate and adaptive immune system.

5.6.1. Modulation of innate immunity by CyaA functions

The important role of CyaA in colonization and pathogenesis is at least in part achieved by the effects of CyaA on bactericidal functions of innate immunity. Andreasen and Carbonetti observed no differences in bacterial loads of *B. pertussis* in naïve mice with depleted neutrophils versus control mice (Andreasen and Carbonetti, 2009). However, CyaA was still required for colonization in this model, since bacteria lacking CyaA were unable to colonize animals (Andreasen and Carbonetti, 2009; Harvill et al., 1999). In contrast, neutrophils seemed to be necessary for bacterial clearance in mice actively or passively immunized before the challenge with *B. pertussis*, since immunized neutropenic mice showed higher loads of bacteria in the lungs in comparison with normal mice. Moreover, neutrophils were the primary target of CyaA in immunized mice, as shown by using CyaA deficient bacteria (Andreasen and Carbonetti, 2009). This is consistent with findings that neutralizing antibodies against CyaA may restore functions of neutrophils (Mobberley-Schuman et al., 2003; Weingart et al., 2000). Indeed, CyaA is able to abolish the functions of neutrophils, such as chemotaxis, phagocytosis, reactive oxygen species (ROS) production, and neutrophil extracellular trap (NET) formation. The inhibition of superoxide production by CyaA-produced cAMP had already been described in 1982 by Confer and Eaton (Confer and Eaton, 1982) and it likely

accounts for the inhibition of NET formation and neutrophil apoptosis (Eby et al., 2014). Following on the study of Confer and Eaton, Friedman and coworkers showed the inhibition of chemotaxis and superoxide production by human polymorphonuclear leukocytes exposed to CyaA, but did not observe changes in phagocytic capacities of these cells using light microscopy (Friedman et al., 1987). The inhibition of phagocytosis by toxin-treated macrophages was, however, observed by Weingart and Weiss, who showed that the *B. pertussis* mutant lacking CyaA is approximately 10 times more efficiently phagocytosed by human neutrophils than wild-type bacteria (Weingart et al., 2000). Moreover, the addition of purified CyaA to human neutrophils incubated with the mutant bacteria led to the impairment of phagocytosis (Weingart et al., 2000). It was also shown that neutralizing antibodies against CyaA, or a human convalescent serum containing such antibodies, restored the phagocytic capacity of human neutrophils exposed to CyaA (Weingart et al., 2000). More specifically, CyaA was found to be able to inhibit CR3-mediated phagocytosis in human neutrophils (Mobberley-Schuman et al., 2003). Thus, CyaA inhibits a broad spectrum of bactericidal activities of neutrophils.

Similar observations as those for neutrophils were obtained using monocytes/macrophages. It was shown that CyaA inhibits the production of reactive oxygen species and impairs opsonophagocytic killing of bacteria by alveolar macrophages and neutrophils (Confer and Eaton, 1982). CyaA is able to inhibit both CR3- and FcR-mediated phagocytosis and this depends on its ability to increase cAMP levels in macrophages (Kamanova et al., 2008). CR3-mediated phagocytosis appears to be much more sensitive to CyaA-mediated cAMP elevation than FcR-mediated phagocytosis and its inhibition is accompanied by actin cytoskeleton rearrangement and membrane ruffling due to inhibition of RhoA (Kamanova et al., 2008). CyaA mediated cAMP production also leads to a rapid inhibition of macropinocytosis (Kamanova et al., 2008).

The expression of CyaA is important for the survival of *B. pertussis* in phagosomes. Once *B. pertussis* is engulfed by a human macrophage, it is able to survive within the phagosome if the multiplicity of infection reaches 100 bacteria per macrophage (Friedman et al., 1992). This can be important for bacterial survival in host airways and may be related to the clinical manifestation of whooping cough.

Mutants with repressed expression of CyaA were shown to have a decreased ability to survive inside macrophages, whereas, induction of CyaA expression enabled the bacteria to survive inside primary macrophages for several days (Friedman et al., 1992).

In addition to the blocking of bactericidal functions of phagocytes, CyaA is also able to induce apoptosis of macrophages both *in vivo* and *in vitro* (Gueirard et al., 1998; Khelef et al., 1993). First apoptotic cells can be observed after 2 hours of incubation of macrophages with the *B. pertussis* strain 18323 cells at a bacterium to macrophage ratio of 100:1. After 6 to 8 hours, almost 100% of macrophages are killed (Khelef et al., 1993). It was also shown that the engulfment of bacteria is not important for apoptosis induction by *B. pertussis* (Khelef et al., 1993). The use of bacterial mutants showed that CyaA, but not the pertussis toxin, was needed for *B. pertussis*-provoked macrophage apoptosis (Gueirard et al., 1998; Khelef et al., 1993). Moreover, incubation of macrophages with purified CyaA was found to be sufficient for induction of apoptosis (Hewlett et al., 2006; Khelef and Guiso, 1995). In contrast, CyaA at a physiological concentration of (10 ng/ml) blocks spontaneous apoptosis of neutrophils (Eby et al., 2014).

CyaA-caused apoptosis depends on both the cell-invasive AC enzyme activity (conversion of ATP to cAMP) and on the pore-forming activity (Hewlett et al., 2006). Whereas CyaA at higher concentrations causes a loss of cell membrane integrity, incubation of macrophages with lower concentrations of CyaA leads to the induction of apoptosis due to the activation of caspase 3 and 7 (Hewlett et al., 2006). The activation of caspase 3/7 by CyaA depends on cAMP production (Hewlett et al., 2006). Non-acylated CyaA induced apoptosis at a toxin concentration that was sufficient for cAMP production, but not for erythrocyte lysis (hemolysis). This supports the role of hemolytic activity in the induction of apoptosis when higher toxin doses (>100 ng/ml) are used (Hewlett et al., 2006; Cheung et al., 2009). Damage of cellular membrane integrity by CyaA-formed pores leads to LDH release into the medium before macrophages lose their ability to reduce MTT into the formazan dye (Basler et al., 2006). MTT reduction depends on oxidative phosphorylation occurring in mitochondria. Bachelet and coworkers then showed

that CyaA of wild-type *B. pertussis* induces the loss of mitochondrial membrane potential (Bachelet et al., 2002).

We have recently shown that the enzymatic activity of CyaA causes induction of apoptosis by promoting the translocation of the pro-apoptotic protein Bax into the mitochondrial membrane. This is preceded by cAMP-dependent accumulation of the pro-apoptotic protein BimEL by the process dependent on the activation SHP-1 and the inhibition of AKT (Ahmad *et al.*, in press).

In vitro, CyaA provokes a decrease in the phagocyte number also by an arrest of the cell cycle. Incubation of mouse macrophages with CyaA led to accumulation of cells arrested in the G1/G0 phase. This cell cycle arrest was, however, reversible at physiologically relevant (~10 ng/ml) toxin concentrations (Gray and Hewlett, 2011). Gray and colleagues further showed that CyaA is responsible for a decrease of cyclin D1 concentration in macrophages, as well as for an increase of levels of $p27^{kip1}$, a CDK inhibitor. Both these processes, as well as CyaA-provoked inhibition of ERK 1/2 kinase, contribute to cell cycle dysregulation (Gray and Hewlett, 2011). These changes in the presence and activity of proteins important for passing through the cell cycle are mediated by the elevation of cAMP by the toxin (Gray and Hewlett, 2011).

In addition to the altered expression of cyclin D1 and $p27^{kip}$, it was shown that CyaA is able to promote important changes in transcription of a whole range of genes of murine bone marrow-derived macrophages. Using a microarray analysis, Cheung and coworkers showed that the incubation of bone marrow-derived macrophages with 20 ng/ml of CyaA for 24 hours led to more than a two-fold change in the expression of ~5.8% (2613 genes) of genes (45,000 probe set) (Cheung et al., 2008). By comparison, exposure to the CyaA-AC^- toxoid, which was not able to produce cAMP, or to nonacylated pro-CyaA caused a significant up-regulation of only 12 and 2 genes, respectively. Cheung and coworkers also found that the majority of the up-regulated genes were connected with host immune responses and inflammation. CyaA caused increased transcription of CD80 and CD86 genes (Cheung et al., 2008), which corresponds to the observation of Bagley and coworkers, showing the up-regulation of these genes after CyaA treatment in dendritic cells (Bagley et al., 2002). Cheung and coworkers further observed

increased transcription of genes for chemokines involved in adhesion and transmigration of neutrophils (Cxcl5, Cxcl7). By contrast, about 40 % of the down-regulated genes were involved in cell proliferation (down-regulation of genes for cyclins B1 and B2 and their CDK1 partner) (Cheung et al., 2008). This is in agreement with the above-described effect of CyaA on cell cycle.

Besides professional phagocytes, *B. pertussis* also interacts with tracheal epithelial cells, which are among the first targets of *B. pertussis* in the course of infection. The epithelial layer, formed by these cells, serves not only as a mechanical barrier, but it also produces various anti-bacterial agents, cytokines, and immunomodulators. Bacterial tracheal cytotoxin (TCT) and LOS were shown to synergize in the induction of IL-1α and NO production in hamster tracheal epithelial cells (Flak et al., 2000). Furthermore, bacterial attachment to ciliated cells causes mucin hypersecretion and epithelial damage, which all together result in decreased mucociliary clearance (Soane et al., 2000). Consistent with these findings, genes encoding IL-6, IL-8, chemokine MCP-1 and two genes for mucin secretion: MUC2 and MUC5AC were shown to be up-regulated in the human bronchial epithelial cell line (BEAS-2B) after infection with *B. pertussis* (Belcher et al., 2000).

After attachment, *B. pertussis* was shown to invade human tracheal epithelial cells (Bassinet et al., 2000). Originally, it was thought that the bacteria within the cells are rapidly killed (Bassinet et al., 2000; Gueirard et al., 2005). Recently, however, Lamberti and coworkers showed that a significant proportion of *B. pertussis* cells is able to survive within the human epithelial cell line A549 for several days (Lamberti et al., 2013). Interestingly, CyaA inhibits bacterial uptake into human tracheal epithelial cells (Bassinet et al., 2000) and causes production of cytokine IL-6 in these cells (Bassinet et al., 2004). However, the immunological consequences of this process remain unknown.

In addition to the invasion of epithelial cells, CyaA was shown to cause epithelial cell rounding due to its AC activity (Ohnishi et al., 2008; Westrop et al., 1994), which may support the toxin-provoked loss of tightness of the epithelial barrier. Furthermore, *B. pertussis* was found to efficiently translocate across the basolateral membrane of polarized epithelial cells (Eby et al., 2010). The basolateral side of epithelial cells seems to be quite sensitive to CyaA action despite the absence

of the CD11b/CD18 receptor. This mechanism could be used by CyaA to change the expression of cytokines by epithelial cells and thus to further manipulate innate immunity or the maturation of dendritic cells on epithelial surfaces, and thereby also the specific immune response (Diamond et al., 2000; Hammad and Lambrecht, 2008; Kato and Schleimer, 2007; Mayer and Dalpke, 2007; Schleimer et al., 2007).

5.6.2. Modulation of adaptive immunity by CyaA functions

Dendritic cells (DCs) express high amounts of the CD11b/CD18 integrin, and are thus sensitive targets of CyaA (Guermonprez et al., 2001). These cells represent the bridge between innate and adaptive immune systems, where the immature DCs sample the environment by phagocytosis of particulate matter and by macropinocytosis of extracellular fluid and its contents. Any contact with PAMPs leads to maturation of DCs. Mature DCs then migrate to lymph nodes, where they can activate particular subsets of T and B cells by displaying antigens derived from the pathogen on their surface and by production of cytokines.

CyaA was shown to interfere with adaptive immune functions of DCs, such as the maturation and cytokine production by murine bone marrow-derived DCs (BMDC), as well as of the human peripheral blood monocytes, the precursors of DCs (Adkins et al., 2014; Ross et al., 2004). In LPS-stimulated DCs, CyaA enhances up-regulation of CD80 on the cell surface, while concomitantly reducing CD86, CD40 and CD54 surface exposure (Adkins et al., 2014; Boyd et al., 2005; Ross et al., 2004; Skinner et al., 2004). Moreover, the toxin strongly suppresses LPS-stimulated production of TNF-α, IL-12p70 and MIP-1α, while it potentiates IL-6 and IL-10 production in DCs (Bagley et al., 2002; Boyd et al., 2005; Njamkepo et al., 2000; Ross et al., 2004; Siciliano et al., 2006; Skinner et al., 2004; Spensieri et al., 2006). The effects of CyaA on DCs are mainly dependent on toxin-induced cAMP signaling, as these effects could be mimicked by cell-permeable cAMP analogues db-cAMP or 8-Br-cAMP, or by the cAMP-elevating agent forskolin (Bagley et al., 2002).

On the other hand, the impact of the CyaA-AC$^-$ toxoid action, when used in high concentrations, was also described on DCs. Toxin-induced increase in cell surface exposure of CD80 and CD86 maturation markers as well as production of TNF-α, IL-1β, IL-6, and IL-12 was dependent on CD14 and TLR4 signaling both in

mice and in bone-marrow-derived DCs as well as in primary human monocytes (Dadaglio et al., 2014). In contrast, the pore-forming activity of CyaA was observed to drive DC maturation when physiological concentrations of highly active CyaA-AC^- toxoid were used (Svedova et al., under revision).

DC maturation and cytokine production induced by TLR signaling is controlled mainly by mitogen-activated protein kinases (MAPKs) like p38 and ERK1/2, and nuclear factor (NF)-κB signaling pathways (Rescigno et al., 1998; Sato et al., 1999). CyaA of *Bordetellae* was shown to differentially regulate MAPK signaling in DCs. Exposure to CyaA produced by *B. bronchiseptica* was shown to account for the inhibition of p38 MAPK signaling in BMDCs, but no effect on ERK1/2 was observed (Skinner et al., 2004). On the other hand, recombinant CyaA enhanced LPS-induced MAPK phosphorylation and inhibited IRF-1 and IRF-8 expression, thus modulating TLR-agonist-induced IL-10 and IL-12p70 production by DCs (Hickey et al., 2008; Spensieri et al., 2006). Furthermore, wild-type *B. pertussis* as well as the CyaA-deficient strain was shown to increase phosphorylation of p38, ERK1/2, SAPK/JNK and IκBα in monocyte-derived DCs, suggesting activatory effects of CyaA on MAPKs and NF-κB signaling (Fedele et al., 2010). It appears that dysregulation of MAPK and IRF signaling by CyaA action could be a way to dysregulate DC maturation on infected epithelia.

CyaA-promoted aberrant maturation of DCs might affect the onset of adaptive immune responses and may delay bacterial clearance. Recently, the role of CyaA-mediated K^+ efflux from DCs was shown *in vivo*, as it activated the NALP3 inflammasome and IL-1β production in LPS-stimulated DCs. IL-1β subsequently mediated induction of a Th17 response, which is crucial for the clearance of *Bordetella* infection from the respiratory tract (Dunne et al., 2010). Moreover, human monocytes infected by *B. pertussis*, but not by the CyaA-deficient mutant strain, displayed suppressed capacity to induce antigen-dependent $CD4^+$ T cell proliferation (Boschwitz et al., 1997). Similarly, CyaA of closely related *B. bronchiseptica* inhibited antigen-induced $CD4^+$ T cell proliferation stimulated by macrophages and induced a Th17 response (Siciliano et al., 2006). The ability of DCs to present antigens to $CD4^+$ T cells and to promote $CD8^+$ T cell proliferation was also shown to be inhibited by CyaA. CyaA enabled the migration of DCs towards CCL19 and

CCL21 and the CyaA-treated DCs may therefore subsequently shape the development of T cells into immunosuppressive T_{reg} cells (Adkins et al., 2014). This may serve in inhibition of anti-*Bordetella* adaptive immunity by CyaA-dependent modulation of DCs.

In addition, CyaA has also been shown to shape T cell responses directly by interfering with their activation and chemotaxis. Although T cells do not express the CD11b/CD18 receptor of CyaA, the toxin may still bind these cells through its lectin-like activity when used in high concentrations and may thus modulate T cell functions directly. This is, however, not very likely in the course of natural infection due to low CyaA production levels. Nevertheless, CyaA was shown to promote the polarization of T cells into Th2 and IL-10-producing T cells with a regulatory phenotype (Tr1), while limiting Th1 responses *in vitro* (Paccani et al., 2008; Paccani et al., 2011; Ross et al., 2004; Rossi Paccani et al., 2009). T-cell antigen receptor and chemokine receptor signaling, as well as MAPK signaling, were inhibited by CyaA via a cAMP/PKA-dependent pathway. Similarly, CyaA potently promoted Th2 cell differentiation by inducing expression of the master Th2 transcription factors c-maf and GATA-3 (Rossi Paccani et al., 2009).

6. Aims of the Thesis

Although the global effect of CyaA action on immune cells has been extensively studied, the exact mechanism of CyaA action and signaling pathways activated by this toxin remain poorly characterized. Even less is known about the effects of particular CyaA activities on signaling in the targeted cell leading to a disruption of bactericidal activities of the host.

To clarify the issues mentioned above, the aims of this thesis were:

1) to characterize the impact of CyaA action on the most important bactericidal activities of phagocytes, such as the production of reactive oxygen and nitrogen species, and on processes leading to the activation of the adaptive immune system and

2) to describe the signaling pathways involved in the CyaA-provoked inhibition of the immune response to *B. pertussis*.

7. Materials and Methods

Antibodies and Reagents

Escherichia coli 0111:B4 lipopolysaccharide (LPS), zymosan, poly-RGD, anti-BSA antibody, 3-isobutyl-1-methylxanthine (IBMX), N-6,2'-O-Dibutyryladenosine-3',5'-cyclic monophosphate (db-cAMP), horse radish peroxidase (HRP), formyl-Met-Leu-Phe (fMLP), and luminol were obtained from Sigma-Aldrich; N6-Benzoyladenosine-3',5'-cyclic monophosphate (6-Bnz-cAMP), 8-(4-chlorophenylthio)-2'-O-methyladenosine-3',5'-cyclic monophosphate (8-CPT-cAMP), and 8-Bromoadenosine-3',5'-cyclic monophosphorothioate (cAMPS) were from BIOLOG Life Science Institute; NSC87877 and H-89 were purchased from Calbiochem; DAE-NONOate was from Cayman Chemical; and hydrogen peroxide was from Lach-Ner. Antibodies were purchased from Santa Cruz Biotechnology (anti-SHP-1 (C-19), anti-SHP-2 (c-18)) or from Cell Signaling Technology (anti-p38 MAPK (D13E1), anti-P-p38 MAPK (D3F9), anti-p44/42 MAPK, anti-P-p44/42 MAPK (20G11), anti-p65 (D14E12), anti-Akt (C67E7), anti-Akt P-Ser473 (D9E), anti-Akt P-Thr308 (C31E5E), anti-P-c-Fos (D82C12), anti-FoxO3a, anti-P-FoxO3a, anti-iNOS, anti-β actin, anti-IRF1 (D5E4), anti-P-IκB, anti-IκB, anti-JNK, anti-P-JNK (98F2), anti-Stat1 (9H2), anti-P-Tyr701 Stat1, anti-P-Ser727 Stat1). All siRNAs (ON TARGETplus SMARTpool, si-PTPN6, si-PTPN11 and non-targeting siRNA control) as well as DharmaFECT 4 were obtained from Dharmacon.

Bacterial strains

Bacterial strains were derived from *Bordetella pertussis* Tohama I (*B.p. cyaA-wt*) obtained as strain CIP 81.32 from the Collection of Institute Pasteur, Paris, France. The *B.p. ΔcyaA* and *B.p. cyaA-AC*$^-$ strains, carrying an in-frame deletion of the *cyaA* open reading frame on the chromosome or secreting an enzymatically inactive CyaA-AC$^-$ toxoid, created by the insertion of GlySer dipeptide into the positions 188 and 189 (Osickova et al., 2010), respectively, were constructed using the pSS4245 allelic exchange vector kindly provided by Dr. S. Stibitz (Buasri et al., 2012). The pSS4245 plasmid carries a gene encoding the I-SceI restriction endonuclease that is expressed in *B. pertussis* under Bvg$^+$ conditions. Briefly, the parental strain was grown for 4 days under modulating conditions (Bvg$^-$) on BGA plates (Bordet-Gengou agar,

Becton Dickinson) containing 15% defibrinated sheep blood and 50 mM $MgSO_4$. Plasmid constructs were transformed into *E. coli* SM10 λpir and transferred by conjugation into the recipient *B. pertussis*. Matings were performed for 3 h at 37°C on fresh BGA plates containing 10 mM $MgCl_2$ and 50 mM $MgSO_4$ (modulating, Bvg^- conditions). *B. pertussis* clones having the plasmid construct inserted into the chromosome by single crossing-over were selected for 5 days at 37°C on plates that contained 50 mM $MgSO_4$, 500 μg/ml of streptomycin, 30 μg/ml of ampicillin and 40 μg/ml of kanamycin. The clones were restreaked on the same media for additional 5 days and then plated on BGA lacking $MgSO_4$ (Bvg^+ conditions) in order to select for the second crossing-over and excision of the rest of the allelic exchange vector from the bacterial chromosome. For each construct, several individual clones were characterized for phenotypic change and presence of introduced and absence of undesired mutations was verified by the sequencing of relevant portions of PCR-amplified segments of the *cyaA* gene. Production of key virulence factors like PTX, PRN, FHA and CyaA was verified by Western blotting of bacterial lysates with specific antibodies (Weber et al., 2001). The construction of *B. pertussis* strains carrying mutation in *cyaA* gene was performed by Ing. K. Skopova (Institute of Microbiology, ASCR, v.v.i., Prague).

The plasmid pBBRcyaGFP encoding GFP under the control of the *cyaA* gene promoter was kindly provided by Dr. B. Vecerek (Institute of Microbiology, ASCR, v.v.i., Prague) and was introduced into *Bordetella* strains by conjugation, using 50 μg/ml kanamycin and 150 μg/ml cephalexin for selection.

Cell cultures and handling

The L929 CMG cells (a kind gift from Dr. T. Brdicka from the Institute of Molecular Genetics, ASCR, v.v.i., Prague) were used for M-CSF production (Weischenfeldt and Porse, 2008). The L929 CMG cells were cultivated until full confluence in D-MEM containing 10% (v/v) fetal calf serum (FCS). The medium was subsequently changed and the cells were kept in the fresh D-MEM medium for three days to produce sufficient amounts of M-CSF. Bone marrow macrophage-like cells (BMDM) and the bone-marrow-derived dendritic cells (BMDC) were obtained from femoral and tibial bones of 6-week-old female C57BL/6 mice. Briefly, the bone marrow was flushed out of the bones using 5 ml of sterile, ice-cold PBS and washed

3-times with cold PBS. After the last washing, the pellet was filtered through an 80 μm filter to remove all fragmented parts of the tissue. For BMDM preparation, washed cells were cultivated in D-MEM containing 10% (v/v) FCS in the presence of 10% (v/v) of conditioned media of L929 CMG cells, and antibiotic antimycotic solution (0.1 mg/ml streptomycin, 100 U/ml penicillin and 0.25 μg/ml amphotericin, Sigma Aldrich) for 7 days at 37°C in a humidified air-CO_2 (5%) atmosphere. The obtained cells were tested for the presence of F4/80 and CD11b/CD18. At least 90% of matured cells displayed macrophage markers, and of these more than 95% were viable. For BMDC preparation, the washed cells were cultivated in D-MEM containing 10% (v/v) FCS in the presence of mouse recombinant GM-CSF (20ng/ml), nonessential amino acids (Biochrom AG) and antibiotic antimycotic solution (0.1 mg/ml streptomycin, 100 U/ml penicillin and 0.25 μg/ml amphotericin, Sigma Aldrich) for 7 days at 37°C in a humidified air-CO_2 (5%) atmosphere. Only loosely attached cells were used for the experiments. The obtained cells were tested for the presence of CD11b, CD11c, I-A/I-E+, Gr-1, F4/80 and the absence of B220. Approximately 80% of the cells displayed DC markers, and of these more than 95% were viable.

RAW264.7 mouse macrophage cells (ATCC Cat. No. TIB 71) were grown in RPMI 1640 medium supplemented with 10% (v/v) FCS and antibiotic antimycotic solution. Prior to assays, the phosphate-buffered RPMI medium was replaced with HEPES-buffered D-MEM (containing 1.9 mM Ca^{2+}) supplemented with 10% (v/v) FCS and the cells were allowed to rest in D-MEM for 2 hours before the toxin addition.

Human neutrophils were purified from full blood obtained at the transfusion unit of the Thomayer Hospital in Prague as described elsewhere (Anderson et al., 2008). Briefly, blood was centrifuged (1.200 RPM, 20 min, 17°C, without brakes) to remove platelet rich plasma (PRP). Pellet was resuspended in 0.72% Dextran T500 in 0.9% NaCl and left to sediment (30 min, RT, in dark). After sedimentation, the upper layer containing leukocytes was centrifuged (1.200 RPM, 6 min, 17°C) and the pellet was resuspended in platelet poor plasma (PPP) obtained by centrifugation of PRP (3.000 RPM, 30 min, 17°C). Granulocytes were obtained by centrifugation of leukocytes through Percoll gradient from the 37.8%/45.9% interface.

All experiments with the CyaA toxin were performed in phosphate-free medium containing 2 mM Ca^{2+} necessary for full CyaA activity.

Production and purification of CyaA variants

Intact CyaA toxin, an enzymatically inactive CyaA-AC^{-} toxoid (Osicka et al., 2000), a toxoid with increased pore-forming capacity CyaA-E509K+E516K-AC^{-} (CyaA-KK-AC^{-}) and a toxoid with decreased pore-forming capacity CyaA-E570Q+K860R-AC^{-} (CyaA-QR-AC^{-}) were produced in *E. coli* XL1-Blue (Stratagene) transformed with the pCACT3- or pT7CACT1-derived constructs, as appropriate (Osicka et al., 2000). Exponential-phase 500-ml cultures were grown at 37°C and induced by isopropyl-1-thio-β-d-galactopyranoside (IPTG; 1 mM) for 4 h before the cells were washed in 50 mM Tris-HCl (pH 8.0), 150 mM NaCl, resuspended in 50 mM Tris-HCl (pH 8.0), 0.2 mM $CaCl_2$, and disrupted by sonication. The insoluble cell debris was resuspended in 8 M urea, 50 mM Tris-HCl (pH 8.0), 50 mM NaCl, and 0.2 mM $CaCl_2$ to extract the CyaA proteins. Upon centrifugation at 25,000 × g for 20 min, clarified urea extracts were loaded onto a DEAE-Sepharose column equilibrated with 8 M urea, 50 mM Tris-HCl (pH 8.0), 120 mM NaCl. After washing, the CyaA was eluted with 8 M urea, 50 mM Tris-HCl (pH 8.0), 2 M NaCl, diluted four times with 50 mM Tris-HCl (pH 8.0), 1mM $CaCl_2$, 1 M NaCl buffer, and further purified on a phenyl-Sepharose column equilibrated with the same buffer. Unbound proteins were washed out with 50 mM Tris-HCl (pH 8.0), and the CyaA was eluted with 8 M urea, 50 mM Tris-HCl (pH 8.0), 2 mM EDTA and stored at -20°C. The protein concentration was determined by the Bradford assay (Bio-Rad, Hercules, CA) using bovine serum albumin as a standard.

Determination of ROS production

ROS production was measured using a luminol-based assay as described previously (Anderson et al., 2008). Briefly, 5 x 10^5 RAW264.7 macrophages or primary human neutrophils in HBSS supplemented with 1% glucose, 2 mM $MgCl_2$ and 2 mM $CaCl_2$ were incubated as indicated in the figure legend at 37°C with 150 μM luminol and 18.75 U of HRP, before the cells were transferred to wells containing the given activator (*e.g.* fMLP, human complement-opsonized zymosan, complement-opsonized *B. pertussis*, or unopsonized *B. pertussis* at an MOI of 10:1, respectively). Luminescence was recorded using a Safire2 microplate reader (Tecan). ROS

production in time was plotted and the area under the curve was calculated. The effect of treatment was calculated as percentage of ROS production compared to the positive control.

Determination of PIP3 amounts in cell membranes

The amount of PIP3 in membranes of neutrophils was determined as described elsewhere (Clark et al., 2011). Briefly, purified neutrophils were pre-incubated with 100 ng/ml CyaA for 5 minutes at 37°C in a chloroform resistant tube. Neutrophils were subsequently activated by the indicated concentration of fMLP for 1 minute. The PIP3 production was then stopped by the addition of a mixture of 64.5% methanol, 32.3% chloroform, and 3.14% of 1M HCl. C16/17 PIP3 was added into the final concentration of 1 ng/µl as an internal standard. To the mixture, an equal volume of chloroform was added and the mixture was incubated for 5 minutes at room temperature leading to separation of aqueous and organic phases. The organic phase was removed and washed with the equal amount of a mixture of 53.3% methanol, 26.6% chloroform, and 20% 0.01M HCl. The washed organic phase was derivatized with 133.3 mM TMS-diazomethan (Sigma) for 10 minutes and derivatization was stopped by the addition of glacial acetic acid to the final concentration of 0.8%. The derivatized organic phase was washed twice with a mixture of 53.3% methanol, 26.6% chloroform, and 20% water, followed by addition of 0.125 volume of the mixture of methanol and water (9:1). The mixture was dried in a speed-vac and resuspended in 80% methanol. The amount of PIP3 was measured at the mass spectrometry core facility of Babraham Institute.

Determination of diacylglycerol in cell membranes

The amount of diacylglycerol was determined as described elsewhere (Bierhanzel *et al.*, in preparation). Briefly, purified neutrophils were pre-incubated with 10 ng/ml of CyaA for 10 minutes at 37°C prior to activation by 3 µM fMLP for 1 minute. The reaction was stopped by the addition of ice cold PBS and the cells were subsequently lysed by the mixture of hexane with isopropanol (3:2). The amount of DAG in the mixture was determined by Ing. Bierhanzel at the Charles University in Prague.

Opsonization of bacteria and zymosan with human complement

Anonymous fresh human blood was purchased at the transfusion unit of the Thomayer Hospital in Prague, and complete human sera were obtained by centrifugation at 1,200 RPM, for 20 minutes at 17°C. Prior to use, the sera were controlled by ELISA for presence of any detectable amounts of antibodies recognizing the PTX, CyaA and FHA antigens of *B. pertussis*. For the opsonization by human complement, 1 x 10^8 heat-killed *B. pertussis* cells (70°C, 30 minutes), or 1 mg of zymosan, were incubated with 50% human serum for 30 minutes at 37°C under gentle shaking and the suspensions were washed twice with serum-free HBSS.

B. pertussis-specific antigens detection by ELISA

Anti-*Bordetella* specific antibody titers were detected in all sera used for opsonization as described by Villarino Romero (Villarino Romero et al., 2013) with minor modifications. PolySorp 96-well ELISA plates (Nunc) were coated with purified FHA, CyaA-AC^-, or heat-killed, or 0.1% formaldehyde-killed *Bordetella pertussis* at 10 μg/ml in 100 mM sodium carbonate buffer (pH 9.5) overnight at 4°C. Heat-killed *E. coli* XL-1 bacteria were used as a control for unspecific binding. Plates were blocked for 3 hours at room temperature with 0.1% Tween 20 (TBST) and 2% bovine serum albumin (BSA) in TBS (TBST-BSA). Diluted human serum samples (1:2, 1:10, 1:100, and 1:1,000) in TBST-BSA were added and the plate was incubated overnight at 4°C. Positive humane sera (Villarino Romero et al., 2013) were used as a positive control. Upon three washes, the reactions were revealed using horseradish peroxidase conjugates of swine anti-human IgG (1:5,000; SEVAC) and o-phenylenediamine as a substrate. Serum levels of IgG antibodies directed against pertussis toxin (PTX) were determined by using the *B. pertussis* IgG-PTX ELISA kit validated for clinical diagnosing of pertussis (Statens Serum Institute Diagnostica) according to the manufacturer's instructions.

Determination of NO production

The production of NO was measured either as nitrite accumulation in the medium using the Griess reaction (Marletta et al., 1988), or as the accumulation of both nitrite and nitrate using fluorescent 4-Amino-5-Methylamino-2',7'-Difluorofluorescein Diacetate (DAF-FM; Life Technologies) (Cortese-Krott et al., 2012). RAW264.7 cells were seeded into 96-well plates (10^5 per well) and incubated with the indicated

inhibitors for 1 h prior to toxin addition. After 24 h of continued incubation, 100 µl aliquots of culture supernatants were mixed with 100 µl of Griess reagent (2% sulfanilamide, 0.2% N-(1-napthyl)-ethylenediamine dihydrochloride, 2.5% orthophosphoric acid) and OD_{540} was measured using Safire2 microplate reader (Tecan). For measurement with DAF-FM, the fluorescent probe (10 µM) was added to cell suspensions 22 h after stimulation. 2 hours later, cells were washed 5-times with ice-cold PBS and fluorescence (excitation 485 nm, emission 520 nm) was measured using Safire2 microplate reader (Tecan).

FACS analysis of neutrophils apoptosis

Apoptosis of neutrophils was determined using double staining with Annexin V and Hoechst 33258. Cells were pre-incubated with 100 ng/ml of either CyaA or CyaA-AC^- for 5 minutes prior to stimulation with 1 mg/ml of serum-opsonized zymosan for 1 hour at 37°C under continuous gentle shaking. Cells were next washed 3-times with ice-cold HBSS to remove any excess of the unbound toxin. Subsequently, the cells were stained by 10 µl Annexin V-FITC in Annexin buffer for 15 minutes in the dark at room temperature. 5 minutes before FACS analysis, 1 µg/ml of Hoechst 33258 was added to cells on ice. 20,000 cells per sample were analyzed by flow cytometry (LSR II instrument, BD Biosciences). The data was analyzed by FlowJo (version 7.6.1).

cAMP ELISA

The accumulation of cAMP in RAW264.7 cells and in primary human neutrophils was measured using a competition ELISA as described earlier (Kamanova et al., 2008). Cells were incubated for the indicated times with CyaA at indicated concentration in D-MEM in the presence or absence of 100 ng/ml of LPS from *E. coli* 0111:B4, or were infected with live *B. pertussis* bacteria at the MOI 10:1, as described in the infection assay, respectively. After the time indicated in the figure legend, the reaction was stopped by the addition of 0.2% Tween 20 in 50 mM HCl. The samples were boiled for 15 minutes at 100°C, neutralized with 150 mM unbuffered imidazole and cAMP concentration was determined by ELISA. MaxiSorp 96-well ELISA plates (Nunc) were coated with cAMP-BSA conjugate (1:6,000 dilution) in 100 mM sodium carbonate buffer (pH 9.5) overnight at 4°C. Plates were blocked for 3 hours at room temperature with 0.1% Tween 20 (TBST) and 2%

bovine serum albumin (BSA) in TBS (TBST-BSA). Cell lysates and rabbit anti-cAMP polyclonal antibody (1:3,000 dilution, kind gift of Agnes Ullmann, Institute Pasteur, Paris) were incubated in the coated and blocked plate over night at 4°C. The unbound primary antibody was washed out by three washing steps, and the secondary goat anti-rabbit HRP-conjugated antibody (1:1,000 dilution, GE Healthcare) was added. After three washes, the reactions were revealed using o-phenylenediamine as a substrate.

Determination of arginase activity

Arginase activity was measured as previously described (Corraliza et al., 1994). RAW264.7 cells were seeded into 96-well plates (10^5 per well) and incubated with indicated concentrations of CyaA for 24 hours and lyzed in 50 µl of buffer that contained 50 mM Tris HCl (pH 7.5), 0.1% Triton X-100, 50 mM NaF, 10 mM $Na_4P_2O_7$, 1 mM Na_3VO_4, 50 nM Calyculin A and the Complete mini EDTA-free protease cocktail inhibitor (Roche). After 30 minutes at RT, 10 mM $MnCl_2$ was added and the samples were heated for 10 minutes at 55°C. An equal volume of 0.5 M L-arginine was added and the mixture was incubated for 60 minutes at 37°C. The reaction was stopped by the addition of 8 volumes of a mixture of H_2SO_4 and H_3PO_4 in water (1:3:7) with half a volume of 9% α-isonitrosopropiophenone (ISPF) dissolved in ethanol. Samples were boiled for 45 minutes at 100°C, chilled for 10 minutes in the dark and absorbance was read at 540 nm.

Immunodetection of proteins (Western blotting)

RAW264.7 cells were seeded into 12-well plates (10^6 per well) and cultured in RPMI medium overnight. RPMI medium was then replaced with D-MEM and inhibitors were added 1 hour before the addition of CyaA, and incubated for the indicated times. Cells were washed two-times with ice-cold PBS (137 mM NaCl, 2.7 mM KCl, 10 mM Na_2HPO_4, 2 mM KH_2PO_4, pH = 7.4) and lysed with 1% Nonidet P-40 in 20 mM Tris-HCl (pH 8.0) buffer containing 100 mM NaCl, 10 mM EDTA, 10 mM $Na_4P_2O_7$, 1 mM Na_3VO_4, 50 mM NaF, 10 nM CalyculinA, and Complete Mini protease inhibitors (Roche). Upon separation by SDS-PAGE and transfer onto nitrocellulose membranes, proteins were probed by the indicated mAbs and revealed by corresponding peroxidase-conjugated secondary antibody (1/5,000, GE Healthcare) using the West Femto Maximum Sensitivity Substrate (Pierce).

Chemiluminescence signals were quantified using ImagQuant LAS 4000 imaging system instrument (Fuji) and images were analyzed using AIDA two-dimensional densitometry software (version 3.28, Raytest Isotopenmessgeraete GmbH).

Protein immunoprecipitation

The immunoprecipitation was performed using the Pierce Co-Immunoprecipitation (CO-IP) Kit. Cells, treated as indicated in the figure legend, were lysed using the IP Lysis/Wash Buffer. Lysates were pre-cleared with 40 µl of control resin slurry for 1 hour at 4°C and the protein of interest was subsequently allowed to bind to a specific antibody coupled to resin beads with gentle rocking for 2 hours at 4°C. The beads were washed twice with ice-cold lysis buffer. Proteins were eluted using Elution Buffer and analyzed by western blotting or by SHP-1 activity assay.

SHP-1 activity assay

$5x10^6$ RAW264.7 cells were incubated in D-MEM with 100 ng/ml LPS and/or 10 ng/ml CyaA and washed twice with ice-cold PBS. Cells were lyzed and SHP-1 was immunoprecipitated from post-nuclear fractions using the Pierce Co-Immunoprecipitation (Co-IP) Kit. The columns with bound SHP-1 were washed 6-times with reaction buffer (25 mM imidazole pH 7.2, 45 mM NaCl, 1 mM EDTA in phosphate-free water). 250 µM tyrosine phosphopeptide (RRLIEDAEpYAARG, Upstate Biotechnologies) was then loaded on the columns. After 30 min at 37°C the free phosphate was determined in column eluates using Malachite Green Phosphate assay (ScienCell). SHP-1 was next eluted from the columns and detected by immunoblotting. Specific SHP-1 activity was calculated as the amount of free phosphate normalized to the total eluted SHP-1 protein amount.

RNA Isolation and Quantitative Real Time PCR

$2x10^6$ RAW264.7 cells per well were incubated in D-MEM with 100 ng/ml of *Escherichia coli* 0111:B4 lipopolysaccharide and/or CyaA toxin at the indicated concentration for 24 hours. Cells were washed twice with ice-cold PBS and lysed with TRIzol Reagent (Life Technologies). Total RNA was extracted using the RNeasy Mini Kit (Qiagen), including a treatment with DNase I (Ambion), and 1 µg of total RNA was reverse-transcribed into cDNA following the manufacturer's instructions in a 25-µL reaction using M MLV Reverse Transcriptase (Promega) and

0.5 µg of random hexamers and oligo dT mixture. Quantitative PCR was performed on Bio-Rad CFX96 instrument using SYBR® Green JumpStart™ Taq ReadyMix™ (Sigma) and gene-specific primers (Supplementary Table 1). 200 nM of each primer together with 40 ng of reverse transcribed RNA were used in a 20-µl qPCR reaction volume, with an initial step at 95°C for 2 min, followed by 40 cycles of 95°C for 15 s, 60°C for 30 s, 72°C for 30 s, followed by recording the melting curve. The *actin* gene was used as the reference gene, and relative gene expression was quantified using amplification efficiency values (Kubista et al., 2006).

siRNA silencing

siRNA transfections were performed according to manufacturer's recommendation (Dharmacon) and the protocol was optimized for RAW264.7 cells using FITC-labeled siGlo RNAi control (Dharmacon). $2x10^4$ cells per well were seeded into 96-well plates and grown overnight in RPMI medium without antibiotics. The cells were next transfected with 50 nM siRNA using 0.05% DharmaFECT 4 reagent (Dharmacon) and the transfection procedure was repeated 48 hours later to increase silencing efficacy. After an additional 48 hours, the cells were repeatedly washed with prewarmed D-MEM medium and tested for NO production and/or target-protein expression. Unspecific effects of transfection were systematically controlled for by including untreated cells, cells treated with DharmaFECT 4 reagent only, and cells transfected with verified non-targeting siRNA in all experiments, respectively.

In Vitro Killing Assay

Bordetella pertussis suspensions were grown in liquid Stainer-Scholte medium (Stainer and Scholte, 1970) to OD_{600} = 1. DAE-NONOate or hydrogen peroxide was added and after 2 hours of incubation at 37°C, serial dilutions of the cultures were plated on BGA plates for the determination of viable CFU after 5 days of growth.

Infection of RAW264.7 cell by B. pertussis

Cell infection assays were performed as described by Lamberti *et al.* (Lamberti et al., 2010), with minor modifications. RAW264.7 cells (10^5 per well) were seeded into 24-well plates and cultured overnight in complete RPMI medium with 10% heat-inactivated FCS and without antibiotics. Prior to infection, RPMI medium was replaced by D-MEM (containing 1.9 mM Ca^{2+} and 10% (v/v) HIFCS) and

exponentially growing *B. pertussis* cells expressing GFP from the pBBRcyaGFP plasmid were added at MOI 10:1. The bacteria were gently spun onto the cells at 640 x g for 5 minutes to facilitate bacterial attachment to macrophages. Co-incubation was continued for 1 hour at 37°C and unbound bacteria were removed by rinsing cells 3 times with prewarmed D-MEM. Cells were fixed for microscopic analysis or replaced for one hour into a medium containing 100 μg/ml of polymyxin B, to kill the attached extracellular bacteria. Polymyxin B concentration was next decreased to 20 μg/ml in the culture medium in order to avoid killing of the internalized bacteria during continued cell culture for the indicated times (24, 48 and 72 hours, respectively). Finally, RAW264.7 cells were washed 3-times with a prewarmed medium without antibiotics and lysed with sterile dH_2O. Lysates of macrophage cells were serially diluted in Stainer-Scholte medium and plated on BGA. *B. pertussis* CFUs were counted after 5 days of growth.

Infection of neutrophils by B. pertussis

Primary human neutrophils (2 x 10^6 cells/ml) were mixed with exponentially growing *B. pertussis* cells at MOI 100:1 and the cultures were incubated at 37°C under continuous gentle shaking. At time points indicated in the figure legend, the aliquots were serially diluted in Stainer-Scholte medium and plated on BGA. *B. pertussis* CFUs were counted after 5 days of growth.

Fluorescence microscopy of cell-associated bacteria

After 1 hour of incubation with *B. pertussis*/pBBRcyaGFP bacteria, the RAW264.7 cells were washed three times with prewarmed D-MEM medium and fixed with 4% paraformaldehyde in PBS for 20 minutes. Non-phagocytosed bacteria attached to the surface of macrophage cells were decorated with rabbit polyclonal antiserum against *B. pertussis* (kind gift of Dr. B. Vecerek, Institute of Microbiology, ASCR, v.v.i., Prague) and stained with goat anti-rabbit IgG conjugated with Cy5. F-actin was stained with TRITC-conjugated phalloidin (0.5 μg/ml, Sigma-Aldrich) and DNA with DAPI (10 μg/ml, Sigma-Aldrich) in PBS supplemented with 3% BSA (v/v) for 30 min. Samples were mounted on glass coverslips in Mowiol and images were captured using CellR Imaging Station (Olympus) based on Olympus IX81 fluorescence microscope using 100×/1.35 oil objective. Images were captured in 0.1 μM Z-stack layers across complete cell and 3D image was reconstructed using 3D

deconvolution. Internalized bacteria, emitting only green fluorescence (GFP^+) and cell surface-associated yellow bacteria emitting both red (Cy5) and green (GFP) fluorescence, were counted for at least 50 cells per sample and experiment.

Ethics Statement

All animal experiments were approved by the Animal Welfare Committee of the Institute of Microbiology of the ASCR, Prague, Czech Republic. The handling of animals was performed according to the Guidelines for the Care and Use of Laboratory Animals, the Act of the Czech National Assembly, Collection of Laws no. 149/2004, inclusive of the amendments, on the Protection of Animals against Cruelty, and Public Notice of the Ministry of Agriculture of the Czech Republic, Collection of Laws no. 207/2004, on care and use of experimental animals.

Human peripheral blood neutrophils were purified from healthy human volunteers. All human participants gave written informed consent, and all studies complied with the Declaration of Helsinki.

Statistical Analysis

The significance of differences in values was assessed by Students' t-test.

8. Results

Upon colonization of the respiratory tract of a new host, *B. pertussis* has to deal with oxidative stress caused by the production of reactive oxygen and nitrogen species by infiltrating neutrophils and macrophages. We, therefore, analyzed the susceptibility of *B. pertussis* to oxidative stress-mediated killing. *B. pertussis* cells were exposed to H_2O_2 (ROS-mediated killing; (Mandell and Hook, 1969)), or DEA-NONOate (NO donor, RNS-mediated killing; (Dyet and Moir, 2006; Potter et al., 2009)) for 2 h at 37°C. As shown in Fig. 16, a significant drop of bacterial viability was observed in cultures treated with DEA-NONOate or H_2O_2 in comparison with the control culture. While these results showed that *B. pertussis* is highly sensitive to oxidative killing, it has been shown previously that the bacterium has mechanisms allowing it to suppress the oxidative burst of neutrophils and macrophages (Confer and Eaton, 1982)

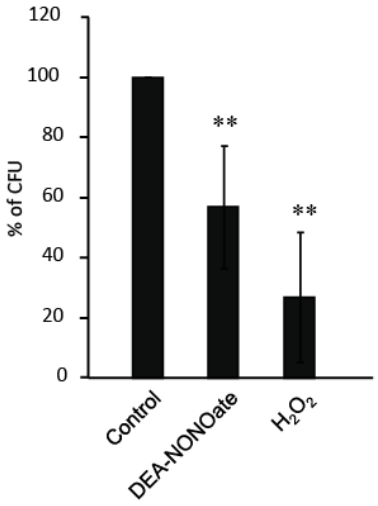

Fig. 16: *Bordetella pertussis* is sensitive to oxidative stress-mediated killing. Exponentially growing cultures of *B. pertussis* (OD_{600} = 1) were divided into aliquots to which corresponding volumes of solvent control (ethanol), or of the 400 µM DAE-NONOate solution, or of 100 µM H_2O_2 were added for 2 h. Following plating on BGA, the numbers of viable CFU were counted after 5 days of growth. The values are means ±SD from at least 5 independent experiments performed in duplicates (n=10). **, $p<0.001$ *vs*. control.

8.1. CyaA-provoked inhibition of ROS production by neutrophils

Bordetella pertussis employs enzymatic activity of CyaA to escape killing by neutrophils

In order to identify the mechanisms used by *B. pertussis* to impair killing by ROS-producing neutrophils, we evaluated the survival of a hemolytic *B. pertussis* strain producing a catalytically inactive CyaA-AC$^-$ toxoid unable to convert cellular ATP to cAMP (*B.p. cyaA-AC*$^-$) in the presence of primary human neutrophils, and compared it to the survival of the parental *B. pertussis* Tohama I strain (*B.p. cyaA-wt*) producing intact CyaA. As a negative control, a mutant not producing CyaA due to the deletion of the entire *cyaA* open reading frame (*B.p. ΔcyaA*) was used. As shown in Fig. 17, growth of *B.p. cyaA-AC*$^-$ as well as *B.p. ΔcyaA* was completely blocked in comparison with the parental *B.p. cyaA-wt* strain when mixed with neutrophils at MOI 100:1. While *B.p. cyaA-wt* culture continued to grow in a manner close to the theoretical growth curve in the presence of neutrophils, the *B.p. cyaA-AC*$^-$ and *B.p. ΔcyaA* cells did not multiply during the entire experiment. This result suggests that the CyaA enzymatic activity impairs the bactericidal capacity of neutrophils and their ability to control the growth of *B. pertussis*.

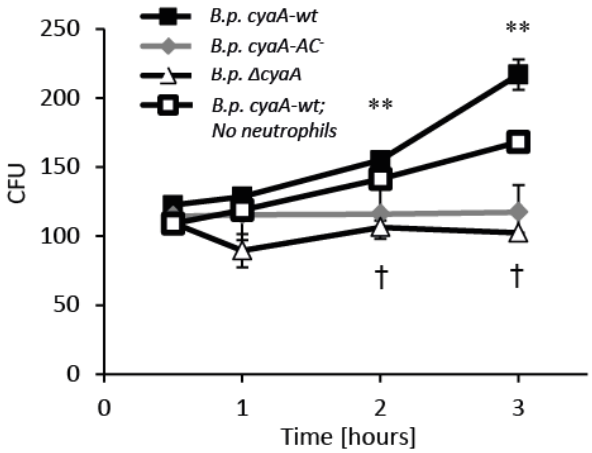

Fig. 17: Growth of *B. pertussis* in the presence of neutrophils. Primary human neutrophils were mixed with either *B.p. cyaA-wt, B.p. cyaA-AC*$^-$, or *B.p. ΔcyaA* at MOI 100:1. At the indicated time, aliquots of cultures were diluted and plated on BGA. CFU of recovered bacteria were counted 5 days later. Values represent one representative result out of 5 independent experiments performed in triplicates. **, p<0.001 *versus B.p. cyaA-wt* starting inoculum; †, p<0.001 *versus B.p. cyaA-wt* at the indicated time point

Bordetella pertussis inhibits ROS production by neutrophils

As shown in Fig. 16, *B. pertussis* is sensitive to ROS-mediated killing. However, it is also known that CyaA inhibits ROS production by neutrophils (Confer and Eaton, 1982; Pearson et al., 1987). We, therefore, examined if the inhibition of ROS production by CyaA is the reason for the prolonged survival of *B.p. cyaA-wt*. Primary human neutrophils were infected by *B.p. cyaA-wt*, *B.p. cyaA-AC*$^-$, and *B.p. ΔcyaA* at MOI 100:1 and the production of ROS was examined. As shown in the Fig. 18, non-opsonized *B.p. cyaA-wt* was able to efficiently inhibit ROS production by human neutrophils. In contrast, neither *B.p. ΔcyaA* nor *B.p. cyaA-AC*$^-$ were able to diminish ROS production by neutrophils. This suggests that the prolonged survival of non-opsonized *B.p. cyaA-wt* in the presence of neutrophils was due to the inhibition of ROS production by the enzymatic activity of CyaA.

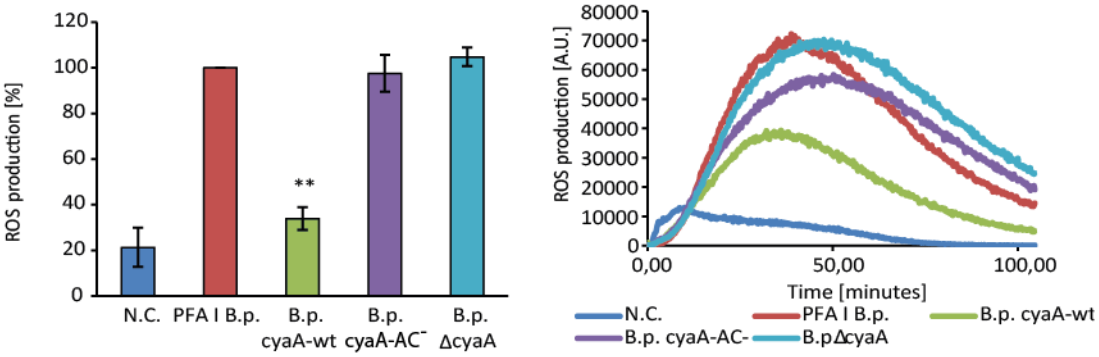

Fig. 18: *B. pertussis* inhibits ROS production in neutrophils. Primary human neutrophils were activated either with unopsonized paraformaldehyde-inactivated (PFA I *B.p.*), or with live *B.p. cyaA-wt* or mutant bacteria lacking the CyaA enzymatic activity *B.p. cyaA-AC*$^-$, or with mutant bacteria defective in production of whole CyaA toxin *B.p. ΔcyaA*. at MOI 100:1. The values in left panel represent relative ROS production to PFA I *B.p.* control from three independent experiments (n=3). In the right panel, the time dependence of ROS production is shown and the values represent the results of one representative out of three independent experiments. **, $p<0.001$ *versus* PFA I *B.p.*

CyaA inhibits ROS production stimulated by opsonized zymosan, fMLP, adhesion, or phagocytosis in a time and toxin dose-dependent manner

In order to characterize the CyaA-hijacked mechanism by which *B. pertussis* inhibits ROS production, we first induced ROS production in primary human neutrophils using serum opsonized-zymosan, in order to mimic ROS production stimulated by binding of complement-opsonized bacteria and phagocytosis. As shown in Fig. 19 and in agreement with previously published observations (Confer and Eaton, 1982), ROS production triggered by complement-opsonized zymosan was inhibited upon pre-incubation of neutrophils with CyaA (10 and 100 ng/ml).

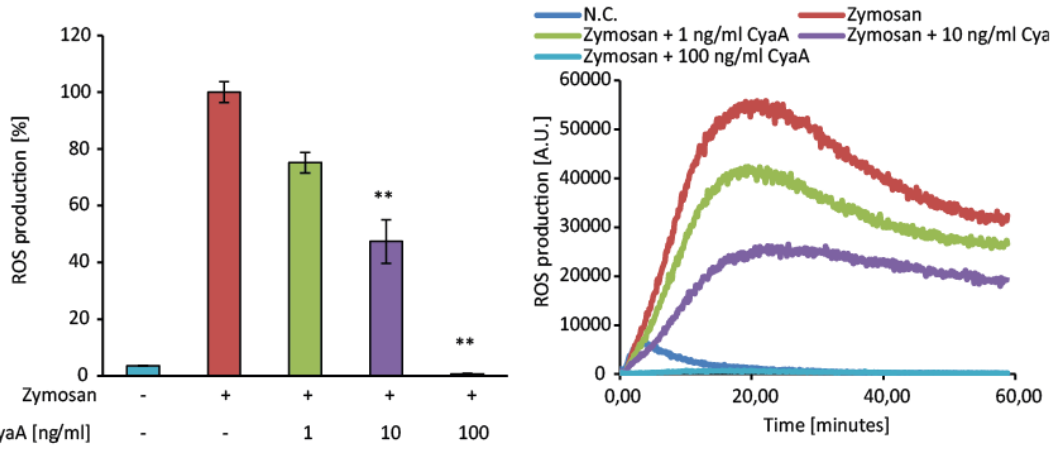

Fig. 19: CyaA inhibits ROS production induced by opsonized-zymosan in neutrophils. Primary human neutrophils were pre-incubated with CyaA at the indicated concentration for 5 minutes prior to stimulation with 1 mg/ml of serum-opsonized zymosan. ROS production was measured over the indicated period of time. The values in the left panel represent relative ROS production from three independent experiments (n=3). In the right panel, the time dependence of ROS production is shown and the values represent the results of one representative experiment out of three performed. **, $p<0.001$ versus opsonized-zymosan control.

To verify that the observed inhibition of ROS production was not due to the induction of neutrophil apoptosis by CyaA, we examined the presence of apoptosis markers on neutrophils. Hoechst 33258 exclusion and cell surface-exposed phosphatidyl serine staining by Annexin V was examined. This allowed us to distinguish between living cells (Hoechst 33258 neg., Annexin V neg.), cells in the state of early apoptosis (Hoechst 33258 neg., Annexin V pos.), cells in late apoptosis state (Hoechst 33258 pos., Annexin V pos.), and cells undergoing necrosis (Hoechst 33258 pos., Annexin V neg.). As shown in Fig. 20, addition of CyaA-AC$^-$ had no impact on the spontaneous apoptosis of neutrophils, as compared to non-stimulated cells, or to cells stimulated with 1 mg/ml of opsonized zymosan. In contrast, neutrophils treated with 100 ng/ml of CyaA remained viable and underwent spontaneous apoptosis to a much lower extent. No necrosis was detected in either case. The action of active CyaA toxin thus inhibited the spontaneous apoptosis of neutrophils, as also reported by Eby *et al.* (Eby et al., 2014).

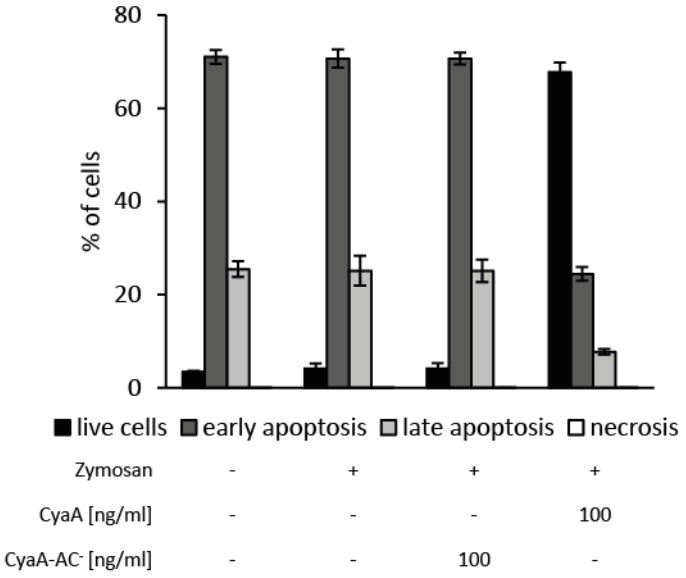

Fig. 20: CyaA inhibits spontaneous apoptosis in neutrophils. Primary human neutrophils were pre-incubated with 100 ng/ml of either CyaA or CyaA-AC$^-$ for 5 minutes prior to stimulation with 1 mg/ml of serum-opsonized zymosan. Apoptosis was detected by FACS using Hoechst 33258 and Annexin V staining. The values represent data for one representative experiment out of three performed in triplicates.

As further shown in Fig. 21, CyaA also inhibited ROS production elicited by formyl-methionyl-leucinyl-phenylalanine (fMLP), by phagocytosis of complement-opsonized *E. coli*, or by the adhesion to surface coated by IgG-opsonized BSA, or poly-RGD peptide. It is, however, important to note that the sensitivity of neutrophils to CyaA differed in function of the source of neutrophils (donor), which lead to high inter-experimental variability. As could be expected, neutrophils obtained from one donor may respond to lower CyaA concentration than cells from another donor (*cf.* Fig. 21*A*). The effects of CyaA treatment of neutrophils depended on the time of pre-incubation with the toxin and on the concentration of the toxin.

Based on these experiments, fMLP stimulation of neutrophils was used for further dissection of the signaling pathway leading to the inhibition of ROS production by CyaA.

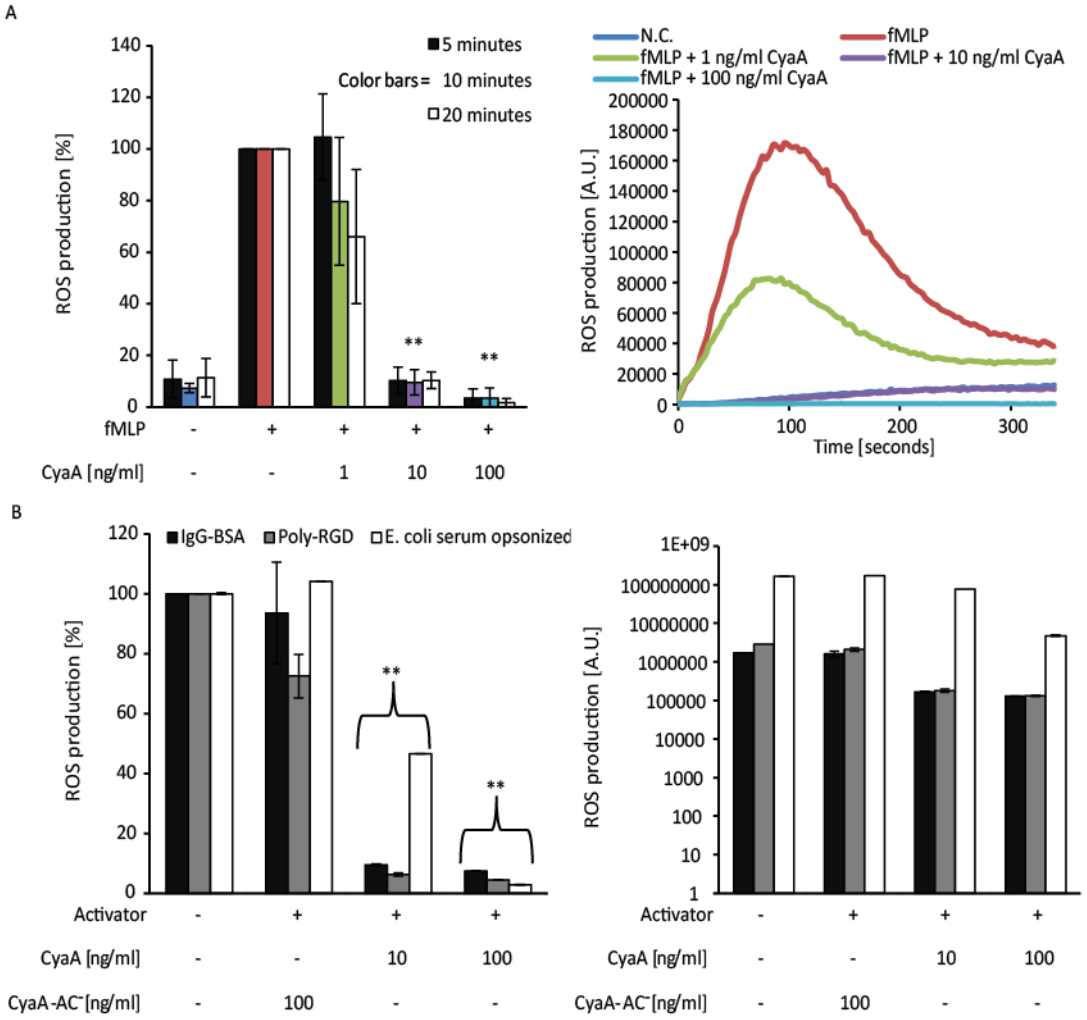

Fig. 21: CyaA inhibits ROS production induced by fMLP, phagocytosis, and attachment. *A.* Primary human neutrophils were pre-incubated with CyaA at the indicated concentration for 5, 10, or 20 minutes prior to stimulation with 300 nM fMLP and ROS production was measured for 330 seconds. Mean values for relative ROS production (left panel; mean values out of three independent experiments) and time-course of ROS production by neutrophils pre-incubated with CyaA for 10 minutes (right panel; one representative result out of three independent experiments) are shown. *B.* Primary human neutrophils were pre-incubated with CyaA variants at the indicated concentration for 5 minutes prior to stimulation with the indicated agent. ROS production was measured for 1 hour. Mean values for relative (left panel) and absolute (right panel) ROS production out of three independent experiments (n=3) are shown. **, $p<0.001$ versus activator-only treated control

Enzymatic activity of CyaA is sufficient for the inhibition of ROS production

The results presented in Fig. 18 suggested that the enzymatic activity (cAMP production) of the CyaA toxin played a crucial role in inhibition of ROS production. To corroborate this, we evaluated the contribution of the other CyaA activities to inhibition of ROS production. Therefore, we compared wild-type CyaA causing conversion of ATP into cAMP, Ca^{2+} influx, and forming pores in target membrane, to the effects of enzymatically inactive CyaA-AC^- toxoid that is unable to convert ATP into cAMP, while it still causes Ca^{2+} influx and forms pores in cell membranes.

Finally, we used also the CyaA-E509K+E516K-AC$^-$ toxoid (CyaA-KK-AC$^-$) that is devoid of enzymatic activity and causes much lower Ca^{2+} entry, while it exhibits a strongly increased pore-forming activity. The activities of the used CyaA variants are summarized in Table 2.

Table 2.: Comparison of activities of used CyaA variants.

Toxoid	cAMP production	Ca^{2+} influx	Pore formation
CyaA	+	+	+
CyaA-AC$^-$	-	+	+
CyaA-KK-AC$^-$	-	+/-	+++

The activity of recombinant wild-type CyaA, of the detoxified CyaA-AC$^-$, lacking the ATP to cAMP-converting activity, and of the hyperhemolytic and detoxified CyaA-KK-AC$^-$ are given. +, activity at wild-type toxin level; +/-, activity decreased in comparison with wild-type toxin; -, activity is missing in comparison with wild-type toxin; +++, activity is strongly increased in comparison with the wild-type toxin

As shown in Fig. 22, CyaA almost completely blocked fMLP-stimulated ROS production at the concentration of 10 ng/ml. On the other hand, neither CyaA-AC$^-$, nor CyaA-KK-AC$^-$ toxoids inhibited oxidative burst in neutrophils even at 100 ng/ml concentration. In addition, membrane-permeable cAMP analogue, db-cAMP, ablated ROS production in a manner similar to CyaA. The combination of db-cAMP with either CyaA-AC$^-$ or CyaA-KK-AC$^-$ did not exhibit any additive effect, as compared to the activity of db-cAMP alone. Taken together, these results show that the inhibition of oxidative burst capacity of neutrophils was specifically due to the elevation of cytosolic cAMP concentration by the AC enzyme activity of the CyaA toxin.

We next measured cAMP accumulation in CyaA-treated neutrophils in order to correlate the CyaA enzymatic activity with its inhibitory effect on ROS production. As shown in Fig. 23, CyaA at a concentration of 1 ng/ml, at which it did not significantly inhibit ROS production, did not cause any significant accumulation of cAMP in neutrophils even after 20 minutes of co-incubation. In contrast, 10 ng/ml of CyaA increased intracellular concentration of cAMP already in 5 minutes, and the production was rising even at 20 minutes after the toxin addition. Similarly, 100 ng/ml of CyaA caused strong cAMP production already at 5 minutes, reaching a plateau already at 10 minutes of co-incubation with neutrophils.

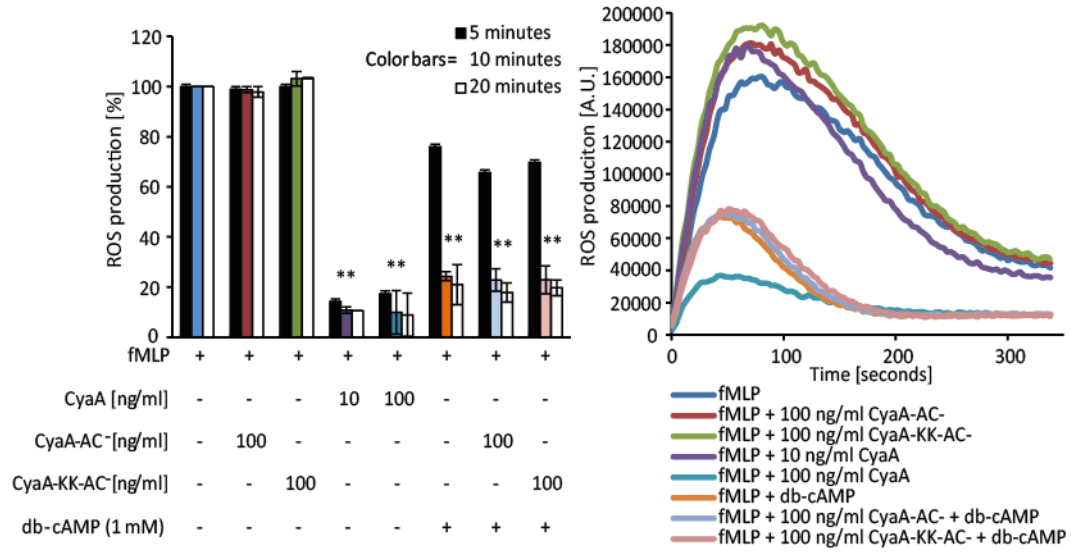

Fig. 22: CyaA-provoked cAMP accumulation is sufficient for inhibition of ROS production by neutrophils. Primary human neutrophils were pre-incubated with CyaA variants at the indicated concentration in the presence or absence of 1mM db-cAMP for the indicated time prior to stimulation with 300 nM fMLP. ROS production was measured over time as shown in right panel (330 seconds). Mean values for relative ROS production (left panel) and time-course (right panel) of ROS production by neutrophils pre-incubated with CyaA for 10 minutes are shown. The time-course of ROS production is from one representative experiment out of three performed. **, $p<0.001$ versus fMLP treated control

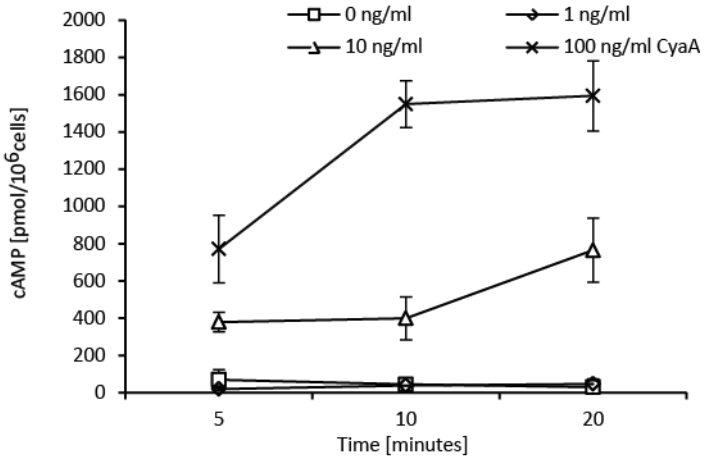

Fig. 23: CyaA-mediated accumulation of cAMP in neutrophils. Primary human neutrophils (2 x 10^6 cells/ml) were incubated with CyaA for the indicated time. The total amount of cAMP in cell lysates was measured using a competition ELISA assay. Mean values for one representative experiment out of three independent experiments performed in triplicates are given.

Both PKA and Epac activation yield inhibition of ROS production

To define the role of CyaA-provoked PKA and Epac signaling in inhibition of ROS production, neutrophils were pre-incubated with unspecific (db-cAMP), PKA-specific (6-Bnz-cAMP), or Epac-specific (8-CPT-cAMP) membrane-permeable cAMP analogues for 20 minutes prior to stimulation by fMLP. As shown in Fig. 24, all cAMP analogues were able to inhibit ROS production, although the PKA

activator (6-Bnz-cAMP) was less potent than the Epac-specific activator (8-CPT-cAMP) or the unspecific activator (db-cAMP).

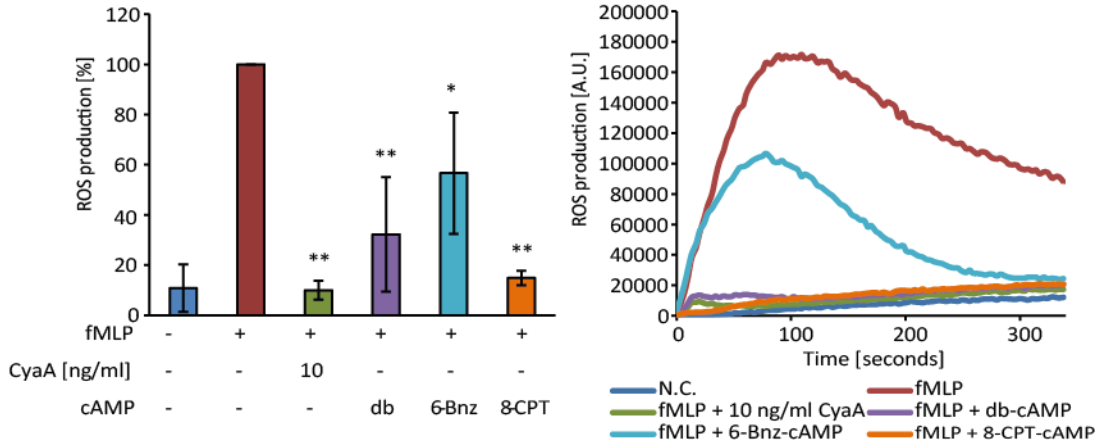

Fig. 24: Both PKA and Epac inhibit ROS production in neutrophils. Primary human neutrophils were pre-incubated with 10 ng/ml of CyaA or with 1 mM cAMP analogues for 20 minutes at 37°C prior to stimulation with 300 nM fMLP. ROS production was measured over time as documented in the right panel (330 seconds). The values in the left panel represent relative ROS production from three independent experiments (n=3). In the right panel, the time dependence of ROS production is shown and the values represent the results of one representative out of three independent experiments. *, p<0,01; **, p<0.001 versus fMLP treated control

To verify the involvement of PKA in the inhibition of ROS production in neutrophils, PKA activity was blocked by the cAMPS or H-89 inhibitors. As shown in Fig. 25, CyaA was still able to block ROS production in neutrophils treated with PKA inhibitors. The presence of either PKA inhibitor diminished but did not completely reverse the inhibitory effects of CyaA action on fMLP-induced ROS production. These results suggest that both PKA and Epac are involved in CyaA-provoked inhibition of ROS production by neutrophils.

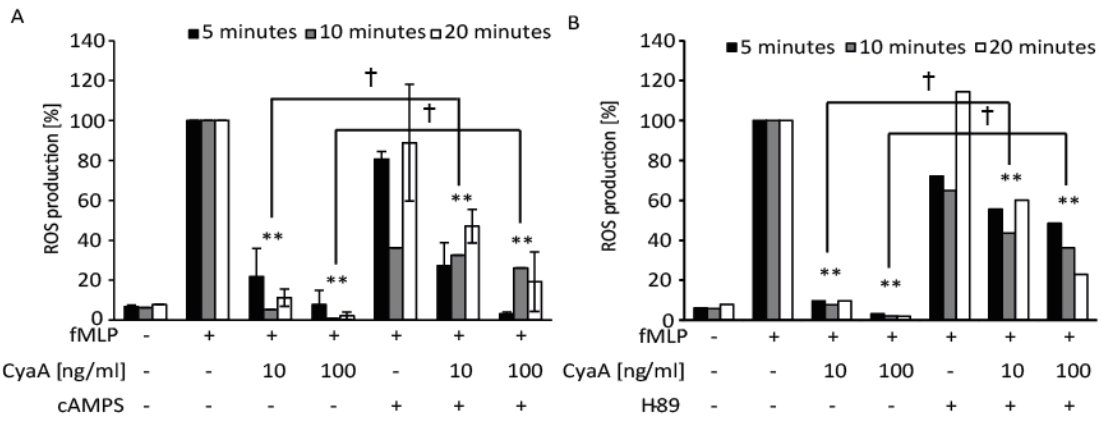

Fig. 25: Inhibition of PKA reverses in part the inhibitory effect of CyaA action on ROS production in neutrophils. Neutrophils were pretreated with PKA inhibitors cAMPS (1 mM; *A.*) or H-89 (10 µM; *B.*) for 20 minutes prior to the addition of CyaA. ROS production was subsequently induced by the addition of 300 nM fMLP and measured over 330 seconds. The results represent mean

values from 3 independent experiments (n=3). **, p<0.001 versus fMLP treated control; †, p<0,01 versus each other

CyaA blocks ROS production in neutrophils by the inhibition of PLC

As illustrated in Fig. 4, ROS production requires the activity of PI3K and of PLC. To examine the effects of CyaA treatment on PI3K activity, we pre-incubated neutrophils for 5 minutes with 100 ng/ml of CyaA prior to fMLP stimulation for 1 minute. As shown in Fig. 26, CyaA was unable to inhibit production of PIP3 in neutrophils stimulated by fMLP.

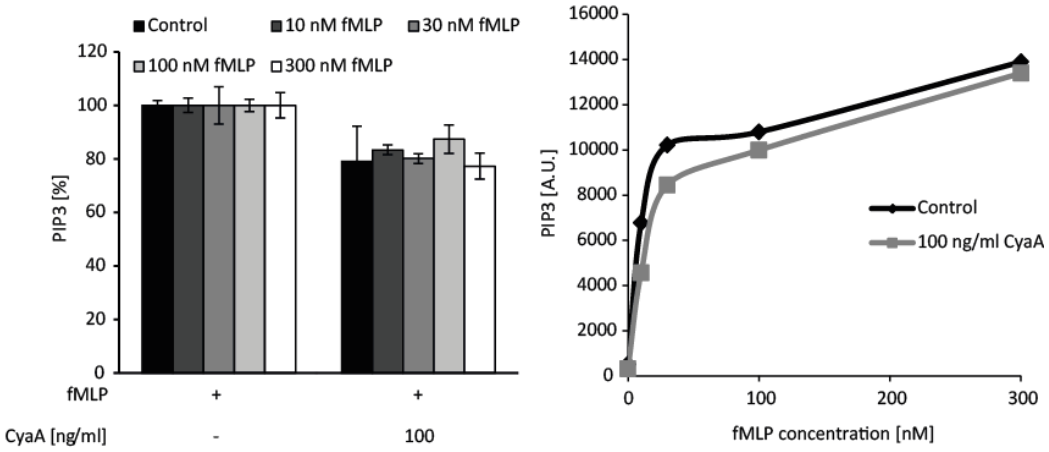

Fig. 26: CyaA does not block PIP3 accumulation in neutrophils. Primary human neutrophils were pre-incubated with 100 ng/ml of CyaA for 5 minutes prior to stimulation with the indicated concentration of fMLP for 1 minute. The total amount of PIP3 in cells was determined by mass spectrometric analysis following the extraction of lipids. The values in left panel represent relative PIP3 production from two independent experiments. In the right panel, the total PIP3 production is shown and the values represent the results of one representative out of two independent experiments.

To assess the effect of CyaA on PLC activity, ROS production was triggered by the PLC activator m-3M3FBS. As shown in Fig. 27*A*, pre-incubation of neutrophils with CyaA blocked m-3M3FBS-induced ROS production. However, in m-3M3FBS activated neutrophils, CyaA exhibited slightly lower inhibitory potency when compared to fMLP stimulated cells. o-3M3FBS was used as a negative control as this compound activates neither PLC nor ROS production (Bae et al., 2003). In contrast, neutrophils activated with 1 µM PMA, a direct PKC activator, were completely resistant to CyaA-provoked inhibition of ROS production (Fig. 27*B*).

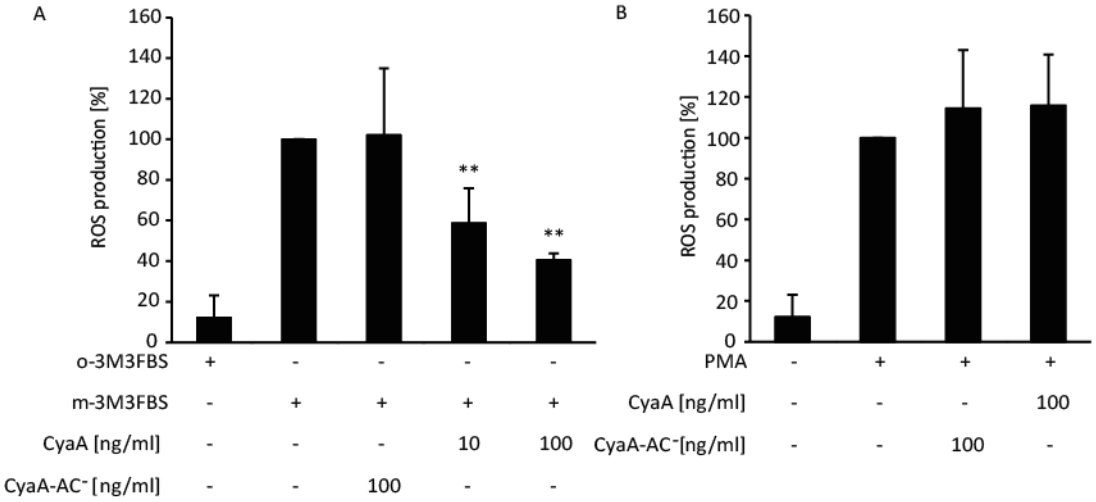

Fig. 27: CyaA differentially regulates PLC and PKC. Primary human neutrophils were pre-incubated with CyaA variants at the indicated concentration prior to stimulation with either 12.5 µM m-3M3FBS (*A*) for direct PLC stimulation or 1 µM PMA (*B*) for direct PKC stimulation. ROS production was measured over 5 minutes or 1 hour, respectively. Mean values for relative ROS production compared to positive control are given (n=3). **, p<0.001 versus positive control

We further examined the impact of CyaA on ROS production stimulated with lower PMA concentrations. Although PMA did not induce significant ROS production at the lowest concentrations used (0.01 and 0.03 µM), signaling started by higher PMA doses (0.3 µM) was already resistant to CyaA action. As shown in Fig. 28, only signaling provoked by moderate PMA concentrations, at ~ 0.1 µM, was sensitive to CyaA action. These results suggest that CyaA inhibited PLC, whereas PI3K and PKC were not strongly influenced by the cAMP signaling that resulted from CyaA action.

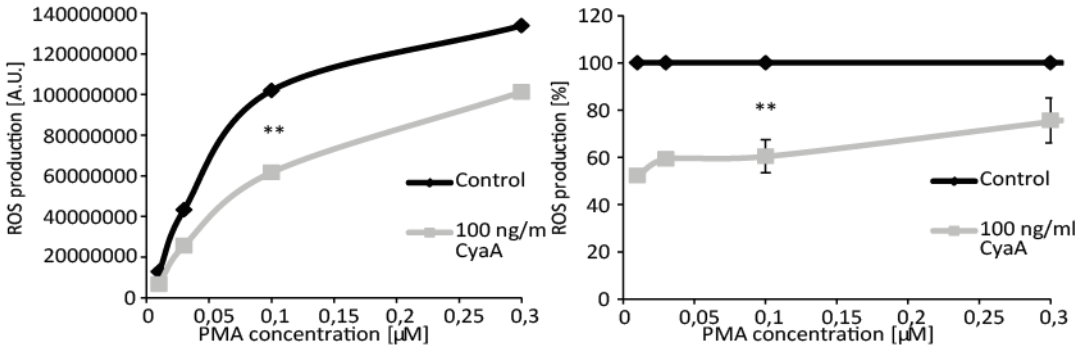

Fig. 28: PMA stimulates ROS production in a dose-dependent manner. Primary human neutrophils were pre-incubated for 20 minutes with 100 ng/ml CyaA prior to stimulation with indicated concentrations of PMA. The ROS production was measured for 1 hour. Mean values represent the total amount of ROS produced (left panel) and the normalized ROS production (right panel) for one out of three independent experiments performed in triplicates (n=9). **, p<0,001 versus control

To test the hypothesis that CyaA inhibits PLC, we measured the total amount of its diacylglycerol (DAG) product in the membranes of CyaA treated neutrophils. The cells were treated with 10 ng/ml of CyaA for 10 minutes before fMLP stimulation for 1 minute. As shown in Fig. 29, CyaA completely blocked the fMLP-stimulated conversion of PIP2 into DAG.

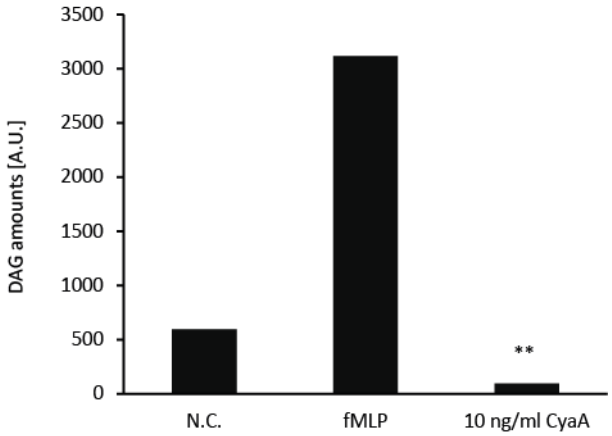

Fig. 29: CyaA inhibits fMLP-stimulated DAG formation. Primary human neutrophils were pre-incubated with 10 ng/ml CyaA for 20 minutes prior to stimulation with 300 nM fMLP for 1 minute. The total amount of DAG in cells was determined by mass spectrometry of extracted lipids. The values represent one representative result out of three independent experiments. **, $p<0,001$ versus fMLP control

CyaA does not inhibit ROS production in primed neutrophils

Neutrophils were previously shown to be important for the clearance of *B. pertussis* in immunized mice (Andreasen and Carbonetti, 2009) that respond to antigenic restimulation by TNFα secretion from macrophages (Macdonald-Fyall et al., 2004). To examine why do neutrophils play a more important role in immunized animals than in the non-immunized ones, we mimicked the effect of immunization by priming of neutrophils *in vitro* with either 2 U/ml TNFα or with 3 nM fMLP. As shown in Fig. 30, the primed neutrophils were completely resistant to CyaA and no inhibition of ROS production was found, in contrasts to unprimed cells (*cf.* Fig. 21*A*).

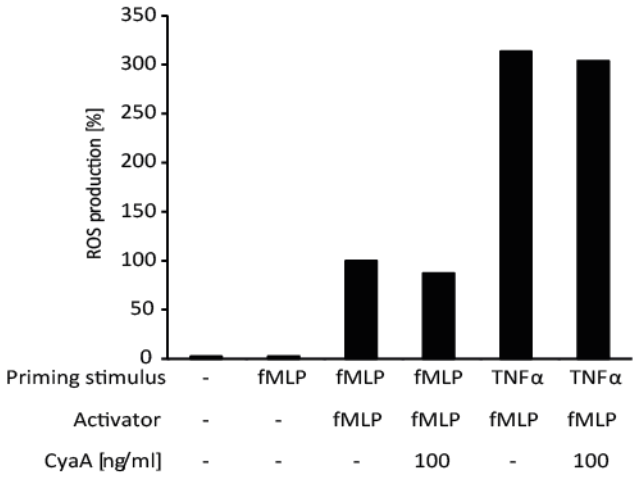

Fig. 30: CyaA does not inhibit ROS production by primed neutrophils. Primary human neutrophils were primed by 3 nM fMLP or 2 U/ml of TNFα for 30 minutes at 37°C prior to addition of indicated concentration of CyaA for 5 minutes. ROS production was subsequently induced by 300 nM fMLP. Mean values represent the total amount of ROS produced and normalized ROS production out of three independent experiments (n=3).

8.2. CyaA-provoked inhibition of RNS production by macrophages

Bordetella pertussis employs enzymatic activity of CyaA to protract its survival inside macrophages

CyaA toxin production was previously found to be required for the persistence of unopsonized *B. pertussis* in macrophages (Friedman et al., 1992). The precise mechanism employed by CyaA to corrupt bactericidal mechanisms of macrophages remained, however, unclear. To set up a working model of *B. pertussis* interaction with macrophages, the survival of *B.p. cyaA-AC*$^-$ (a hemolytic *B. pertussis* strain producing a catalytically inactive CyaA-AC$^-$ toxoid) in murine RAW264.7 macrophage cells was compared at MOI 10:1 to the persistence of the parental *B. pertussis* Tohama I strain (*B.p. cyaA-wt*) producing intact CyaA. As a negative control, *B.p. ΔcyaA* (a mutant not producing CyaA due to the deletion of the entire *cyaA* open reading frame) was used. As shown in Fig. 31, the association of *cyaA-AC*$^-$ or of *ΔcyaA* bacteria with the RAW264.7 macrophages after 1 h of co-incubation was not impaired by the inability to produce enzymatically active CyaA toxin. When compared to the *cyaA-wt* strain, internalization of bacteria producing the AC$^-$ toxoid (*cyaA-AC*$^-$), or not producing CyaA at all (*ΔcyaA*), was even enhanced (~120%). Although the differences were not statistically significant, this observation would go well with the previously shown capacity of CyaA to provoke cAMP-triggered unproductive actin cytoskeleton rearrangements and macrophage ruffling (Kamanova et al., 2008).

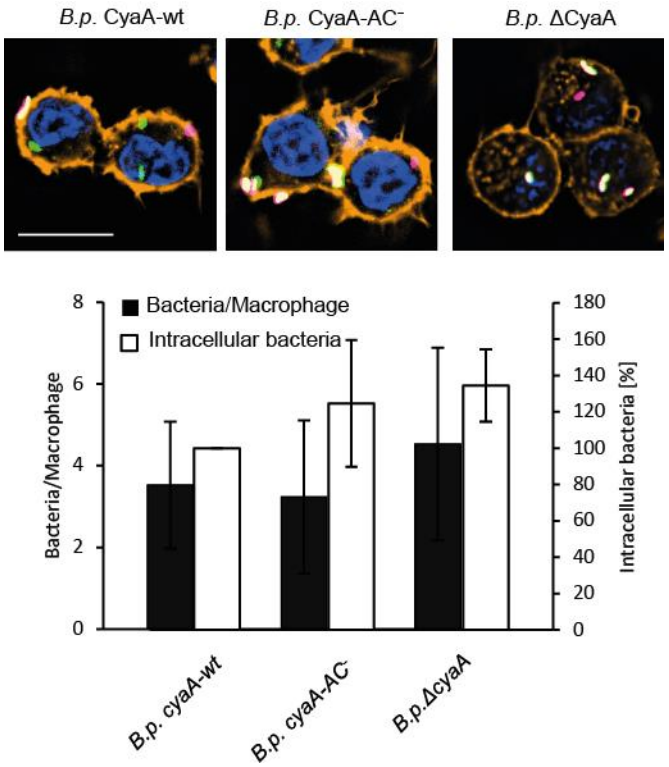

Fig. 31: Interaction of *B. pertussis* with macrophage cells. RAW264.7 cells were infected at MOI 10:1 for 1 h (37°C, 5% CO_2) by centrifuging (640 x g, 5 min) onto macrophages the GFP-expressing wild-type *B. pertussis* Tohama I (*B.p. cyaA*-wt), the bacteria producing enzymatically inactive CyaA-AC$^-$ toxoid (*B.p. cyaA-AC*$^-$), or *B. pertussis* lacking the *cyaA* gene (*B.p. ΔcyaA*), respectively. Upon co-incubation for 1 h at 37°C, the cells were washed and fixed with 4% PFA (20 min). Extracellular bacteria were stained with rabbit anti-*B. pertussis* serum and detected with the Cy5-labeled goat anti-rabbit IgG conjugate. TRITC-phalloidin (1 µg/ml) was used for actin staining and DAPI (10 µg/ml) for visualization of nuclei. Representative images from one out of five independent experiments are shown (scale bar = 5 µm).

In contrast to enhanced initial uptake, the survival of the *cyaA-AC*$^-$ and *ΔcyaA* bacteria within murine macrophages was significantly impaired in 24 h compared to the survival of *B.p. cyaA-wt* as shown in Fig. 32. After 48 h of incubation, about two orders of magnitude lower viable counts of the mutants were recovered from RAW264.7 cells. Hence, the enzymatic AC activity of CyaA was crucial for extended survival of unopsonized *B. pertussis* inside murine macrophages.

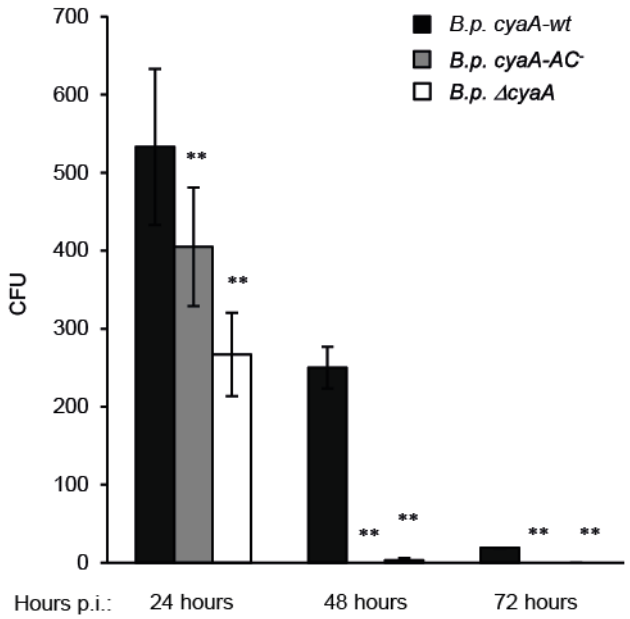

Fig. 32: Killing of *B. pertussis* by macrophages. The RAW264.7 cells were infected at MOI 10:1 as above and after 1 h of co-incubation the cells were washed and replaced for 1 h into D-MEM with 100 µg/ml of polymyxin B to kill extracellular bacteria. The infected cells were incubated for additional 24, 48, or 72 h prior to lysis and determination of CFU of recovered bacteria. Values represent the means ±SD from at least 10 independent experiments (n=10). **, $p<0.001$ *versus B.p.* wild-type control

Bordetella pertussis is not killed by ROS in macrophages

CyaA-catalyzed elevation of cAMP was previously shown to efficiently block bactericidal activities of neutrophils (*cf.* Fig. 16)(Confer and Eaton, 1982; Pearson et al., 1987)(Confer and Eaton, 1982; Pearson et al., 1987). However, as shown in Fig. 33, despite responding by the production of ROS to stimulation by complement-opsonized zymosan, the RAW264.7 cells produced little or no ROS upon incubation with heat-killed *B. pertussis* cells, regardless of whether these were opsonized by complement or not. It therefore appeared unlikely that the unopsonized bacteria, eliciting even lower ROS production than opsonized bacteria, were killed in RAW264.7 cells by oxidative burst.

To verify that opsonization of *B. pertussis* used here was due to complement and was not due to contaminating antibodies, we measured titers of anti-*Bordetella* antibodies in the sera used for opsonization. As shown in Fig. 34, no antibodies against *B. pertussis* components were detected in sera used for opsonization experiments. As a positive control, sere obtained from convalescent pertussis patients were used.

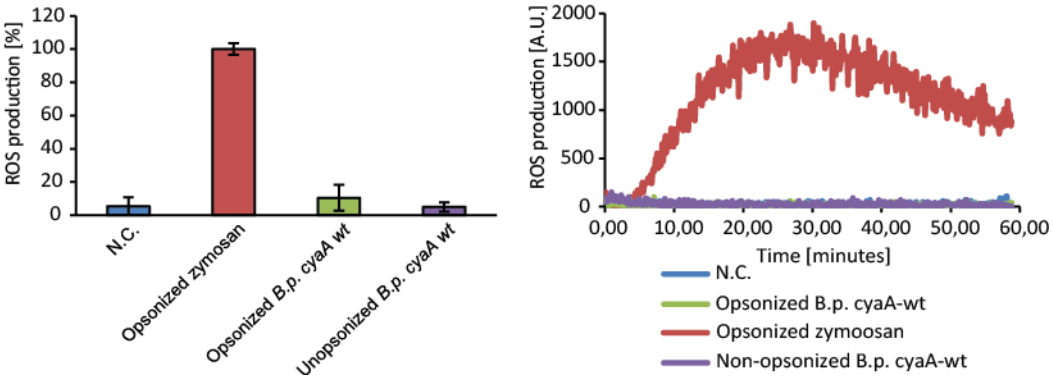

Fig. 33: *B. pertussis* does not induce ROS production in macrophages. RAW 264.7 macrophages were activated with either complement-opsonized zymosan, or with complement-opsonized *B.p. cyaA-wt* or unopsonized *B.p. cyaA-wt* bacteria at MOI 10:1. ROS production was measured over the indicated period of time. The values in the left panel represent means of relative ROS production compared to HI control out of three independent experiments (n=3). The right panel represents the time dependence of ROS production. The values represent the results of one experiment out of three independent.

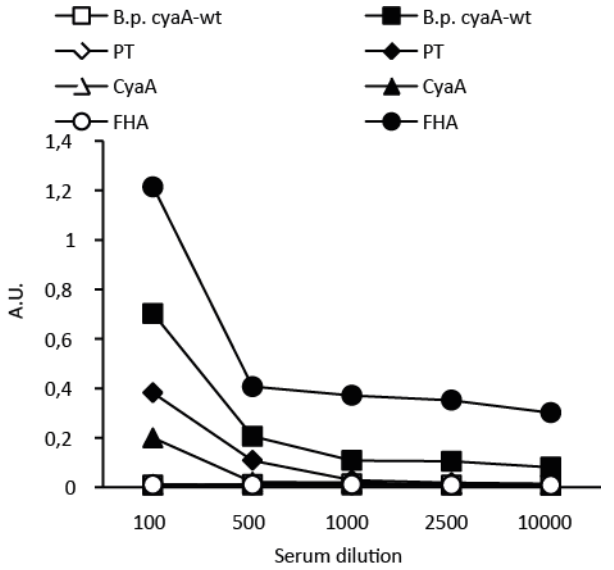

Fig. 34: Sera used for opsonization experiments do not contain anti-*B. pertussis* antibodies. The amounts of antibodies against PTX, CyaA, and FHA as well as against the heat-inactivated *B.p. cyaA*-wt cells were measured in donor sera (empty marks) or in serum from pertussis convalescent patients as positive controls (full marks) using an ELISA assay. Pertussis convalescent patient serum was used as a positive control. A representative result for one donor serum is shown.

Bordetella pertussis inhibits NO production by macrophages

Macrophage cells are known to produce substantial amounts of bactericidal nitric oxide (Noda and Amano, 1997). Moreover, *B. pertussis* was shown to persist much better inside activated macrophages from iNOS-deficient mice (Canthaboo et al., 2002). We, therefore, tested if *B. pertussis* inhibits NO production by macrophages.

As shown in Fig. 35, significantly decreased NO production was observed in RAW264.7 macrophages infected with bacteria producing intact CyaA (*B.p. cyaA-wt*), as compared to RAW264.7 cells co-incubated with heat-inactivated (HI) *B. pertussis*, or to macrophages infected with *B.p. cyaA-AC*$^-$ or *B.p. ΔcyaA* bacteria, respectively. This suggested that signaling of CyaA-produced cAMP interfered with TLR-triggered induction of NO production.

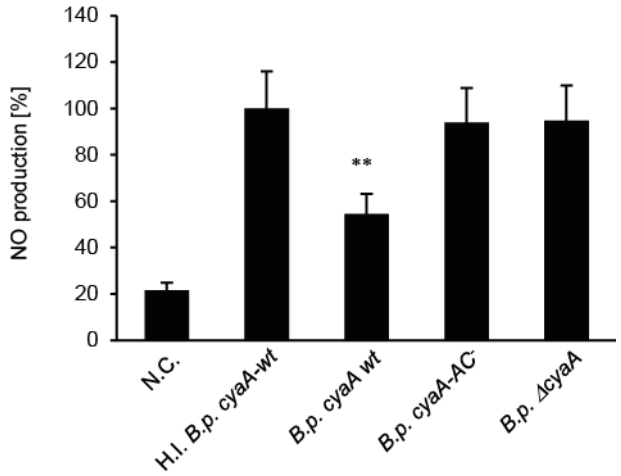

Fig. 35: *B. pertussis* inhibits NO production in macrophages. RAW264.7 macrophages were incubated with heat-inactivated (HI) *B.p. cyaA-wt*, or live *B.p. cyaA-wt*, *B.p.* c*yaA-AC*$^-$, or *B.p. ΔcyaA* cells for 24 h before NO production was measured in culture supernatants. Values represent the means ±SD from three experiments performed in triplicates (n=9). **, $p<0.001$ *vs*. HI *B.p. cyaA-wt* control

As shown in Fig. 36*A*, exposure to as little as 1 ng/ml of CyaA did significantly decrease LPS-induced NO production in RAW264.7 macrophages and the higher concentrations of CyaA blocked it nearly completely. This was clearly and specifically due to the elevation of cAMP concentration by the AC enzyme activity of the CyaA toxin, as the LPS-inducible NO production was also inhibited upon RAW264.7 cell exposure to the membrane-permeable cAMP analog db-cAMP (1 mM). In contrast, cell exposure to the non-enzymatic CyaA-AC$^-$ toxoid, unable to raise cAMP levels, had no effect on the induction of NO production by LPS. As further shown in Fig. 36*B*, the inhibition of NO production by CyaA was also fully reproduced in bone marrow-derived macrophages (BMDM) stimulated by LPS, showing that CyaA activity (cAMP elevation) blocked the induction of bactericidal NO production in primary murine macrophages.

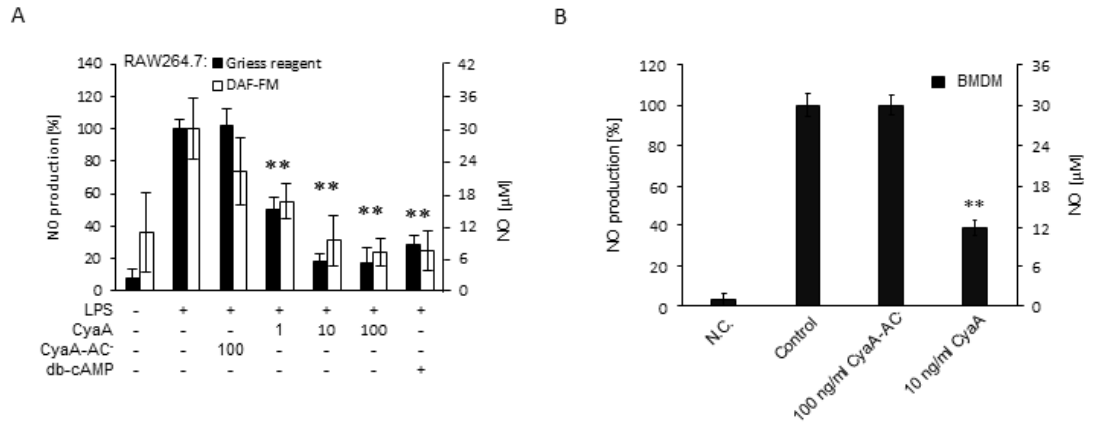

Fig. 36: CyaA inhibits NO production in macrophages. RAW264.7 macrophages (*A.*) or BMDM (*B.*) were treated in the presence or absence of 100 ng/ml of LPS from *E. coli* with the CyaA variants or with 1 mM db-cAMP for 24 h. 10 µM IBMX was added 1 h prior to the db-cAMP addition to cells and the produced NO was measured by the Griess reagent or by the DAF-FM probe. Values represent means ±SD from three independent experiments performed in triplicates (n=9). **, p<0.001 *versus* LPS-treated control

As shown in Fig. 37, a detectable increase of intracellular cAMP concentration in RAW264.7 cells was observed already upon exposure of RAW264.7 macrophages for 5 minutes to CyaA at a concentration of 10 ng/ml, which corresponds well to toxin amounts detected in nasopharyngeal fluids from *B. pertussis*-infected humans and primates (Eby et al., 2013). The CyaA-catalyzed cAMP production in cells then peaked within 1 h and intracellular cAMP concentrations remained elevated for 24 h, regardless of whether the cells were activated by the addition of *E. coli* LPS (100 ng/ml) or not. Hence, signaling of LPS used for the induction of NO production did not interfere with cAMP elevation in macrophage cells. The peak amounts of cAMP produced upon exposure to 10 ng/ml of CyaA were fully comparable to cAMP levels resulting from infection of macrophages by wild-type *B. pertussis* for 24 h at the MOI 10:1, as used in the intracellular survival assay (*cf.* Fig. 32). It should, however, be noted that some increase of cAMP levels was also observed upon prolonged macrophage infection by the AC enzyme-deficient cyaA-AC$^-$ mutant (Fig. 37). This was most likely due to the action of the pertussis toxin (PTX) produced by the mutant strain, as PTX can dysregulate the activity of the cellular adenylyl cyclase enzymes through inhibitory ADP-ribosylation of the $G_{i\alpha}$ subunits of the trimeric G proteins (Katada and Ui, 1982). The PTX-triggered cAMP elevation occurs, however, several hours after PTX penetration into cells and requires external stimuli activating the endogenous AC enzyme, while yielding substantially lower levels of cAMP than what CyaA

produces within minutes of contact with phagocytes (Bokoch et al., 1983). Hence, likely due to the delay in the onset of PTX-mediated cAMP elevation, which takes 8 to 12 h to manifest (Bokoch et al., 1983), the PTX-mediated elevation of cAMP did not prevent the rapid killing of the *cyaA-AC*$^-$ bacteria inside RAW264.7 cells (*cf.* Fig. 32).

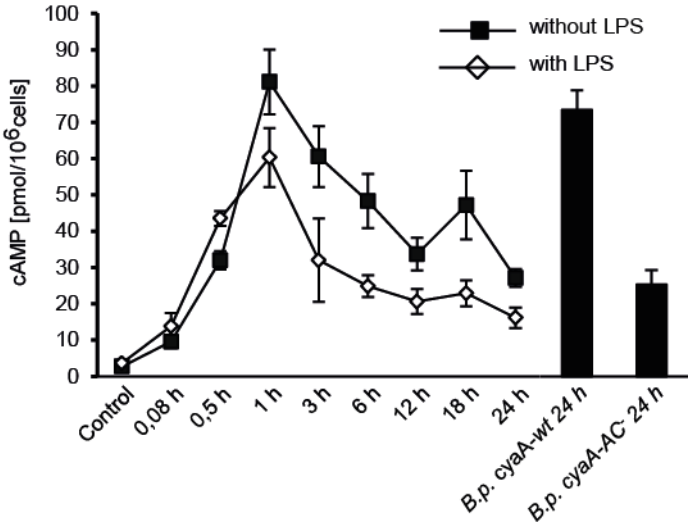

Fig. 37: CyaA-mediated accumulation of cAMP in macrophages. RAW264.7 macrophages were treated with 10 ng/ml CyaA, in the presence or absence of 100 ng/ml of LPS for the indicated times, or were infected for 24 hours with the indicated *B. pertussis* strains as described in Fig. 30. The concentration of cAMP was measured in cell lyzates by competition ELISA assay. One representative result out of three independent experiments performed in triplicates is shown.

CyaA-provoked inhibition of NO production is not due to the activation of arginases in macrophages

Previously, Cheung and co-workers suggested that CyaA might interfere with bactericidal NO production through the induction of arginase expression (Cheung et al., 2008). A cAMP-dependent increase of arginase activity was, indeed, observed in CyaA-treated RAW264.7 cells, as shown in Fig. 38*A*. However, as shown in Fig. 38*B*, the production of NO was not restored in CyaA-treated macrophages, neither upon selective inhibition of arginases by 100 μM nor-NOHA, nor at saturating concentrations of the arginase substrate L-arginine (12.8 mM), as shown in Fig. 38*C*. Thus, in contrast to the predicted role, arginases do not play any role in the inhibition of NO production by CyaA.

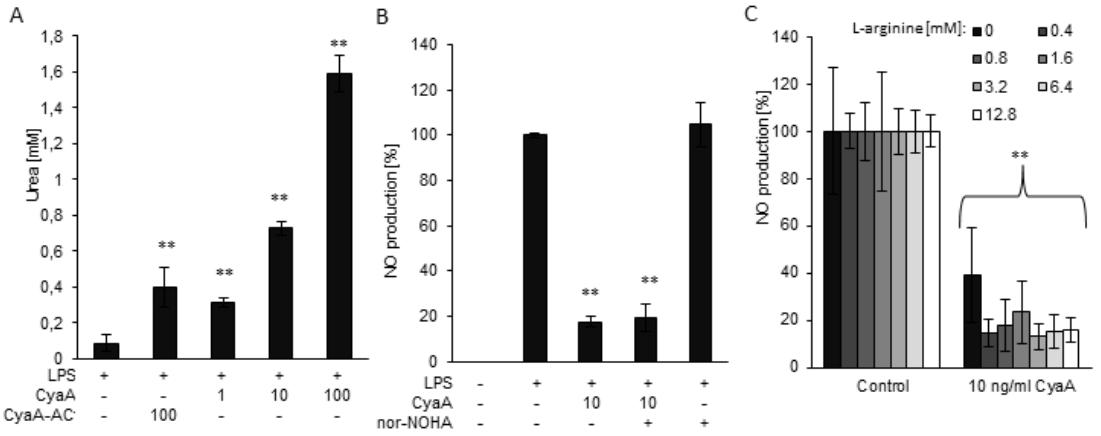

Fig. 38: CyaA induces increase in arginase activity. *A.* RAW264.7 cells were incubated with CyaA and 100 ng/ml LPS for 24 h before total arginase activity was measured in cell lyzates. The values are means ±SD from three independent experiments performed in triplicates (n=9). *B.* RAW264.7 cells were pre-incubated for 1 h in the presence or absence of 100 μM nor-NOHA prior to activation with 100 ng/ml of LPS and/or addition of 10 ng/ml CyaA for 24 h. Values represent means ±SD from three independent experiments performed in triplicates (n=9). *C.* RAW264.7 cells were incubated with 100 ng/ml of LPS and 10 ng/ml of CyaA in the presence of the indicated concentration of L-arginine for 24 h. Values represent the means ±SD from three independent experiments performed in triplicates (n=9). **, $p<0.001$ *vs*. LPS-treated control

CyaA inhibits the expression of iNOS in macrophages

To corroborate the evidence that CyaA inhibits NO production by a mechanism independent of arginases, we examined the iNOS enzyme expression in RAW264.7 macrophages treated with CyaA. As revealed by immunodetection with specific antibodies in Fig. 39*A*, exposure to 1 ng/ml of CyaA resulted in a significant decrease of iNOS production in LPS-stimulated RAW264.7 cells, or primary BMDM. Moreover, no iNOS protein was detected in cells exposed to higher toxin concentrations (10 or 100 ng/ml) or to 1 mM db-cAMP. In line with this, a strong decrease of iNOS mRNA level was detected by quantitative PCR in such-treated RAW264.7 cells, as shown in Fig. 39*B*. Hence, treatment with the cell-permeable cAMP analogue fully reproduced the impact of CyaA toxin action, while cell exposure to the CyaA-AC$^-$ toxoid had no effect. It can thus be concluded that the CyaA-produced cAMP signaling suppressed NO production in LPS-stimulated RAW264.7 cells through the inhibition of iNOS gene expression, rather than by the enhancement of arginase activity and the degradation of the L-arginine substrate.

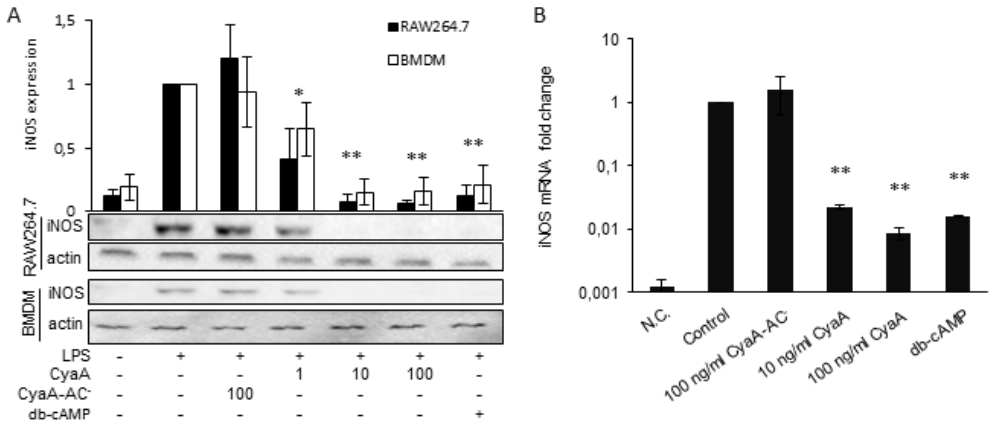

Fig. 39: CyaA down-regulates iNOS expression in macrophages. *A.* RAW264.7 macrophages or BMDM were treated at the indicated concentration of the indicated CyaA variant in the presence of 100 ng/ml LPS. After 24 h, iNOS protein levels were detected by immunoblotting. For experiments with RAW264.7 cells, one representative blot out of three independent experiments is shown (n=3). For experiments with BMDM, cells were isolated from three animals and one blot representative out of 3 experiments is shown (n=3). Mean ±SD iNOS amounts were determined by densitometric analysis. *B.* RAW264.7 cells were treated as in *A*. After 24 h iNOS mRNA was quantified by qRT-PCR. Relative iNOS mRNA levels normalized to iNOS mRNA extracted from LPS-treated control cells are expressed as fold change. Means ±SD of three independent experiments performed in duplicates (n=6) are given. *, $p<0.01$; **, $p<0.001$ versus LPS-treated control

Intriguingly, the induction of arginases would be indicative of macrophage polarization towards the M2 phenotype, while the induction of the M1 phenotype-associated COX-2 enzyme activity in murine macrophages by CyaA was previously reported (Perkins et al., 2007). We also did not observe here any alteration of the Mox macrophage markers NRF2 or HO-1 protein levels (Fig. 40) (Kadl et al., 2010). It appears, therefore, that the subversive cAMP-dependent signaling elicited by CyaA does not yield any clear macrophage polarization.

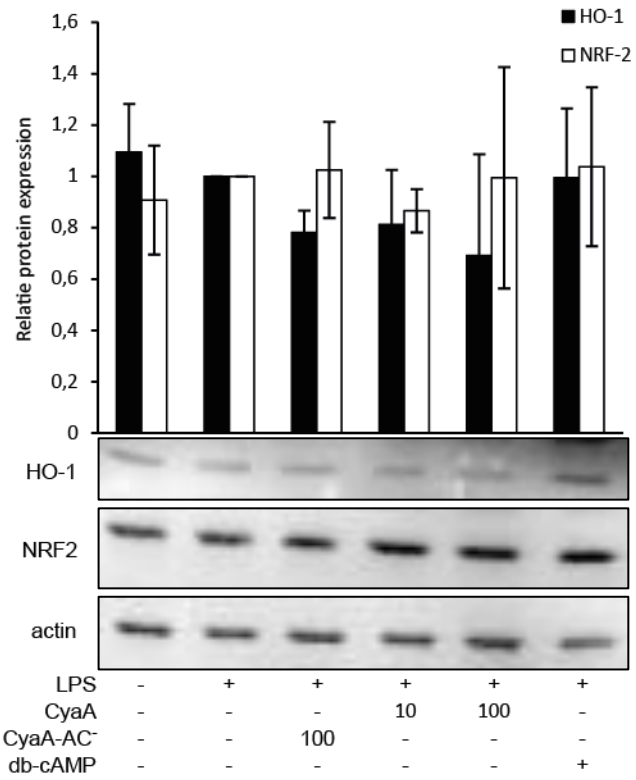

Fig. 40: CyaA does not influence NRF2 and HO-1 protein abundance. Raw264.7 cells were treated with or without 100 ng/ml LPS and with the indicated concentrations of CyaA variants or 1 mM db-cAMP with 10 μM IBMX for 24h. The presence of NRF2 and HO-1 was detected by immunoblotting. One representative blot out of three independent experiments is shown. The mean ±SD of densitometric analysis from all three experiments is shown (n=3).

CyaA blocks iNOS expression by cAMP-dependent activation of PKA

cAMP activates signaling of the protein-kinase A (PKA) and of the Epac protein (Peters-Golden, 2009). To determine if PKA or Epac activities were involved in the suppression of LPS-induced iNOS expression by cAMP signaling, RAW264.7 cells were pre-incubated with 10 μM phosphodiesterase inhibitor IBMX and stimulated by LPS in the presence of 1 mM cell-permeable cAMP analogues that (i) activate both PKA and Epac, such as db-cAMP, or (ii) selectively activate PKA, like 6-Bnz-cAMP, or (iii) only Epac, like 8-CPT-cAMP, respectively. As shown in Fig. 41*A*, signaling of 1 mM db-cAMP or of the PKA-specific activator 6-Bnz-cAMP provoked as significant inhibition of LPS-triggered NO production as exposure of cells to CyaA toxin (10 ng/ml). In contrast, treatment with the Epac-selective activator 8-CPT-cAMP had little effect on LPS-triggered NO production. As further shown in Fig. 41*B*, the 6-Bnz-cAMP (PKA activation) and db-cAMP treatments, but not the signaling of 8-CPT-cAMP (Epac activation), also provoked a loss of iNOS production in LPS-activated RAW264.7 macrophages. An insignificant effect of the

Epac activator was, however, also observed and it remains to be clarified whether it was due to a low level of unspecific activation of PKA by 8-CPT-cAMP, or whether Epac signaling also contributed to some extent to the suppression of iNOS gene expression. Nevertheless, as is also shown in Fig. 41*C*, activation of PKA by toxin-produced cAMP appeared to be the dominant pathway through which the CyaA-produced cAMP suppressed iNOS-mediated NO production in macrophages. The inhibition could be reversed to a great extent, though not fully, by the pre-incubation of cells with the PKA inhibitor H-89 (10 μM). Besides of the possibly incomplete inhibition of PKA at high cAMP levels produced by CyaA, the incomplete restoration of iNOS expression in H-89-treated cells was also likely due to some unspecific off-target effects of H-89. Indeed, as shown in Fig. 41*C*, the H-89 inhibitor (10 μM) caused some observable reduction of LPS-stimulated iNOS expression on its own. H-89 is, indeed, known to be not entirely specific for PKA and to influence activities of other AGC kinases at concentrations used here (Bain et al., 2007). Moreover, the more specific inhibitors of PKA, such as mPKI or cAMPS, were found to be less potent in the reversal of the overwhelming cAMP-mediated impact of CyaA action on iNOS expression (data not shown). It remains, therefore, possible that H-89 may also interfere with the induction of iNOS expression at some step downstream of PKA signaling. Collectively, these results show that the CyaA toxin inhibits iNOS expression predominantly through cAMP-mediated hijacking of the PKA signaling pathway.

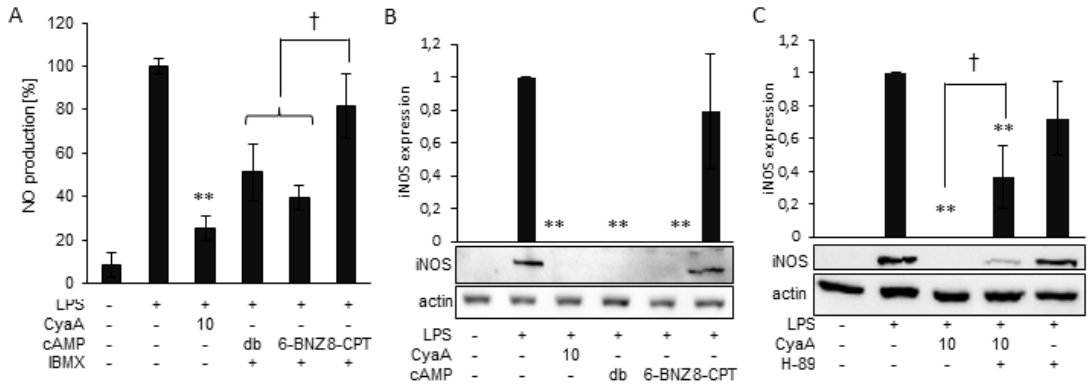

Fig. 41: PKA activation by CyaA inhibits NO production *A.* RAW264.7 cells were pre-incubated for 1 h in the presence or absence of 10 μM IBMX before LPS (100 ng/ml) and 8-CPT-cAMP, 6-Bnz-cAMP, or db-cAMP (1 mM) were added, respectively. NO production was detected after 24 h. Values represent the means ±SD from three independent experiments performed in triplicates (n=9). *B.* RAW264.7 cells were treated as in *A.* CyaA was added to the cells concomitantly with LPS and iNOS was detected by immunoblotting. One representative blot out of three independent experiments is shown. *C.* RAW264.7 cells were pre-incubated for 1 h with or without the PKA inhibitor H-89 (10

μM) prior to stimulation with 100 ng/ml LPS and 10 ng/ml of CyaA. After 24 h, the levels of iNOS protein were detected by immunoblotting. One representative blot out of three independent experiments is shown. The means ±SD of densitometric analysis from three experiments are shown (n=3). **, p<0.001 *versus* LPS treated control; †, p<0.01 *versus* each other

CyaA-provoked inhibition of JNK causes the block of NO production

NO production and iNOS expression is known to be regulated by the activity of MAPK (Brubaker et al., 2011), which was previously shown to be influenced by CyaA-mediated production of cAMP. We, therefore, analyzed the impact of MAPK inhibition on NO production and compared it with the effects of CyaA. As shown in Fig. 42, neither inhibition of p38, nor inhibition of ERK signaling due to the inhibition of its MEK activators did result in any major changes in NO production. In contrast, the inhibition of JNK led to a weak but statistically significant decrease of NO production. This result suggests that while JNK activity is required for NO production, neither p38, nor ERK signalization is needed for LPS-stimulated NO production.

As further shown in Fig. 42, neither JNK, nor MEK inhibitors exhibited any additive effect to CyaA-provoked inhibition of NO production. In contrast, p38 inhibitor potentiated the effects of CyaA. Taken together, these results suggest that neither ERK, nor p38 play any role in the effects of CyaA on NO production. In contrast, CyaA likely provoked inhibition of NO production through inhibition of JNK.

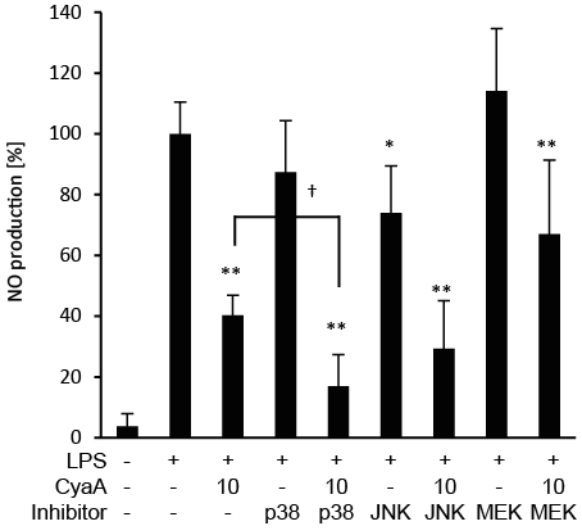

Fig. 42: CyaA-triggered inhibition of JNK contributes to inhibition of NO production in macrophages. RAW264.7 macrophages were pre-incubated with inhibitors of indicated MAPKs for 1 hour prior to the addition of 100 ng/ml LPS and/or 10 ng/ml CyaA. NO production was detected after

24 h. Values represent the means ±SD from three independent experiments performed in triplicates (n=9). *, p<0.01; **, p<0.001 *versus* LPS treated control; †, p<0.01 *versus* each other's

Pore-forming capacity of CyaA activates MAPKs

It was previously hypothesized that CyaA influences different MAPK pathways leading to dysregulation of immune functions of leukocytes. In addition to our above described finding that CyaA employs the inhibition of JNK to decrease NO production, p38 was shown to be activated by CyaA in DCs and T lymphocytes (Hickey et al., 2008; Rossi Paccani et al., 2009). To study this in more detail, we incubated BMDCs with a detoxified CyaA-AC$^-$ toxoid, with a detoxified toxoid that had a decreased pore-forming capacity CyaA-E570Q+K860R-AC$^-$ (CyaA-QR-AC$^-$), and with a detoxified toxoid with increased specific pore-forming capacity CyaA-E509K+E516K-AC$^-$ (CyaA-KK-AC$^-$). The activities of the used CyaA variants are summarized in Table 3.

Table 3.: Comparison of activities of used CyaA variants.

Toxoid	cAMP production	Ca^{2+} influx	Pore formation
CyaA	+	+	+
CyaA-AC$^-$	-	+	+
CyaA-QR-AC$^-$	-	+	+/-
CyaA-KK-AC$^-$	-	+/-	+++

The activity of recombinant CyaA, of detoxified CyaA-AC$^-$ lacking the ATP to cAMP-converting activity, of detoxified CyaA-QR-AC$^-$ toxoid with decreased pore-forming activity, and of hyperhemolytic and detoxified CyaA-KK-AC$^-$ are given. +, activity at wt toxin level; +/-, activity decreased in comparison with wt toxin; -, activity is missing in comparison with wt toxin; +++, activity is strongly increased in comparison with wt toxin

As shown in Fig. 43, toxoids with either preserved, or increased pore-forming capacity highly increased the activatory phosphorylation of JNK, while the toxoid with decreased pore forming capacity failed to influence JNK phosphorylation. As further shown in Fig. 43, p38 was also more phosphorylated in cells exposed to the CyaA variant exhibiting enhanced specific pore-forming activity. Thus p38 was activated by CyaA pore-dependent signaling, while the enzymatic activity of the toxin played a minor role. In contrast, while JNK could be also activated by signaling provoked by CyaA pores, the enzymatic activity of the toxin reverted this process and yielded JNK inhibition (*cf.* Fig. 42).

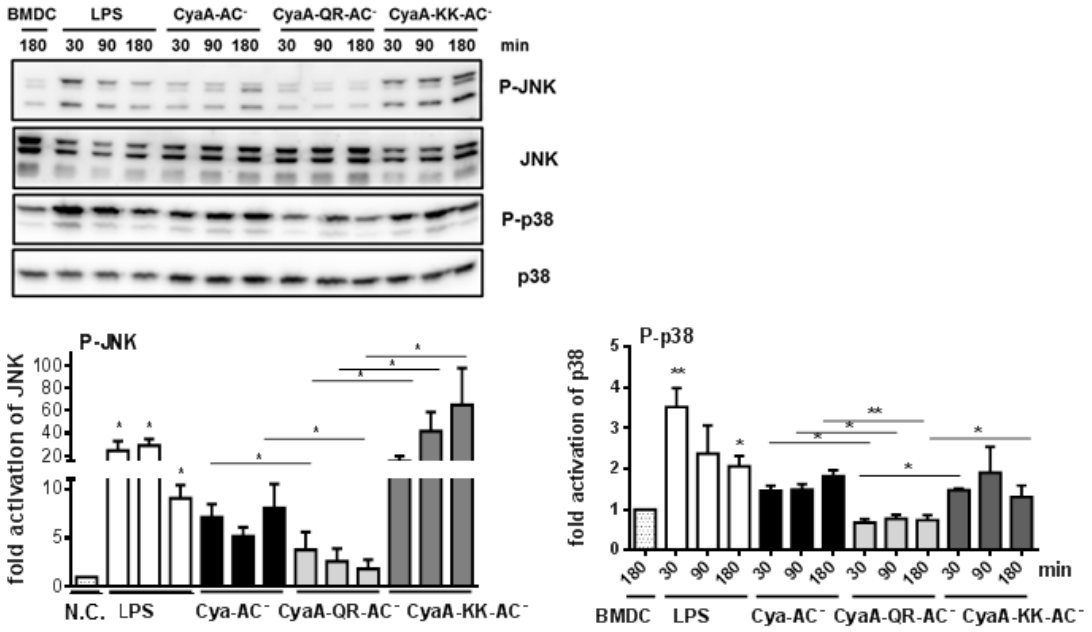

Fig. 43: Pore-forming activity of CyaA induces JNK and p38 phosphorylation. BMDC were incubated either with 100 ng/ml of LPS, or with 300 ng/ml of CyaA variants – CyaA-AC$^-$, CyaA-QR-AC$^-$, or CyaA-KK-AC$^-$ for the indicated time. Phosphorylation of JNK and p38 was determined by immunoblotting. One representative blot out of three experiments on independent BMDC preparations is shown. The means ±SD of densitometric analysis from three experiments are shown (n=3). *, $p<0.001$ *versus* LPS treated control

CyaA potentiates LPS-mediated NF-κB activation

MAPKs are known to regulate a broad range of transcription factors (Seger and Krebs, 1995) and some of them, such as NF-κB, Stat1, IRF1, and AP-1, are known to regulate iNOS expression (Kleinert et al., 2003; Lee et al., 2005a; Pautz et al., 2010). The NF-κB transcription factor is sequestered in the cytoplasm by its inhibitor IκB that can be phosphorylated in activated cells. This leads to IκB ubiquitination and proteasomal degradation. Therefore, we first analyzed the phosphorylation status of IκB. As shown in Fig. 44*A*, the basal level of IκB protein, as well as its basal phosphorylation was detected in non-activated RAW264.7 macrophages. Although some increase in IκB protein was observed after LPS activation of macrophages, the increase in its phosphorylation was much more dramatic. This suggests that after LPS activation of macrophages, NF-κB is, indeed, activated. As further shown in Fig. 44*A*, however, a decrease in IκB protein level was provoked by CyaA, but not by CyaA-AC$^-$. This suggests that NF-κB was activated by signaling of CyaA-produced cAMP.

To corroborate that NF-κB was not sequestered in the cytoplasm of toxin-treated cells by another mechanism than by IκB binding, we monitored the translocation of the p65 subunit of NF-κB into cell nucleus. As shown in Fig. 44*B*, LPS caused a strong translocation of p65 into the nucleus. In agreement with our observation shown in the Fig. 44*A*, CyaA action itself caused a weak p65 nuclear transport. Moreover, CyaA action potentiated p65 nuclear export in LPS treated RAW264.7 macrophages. Therefore, we examined the effect of CyaA treatment on NF-κB-dependent transcription in RAW264.7 macrophages transfected with a plasmid encoding GFP under the control of NF-κB promoter. As shown in Fig. 44*C.*, a significant increase in the amount of GFP-expressing cells was observed upon treatment of transfected macrophages with 100 ng/ml of LPS in combination with 100 ng/ml of CyaA, as compared to LPS-treated control. This shows that NF-κB activity is increased in response to LPS and CyaA treatment. For this reason, the effect of the CyaA/cAMP on NF-κB activation likely played no role in the inhibition of iNOS expression.

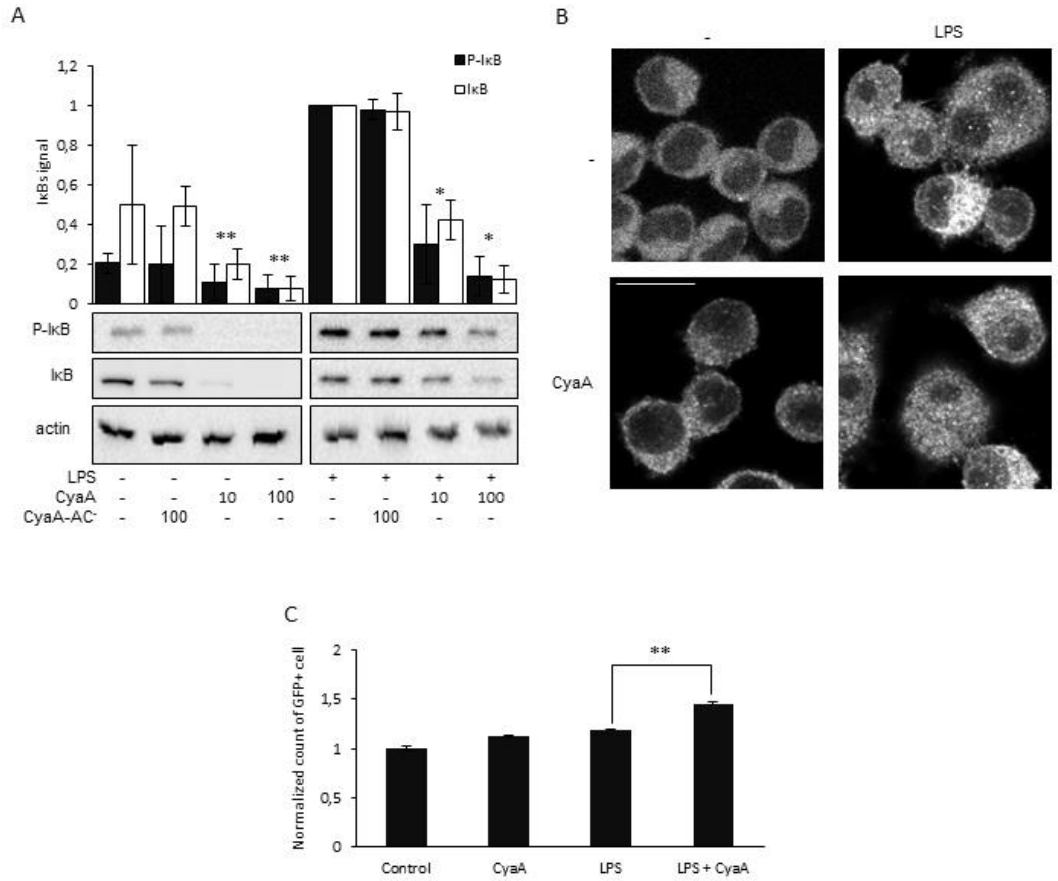

Fig. 44: CyaA activates NF-κB. *A.* RAW264.7 cells were treated with or without 100 ng/ml LPS and with the indicated concentrations of CyaA for 24 h. The presence and phosphorylation of IκB was

detected by immunoblotting. One representative blot out of three independent experiments is shown. The mean ±SD of densitometric analysis from three experiments is shown (n=3). *B.* RAW264.7 cells were treated with or without 100 ng/ml LPS and/or 10 ng/ml CyaA for 1 hour. Subcellular localization of p65 was detected by specific antibody and visualized using confocal microscopy. Images representative of 3 independent experiments are shown. The scale bar corresponds to 5 μm. *C.* RAW264.7 macrophages were transfected with a plasmid carrying the GFP gene under the control of the NF-κB promoter. 24 hours after transfection, cells were treated with or without 100 ng/ml LPS and/or 10 ng/ml CyaA for an additional 6 hours. GFP expression was quantified using FACS. Values represent the mean of relative amounts of GFP expressing cells ±SD from three independent experiments performed in triplicates (n=9). *, p< 0,01; **, p<0.001 vs. control

CyaA inhibits Stat1 and IRF1

We further examined the effect of CyaA on the activity of Stat1 transcription factor. Stat1 activity correlates with its phosphorylation on the Y701 and S727 residues. As shown in Fig. 45, CyaA caused dephosphorylation of LPS-activated Stat1 both on Y701, as well as on S727 in a dose dependent manner during the 24 hours after toxin addition. Similarly, treatment of RAW264.7 macrophages with 10 μM IBMX and 1 mM db-cAMP led to the complete dephosphorylation of Stat1. In contrast, Stat1 dephosphorylation was not observed in RAW264.7 macrophages treated with 100 ng/ml of CyaA-AC$^-$. CyaA and db-cAMP, but not CyaA-AC$^-$, also caused a decrease in the total amount of transcription factor IRF1. Thus, CyaA causes inhibition of Stat1 and IRF1 transcription factors by a mechanism dependent on cAMP production.

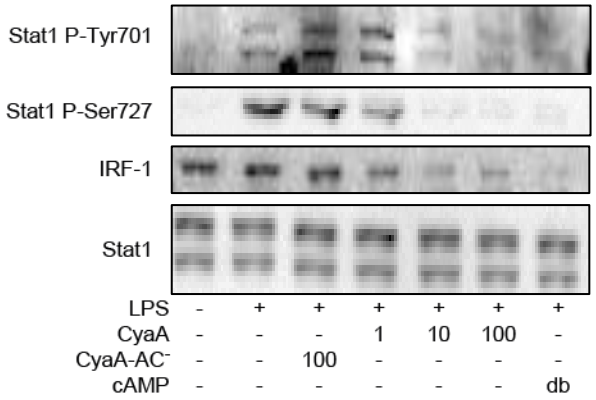

Fig. 45: CyaA inhibits Stat1 and IRF1. RAW264.7 cells were incubated with or without 100 ng/ml LPS and/or the indicated concentration of CyaA, or with 1 mM db-cAMP with 10 μM IBMX for 24 hours. Specific phosphorylation of Stat1 and the presence of IRF1 were detected by immunoblotting.

To examine if inhibition of iNOS expression and NO production by CyaA was due to inhibition of Stat1 and IRF1, we examined the time dependence of Stat1 dephosphorylation and inhibition of iNOS expression by CyaA. As shown in Fig. 46, iNOS expression could not be observed earlier than 6 hours after RAW264.7 cells

stimulation by 100 ng/ml LPS. Similarly, neither Stat1 activation nor the inhibitory effect of CyaA on Stat1 phosphorylation preceded iNOS expression.

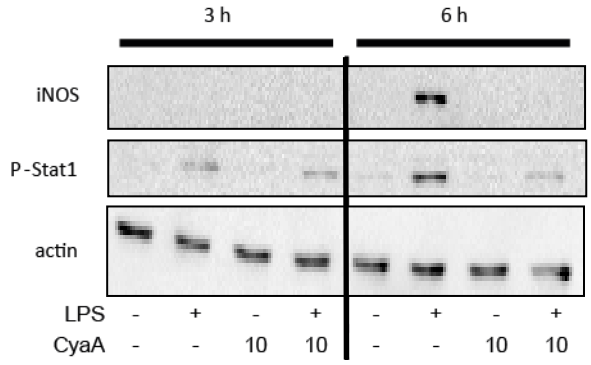

Fig. 46: Inhibition of Stat1 does not precede the block of iNOS expression. RAW264.7 cells were incubated with or without 100 ng/ml LPS and/or 10 ng/ml of CyaA. Expression of iNOS and specific phosphorylation of Stat1 were detected by immunoblotting.

cAMP signaling through PKA causes the dephosphorylation of AP-1

Another major transcription factor required for iNOS expression is AP-1 (Bonaparte et al., 2006; Pautz et al., 2010). Therefore, we next examined if cAMP signaling of CyaA affected the regulatory phosphorylation of the c-Fos subunit of AP-1. As shown in Fig. 47, no phosphorylation of c-Fos was detected in untreated cells, while the activation of RAW264.7 macrophages by LPS resulted in hyperphosphorylation of c-Fos, which was detected as two bands in immunoblots with P-c-Fos antibody. Exposure of LPS-activated RAW264.7 cells to 10 ng/ml of CyaA then provoked a near-complete disappearance of the upper hyperphosphorylated c-Fos isoform, while the hypophosphorylated lower band of P-c-Fos form was detected at comparable levels as in LPS-activated and mock-treated cells. In contrast, specific activation of Epac with 1 mM 8-CPT-cAMP did not affect TLR(LPS)-signaling-triggered phosphorylation of c-Fos, while the action of CyaA was almost fully reproduced by the PKA-activating analogues db-cAMP (1 mM) and 6-Bnz-cAMP (1 mM), respectively. Activation of PKA by the cAMP analogues yielded a less complete dephosphorylation of the hyperphosphorylated P-c-Fos species (upper band) as that provoked by CyaA action. It, however, increased the relative detected amounts of the hypophosphorylated P-c-Fos isoform. Altogether, these data suggest that the activation of PKA signaling by CyaA-produced cAMP provokes dephosphorylation of the c-Fos subunit of the AP-1 transcription factor that is required for iNOS gene expression in LPS-activated macrophages.

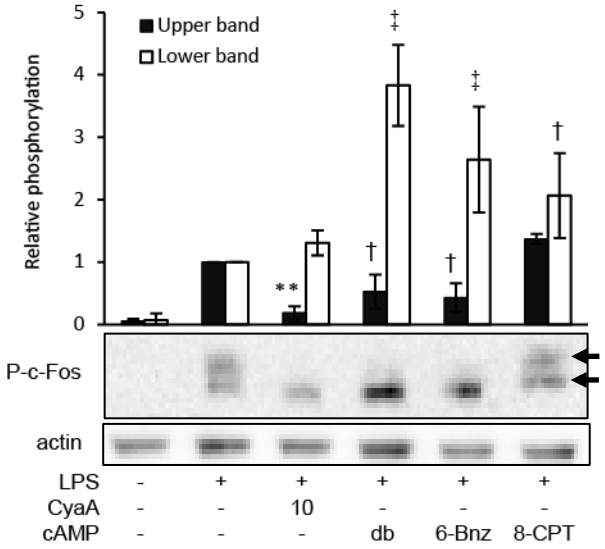

Fig. 47: CyaA provokes dephosphorylation of the P-c-Fos subunit of AP-1 *via* PKA-mediated signaling. RAW264.7 macrophages were pre-incubated with or without 10 µM IBMX for 1 h before the addition of LPS (100 ng/ml) and/or CyaA (10 ng/ml), or db-cAMP, 6-Bnz-cAMP or 8-CPT-cAMP (1 mM), respectively. After 24 h, the active hyperphosphorylated P-c-Fos form (slower migrating upper band) and the inactive hypophosphorylated form (lower band) were detected by immunoblotting and are indicated by arrows, respectively. **, $p<0.001$ *versus* LPS treated control; †, $p<0.01$; ‡, $p<0.001$ *versus* IBMX control.

CyaA/cAMP signaling blocks iNOS expression through activation of the SHP-1 phosphatase

No protein phosphatases directly activated by cAMP signaling have as yet been identified, but the tyrosine phosphatase SHP-1 is known to be involved in the regulation of numerous receptor signaling pathways in leukocytes and was previously implicated also in the regulation of iNOS expression (Blanchette et al., 2009) and MAPK activity (Mizuno et al., 2002; Zhang et al., 2000). Therefore, we examined if SHP-1 activity played a role in cAMP/PKA-regulated dephosphorylation of c-Fos. As shown in Fig. 48, the CyaA-provoked dephosphorylation of the hyperphosphorylated (upper band) form of c-Fos was partly inhibited upon pretreatment of LPS-activated cells with NSC87877 (500 nM), an inhibitor of the SHP-1 and SHP-2 phosphatases. Moreover, increased amounts of the hypophosphorylated (faster migrating) isoform of c-Fos were observed in NSC87877-treated cells exposed to CyaA, indicating that SHP-1/2 activity may be regulated by cAMP signaling.

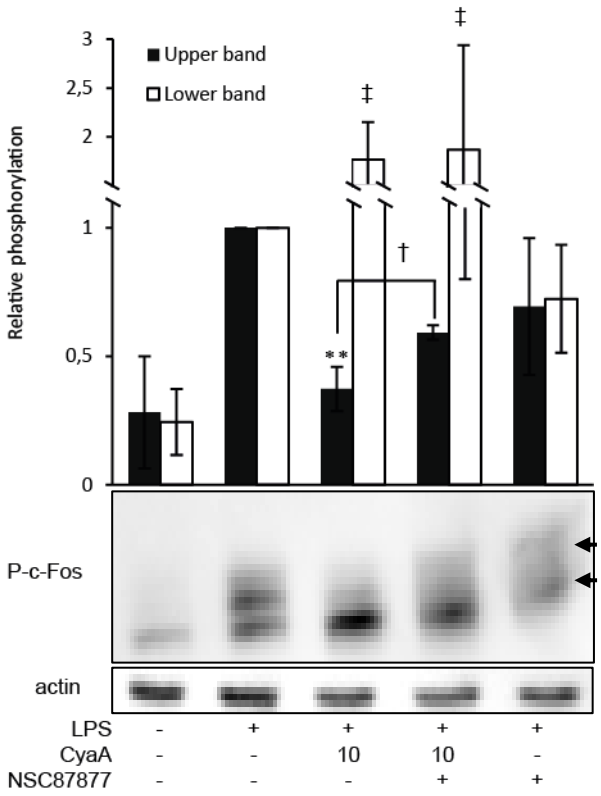

Fig. 48: NSC87877 reverts CyaA-provoked dephosphorylation of c-Fos. RAW264.7 macrophages were pretreated with or without the 500 nM NSC87877 inhibitor of SHP-1/2 phosphatases for 1 h before 100 ng/ml LPS and 10 ng/ml of CyaA were added for 24 h and phosphorylation status of P-c-Fos was analyzed by immunoblotting of cell lyzates. One representative blot out of three independent experiments is shown. The mean values ±SD from densitometric analysis are shown (n=3). **, $p<0.001$ *versus* LPS treated control; †, $p<0.01$ versus each other; ‡, $p<0.001$ *versus* NSC87877 control

Moreover, pretreatment with NSC87877 also restored in part the production of NO and the expression of iNOS in toxin-treated RAW264.7 cells (Fig. 49*A* and *B*, respectively).

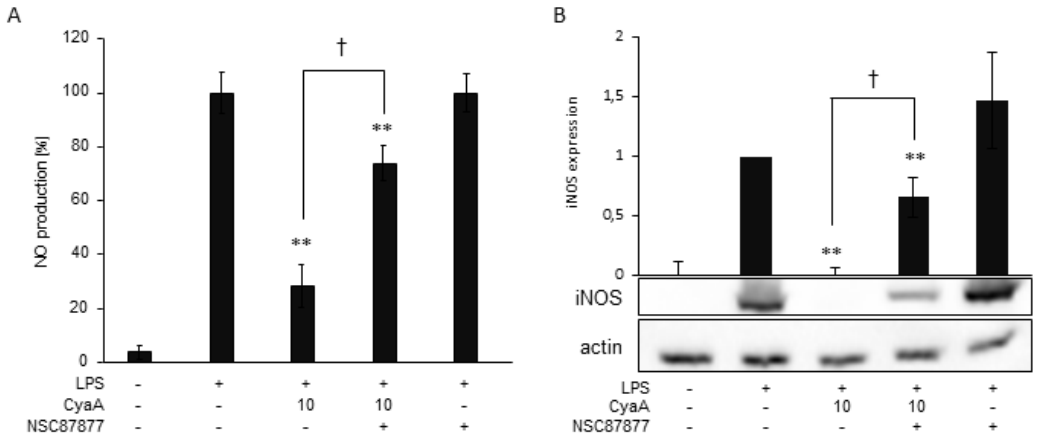

Fig. 49: NSC87877 reverts inhibition of NO production and iNOS expression by CyaA. *A.* RAW264.7 macrophages were pretreated with or without the 500 nM NSC87877 inhibitor of SHP-1/2 phosphatases for 1 h before 100 ng/ml LPS and 10 ng/ml of CyaA were added for 24 h and the production of NO was assessed. Values represent the means ±SD from three independent experiments performed in triplicates (n=9). *B.* RAW264.7 cells were treated as in *A* and after 24 h, the levels of iNOS protein were detected by immunoblotting. One representative blot out of three independent experiments is shown. The means ±SD form densitometric analysis of three experiments is shown (n=3). **, $p<0.001$ *versus* LPS treated control; †, $p<0.01$ versus each other

Therefore, SHP-1 and SHP-2 expression was selectively knocked-down by siRNA and cAMP-induced inhibition of iNOS expression was examined. As shown in Fig. 50, CyaA fully suppressed production of NO in RAW264.7 macrophages transfected with non-targeting siRNA or with SHP-2-specific siRNA. Such cells expressed normal levels of the SHP-1 protein, as detected in immunoblots of cell lyzates with SHP-1-specific antibodies. In contrast, no detectable amounts of the SHP-1 protein were produced in cells repeatedly transfected with SHP-1-specific siRNA, in which exposure to CyaA provoked only a mild decrease of the LPS-induced NO production. Moreover, in the absence of CyaA the cells with SHP-1 knocked-down reproducibly responded to activation by LPS with a ~50% higher production of NO than control cells, or cells transfected by non-targeting or SHP-2-specific siRNA. It can, therefore, be concluded that it was specifically the SHP-1 tyrosine phosphatase that translated the PKA-mediated signaling of toxin-produced cAMP into inhibition of iNOS expression and loss of NO production.

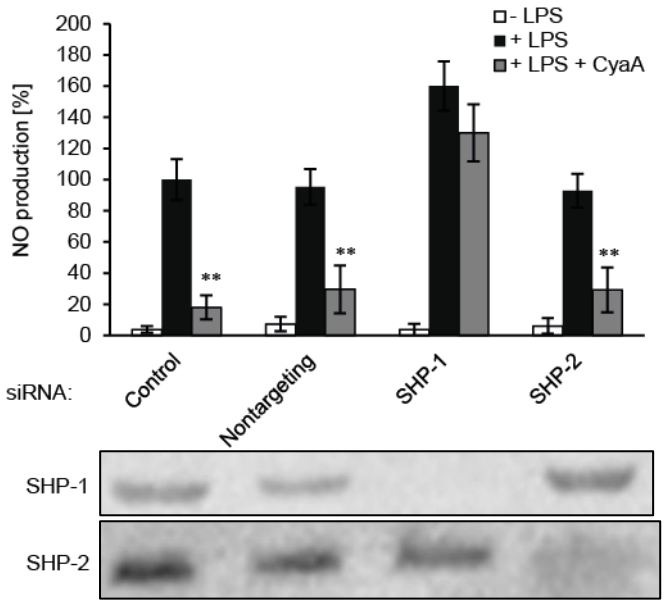

Fig. 50: SHP-1 is responsible for CyaA-provoked inhibition of NO production. RAW264.7 cells were transfected with either non-targeting, or SHP-1-, or SHP-2-specific siRNA, respectively. LPS (100 ng/ml) and/or CyaA (10 ng/ml) were added and incubation was continued for 24 h. The production of SHP proteins was analyzed by immunoblotting. Values represent the means ±SD from three independent experiments performed in triplicates (n=9). **, $p<0.001$ *versus* LPS treated control

To corroborate that cAMP/PKA signaling activated the SHP-1 phosphatase, its activity was measured in the material pulled-down by SHP-1-specific antibody from lyzates of CyaA-treated cells. As documented in Fig. 51, about a two-fold higher SHP-1 phosphatase activity was, indeed, detected in immunoprecipitates from LPS-activated cells exposed to 10 ng/ml of CyaA for 10 or 30 min, compared to lyzates from cells exposed to LPS only. Intriguingly, this activation of SHP-1 was only transient and at 60 min of cell exposure to CyaA the levels of SHP-1 activity in cells decreased back to the steady state levels.

To gain more insight into the possible mechanism of SHP-1 activity regulation by signaling of cAMP, we examined the phosphorylation of SHP-1 on residues known to be involved in up-regulation of the specific phosphatase activity. As shown in Fig. 52, at 30 min of cell exposure to toxin, no alteration of the activatory phosphorylation of Y564 and Y536 residues was detected, while a decrease of the inhibitory phosphorylation on S591 in 30 minutes was reproducibly observed. The exact mechanism of cAMP-dependent regulation of SHP-1 activity will, however, require further analysis, as at 60 min of CyaA action, where the SHP-

1 activity was already back to initial level, no increase of the inhibitory phosphorylation of the S591 residue was observed.

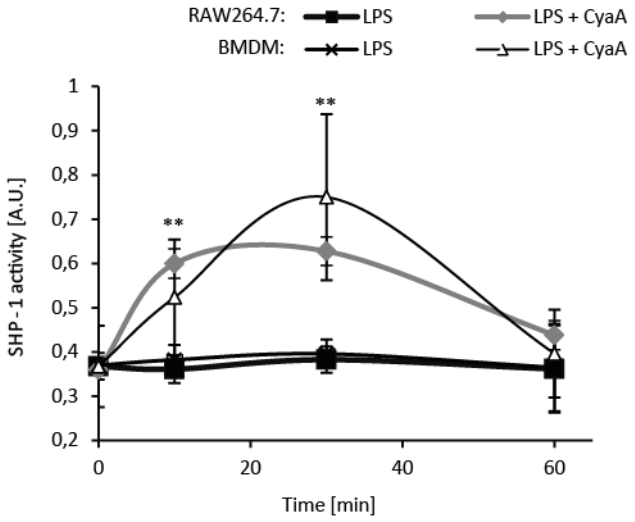

Fig. 51: CyaA induces SHP-1 activity. RAW264.7 or BMDM cells were treated with 10 ng/ml of CyaA for the indicated time in the presence of 100 ng/ml LPS. SHP-1 was immunoprecipitated and its phosphatase activity was measured and expressed relative to phosphatase activity. Mean values ±SD from three independent experiments are given. **, p<0.001 *versus* LPS treated control

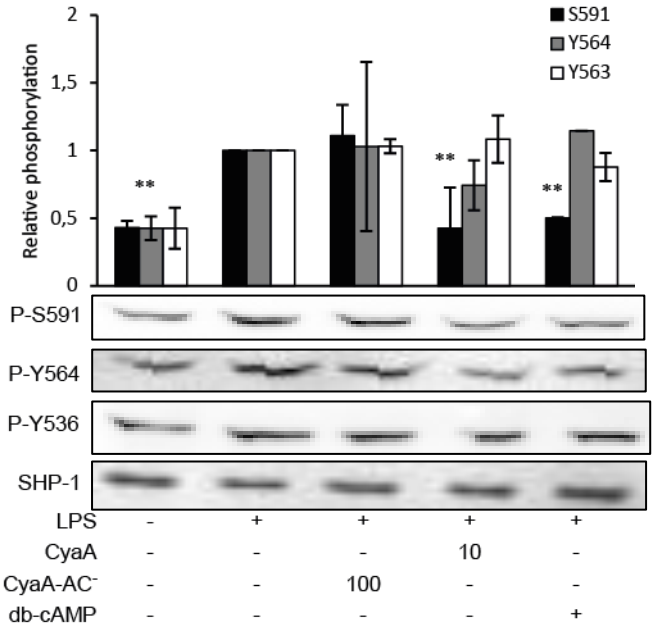

Fig. 52: CyaA causes decrease in inhibitory phosphorylation of SHP-1. RAW264.7 cells were treated with indicated CyaA variants for 30 minutes and the phosphorylation status of SHP-1 was analyzed by immunoblotting. One representative blot out of three independent experiments is shown. Mean values ±SD from densitometric analysis are given (n=3). **, p<0.001 *versus* LPS treated control; †, p<0.01 versus each other; ‡, p<0.001 *versus* NSC87877 control.

Inhibition of SHP phosphatase activity abrogates B. pertussis survival in macrophages

It was then important to examine if SHP-1 activation by CyaA accounted for the extended survival of unopsonized *B. pertussis* inside mouse macrophages. As shown in Fig. 53*A*, treatment with the SHP-1/2 inhibitor NSC87877 (500 nM) enhanced by about two to three fold the total number of *B. pertussis* cells associated with and internalized by the RAW264.7 macrophages. This goes well with an earlier observation that the inhibition of the SHP-1 phosphatase enhances phagocytic activity of macrophages (Kant et al., 2002; Lee et al., 2011). In sharp contrast, the presence of the SHP inhibitor completely abrogated the capacity of *B. pertussis* to survive within macrophages, as documented in Fig. 53*B*. Almost no viable bacteria could be recovered from macrophages incubated with NSC87877 at 24 hours after infection, while in the absence of the SHP inhibitor the bacterial viability inside cells was decreasing gradually over 72 hours. Collectively, these data show that the activation of the SHP-1 phosphatase by CyaA-elicited signaling of cAMP enables unopsonized *B. pertussis* bacteria to extend their survival inside macrophage cells.

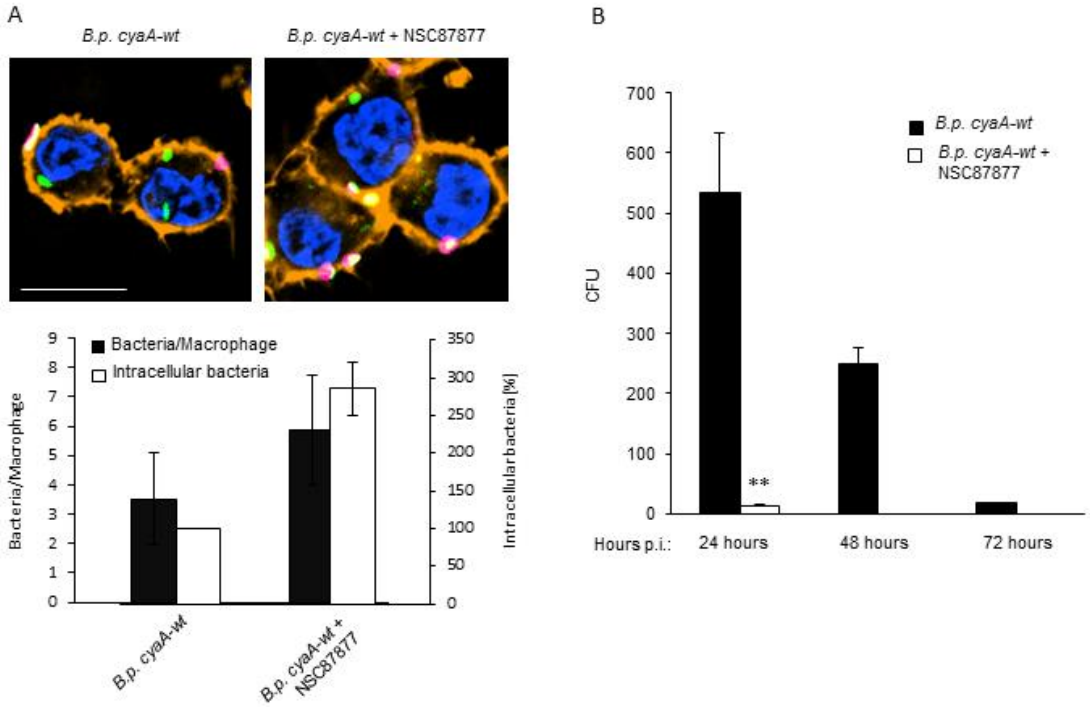

Fig. 53: SHP-1 inhibition abrogates survival *of Bordetella pertussis* inside macrophages. Prior to infection with GFP-expressing *B.p. cvaA-wt*, the RAW264.7 macrophages were pre-incubated for 1 h with or without SHP-1/2 inhibitor NSC87877 (500 nM). *A.* After 1 h, the cells were washed, fixed, and analyzed as described in legend to Fig. 31. Representative images from at least five independent experiments are shown. The scale bar corresponds to 5 μm. *B.* The RAW264.7 cells were treated as described in legend to Fig. 32. Cell lyzates were plated on BGA and bacterial CFU were counted after

5 days. Values represent the means ±SD from at least 10 independent experiments (n=10). **, p<0.01 vs. Control

CyaA-dysregulates AKT and FoxO3a activity

In Fig. 32, we show that *B. pertussis* survives inside phagocytes for a limited period of time. Some authors have hypothesized that this could be an important virulence mechanism contributing to the long-lasting symptoms of whooping cough (Lamberti et al., 2010). This may, however, be also influenced by the CyaA-dependent induction of apoptosis of phagocytes (Gueirard et al., 1998; Khelef et al., 1993). The CyaA-provoked apoptosis of monocytes was shown to be due to the accumulation of the pro-apoptotic BimEL protein and the association of the pro-apoptotic factor Bax with mitochondria (Ahmad *et al.*, in press). This required cAMP/PKA signaling and depended on SHP-1 activity, being selectively inhibited upon siRNA knockdown of SHP-1. Moreover, signaling of CyaA-produced cAMP further inhibited the AKT/PKB pro-survival cascade, enhancing activity of the FoxO3a transcription factor and inducing *Bim* transcription. Hence, synergy of the FoxO3a activation with SHP-1 hijacking enabled the toxin to rapidly trigger a persistent accumulation of BimEL, thus activating the pro-apoptotic program of phagocytes and subverting the innate immunity of the host (Ahmad *et al.*, in press). As shown in Fig. 54, cAMP production by 20 ng/ml of CyaA leads to dephosphorylation of AKT on both S473 and T308 residues and thus inhibits AKT pro-survival activity within 30 minutes of toxin action. In contrast, CyaA-AC$^-$ toxoid did not influence or maybe even increased the AKT phosphorylation at the concentration of 100 ng/ml.

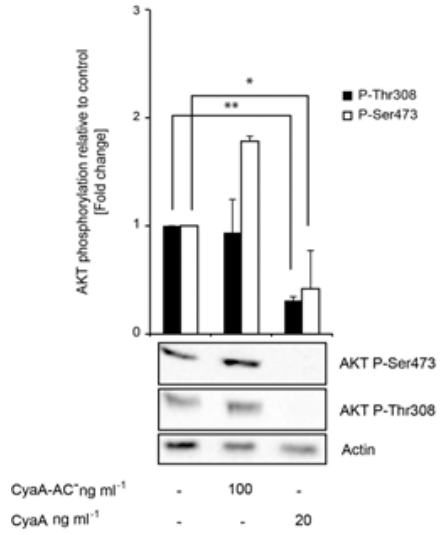

Fig. 54: CyaA inhibits AKT. THP-1 monocytes were incubated with the indicated concentration of CyaA variants for 30 minutes and the phosphorylation status of AKT was analyzed by immunoblotting. One representative blot out of three independent experiments is shown. Mean values ±SD from densitometric analysis are given (n=3). *, p<0,05; **, p<0.01 *versus* control

As further shown in Fig. 55, CyaA provoked the loss of FoxO3a inhibitory phosphorylation in monocytes. In contrast, exposure of monocytes to CyaA-AC$^-$ slightly increased FoxO3a phosphorylation.

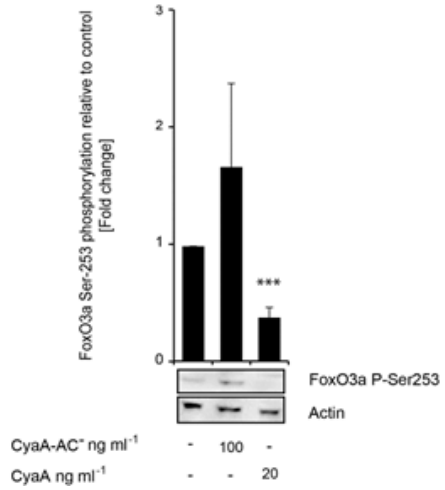

Fig. 55: CyaA causes decrease in inhibitory phosphorylation of FoxO3a. THP-1 monocytes were incubated with indicated concentration of CyaA variants for 30 minutes and phosphorylation status of FoxO3a was analyzed by immunoblotting. One representative blot out of three independent experiments is shown. Mean values ±SD from densitometric analysis are given (n=3). ***, p<0.001 *versus* control

AKT and PI3K signaling is not involved in the CyaA-provoked inhibition of NO production

AKT and its upstream activator PI3K were previously also shown to play an important role in regulation of NO production (Tsukamoto et al., 2008). Therefore, to

determine if the above observed inhibition of AKT by CyaA action may be contributing to the inhibition of NO production, we compared the effect of the toxin with that of the AKT inhibitor IV and the PI3K inhibitor wortmanin. While CyaA at concentrations of 10 ng/ml inhibited LPS-induced NO production, neither AKT inhibitor IV at concentration of 200 nM, nor 1 μM wortmanin exhibited any effect on NO production, as shown in Fig. 56. This result suggests that in the used cellular model, the AKT and PI3K signaling did not influence NO production.

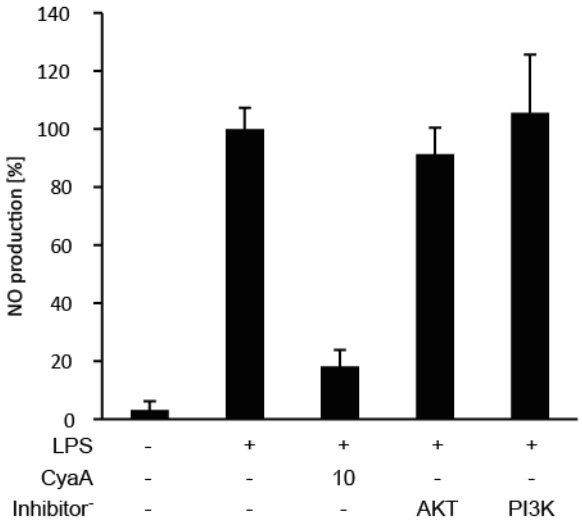

Fig. 56: CyaA does not inhibit LPS-stimulated NO production in RAW264.7 macrophages through AKT and PI3K. RAW264.7 macrophages were pre-treated with either a 200 nM AKT inhibitor IV or 1 μM wortmanin for 1 hour prior to the addition of 100 ng/ml of LPS for 24 hours. 10 ng/ml of CyaA was added concomitantly with LPS. Values represent the means ±SD from three independent experiments performed in triplicates (n=9). **, $p<0.001$ *versus* LPS treated control

9. Discussion

Whooping cough caused by *Bordetella pertussis* is a reemerging disease with an insufficiently understood mechanism of pathogenesis. Deeper characterization of processes involved in the interaction of *B. pertussis* with the innate immune system is, therefore, of high importance. In this thesis, we describe how CyaA, a key virulence factor of *Bordetella pertussis*, modulates bactericidal mechanisms of a host. *B. pertussis* survival is mainly dependent on the inhibition of ROS and RNS production by neutrophils and macrophages, respectively. We confirmed that the enzymatic activity of the adenylate cyclase toxin plays a crucial role in *Bordetella* escape from innate immunity control. This is in agreement with the already published studies showing the importance of CyaA for *B. pertussis* virulence (Goodwin and Weiss, 1990; Khelef et al., 1994; Khelef et al., 1992). The proposed model of CyaA-hijacked signaling pathways leading to the inhibition of the innate immune mechanisms of phagocytes is shown in Fig. 57.

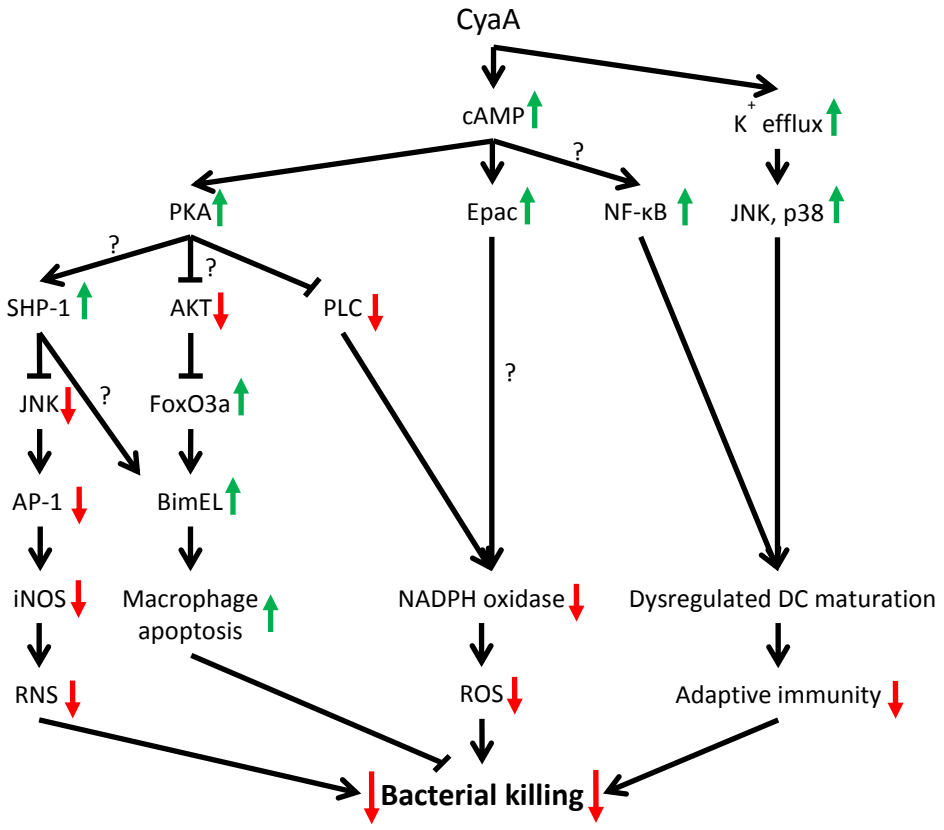

Fig. 57: Scheme of the CyaA-provoked signaling in cells of innate immune system. After binding of CyaA to the receptor, the toxin promotes pore-dependent potassium efflux and delivers the AC domain into the cytosol of phagocytes.

There, the AC domain of CyaA is activated by the binding of calmodulin and catalyzes uncontrolled conversion of cytosolic ATP into cAMP. This activates PKA- and Epac-dependent signaling. By an as yet uncharacterized mechanism, PKA activation leads to the enhancement of activity of the SHP-1 phosphatase, which yields dephosphorylation and loss of activity of the c-Fos subunit of the transcription factor AP-1. The loss of P-c-Fos function then prevents iNOS expression and NO production in TLR-activated macrophages. PKA simultaneously inhibits AKT by a mechanism that remains unknown. This leads to the activation of FoxO3a, which together with activated SHP-1 promotes Bim-dependent apoptosis. PKA-dependent inhibition of PLC together with an as yet unknown Epac-dependent mechanism leads to the blocking of NADPH assembly and the inhibition of ROS production.

Further, the potassium efflux through CyaA-formed pores activates MAPKs in DCs. This leads, together with cAMP-activated NF-κB translocation into cell nuclei, to dysregulation of maturation of DCs and to the shift in the development of anti-*Bordetella* adaptive immunity.

Block of ROS and RNS production, induction of apoptosis, and dysregulation of adaptive immune responses finally facilitate the survival of *Bordetella pertussis* in the infected host.

9.1. CyaA-provoked inhibition of ROS production by neutrophils

We have shown here that CyaA-provoked cAMP signaling enables *Bordetella pertussis* to escape rapid killing by neutrophils. As summarized in the model in Fig. 56, this process involves the blocking of PLC, resulting in the loss of ROS production by neutrophils. To target this important bactericidal mechanism, CyaA employs both PKA and Epac. Hijacking of this signaling pathway thus leads to overcoming of one of the first line defense mechanisms of the host.

Although, the capability of CyaA to inhibit ROS production has already been known for some time (Confer and Eaton, 1982), a mechanistic analysis of this phenomenon was missing. Previous studies examined the impact of CyaA action on ROS production stimulated by either serum-opsonized zymosan (Confer and Eaton, 1982; Pearson et al., 1987) or PMA (Eby et al., 2014). Neither zymosan nor PMA do, however, play any role in natural *B. pertussis* infection. In contrast, we used here fMLP, naturally originating from the bacterial lipoproteins, in order to induce ROS production in primary human neutrophils. We took an advantage here from the properly understood signaling pathway of this G Protein-Coupled Receptor (GPCR) agonist (Stadtmann and Zarbock, 2012). Moreover, fMLP-provoked signaling shares the production of two main second messengers with the signaling promoted by complement- or antibody-opsonized compounds. These second messengers are PIP3 formed by PI3K and DAG generated by PLC. Furthermore, the usage of fMLP stimulation instead of the use of specific immunocomplexes allowed us to explore signaling pathways that are independent of a broad range of immunoreceptor-

activated tyrosine kinases such as LYN and SYK (Nakayama et al., 2013; Tohyama and Yamamura, 2009). Note worthily, it was previously shown that CyaA provokes SYK inactivation by interfering with its phosphorylation in monocytes (Osicka *et al.*, manuscript in preparation). We were, however, unable to show the same in neutrophils (data not shown). Taken together, the model proposed in this thesis provides a more general inhibitory mechanism than simple targeting of SYK-mediated signaling of particular immunoreceptors.

We also show here that the inhibition of ROS production by cAMP is due to the inhibition of PLC activity. When the ROS production was stimulated by a direct PLC activator m-3M3FBS (Bae et al., 2003), it was still sensitive to CyaA, while the activation of PKC by PMA was resistant to CyaA action (cAMP signaling). This indicates that the inhibition of PLC by cAMP-dependent signaling is a general mechanism of the blocking of ROS production by CyaA.

The fact that ROS production stimulated by direct activation of PKC by PMA was resistant to CyaA action (*cf.* Fig. 26) is, however, in contrast with some previously published observations (Eby et al., 2014). The PMA concentration used by Eby (0.02 μM) was, however, not sufficient to induce a robust and thus potentially bactericidal ROS production (*cf.* Fig. 27), as the primary aim of that study was analysis of NETosis. The finding that the inhibition of PKC by CyaA leads to the inhibition of NETosis thus suggests that partially activated PKC can be sensitive to CyaA action and cAMP signaling. This is in agreement with our data showing that incomplete PKC activation can be partially overcome by CyaA action (*cf.* Fig. 27). Other possible explanations could be the different sensitivity of particular PKC isoforms to PMA (Nixon and McPhail, 1999). NETosis is driven selectively by PKC_{β} isoform, whereas ROS production could be activated by a broader range of PKCs (Gray et al., 2013). Hence, the PKC_{β} isoform could be sensitive to CyaA-promoted signaling, while other PKC isoforms may be resistant to the action of CyaA toxin.

Similarly to PKC, we have not observed a strong effect of CyaA on PI3K-produced PIP3 (*cf.* Fig. 25). This is in contrast to the results reported by others showing both activatory and inhibitory effects of cAMP signaling on the activity of PI3K isoforms (Cosentino et al., 2007; Feola et al., 2013; Rotfeld et al., 2014; Shen et al., 2011; Wang et al., 2001). The influence of cAMP signaling on PI3K activity

is, however, mainly described on non-immune cells. Moreover, our study was limited to PI3K$_\gamma$ and PI3K$_\beta$, which are the only PI3K isoforms activated by fMLP. Studies on other PI3K isoforms are currently in progress.

Finally, the inhibition of PLC by CyaA/cAMP signaling action could be explained by the PKA-dependent phosphorylation of PLC. PKA and its cell permeable activator 8-[4-chlorophenythio]-cAMP were found to provoke phosphorylation of PLC$_\beta$3 isoform on the S1105 residue, which led to its inhibition (Yue et al., 1998). It is important to note here that 8-[4-chlorophenythio]-cAMP analogue is not strictly PKA-specific. It was also found to activate the cGMP-dependent Protein Kinase G (PKG) (Sugita et al., 1994), cGMP-specific phosphodiesterase (Connolly et al., 1992), and the Epac protein, and this was described only after Yue's work was published (Rehmann et al., 2003). On the other hand, the phosphorylation of PLC by PKA could be specific, as the authors also detected PLC phosphorylation by PKA *in vitro* (Yue et al., 1998). The inhibition of PLC by PKA and not by Epac could also be the reason why CyaA action had a weaker effect on m-3M3FBS-induced ROS production as compared to fMLP-induced ROS production (*cf.* Fig. 26). In such a case, the additive effect of Epac activation would not be involved in the toxin-initiated inhibitory pathway, yielding a less effective inhibition of m-3M3FBS-induced ROS production. The contribution of Epac to inhibition of ROS production is thus more likely mediated by an interference of the Epac effector Rap1 with NADPH oxidase assembly. Indeed, Rap1 was recently found to interact with p47^{PHOX}, thus blocking Rac-mediated NADPH oxidase activation (Wang et al., 2014). The possibility of Rap1 interaction with NADPH oxidase has already been described by several *in vitro* studies (Vignais, 2002), although it was only thought to play an activatory role. The precise mechanism by which CyaA-mediated Epac/Rap1-activation leads to the blocking of ROS production remains to be elucidated in the future.

In addition to PKA and Epac activation by CyaA-produced cAMP, no other CyaA activity was found to contribute to the inhibition of ROS production (*cf.* Fig. 21). The role of enzymatic activity of CyaA in the inhibition of ROS production had also been described earlier (Confer and Eaton, 1982). Until now, however, the contribution of other activities of the toxin was not disqualified. The contribution of

other CyaA activities could be expected, as toxin-provoked calcium influx may have an impact on the PKC activity. Moreover, dysbalance of ion homeostasis and membrane potential due to the pore-forming activity of CyaA may also have an influence on NADPH assembly (Browning et al., 2014; Norton et al., 2013). Indeed, action of another pore-forming toxin, HlyA, was found to inhibit the AKT kinase required for NADPH oxidase assembly (Wiles et al., 2008).

The concentration of CyaA used here is likely biologically relevant, as the same amounts of CyaA were detected in mucosal fluids of *B. pertussis*-infected infants and experimentally challenged baboons (Eby et al., 2013). Moreover, AC activity of CyaA in the culture supernatant of neutrophils infected with *B. pertussis* at MOI 100:1 (*cf.* Fig. 17) corresponds to the activity of purified toxin used in our experiments (*cf.* Figs. 18 and 20). A lower concentration of the toxin was ineffective in blocking ROS production even after prolonged pre-incubation with neutrophils. This is in line with the amount of cAMP produced by different CyaA concentrations (*cf.* Fig. 22).

In contrast to the above described data, CyaA was unable to block ROS production in fMLP- or TNFα-primed neutrophils (*cf.* Fig. 29). This may explain why neutrophils are crucial for *B. pertussis* clearance from immunized mice, whereas they play no role in control of *B. pertussis* infection of naïve animals (Andreasen and Carbonetti, 2009). The most potent bactericidal activity of neutrophils – production of ROS – appears to be effectively blocked by physiological concentrations of CyaA. After immunization of mice, which leads to neutrophil priming by TNFα released by macrophages upon antigenic restimulation, neutrophils, however, become resistant to CyaA action. This observation may be of high interest for the development of the next generations of vaccines against *B. pertussis*. The vaccines should be examined for the capacity to induce TNFα-dependent priming of innate immunity (Quintin et al., 2014), which could protect against colonization by *B. pertussis*. This is not a case of current acellular pertussis vaccines, which protect against pertussis symptoms but not against colonization (Sebo et al., 2014).

Taken together, the here reported blocking of ROS production by CyaA is controlled by cAMP-activated PKA- and Epac-dependent signaling pathways. Moreover, the observed inhibition of PLC activity reveals that the composition of a

host membranes is a new target of CyaA action. Furthermore, the inhibition of PLC-dependent DAG production and subsequent ROS production in CyaA toxin-treated cells provoked a steep decrease of *B. pertussis* survival inside primary neutrophils. These observations reveal an as yet undescribed CyaA-provoked signaling mechanism by which the whooping cough agent *B. pertussis* achieves the ablation of bactericidal mechanisms of the innate immune system of the host.

9.2. CyaA-provoked inhibition of RNS production by macrophages

We further show here that cAMP-activated signaling through PKA yields the activation of the tyrosine phosphatase SHP-1. Hijacking of this novel cAMP-regulated signaling pathway by the adenylate cyclase toxin then enables *Bordetella pertussis* to evade NO-mediated killing inside macrophage cells. As summarized in the model shown in Fig. 56, the CyaA-cAMP-triggered activation of SHP-1 leads to dephosphorylation of the P-c-Fos subunit of the transcription factor AP-1 and results in the loss of TLR-induced expression of the iNOS enzyme and the loss of production of bactericidal levels of NO. This novel mechanism adds to the broad spectrum of immunosubversive outcomes of CyaA-catalyzed synthesis of cAMP in host phagocytes.

Somewhat controversial results were previously reported on the role of cAMP in the regulation of iNOS expression in different cell types and tissues. While cAMP was found to be a strong inducer of iNOS gene expression in rat vascular smooth muscle and mesangial cells, the elevation of cAMP in other rodent cells yielded a reduction of iNOS expression (Koide et al., 1993; Messmer and Brune, 1994; Pang and Hoult, 1997). In fact, it has been previously observed that a modulation of cAMP levels in RAW264.7 macrophages may impact LPS-induced expression of iNOS and NO production (Chang et al., 2013; Koide et al., 2003). We show here that low amounts of the CyaA toxin as 1 ng/ml do produce sufficient amounts of cAMP to cause a strong reduction of iNOS expression in LPS-activated macrophage cells (*cf.* Fig. 38). In agreement with a previous report (Kuo et al., 1997) and by contrast to CyaA, the pertussis toxin (PTX) produced by the mutant *cyaA-AC*$^{-}$ bacteria was unable to increase cAMP concentrations through dysregulation of the endogenous adenylyl cyclase to a level that would provoke a block of induction of bactericidal NO production in LPS-activated macrophage cells (*cf.* Fig. 36). Indeed, PTX action takes hours to translate into a cAMP increase in cells and it depends on an additional receptor signaling-mediated activation of the endogenous adenylyl cyclase enzyme. It is, therefore, plausible to propose that the steep increase of cAMP concentration, accomplished early upon bacterial contact with phagocytes by the CyaA toxin, was required for the prevention of TLR-activated iNOS expression. This is likely to have been made possible by two unique features of CyaA. Firstly, CyaA exhibits an

extraordinarily rapid mechanism of target cell penetration, where translocation the AC domain into cells occurs by an endocytosis-independent mechanism directly across the cytoplasmic membrane of cells, and it proceeds with a halftime of only about 30 seconds (Bumba et al., 2010; Gordon et al., 1988; Gordon et al., 1989; Rogel and Hanski, 1992). Secondly, the calmodulin-activated catalytic domain of CyaA possesses an extremely high specific AC enzyme activity, with a turnover number of about 2,000 s^{-1} (Rogel and Hanski, 1992). As a result, CyaA concentrations as low as used *in vitro* here (10 ng/ml) and detected in mucosal fluids of infected infants and experimentally challenged baboons (Eby et al., 2013), are not only sufficient for the ablation of superoxide production and NET release by host neutrophils (Confer and Eaton, 1982; Eby et al., 2014; Pearson et al., 1987), but also provoke the inhibition of bactericidal NO production in macrophages. This explains why CyaA expression is crucial for the extended survival of unopsonized *B. pertussis* bacteria in macrophages. These results further highlight the unique role played by CyaA in the subversion of the innate immunity mechanisms, explaining the importance of the role played by CyaA in the early phases of bacterial colonization of host airways (Goodwin and Weiss, 1990; Khelef et al., 1992; Sebo et al., 2014; Vojtova et al., 2006).

While major differences exist in iNOS expression regulation in man and mice, the expression of bactericidal iNOS in human phagocytes and the role of NO in innate immunity in man is now well established (Fang and Vazquez-Torres, 2002). iNOS expression in human macrophages, however, require, besides activation by LPS, the simultaneous involvement of several cytokine signals (e.g. IFNγ, TNFα, and IL-1β). This makes the deciphering of signaling pathways leading to iNOS expression in human phagocytes difficult. In contrast, LPS alone is sufficient for strong iNOS expression in murine macrophages (Pautz et al., 2010). Therefore, mouse cells like the RAW264.7 macrophages are preferentially used for analysis of signaling that leads to bactericidal iNOS expression in phagocytes (Chang et al., 2013; Koide et al., 2003; Tsukamoto et al., 2008). Using these cells, we reveal here the prominent role played by cAMP signaling in the regulation of the activity of the transcription factors involved in iNOS expression in phagocytes. This remains scarcely documented in the literature. The activation of the NF-κB transcription factor in human keratinocytes by db-cAMP or forskolin has previously been reported

(Qi et al., 2009), which goes well with the here observed triggering of NF-κB translocation into cell nuclei by the cAMP-elevating activity of CyaA (*cf.* Fig. 43). While NF-κB activation alone cannot lead to the blocking of iNOS expression, Hickey and co-workers observed previously that cAMP production by CyaA caused a decrease of levels of both IRF1 and IRF8 transcription factors (Hickey et al., 2008). Similarly, cAMP elevation by cholera toxin was found to cause inhibition of IRF1-IRF8 interaction (la Sala et al., 2009). Furthermore, IRF1 and STAT1 activities were also found to be inhibited upon VPAC1-mediated PKA activation by a mechanism independent of Suppressor Of Cytokine Signaling 1/3 (Delgado and Ganea, 2000). Hence, the previous observations that IRF1 and Stat1 activities are regulated by cAMP go well with our results showing that CyaA activity concomitantly decreased Stat1 phosphorylation and IRF1 levels (*cf.* Fig. 44). While Stat1 activation was previously found to be inhibited via cAMP/PKA signaling-triggered activation of SHP-2 (Tai et al., 2014), we observed here a highly SHP-1-specific effect of cAMP increase on LPS-triggered iNOS expression in murine macrophage cells. Moreover, inhibition of Stat1 by CyaA did not occur before the inhibition of iNOS expression (*cf.* Fig. 45), showing that Stat1 inhibition does not play a major role in the first phase of inhibition of iNOS expression. In contrast, the effects of CyaA-provoked cAMP signaling on phosphorylation of the c-Fos subunit of AP-1 correlated in time with the observed inhibition of iNOS expression.

The c-Fos subunit of the transcription factor AP-1 was, indeed, shown to undergo hyperphosphorylation at multiple sites upon macrophage activation by LPS. This increases its activity (Pellegrino and Stork, 2006) and accounts for the appearance of several P-c-Fos bands, or a smear of hyperphosphorylated P-c-Fos, in immunoblots with P-c-Fos-specific antibodies. The here analyzed CyaA-produced cAMP signaling then caused dephosphorylation of the hyperphosphorylated P-c-Fos into the hypophosphorylated c-Fos. This suggests that P-c-Fos was, indeed, the primary target of PKA activation-dependent signaling in the course of CyaA action and that dephosphorylation of P-c-Fos accounted for the inhibition of iNOS expression.

The inhibitory effect of CyaA on the transcription factor AP-1 is very likely due to interference with MAPK signaling, which is known to play a major role in

regulation of AP-1. The here described results are in agreement with the effect of CyaA on the MAPK activity described elsewhere.

Intriguingly, manipulation of iNOS expression through a very different mechanism of protease-dependent activation of SHP-1 and a subsequent modulation of c-Fos activity has been previously observed in mouse macrophages infected with *Leishmania donovani* (Blanchette et al., 2009; Gomez et al., 2009; Nandan et al., 1999). Moreover, LPS-triggered iNOS expression in murine macrophages could previously have been blocked by the activation of SHP-1 (Hardin et al., 2006). We describe here, however, the activation of SHP-1 by a mechanism dependent on cAMP elevation and PKA activity. Intriguingly, while the cAMP levels increased with time of toxin action (*cf.* Fig. 36) and presumably the PKA activity remained high over the duration of cell exposure to CyaA, the activation of SHP-1 by toxin-produced cAMP signaling was only transient. The mechanism underlying the down-regulation of SHP-1 activity after prolonged cell exposure to CyaA (60 min, *cf.* Fig. 50) remains unknown but correlates in time with the cAMP-provoked transient inhibition of the small GTPase RhoA activity in CyaA-treated murine macrophages, which was maximal at 30 minutes from the toxin addition (Kamanova et al., 2008). It will, therefore, be of interest to determine if the same regulatory circuit is involved in the modulation of both RhoA and SHP-1 activities by toxin-produced cAMP signaling. PKA, in fact, likely exerts its effect on SHP-1 activity by an indirect mechanism, as no phosphorylation consensus sequence for PKA (-RRXS/T- where X stands for any amino acid) is found in SHP-1 sequence, in contrast to SHP-2. We then conclude that it is selectively the cAMP-activated PKA signaling that leads to the activation of SHP-1. This is based on the observation that the Epac-specific cell-permeable activator 8-CPT-cAMP exerted little, if any, effect on c-Fos phosphorylation, iNOS expression and NO production. In contrast, the PKA specific activator 6-Bnz-cAMP mimicked to a large extent the impact of CyaA action on cells. Hence, cAMP-dependent activation of PKA clearly played a dominant role in CyaA-provoked suppression of iNOS expression in macrophages. However, it cannot be definitively concluded at present that only PKA signaling was involved and Epac did not play any role in the control of TLR-induced iNOS expression. PKA inhibition with H-89 did not fully revert the impact of CyaA action on iNOS expression. Moreover, H-89 is known to exert some off-target effects (Bain et al.,

2007) and H-89 on its own was found to partially impair iNOS expression (*cf.* Fig. 40). It is thus possible that due to high levels of cAMP produced in cells by CyaA, the H-89 inhibitor at the usual concentration of 10 μM was just unable to completely inhibit the fully activated PKA signaling.

Taken together, the here reported modulation of iNOS expression by the cAMP/PKA-regulated SHP-1 activity indicates that SHP-1 plays a rather central role in the control of iNOS expression and *B. pertussis* survival in macrophages. Furthermore, selective silencing of SHP-1 expression led to the restoration of NO production in CyaA toxin-treated RAW264.7 cells and the inhibition of SHP-1/2 phosphatases by NSC87877 provoked a steep decrease of *B. pertussis* survival inside macrophages. These observations reveal an as yet undescribed cAMP/PKA-regulated signaling mechanism that is manipulated by the CyaA toxin of the whooping cough agent *B. pertussis*. This reveals an opportunity for the development and testing of novel SHP-1-specific inhibitors as potential drugs for the treatment of pertussis in the early phases of *B. pertussis* infections.

10. Conclusions

In this thesis we describe the achieved progress in our understanding of mechanisms that underlie the ablation of the innate immunity by the causative agent of whooping cough – *Bordetella pertussis.*

1) We showed that *B. pertussis* employs the enzymatic activity of CyaA in order to survive the initial contact with innate immune cells and to avoid being killed by oxidative burst of these sentinel cells of innate immunity.
2) We showed that PKA and Epac collaborate in CyaA/cAMP-triggered inhibition of ROS production by neutrophils.
3) We identified PLC as the primary target of CyaA-induced signaling that leads to the blocking of ROS production by neutrophils.
4) Using primed neutrophils, we reveal a mechanism that potentially enables vaccinated animals to clear *B. pertussis* infection.
5) In contrast to the blocking of ROS production, CyaA-dependent PKA activation is sufficient to block NO production and iNOS expression in macrophages.
6) We describe here, that the enzymatic activity of CyaA yielding cAMP signaling does inhibit Stat1 and IRF1 transcription factors and JNK signaling, while it activates the NF-κB transcription factor. Moreover, the pore-forming activity of CyaA activates JNK and p38. This dysregulation of signaling pathways then leads to altered gene expression patterns and finally yields dysregulation of DC maturation.
7) Furthermore, CyaA enzymatic activity accounts for the blocking of the AP-1-dependent iNOS expression by the activation of the tyrosine phosphatase SHP-1.
8) We have identified the activation of SHP-1 by CyaA as a crucial step in the survival of *B. pertussis* during interaction with macrophages.
9) We also described that the inhibition of AKT by CyaA enzymatic activity is important for the induction of apoptosis of monocytes, while it does not play any role in the inhibition of NO production.

11. Abbreviations

AC	Adenylate Cyclase
AP-1	Activator Protein 1
ATP	adenosine triphosphate
BMDM	bone marrow-derived macrophages
BMDC	bone marrow-derived dendritic cells
B.p. cyaA-wt	*Bordetella pertussis* producing wild type CyaA
B.p. cyaA-AC$^-$	*Bordetella pertussis* producing detoxified CyaA-AC$^-$
B.p. ΔcyaA	*Bordetella pertussis* with in frame deletion of *cyaA* gene
6-Bnz-cAMP	N^6- Benzoyladenosine- 3', 5'- cyclic monophosphate
cAMP	adenosine 3',5'- cyclic monophosphate
cAMPS	8- Bromoadenosine- 3', 5'- cyclic monophosphorothioate, Rp- isomer
CD	cluster of differentiation
CDK	Cyclin-Dependent Kinase
8-CPT-cAMP	8-(4-chlorophenylthio)-2'-O-methyladenosine-3',5'-cyclic monophosphate
CyaA	adenylate cyclase toxin, ACT
CR3	Complement Receptor 3, integrin CD11b/CD18, $\alpha_M\beta_2$, Mac1
DAG	diacylglycerol
DNT	DermoNecrotic Toxin
ERK	Extracellular signal-Regulated Kinase
FHA	Filamentous Hemagglutinin
fMLP	formyl-Methionyl-Leucyl-Phenylalanine
IL	InterLeukin
iNOS	inducible nitric oxide synthase, NOS2
IRF	Interferon Regulatory Factor
LPS	lipopolysaccharide
MAPK	Mitogen-Activated Protein Kinase
NADPH	nicotinamide adenine dinucleotide phosphate
NF-κB	Nuclear Factor κB
NO	nitric oxide
PI3K	PhosphoInositide 3-kinase
PIP3	phosphatidylinositol (3,4,5)-trisphosphate
PKA	cAMP dependent Protein Kinase A
PLC	PhosphoLipase C
PRN	Pertactin
PTX	Pertussis Toxin
ROS	reactive oxygen species
RNS	reactive nitrogen species
RTX	Repeat in ToXin
SHP	SH2 domain-containing protein tyrosine Phosphatase
siRNA	small interfering RNA
Stat	Signal Transducer and Activator of Transcription
TCT	Tracheal CytoToxin
TLR	Toll-Like Receptor
TNF	Tumor Necrosis Factor
T1SS	Type I secretion system
T3SS	Type III secretion system

12. References

Adkins, I., Kamanova, J., Kocourkova, A., Svedova, M., Tomala, J., Janova, H., Masin, J., Chladkova, B., Bumba, L., Kovar, M., *et al.* (2014). *Bordetella* adenylate cyclase toxin differentially modulates toll-like receptor-stimulated activation, migration and T cell stimulatory capacity of dendritic cells. PLoS One *9*, e104064.

Ago, T., Takeya, R., Hiroaki, H., Kuribayashi, F., Ito, T., Kohda, D., and Sumimoto, H. (2001). The PX domain as a novel phosphoinositide- binding module. Biochem Biophys Res Commun *287*, 733-738.

Ahuja, N., Kumar, P., and Bhatnagar, R. (2004). The adenylate cyclase toxins. Crit Rev Microbiol *30*, 187-196.

Akashi, K., Traver, D., Miyamoto, T., and Weissman, I.L. (2000). A clonogenic common myeloid progenitor that gives rise to all myeloid lineages. Nature *404*, 193-197.

Alonso, S., Pethe, K., Mielcarek, N., Raze, D., and Locht, C. (2001). Role of ADP-ribosyltransferase activity of pertussis toxin in toxin-adhesin redundancy with filamentous hemagglutinin during *Bordetella pertussis* infection. Infect Immun *69*, 6038-6043.

Ambagala, T.C., Ambagala, A.P., and Srikumaran, S. (1999). The leukotoxin of *Pasteurella haemolytica* binds to beta(2) integrins on bovine leukocytes. FEMS Microbiol Lett *179*, 161-167.

Amdahl, H., Jarva, H., Haanpera, M., Mertsola, J., He, Q., Jokiranta, T.S., and Meri, S. (2011). Interactions between *Bordetella pertussis* and the complement inhibitor factor H. Mol Immunol *48*, 697-705.

Anderson, K.E., Boyle, K.B., Davidson, K., Chessa, T.A., Kulkarni, S., Jarvis, G.E., Sindrilaru, A., Scharffetter-Kochanek, K., Rausch, O., Stephens, L.R., *et al.* (2008). CD18-dependent activation of the neutrophil NADPH oxidase during phagocytosis of *Escherichia coli* or *Staphylococcus aureus* is regulated by class III but not class I or II PI3Ks. Blood *112*, 5202-5211.

Anderson, K.E., Chessa, T.A., Davidson, K., Henderson, R.B., Walker, S., Tolmachova, T., Grys, K., Rausch, O., Seabra, M.C., Tybulewicz, V.L., *et al.* (2010). PtdIns3P and Rac direct the assembly of the NADPH oxidase on a novel, pre-phagosomal compartment during FcR-mediated phagocytosis in primary mouse neutrophils. Blood *116*, 4978-4989.

Anderson, T.R. (1982). Cyclic cytidine 3',5'-monophosphate (cCMP) in cell regulation. Mol Cell Endocrinol *28*, 373-385.

Andreasen, C., and Carbonetti, N.H. (2008). Pertussis toxin inhibits early chemokine production to delay neutrophil recruitment in response to *Bordetella pertussis* respiratory tract infection in mice. Infect Immun *76*, 5139-5148.

Andreasen, C., and Carbonetti, N.H. (2009). Role of neutrophils in response to *Bordetella pertussis* infection in mice. Infect Immun *77*, 1182-1188.

Arico, B., and Rappuoli, R. (1987). *Bordetella parapertussis* and *Bordetella bronchiseptica* contain transcriptionally silent pertussis toxin genes. J Bacteriol *169*, 2847-2853.

Aronoff, D.M., Canetti, C., and Peters-Golden, M. (2004). Prostaglandin E2 inhibits alveolar macrophage phagocytosis through an E-prostanoid 2 receptor-mediated increase in intracellular cyclic AMP. J Immunol *173*, 559-565.

Aronoff, D.M., Canetti, C., Serezani, C.H., Luo, M., and Peters-Golden, M. (2005). Cutting edge: macrophage inhibition by cyclic AMP (cAMP): differential roles of

protein kinase A and exchange protein directly activated by cAMP-1. J Immunol *174*, 595-599.
Aronoff, D.M., Carstens, J.K., Chen, G.H., Toews, G.B., and Peters-Golden, M. (2006). Short communication: differences between macrophages and dendritic cells in the cyclic AMP-dependent regulation of lipopolysaccharide-induced cytokine and chemokine synthesis. J Interferon Cytokine Res *26*, 827-833.
Atkinson, J.P., Michael, J.M., Chaplin, H., Jr., and Parker, C.W. (1977). Modulation of macrophage C3b receptor function by cytochalasin-sensitive structures. J Immunol *118*, 1292-1299.
Bae, Y.S., Lee, T.G., Park, J.C., Hur, J.H., Kim, Y., Heo, K., Kwak, J.Y., Suh, P.G., and Ryu, S.H. (2003). Identification of a compound that directly stimulates phospholipase C activity. Mol Pharmacol *63*, 1043-1050.
Bagley, K.C., Abdelwahab, S.F., Tuskan, R.G., Fouts, T.R., and Lewis, G.K. (2002). Pertussis toxin and the adenylate cyclase toxin from *Bordetella pertussis* activate human monocyte-derived dendritic cells and dominantly inhibit cytokine production through a cAMP-dependent pathway. J Leukoc Biol *72*, 962-969.
Bachelet, M., Richard, M.J., Francois, D., and Polla, B.S. (2002). Mitochondrial alterations precede *Bordetella pertussis*-induced apoptosis. FEMS Immunol Med Microbiol *32*, 125-131.
Baillie, G.S., Scott, J.D., and Houslay, M.D. (2005). Compartmentalisation of phosphodiesterases and protein kinase A: opposites attract. FEBS Lett *579*, 3264-3270.
Bain, J., Plater, L., Elliott, M., Shpiro, N., Hastie, C.J., McLauchlan, H., Klevernic, I., Arthur, J.S., Alessi, D.R., and Cohen, P. (2007). The selectivity of protein kinase inhibitors: a further update. Biochem J *408*, 297-315.
Barnes, M.G., and Weiss, A.A. (2001). BrkA protein of *Bordetella pertussis* inhibits the classical pathway of complement after C1 deposition. Infect Immun *69*, 3067-3072.
Barry, E.M., Weiss, A.A., Ehrmann, I.E., Gray, M.C., Hewlett, E.L., and Goodwin, M.S. (1991). *Bordetella pertussis* adenylate cyclase toxin and hemolytic activities require a second gene, cyaC, for activation. J Bacteriol *173*, 720-726.
Basar, T., Havlicek, V., Bezouskova, S., Hackett, M., and Sebo, P. (2001). Acylation of lysine 983 is sufficient for toxin activity of *Bordetella pertussis* adenylate cyclase. Substitutions of alanine 140 modulate acylation site selectivity of the toxin acyltransferase CyaC. J Biol Chem *276*, 348-354.
Basar, T., Havlicek, V., Bezouskova, S., Halada, P., Hackett, M., and Sebo, P. (1999). The conserved lysine 860 in the additional fatty-acylation site of *Bordetella pertussis* adenylate cyclase is crucial for toxin function independently of its acylation status. J Biol Chem *274*, 10777-10783.
Basler, M., Knapp, O., Masin, J., Fiser, R., Maier, E., Benz, R., Sebo, P., and Osicka, R. (2007). Segments crucial for membrane translocation and pore-forming activity of *Bordetella* adenylate cyclase toxin. J Biol Chem *282*, 12419-12429.
Basler, M., Masin, J., Osicka, R., and Sebo, P. (2006). Pore-forming and enzymatic activities of *Bordetella pertussis* adenylate cyclase toxin synergize in promoting lysis of monocytes. Infect Immun *74*, 2207-2214.
Bassinet, L., Fitting, C., Housset, B., Cavaillon, J.M., and Guiso, N. (2004). *Bordetella pertussis* adenylate cyclase-hemolysin induces interleukin-6 secretion by human tracheal epithelial cells. Infect Immun *72*, 5530-5533.

Bassinet, L., Gueirard, P., Maitre, B., Housset, B., Gounon, P., and Guiso, N. (2000). Role of adhesins and toxins in invasion of human tracheal epithelial cells by *Bordetella pertussis*. Infect Immun *68*, 1934-1941.
Batra, S., Cai, S., Balamayooran, G., and Jeyaseelan, S. (2012). Intrapulmonary administration of leukotriene B(4) augments neutrophil accumulation and responses in the lung to *Klebsiella* infection in CXCL1 knockout mice. J Immunol *188*, 3458-3468.
Baumann, U. (1994). Crystal structure of the 50 kDa metallo protease from *Serratia marcescens*. J Mol Biol *242*, 244-251.
Baumann, U., Wu, S., Flaherty, K.M., and McKay, D.B. (1993). Three-dimensional structure of the alkaline protease of *Pseudomonas aeruginosa*: a two-domain protein with a calcium binding parallel beta roll motif. EMBO J *12*, 3357-3364.
Beavo, J.A., and Brunton, L.L. (2002). Cyclic nucleotide research -- still expanding after half a century. Nat Rev Mol Cell Biol *3*, 710-718.
Bedard, K., and Krause, K.H. (2007). The NOX family of ROS-generating NADPH oxidases: physiology and pathophysiology. Physiol Rev *87*, 245-313.
Bejerano, M., Nisan, I., Ludwig, A., Goebel, W., and Hanski, E. (1999). Characterization of the C-terminal domain essential for toxic activity of adenylate cyclase toxin. Mol Microbiol *31*, 381-392.
Belcher, C.E., Drenkow, J., Kehoe, B., Gingeras, T.R., McNamara, N., Lemjabbar, H., Basbaum, C., and Relman, D.A. (2000). The transcriptional responses of respiratory epithelial cells to *Bordetella pertussis* reveal host defensive and pathogen counter-defensive strategies. Proc Natl Acad Sci U S A *97*, 13847-13852.
Bellalou, J., Sakamoto, H., Ladant, D., Geoffroy, C., and Ullmann, A. (1990). Deletions affecting hemolytic and toxin activities of *Bordetella pertussis* adenylate cyclase. Infect Immun *58*, 3242-3247.
Bengis-Garber, C., and Gruener, N. (1996). Protein kinase A downregulates the phosphorylation of p47 phox in human neutrophils: a possible pathway for inhibition of the respiratory burst. Cell Signal *8*, 291-296.
Benna, J.E., Dang, P.M., Gaudry, M., Fay, M., Morel, F., Hakim, J., and Gougerot-Pocidalo, M.A. (1997). Phosphorylation of the respiratory burst oxidase subunit p67(phox) during human neutrophil activation. Regulation by protein kinase C-dependent and independent pathways. J Biol Chem *272*, 17204-17208.
Benz, R., Maier, E., Ladant, D., Ullmann, A., and Sebo, P. (1994). Adenylate cyclase toxin (CyaA) of *Bordetella pertussis*. Evidence for the formation of small ion-permeable channels and comparison with HlyA of *Escherichia coli*. J Biol Chem *269*, 27231-27239.
Berger, J.T., Carcillo, J.A., Shanley, T.P., Wessel, D.L., Clark, A., Holubkov, R., Meert, K.L., Newth, C.J., Berg, R.A., Heidemann, S., *et al.* (2013). Critical pertussis illness in children: a multicenter prospective cohort study. Pediatr Crit Care Med *14*, 356-365.
Berggard, K., Johnsson, E., Mooi, F.R., and Lindahl, G. (1997). *Bordetella pertussis* binds the human complement regulator C4BP: role of filamentous hemagglutinin. Infect Immun *65*, 3638-3643.
Berkowitz, S.A., Goldhammer, A.R., Hewlett, E.L., and Wolff, J. (1980). Activation of prokaryotic adenylate cyclase by calmodulin. Ann N Y Acad Sci *356*, 360.
Betsou, F., Sebo, P., and Guiso, N. (1993). CyaC-mediated activation is important not only for toxic but also for protective activities of *Bordetella pertussis* adenylate cyclase-hemolysin. Infect Immun *61*, 3583-3589.

Betsou, F., Sebo, P., and Guiso, N. (1995). The C-terminal domain is essential for protective activity of the *Bordetella pertussis* adenylate cyclase-hemolysin. Infect Immun *63*, 3309-3315.
Bibova, I., Skopova, K., Masin, J., Cerny, O., Hot, D., Sebo, P., and Vecerek, B. (2013). The RNA chaperone Hfq is required for virulence of *Bordetella pertussis*. Infect Immun *81*, 4081-4090.
Birkebaek, N.H., Kristiansen, M., Seefeldt, T., Degn, J., Moller, A., Heron, I., Andersen, P.L., Moller, J.K., and Ostergard, L. (1999). *Bordetella pertussis* and chronic cough in adults. Clin Infect Dis *29*, 1239-1242.
Blanchette, J., Abu-Dayyeh, I., Hassani, K., Whitcombe, L., and Olivier, M. (2009). Regulation of macrophage nitric oxide production by the protein tyrosine phosphatase Src homology 2 domain phosphotyrosine phosphatase 1 (SHP-1). Immunology *127*, 123-133.
Bokoch, G.M., Katada, T., Northup, J.K., Hewlett, E.L., and Gilman, A.G. (1983). Identification of the predominant substrate for ADP-ribosylation by islet activating protein. J Biol Chem *258*, 2072-2075.
Bonaparte, K.L., Hudson, C.A., Wu, C., and Massa, P.T. (2006). Inverse regulation of inducible nitric oxide synthase (iNOS) and arginase I by the protein tyrosine phosphatase SHP-1 in CNS glia. Glia *53*, 827-835.
Boschwitz, J.S., Batanghari, J.W., Kedem, H., and Relman, D.A. (1997). *Bordetella pertussis* infection of human monocytes inhibits antigen-dependent CD4 T cell proliferation. J Infect Dis *176*, 678-686.
Bouhss, A., Krin, E., Munier, H., Gilles, A.M., Danchin, A., Glaser, P., and Barzu, O. (1993). Cooperative phenomena in binding and activation of *Bordetella pertussis* adenylate cyclase by calmodulin. J Biol Chem *268*, 1690-1694.
Boucher, P.E., Menozzi, F.D., and Locht, C. (1994). The modular architecture of bacterial response regulators. Insights into the activation mechanism of the BvgA transactivator of *Bordetella pertussis*. J Mol Biol *241*, 363-377.
Bouin, A.P., Grandvaux, N., Vignais, P.V., and Fuchs, A. (1998). p40(phox) is phosphorylated on threonine 154 and serine 315 during activation of the phagocyte NADPH oxidase. Implication of a protein kinase c-type kinase in the phosphorylation process. J Biol Chem *273*, 30097-30103.
Boulanger, A., Chen, Q., Hinton, D.M., and Stibitz, S. (2013). In vivo phosphorylation dynamics of the *Bordetella pertussis* virulence-controlling response regulator BvgA. Mol Microbiol *88*, 156-172.
Bourdonnay, E., Serezani, C.H., Aronoff, D.M., and Peters-Golden, M. (2012). Regulation of alveolar macrophage p40phox: hierarchy of activating kinases and their inhibition by PGE2. J Leukoc Biol *92*, 219-231.
Boyd, A.P., Ross, P.J., Conroy, H., Mahon, N., Lavelle, E.C., and Mills, K.H. (2005). *Bordetella pertussis* adenylate cyclase toxin modulates innate and adaptive immune responses: distinct roles for acylation and enzymatic activity in immunomodulation and cell death. J Immunol *175*, 730-738.
Brickman, T.J., Cummings, C.A., Liew, S.Y., Relman, D.A., and Armstrong, S.K. (2011). Transcriptional profiling of the iron starvation response in *Bordetella pertussis* provides new insights into siderophore utilization and virulence gene expression. J Bacteriol *193*, 4798-4812.
Brock, T.G., Serezani, C.H., Carstens, J.K., Peters-Golden, M., and Aronoff, D.M. (2008). Effects of prostaglandin E2 on the subcellular localization of Epac-1 and Rap1 proteins during Fcgamma-receptor-mediated phagocytosis in alveolar macrophages. Exp Cell Res *314*, 255-263.

Browning, E., Wang, H., Hong, N., Yu, K., Buerk, D.G., DeBolt, K., Gonder, D., Sorokina, E.M., Patel, P., De Leon, D.D., *et al.* (2014). Mechanotransduction drives post ischemic revascularization through K(ATP) channel closure and production of reactive oxygen species. Antioxid Redox Signal *20*, 872-886.
Brubaker, A.L., Palmer, J.L., and Kovacs, E.J. (2011). Age-related Dysregulation of Inflammation and Innate Immunity: Lessons Learned from Rodent Models. Aging Dis *2*, 346-360.
Buasri, W., Impoolsup, A., Boonchird, C., Luengchaichawange, A., Prompiboon, P., Petre, J., and Panbangred, W. (2012). Construction of *Bordetella pertussis* strains with enhanced production of genetically-inactivated Pertussis Toxin and Pertactin by unmarked allelic exchange. BMC Microbiol *12*, 61.
Bumba, L., Masin, J., Fiser, R., and Sebo, P. (2010). *Bordetella* adenylate cyclase toxin mobilizes its beta2 integrin receptor into lipid rafts to accomplish translocation across target cell membrane in two steps. PLoS Pathog *6*, e1000901.
Byrd, M.S., Mason, E., Henderson, M.W., Scheller, E.V., and Cotter, P.A. (2013). An improved recombination-based in vivo expression technology-like reporter system reveals differential cyaA gene activation in *Bordetella* species. Infect Immun *81*, 1295-1305.
Canetti, C., Serezani, C.H., Atrasz, R.G., White, E.S., Aronoff, D.M., and Peters-Golden, M. (2007). Activation of phosphatase and tensin homolog on chromosome 10 mediates the inhibition of FcgammaR phagocytosis by prostaglandin E2 in alveolar macrophages. J Immunol *179*, 8350-8356.
Canthaboo, C., Xing, D., Wei, X.Q., and Corbel, M.J. (2002). Investigation of role of nitric oxide in protection from *Bordetella pertussis* respiratory challenge. Infect Immun *70*, 679-684.
Carbonetti, N.H., Artamonova, G.V., Van Rooijen, N., and Ayala, V.I. (2007). Pertussis toxin targets airway macrophages to promote *Bordetella pertussis* infection of the respiratory tract. Infect Immun *75*, 1713-1720.
Clark, J., Anderson, K.E., Juvin, V., Smith, T.S., Karpe, F., Wakelam, M.J., Stephens, L.R., and Hawkins, P.T. (2011). Quantification of PtdInsP3 molecular species in cells and tissues by mass spectrometry. Nat Methods *8*, 267-272.
Condliffe, A.M., Davidson, K., Anderson, K.E., Ellson, C.D., Crabbe, T., Okkenhaug, K., Vanhaesebroeck, B., Turner, M., Webb, L., Wymann, M.P., *et al.* (2005). Sequential activation of class IB and class IA PI3K is important for the primed respiratory burst of human but not murine neutrophils. Blood *106*, 1432-1440.
Confer, D.L., and Eaton, J.W. (1982). Phagocyte impotence caused by an invasive bacterial adenylate cyclase. Science *217*, 948-950.
Connolly, B.J., Willits, P.B., Warrington, B.H., and Murray, K.J. (1992). 8-(4-Chlorophenyl)thio-cyclic AMP is a potent inhibitor of the cyclic GMP-specific phosphodiesterase (PDE VA). Biochem Pharmacol *44*, 2303-2306.
Conover, M.S., Sloan, G.P., Love, C.F., Sukumar, N., and Deora, R. (2010). The Bps polysaccharide of *Bordetella pertussis* promotes colonization and biofilm formation in the nose by functioning as an adhesin. Mol Microbiol *77*, 1439-1455.
Cookson, B.T., Tyler, A.N., and Goldman, W.E. (1989). Primary structure of the peptidoglycan-derived tracheal cytotoxin of *Bordetella pertussis*. Biochemistry *28*, 1744-1749.
Corraliza, I.M., Campo, M.L., Soler, G., and Modolell, M. (1994). Determination of arginase activity in macrophages: a micromethod. J Immunol Methods *174*, 231-235.

Cortese-Krott, M.M., Rodriguez-Mateos, A., Kuhnle, G.G., Brown, G., Feelisch, M., and Kelm, M. (2012). A multilevel analytical approach for detection and visualization of intracellular NO production and nitrosation events using diaminofluoresceins. Free Radic Biol Med *53*, 2146-2158.
Cosentino, C., Di Domenico, M., Porcellini, A., Cuozzo, C., De Gregorio, G., Santillo, M.R., Agnese, S., Di Stasio, R., Feliciello, A., Migliaccio, A., *et al.* (2007). p85 regulatory subunit of PI3K mediates cAMP-PKA and estrogens biological effects on growth and survival. Oncogene *26*, 2095-2103.
Cowell, J.L., Hewlett, E.L., and Manclark, C.R. (1979). Intracellular localization of the dermonecrotic toxin of *Bordetella pertussis*. Infect Immun *25*, 896-901.
Cummings, C.A., Brinig, M.M., Lepp, P.W., van de Pas, S., and Relman, D.A. (2004). *Bordetella* species are distinguished by patterns of substantial gene loss and host adaptation. J Bacteriol *186*, 1484-1492.
Curnutte, J.T., Erickson, R.W., Ding, J., and Badwey, J.A. (1994). Reciprocal interactions between protein kinase C and components of the NADPH oxidase complex may regulate superoxide production by neutrophils stimulated with a phorbol ester. J Biol Chem *269*, 10813-10819.
Dadaglio, G., Fayolle, C., Zhang, X., Ryffel, B., Oberkampf, M., Felix, T., Hervas-Stubbs, S., Osicka, R., Sebo, P., Ladant, D., *et al.* (2014). Antigen targeting to CD11b+ dendritic cells in association with TLR4/TRIF signaling promotes strong CD8+ T cell responses. J Immunol *193*, 1787-1798.
Dang, P.M., Morel, F., Gougerot-Pocidalo, M.A., and El Benna, J. (2003). Phosphorylation of the NADPH oxidase component p67(PHOX) by ERK2 and P38MAPK: selectivity of phosphorylated sites and existence of an intramolecular regulatory domain in the tetratricopeptide-rich region. Biochemistry *42*, 4520-4526.
Daniel, D.S., Dai, G., Singh, C.R., Lindsey, D.R., Smith, A.K., Dhandayuthapani, S., Hunter, R.L., Jr., and Jagannath, C. (2006). The reduced bactericidal function of complement C5-deficient murine macrophages is associated with defects in the synthesis and delivery of reactive oxygen radicals to mycobacterial phagosomes. J Immunol *177*, 4688-4698.
de Mendez, I., Adams, A.G., Sokolic, R.A., Malech, H.L., and Leto, T.L. (1996). Multiple SH3 domain interactions regulate NADPH oxidase assembly in whole cells. EMBO J *15*, 1211-1220.
Decker, K.B., James, T.D., Stibitz, S., and Hinton, D.M. (2012). The *Bordetella pertussis* model of exquisite gene control by the global transcription factor BvgA. Microbiology *158*, 1665-1676.
Delepelaire, P. (2004). Type I secretion in gram-negative bacteria. Biochim Biophys Acta *1694*, 149-161.
Delgado, M., and Ganea, D. (2000). Inhibition of IFN-gamma-induced janus kinase-1-STAT1 activation in macrophages by vasoactive intestinal peptide and pituitary adenylate cyclase-activating polypeptide. J Immunol *165*, 3051-3057.
Diamond, G., Legarda, D., and Ryan, L.K. (2000). The innate immune response of the respiratory epithelium. Immunol Rev *173*, 27-38.
Diavatopoulos, D.A., Cummings, C.A., Schouls, L.M., Brinig, M.M., Relman, D.A., and Mooi, F.R. (2005). *Bordetella pertussis*, the causative agent of whooping cough, evolved from a distinct, human-associated lineage of *B. bronchiseptica*. PLoS Pathog *1*, e45.
Ding, J., and Badwey, J.A. (1992). Effects of antagonists of protein phosphatases on superoxide release by neutrophils. J Biol Chem *267*, 6442-6448.

Drummond, G.R., Selemidis, S., Griendling, K.K., and Sobey, C.G. (2011). Combating oxidative stress in vascular disease: NADPH oxidases as therapeutic targets. Nat Rev Drug Discov *10*, 453-471.
Duncan, M.C., Linington, R.G., and Auerbuch, V. (2012). Chemical inhibitors of the type three secretion system: disarming bacterial pathogens. Antimicrob Agents Chemother *56*, 5433-5441.
Dunne, A., Ross, P.J., Pospisilova, E., Masin, J., Meaney, A., Sutton, C.E., Iwakura, Y., Tschopp, J., Sebo, P., and Mills, K.H. (2010). Inflammasome activation by adenylate cyclase toxin directs Th17 responses and protection against *Bordetella pertussis*. J Immunol *185*, 1711-1719.
Dusi, S., and Rossi, F. (1993). Activation of NADPH oxidase of human neutrophils involves the phosphorylation and the translocation of cytosolic p67phox. Biochem J *296 (Pt 2)*, 367-371.
Dyet, K., and Moir, J. (2006). Effect of combined oxidative and nitrosative stress on *Neisseria meningitidis*. Biochem Soc Trans *34*, 197-199.
Eby, J.C., Ciesla, W.P., Hamman, W., Donato, G.M., Pickles, R.J., Hewlett, E.L., and Lencer, W.I. (2010). Selective translocation of the *Bordetella pertussis* adenylate cyclase toxin across the basolateral membranes of polarized epithelial cells. J Biol Chem *285*, 10662-10670.
Eby, J.C., Gray, M.C., and Hewlett, E.L. (2014). Cyclic AMP-Mediated Suppression of Neutrophil Extracellular Trap Formation and Apoptosis by the *Bordetella pertussis* Adenylate Cyclase Toxin. Infect Immun *82*, 5256-5269.
Eby, J.C., Gray, M.C., Warfel, J.M., Paddock, C.D., Jones, T.F., Day, S.R., Bowden, J., Poulter, M.D., Donato, G.M., Merkel, T.J., *et al.* (2013). Quantification of the adenylate cyclase toxin of *Bordetella pertussis* in vitro and during respiratory infection. Infect Immun *81*, 1390-1398.
Edwards, J.A., Groathouse, N.A., and Boitano, S. (2005). *Bordetella bronchiseptica* adherence to cilia is mediated by multiple adhesin factors and blocked by surfactant protein A. Infect Immun *73*, 3618-3626.
Ehrmann, I.E., Gray, M.C., Gordon, V.M., Gray, L.S., and Hewlett, E.L. (1991). Hemolytic activity of adenylate cyclase toxin from *Bordetella pertussis*. FEBS Lett *278*, 79-83.
El-Azami-El-Idrissi, M., Bauche, C., Loucka, J., Osicka, R., Sebo, P., Ladant, D., and Leclerc, C. (2003). Interaction of *Bordetella pertussis* adenylate cyclase with CD11b/CD18: Role of toxin acylation and identification of the main integrin interaction domain. J Biol Chem *278*, 38514-38521.
el Baya, A., Bruckener, K., and Schmidt, M.A. (1999). Nonrestricted differential intoxication of cells by pertussis toxin. Infect Immun *67*, 433-435.
El Benna, J., Dang, P.M., Andrieu, V., Vergnaud, S., Dewas, C., Cachia, O., Fay, M., Morel, F., Chollet-Martin, S., Hakim, J., *et al.* (1999). P40phox associates with the neutrophil Triton X-100-insoluble cytoskeletal fraction and PMA-activated membrane skeleton: a comparative study with P67phox and P47phox. J Leukoc Biol *66*, 1014-1020.
Ellson, C., Davidson, K., Anderson, K., Stephens, L.R., and Hawkins, P.T. (2006). PtdIns3P binding to the PX domain of p40phox is a physiological signal in NADPH oxidase activation. EMBO J *25*, 4468-4478.
Ellson, C.D., Gobert-Gosse, S., Anderson, K.E., Davidson, K., Erdjument-Bromage, H., Tempst, P., Thuring, J.W., Cooper, M.A., Lim, Z.Y., Holmes, A.B., *et al.* (2001). PtdIns(3)P regulates the neutrophil oxidase complex by binding to the PX domain of p40(phox). Nat Cell Biol *3*, 679-682.

Fang, F.C., and Vazquez-Torres, A. (2002). Nitric oxide production by human macrophages: there's NO doubt about it. Am J Physiol Lung Cell Mol Physiol *282*, L941-943.
Fedele, G., Spensieri, F., Palazzo, R., Nasso, M., Cheung, G.Y., Coote, J.G., and Ausiello, C.M. (2010). *Bordetella pertussis* commits human dendritic cells to promote a Th1/Th17 response through the activity of adenylate cyclase toxin and MAPK-pathways. PLoS One *5*, e8734.
Felley-Bosco, E., Bender, F., and Quest, A.F. (2002). Caveolin-1-mediated post-transcriptional regulation of inducible nitric oxide synthase in human colon carcinoma cells. Biol Res *35*, 169-176.
Felley-Bosco, E., Bender, F.C., Courjault-Gautier, F., Bron, C., and Quest, A.F. (2000). Caveolin-1 down-regulates inducible nitric oxide synthase via the proteasome pathway in human colon carcinoma cells. Proc Natl Acad Sci U S A *97*, 14334-14339.
Fennelly, N.K., Sisti, F., Higgins, S.C., Ross, P.J., van der Heide, H., Mooi, F.R., Boyd, A., and Mills, K.H. (2008). *Bordetella pertussis* expresses a functional type III secretion system that subverts protective innate and adaptive immune responses. Infect Immun *76*, 1257-1266.
Feola, A., Cimini, A., Migliucci, F., Iorio, R., Zuchegna, C., Rothenberger, R., Cito, L., Porcellini, A., Unteregger, G., Tombolini, V., *et al.* (2013). The inhibition of p85alphaPI3KSer83 phosphorylation prevents cell proliferation and invasion in prostate cancer cells. J Cell Biochem *114*, 2114-2119.
Fernandez, R.C., and Weiss, A.A. (1994). Cloning and sequencing of a *Bordetella pertussis* serum resistance locus. Infect Immun *62*, 4727-4738.
Fernandez, R.C., and Weiss, A.A. (1998). Serum resistance in bvg-regulated mutants of *Bordetella pertussis*. FEMS Microbiol Lett *163*, 57-63.
Finn, T.M., and Stevens, L.A. (1995). Tracheal colonization factor: a *Bordetella pertussis* secreted virulence determinant. Mol Microbiol *16*, 625-634.
Fiser, R., Masin, J., Basler, M., Krusek, J., Spulakova, V., Konopasek, I., and Sebo, P. (2007). Third activity of *Bordetella* adenylate cyclase (AC) toxin-hemolysin. Membrane translocation of AC domain polypeptide promotes calcium influx into CD11b+ monocytes independently of the catalytic and hemolytic activities. J Biol Chem *282*, 2808-2820.
Fiser, R., Masin, J., Bumba, L., Pospisilova, E., Fayolle, C., Basler, M., Sadilkova, L., Adkins, I., Kamanova, J., Cerny, J., *et al.* (2012). Calcium influx rescues adenylate cyclase-hemolysin from rapid cell membrane removal and enables phagocyte permeabilization by toxin pores. PLoS Pathog *8*, e1002580.
Flak, T.A., and Goldman, W.E. (1999). Signalling and cellular specificity of airway nitric oxide production in pertussis. Cell Microbiol *1*, 51-60.
Flak, T.A., Heiss, L.N., Engle, J.T., and Goldman, W.E. (2000). Synergistic epithelial responses to endotoxin and a naturally occurring muramyl peptide. Infect Immun *68*, 1235-1242.
Forbes, L.V., Moss, S.J., and Segal, A.W. (1999a). Phosphorylation of p67phox in the neutrophil occurs in the cytosol and is independent of p47phox. FEBS Lett *449*, 225-229.
Forbes, L.V., Truong, O., Wientjes, F.B., Moss, S.J., and Segal, A.W. (1999b). The major phosphorylation site of the NADPH oxidase component p67phox is Thr233. Biochem J *338 (Pt 1)*, 99-105.
Forstermann, U., and Sessa, W.C. (2012). Nitric oxide synthases: regulation and function. Eur Heart J *33*, 829-837, 837a-837d.

French, C.T., Panina, E.M., Yeh, S.H., Griffith, N., Arambula, D.G., and Miller, J.F. (2009). The *Bordetella* type III secretion system effector BteA contains a conserved N-terminal motif that guides bacterial virulence factors to lipid rafts. Cell Microbiol *11*, 1735-1749.
Friedman, R.L., Fiederlein, R.L., Glasser, L., and Galgiani, J.N. (1987). *Bordetella pertussis* adenylate cyclase: effects of affinity-purified adenylate cyclase on human polymorphonuclear leukocyte functions. Infect Immun *55*, 135-140.
Friedman, R.L., Nordensson, K., Wilson, L., Akporiaye, E.T., and Yocum, D.E. (1992). Uptake and intracellular survival of *Bordetella pertussis* in human macrophages. Infect Immun *60*, 4578-4585.
Fuchs, A., Bouin, A.P., Rabilloud, T., and Vignais, P.V. (1997). The 40-kDa component of the phagocyte NADPH oxidase (p40phox) is phosphorylated during activation in differentiated HL60 cells. Eur J Biochem *249*, 531-539.
Fulop, T., Jr., Foris, G., Worum, I., and Leovey, A. (1985). Age-dependent alterations of Fc gamma receptor-mediated effector functions of human polymorphonuclear leucocytes. Clin Exp Immunol *61*, 425-432.
Funnell, S.G., and Robinson, A. (1993). A novel adherence assay for *Bordetella pertussis* using tracheal organ cultures. FEMS Microbiol Lett *110*, 197-203.
Galea, E., and Feinstein, D.L. (1999). Regulation of the expression of the inflammatory nitric oxide synthase (NOS2) by cyclic AMP. FASEB J *13*, 2125-2137.
Ganguly, T., Johnson, J.B., Kock, N.D., Parks, G.D., and Deora, R. (2014). The *Bordetella pertussis* Bps polysaccharide enhances lung colonization by conferring protection from complement-mediated killing. Cell Microbiol *16*, 1105-1118.
Garcia, R.C., Whitaker, M., Heyworth, P.G., and Segal, A.W. (1992). Okadaic acid produces changes in phosphorylation and translocation of proteins and in intracellular calcium in human neutrophils. Relationship with the activation of the NADPH oxidase by different stimuli. Biochem J *286 (Pt 3)*, 687-692.
Gasperini, S., Crepaldi, L., Calzetti, F., Gatto, L., Berlato, C., Bazzoni, F., Yoshimura, A., and Cassatella, M.A. (2002). Interleukin-10 and cAMP-elevating agents cooperate to induce suppressor of cytokine signaling-3 via a protein kinase A-independent signal. Eur Cytokine Netw *13*, 47-53.
Geduhn, J., Dove, S., Shen, Y., Tang, W.J., Konig, B., and Seifert, R. (2011). Bis-halogen-anthraniloyl-substituted nucleoside 5'-triphosphates as potent and selective inhibitors of *Bordetella pertussis* adenylyl cyclase toxin. J Pharmacol Exp Ther *336*, 104-115.
Geissmann, F., Jung, S., and Littman, D.R. (2003). Blood monocytes consist of two principal subsets with distinct migratory properties. Immunity *19*, 71-82.
Gentile, F., Raptis, A., Knipling, L.G., and Wolff, J. (1988). *Bordetella pertussis* adenylate cyclase. Penetration into host cells. Eur J Biochem *175*, 447-453.
Gerlach, G., von Wintzingerode, F., Middendorf, B., and Gross, R. (2001). Evolutionary trends in the genus *Bordetella*. Microbes Infect *3*, 61-72.
Geuijen, C.A., Willems, R.J., Bongaerts, M., Top, J., Gielen, H., and Mooi, F.R. (1997). Role of the *Bordetella pertussis* minor fimbrial subunit, FimD, in colonization of the mouse respiratory tract. Infect Immun *65*, 4222-4228.
Geurtsen, J., Fae, K.C., and van den Dobbelsteen, G.P. (2014). Importance of (antibody-dependent) complement-mediated serum killing in protection against *Bordetella pertussis*. Expert Rev Vaccines *13*, 1229-1240.

Gille, A., and Seifert, R. (2003). 2'(3')-O-(N-methylanthraniloyl)-substituted GTP analogs: a novel class of potent competitive adenylyl cyclase inhibitors. J Biol Chem *278*, 12672-12679.
Glaser, P., Danchin, A., Ladant, D., Barzu, O., and Ullmann, A. (1988). *Bordetella pertussis* adenylate cyclase: the gene and the protein. Tokai J Exp Clin Med *13 Suppl*, 239-252.
Glaser, P., Elmaoglou-Lazaridou, A., Krin, E., Ladant, D., Barzu, O., and Danchin, A. (1989). Identification of residues essential for catalysis and binding of calmodulin in *Bordetella pertussis* adenylate cyclase by site-directed mutagenesis. EMBO J *8*, 967-972.
Gomez, M.A., Contreras, I., Halle, M., Tremblay, M.L., McMaster, R.W., and Olivier, M. (2009). *Leishmania* GP63 alters host signaling through cleavage-activated protein tyrosine phosphatases. Sci Signal *2*, ra58.
Goodwin, M.S., and Weiss, A.A. (1990). Adenylate cyclase toxin is critical for colonization and pertussis toxin is critical for lethal infection by *Bordetella pertussis* in infant mice. Infect Immun *58*, 3445-3447.
Gordon, S., and Taylor, P.R. (2005). Monocyte and macrophage heterogeneity. Nat Rev Immunol *5*, 953-964.
Gordon, V.M., Leppla, S.H., and Hewlett, E.L. (1988). Inhibitors of receptor-mediated endocytosis block the entry of Bacillus anthracis adenylate cyclase toxin but not that of *Bordetella pertussis* adenylate cyclase toxin. Infect Immun *56*, 1066-1069.
Gordon, V.M., Young, W.W., Jr., Lechler, S.M., Gray, M.C., Leppla, S.H., and Hewlett, E.L. (1989). Adenylate cyclase toxins from *Bacillus anthracis* and *Bordetella pertussis*. Different processes for interaction with and entry into target cells. J Biol Chem *264*, 14792-14796.
Gotoh, T., and Mori, M. (1999). Arginase II downregulates nitric oxide (NO) production and prevents NO-mediated apoptosis in murine macrophage-derived RAW 264.7 cells. J Cell Biol *144*, 427-434.
Gottle, M., Dove, S., Kees, F., Schlossmann, J., Geduhn, J., Konig, B., Shen, Y., Tang, W.J., Kaever, V., and Seifert, R. (2010). Cytidylyl and uridylyl cyclase activity of *Bacillus anthracis* edema factor and *Bordetella pertussis* CyaA. Biochemistry *49*, 5494-5503.
Graf, R., Codina, J., and Birnbaumer, L. (1992). Peptide inhibitors of ADP-ribosylation by pertussis toxin are substrates with affinities comparable to those of the trimeric GTP-binding proteins. Mol Pharmacol *42*, 760-764.
Gray, M., Szabo, G., Otero, A.S., Gray, L., and Hewlett, E. (1998). Distinct mechanisms for K+ efflux, intoxication, and hemolysis by *Bordetella pertussis* AC toxin. J Biol Chem *273*, 18260-18267.
Gray, M.C., Donato, G.M., Jones, F.R., Kim, T., and Hewlett, E.L. (2004). Newly secreted adenylate cyclase toxin is responsible for intoxication of target cells by *Bordetella pertussis*. Mol Microbiol *53*, 1709-1719.
Gray, M.C., and Hewlett, E.L. (2011). Cell cycle arrest induced by the bacterial adenylate cyclase toxins from *Bacillus anthracis* and *Bordetella pertussis*. Cell Microbiol *13*, 123-134.
Gray, M.C., Lee, S.J., Gray, L.S., Zaretzky, F.R., Otero, A.S., Szabo, G., and Hewlett, E.L. (2001). Translocation-specific conformation of adenylate cyclase toxin from *Bordetella pertussis* inhibits toxin-mediated hemolysis. J Bacteriol *183*, 5904-5910.

Gray, M.C., Ross, W., Kim, K., and Hewlett, E.L. (1999). Characterization of binding of adenylate cyclase toxin to target cells by flow cytometry. Infect Immun *67*, 4393-4399.
Gray, R.D., Lucas, C.D., Mackellar, A., Li, F., Hiersemenzel, K., Haslett, C., Davidson, D.J., and Rossi, A.G. (2013). Activation of conventional protein kinase C (PKC) is critical in the generation of human neutrophil extracellular traps. J Inflamm (Lond) *10*, 12.
Gueirard, P., Bassinet, L., Bonne, I., Prevost, M.C., and Guiso, N. (2005). Ultrastructural analysis of the interactions between *Bordetella pertussis*, *Bordetella parapertussis* and *Bordetella bronchiseptica* and human tracheal epithelial cells. Microb Pathog *38*, 41-46.
Gueirard, P., Druilhe, A., Pretolani, M., and Guiso, N. (1998). Role of adenylate cyclase-hemolysin in alveolar macrophage apoptosis during *Bordetella pertussis* infection in vivo. Infect Immun *66*, 1718-1725.
Guermonprez, P., Khelef, N., Blouin, E., Rieu, P., Ricciardi-Castagnoli, P., Guiso, N., Ladant, D., and Leclerc, C. (2001). The adenylate cyclase toxin of *Bordetella pertussis* binds to target cells via the alpha(M)beta(2) integrin (CD11b/CD18). J Exp Med *193*, 1035-1044.
Guo, Q., Shen, Y., Lee, Y.S., Gibbs, C.S., Mrksich, M., and Tang, W.J. (2005). Structural basis for the interaction of *Bordetella pertussis* adenylyl cyclase toxin with calmodulin. EMBO J *24*, 3190-3201.
Guttman, C., Davidov, G., Shaked, H., Kolusheva, S., Bitton, R., Ganguly, A., Miller, J.F., Chill, J.H., and Zarivach, R. (2013). Characterization of the N-terminal domain of BteA: a *Bordetella* type III secreted cytotoxic effector. PLoS One *8*, e55650.
Haberling, D.L., Holman, R.C., Paddock, C.D., and Murphy, T.V. (2009). Infant and maternal risk factors for pertussis-related infant mortality in the United States, 1999 to 2004. Pediatr Infect Dis J *28*, 194-198.
Hackett, M., Guo, L., Shabanowitz, J., Hunt, D.F., and Hewlett, E.L. (1994). Internal lysine palmitoylation in adenylate cyclase toxin from *Bordetella pertussis*. Science *266*, 433-435.
Hackett, M., Walker, C.B., Guo, L., Gray, M.C., Van Cuyk, S., Ullmann, A., Shabanowitz, J., Hunt, D.F., Hewlett, E.L., and Sebo, P. (1995). Hemolytic, but not cell-invasive activity, of adenylate cyclase toxin is selectively affected by differential fatty-acylation in Escherichia coli. J Biol Chem *270*, 20250-20253.
Hamada, K., Hata, Y., Katsuya, Y., Hiramatsu, H., Fujiwara, T., and Katsube, Y. (1996). Crystal structure of *Serratia* protease, a zinc-dependent proteinase from *Serratia* sp. E-15, containing a beta-sheet coil motif at 2.0 A resolution. J Biochem *119*, 844-851.
Hammad, H., and Lambrecht, B.N. (2008). Dendritic cells and epithelial cells: linking innate and adaptive immunity in asthma. Nat Rev Immunol *8*, 193-204.
Harbecke, O., Liu, L., Karlsson, A., and Dahlgren, C. (1997). Desensitization of the fMLP-induced NADPH-oxidase response in human neutrophils is lacking in okadaic acid-treated cells. J Leukoc Biol *61*, 753-758.
Harbecke, O., Lundqvist, H., and Dahlgren, C. (1996). Okadaic acid inhibits the signal responsible for activation of the NADPH-oxidase in neutrophils stimulated with serum-opsonized yeast. J Leukoc Biol *59*, 754-762.
Hardin, A.O., Meals, E.A., Yi, T., Knapp, K.M., and English, B.K. (2006). SHP-1 inhibits LPS-mediated TNF and iNOS production in murine macrophages. Biochem Biophys Res Commun *342*, 547-555.

Harvill, E.T., Cotter, P.A., Yuk, M.H., and Miller, J.F. (1999). Probing the function of *Bordetella bronchiseptica* adenylate cyclase toxin by manipulating host immunity. Infect Immun *67*, 1493-1500.
Hasan, S., Osickova, A., Bumba, L., Novak, P., Sebo, P., and Osicka, R. (2014). Interaction of *Bordetella* adenylate cyclase toxin with complement receptor 3 involves multivalent glycan binding. FEBS Lett.
Hausel, P., Latado, H., Courjault-Gautier, F., and Felley-Bosco, E. (2006). Src-mediated phosphorylation regulates subcellular distribution and activity of human inducible nitric oxide synthase. Oncogene *25*, 198-206.
Havlicek, V., Higgins, L., Chen, W., Halada, P., Sebo, P., Sakamoto, H., and Hackett, M. (2001). Mass spectrometric analysis of recombinant adenylate cyclase toxin from *Bordetella pertussis* strain 18323/pHSP9. J Mass Spectrom *36*, 384-391.
Heiss, L.N., Moser, S.A., Unanue, E.R., and Goldman, W.E. (1993). Interleukin-1 is linked to the respiratory epithelial cytopathology of pertussis. Infect Immun *61*, 3123-3128.
Henderson, I.R., Navarro-Garcia, F., Desvaux, M., Fernandez, R.C., and Ala'Aldeen, D. (2004). Type V protein secretion pathway: the autotransporter story. Microbiol Mol Biol Rev *68*, 692-744.
Hester, S.E., Lui, M., Nicholson, T., Nowacki, D., and Harvill, E.T. (2012). Identification of a CO2 responsive regulon in *Bordetella*. PLoS One *7*, e47635.
Hewlett, E.L., Burns, D.L., Cotter, P.A., Harvill, E.T., Merkel, T.J., Quinn, C.P., and Stibitz, E.S. (2014). Pertussis pathogenesis--what we know and what we don't know. J Infect Dis *209*, 982-985.
Hewlett, E.L., Donato, G.M., and Gray, M.C. (2006). Macrophage cytotoxicity produced by adenylate cyclase toxin from *Bordetella pertussis*: more than just making cyclic AMP! Mol Microbiol *59*, 447-459.
Hewlett, E.L., Urban, M.A., Manclark, C.R., and Wolff, J. (1976). Extracytoplasmic adenylate cyclase of *Bordetella pertussis*. Proc Natl Acad Sci U S A *73*, 1926-1930.
Heyworth, P.G., and Badwey, J.A. (1990). Continuous phosphorylation of both the 47 and the 49 kDa proteins occurs during superoxide production by neutrophils. Biochim Biophys Acta *1052*, 299-305.
Hickey, F.B., Brereton, C.F., and Mills, K.H. (2008). Adenylate cycalse toxin of *Bordetella pertussis* inhibits TLR-induced IRF-1 and IRF-8 activation and IL-12 production and enhances IL-10 through MAPK activation in dendritic cells. J Leukoc Biol *84*, 234-243.
Hiraiwa-Sofue, A., Ito, Y., Mori, H., Ichiyama, T., and Okumura, A. (2012). Pertussis-associated encephalitis/encephalopathy with marked demyelination in an unimmunized child. J Neurol Sci *320*, 145-148.
Holland, I.B., Schmitt, L., and Young, J. (2005). Type 1 protein secretion in bacteria, the ABC-transporter dependent pathway (review). Mol Membr Biol *22*, 29-39.
Hong, K., Lou, L., Gupta, S., Ribeiro-Neto, F., and Altschuler, D.L. (2008). A novel Epac-Rap-PP2A signaling module controls cAMP-dependent Akt regulation. J Biol Chem *283*, 23129-23138.
Horiguchi, Y., Senda, T., Sugimoto, N., Katahira, J., and Matsuda, M. (1995). *Bordetella bronchiseptica* dermonecrotizing toxin stimulates assembly of actin stress fibers and focal adhesions by modifying the small GTP-binding protein rho. J Cell Sci *108 (Pt 10)*, 3243-3251.
Hoyal, C.R., Gutierrez, A., Young, B.M., Catz, S.D., Lin, J.H., Tsichlis, P.N., and Babior, B.M. (2003). Modulation of p47PHOX activity by site-specific

phosphorylation: Akt-dependent activation of the NADPH oxidase. Proc Natl Acad Sci U S A *100*, 5130-5135.
Chang, C.I., Liao, J.C., and Kuo, L. (1998). Arginase modulates nitric oxide production in activated macrophages. Am J Physiol *274*, H342-348.
Chang, S.Y., Kim, D.B., Ryu, G.R., Ko, S.H., Jeong, I.K., Ahn, Y.B., Jo, Y.H., and Kim, M.J. (2013). Exendin-4 inhibits iNOS expression at the protein level in LPS-stimulated Raw264.7 macrophage by the activation of cAMP/PKA pathway. J Cell Biochem *114*, 844-853.
Chen, L.W., Huang, H.L., Lee, I.T., Hsu, C.M., and Lu, P.J. (2006). Thermal injury-induced priming effect of neutrophil is TNF-alpha and P38 dependent. Shock *26*, 69-76.
Chenal, A., Karst, J.C., Sotomayor Perez, A.C., Wozniak, A.K., Baron, B., England, P., and Ladant, D. (2010). Calcium-induced folding and stabilization of the intrinsically disordered RTX domain of the CyaA toxin. Biophys J *99*, 3744-3753.
Chessa, T.A., Anderson, K.E., Hu, Y., Xu, Q., Rausch, O., Stephens, L.R., and Hawkins, P.T. (2010). Phosphorylation of threonine 154 in p40phox is an important physiological signal for activation of the neutrophil NADPH oxidase. Blood *116*, 6027-6036.
Cheung, G.Y., Dickinson, P., Sing, G., Craigon, M., Ghazal, P., Parton, R., and Coote, J.G. (2008). Transcriptional responses of murine macrophages to the adenylate cyclase toxin of *Bordetella pertussis*. Microb Pathog *44*, 61-70.
Cheung, G.Y., Kelly, S.M., Jess, T.J., Prior, S., Price, N.C., Parton, R., and Coote, J.G. (2009). Functional and structural studies on different forms of the adenylate cyclase toxin of *Bordetella pertussis*. Microb Pathog *46*, 36-42.
Inanami, O., Johnson, J.L., McAdara, J.K., Benna, J.E., Faust, L.R., Newburger, P.E., and Babior, B.M. (1998). Activation of the leukocyte NADPH oxidase by phorbol ester requires the phosphorylation of p47PHOX on serine 303 or 304. J Biol Chem *273*, 9539-9543.
Inatsuka, C.S., Julio, S.M., and Cotter, P.A. (2005). *Bordetella* filamentous hemagglutinin plays a critical role in immunomodulation, suggesting a mechanism for host specificity. Proc Natl Acad Sci U S A *102*, 18578-18583.
Italiani, P., and Boraschi, D. (2014). From Monocytes to M1/M2 Macrophages: Phenotypical vs. Functional Differentiation. Front Immunol *5*, 514.
Iwaki, M., Kamachi, K., and Konda, T. (2000). Stimulation of *Bordetella pertussis* adenylate cyclase toxin intoxication by its hemolysin domain. Infect Immun *68*, 3727-3730.
Iwaki, M., Ullmann, A., and Sebo, P. (1995). Identification by in vitro complementation of regions required for cell-invasive activity of *Bordetella pertussis* adenylate cyclase toxin. Mol Microbiol *17*, 1015-1024.
Iyer, S.S., Pearson, D.W., Nauseef, W.M., and Clark, R.A. (1994). Evidence for a readily dissociable complex of p47phox and p67phox in cytosol of unstimulated human neutrophils. J Biol Chem *269*, 22405-22411.
Jeyaseelan, S., Hsuan, S.L., Kannan, M.S., Walcheck, B., Wang, J.F., Kehrli, M.E., Lally, E.T., Sieck, G.C., and Maheswaran, S.K. (2000). Lymphocyte function-associated antigen 1 is a receptor for *Pasteurella haemolytica* leukotoxin in bovine leukocytes. Infect Immun *68*, 72-79.
Johnson, J.L., Park, J.W., Benna, J.E., Faust, L.P., Inanami, O., and Babior, B.M. (1998). Activation of p47(PHOX), a cytosolic subunit of the leukocyte NADPH oxidase. Phosphorylation of ser-359 or ser-370 precedes phosphorylation at other sites and is required for activity. J Biol Chem *273*, 35147-35152.

Kadl, A., Meher, A.K., Sharma, P.R., Lee, M.Y., Doran, A.C., Johnstone, S.R., Elliott, M.R., Gruber, F., Han, J., Chen, W., *et al.* (2010). Identification of a novel macrophage phenotype that develops in response to atherogenic phospholipids via Nrf2. Circ Res *107*, 737-746.
Kalamidas, S.A., Kuehnel, M.P., Peyron, P., Rybin, V., Rauch, S., Kotoulas, O.B., Houslay, M., Hemmings, B.A., Gutierrez, M.G., Anes, E., *et al.* (2006). cAMP synthesis and degradation by phagosomes regulate actin assembly and fusion events: consequences for mycobacteria. J Cell Sci *119*, 3686-3694.
Kamanova, J., Kofronova, O., Masin, J., Genth, H., Vojtova, J., Linhartova, I., Benada, O., Just, I., and Sebo, P. (2008). Adenylate cyclase toxin subverts phagocyte function by RhoA inhibition and unproductive ruffling. J Immunol *181*, 5587-5597.
Kamenetsky, M., Middelhaufe, S., Bank, E.M., Levin, L.R., Buck, J., and Steegborn, C. (2006). Molecular details of cAMP generation in mammalian cells: a tale of two systems. J Mol Biol *362*, 623-639.
Kanai, F., Liu, H., Field, S.J., Akbary, H., Matsuo, T., Brown, G.E., Cantley, L.C., and Yaffe, M.B. (2001). The PX domains of p47phox and p40phox bind to lipid products of PI(3)K. Nat Cell Biol *3*, 675-678.
Kania, S.A., Rajeev, S., Burns, E.H., Jr., Odom, T.F., Holloway, S.M., and Bemis, D.A. (2000). Characterization of fimN, a new *Bordetella bronchiseptica* major fimbrial subunit gene. Gene *256*, 149-155.
Kant, A.M., De, P., Peng, X., Yi, T., Rawlings, D.J., Kim, J.S., and Durden, D.L. (2002). SHP-1 regulates Fcgamma receptor-mediated phagocytosis and the activation of RAC. Blood *100*, 1852-1859.
Karathanassis, D., Stahelin, R.V., Bravo, J., Perisic, O., Pacold, C.M., Cho, W., and Williams, R.L. (2002). Binding of the PX domain of p47(phox) to phosphatidylinositol 3,4-bisphosphate and phosphatidic acid is masked by an intramolecular interaction. EMBO J *21*, 5057-5068.
Karimova, G., Bellalou, J., and Ullmann, A. (1996). Phosphorylation-dependent binding of BvgA to the upstream region of the cyaA gene of *Bordetella pertussis*. Mol Microbiol *20*, 489-496.
Karimova, G., and Ullmann, A. (1997). Characterization of DNA binding sites for the BvgA protein of *Bordetella pertussis*. J Bacteriol *179*, 3790-3792.
Karst, J.C., Barker, R., Devi, U., Swann, M.J., Davi, M., Roser, S.J., Ladant, D., and Chenal, A. (2012). Identification of a region that assists membrane insertion and translocation of the catalytic domain of *Bordetella pertussis* CyaA toxin. J Biol Chem *287*, 9200-9212.
Katada, T., and Ui, M. (1982). Direct modification of the membrane adenylate cyclase system by islet-activating protein due to ADP-ribosylation of a membrane protein. Proc Natl Acad Sci U S A *79*, 3129-3133.
Kato, A., and Schleimer, R.P. (2007). Beyond inflammation: airway epithelial cells are at the interface of innate and adaptive immunity. Curr Opin Immunol *19*, 711-720.
Kaufmann, S.H. (2008). Immunology's foundation: the 100-year anniversary of the Nobel Prize to Paul Ehrlich and Elie Metchnikoff. Nat Immunol *9*, 705-712.
Khelef, N., Bachelet, C.M., Vargaftig, B.B., and Guiso, N. (1994). Characterization of murine lung inflammation after infection with parental *Bordetella pertussis* and mutants deficient in adhesins or toxins. Infect Immun *62*, 2893-2900.
Khelef, N., and Guiso, N. (1995). Induction of macrophage apoptosis by *Bordetella pertussis* adenylate cyclase-hemolysin. FEMS Microbiol Lett *134*, 27-32.

Khelef, N., Sakamoto, H., and Guiso, N. (1992). Both adenylate cyclase and hemolytic activities are required by *Bordetella pertussis* to initiate infection. Microb Pathog *12*, 227-235.
Khelef, N., Zychlinsky, A., and Guiso, N. (1993). *Bordetella pertussis* induces apoptosis in macrophages: role of adenylate cyclase-hemolysin. Infect Immun *61*, 4064-4071.
Kleinert, H., Schwarz, P.M., and Forstermann, U. (2003). Regulation of the expression of inducible nitric oxide synthase. Biol Chem *384*, 1343-1364.
Knapp, O., Maier, E., Masin, J., Sebo, P., and Benz, R. (2008). Pore formation by the *Bordetella* adenylate cyclase toxin in lipid bilayer membranes: role of voltage and pH. Biochim Biophys Acta *1778*, 260-269.
Knapp, O., Maier, E., Polleichtner, G., Masin, J., Sebo, P., and Benz, R. (2003). Channel formation in model membranes by the adenylate cyclase toxin of *Bordetella pertussis*: effect of calcium. Biochemistry *42*, 8077-8084.
Koide, M., Kawahara, Y., Nakayama, I., Tsuda, T., and Yokoyama, M. (1993). Cyclic AMP-elevating agents induce an inducible type of nitric oxide synthase in cultured vascular smooth muscle cells. Synergism with the induction elicited by inflammatory cytokines. J Biol Chem *268*, 24959-24966.
Koide, N., Sugiyama, T., Mori, I., Mu, M.M., Yoshida, T., and Yokochi, T. (2003). C2-ceramide inhibits LPS-induced nitric oxide production in RAW 264.7 macrophage cells through down-regulating the activation of Akt. J Endotoxin Res *9*, 85-90.
Kopperud, R., Krakstad, C., Selheim, F., and Doskeland, S.O. (2003). cAMP effector mechanisms. Novel twists for an 'old' signaling system. FEBS Lett *546*, 121-126.
Koronakis, V., Hughes, C., and Koronakis, E. (1991). Energetically distinct early and late stages of HlyB/HlyD-dependent secretion across both *Escherichia coli* membranes. EMBO J *10*, 3263-3272.
Koronakis, V., Sharff, A., Koronakis, E., Luisi, B., and Hughes, C. (2000). Crystal structure of the bacterial membrane protein TolC central to multidrug efflux and protein export. Nature *405*, 914-919.
Kotob, S.I., Hausman, S.Z., and Burns, D.L. (1995). Localization of the promoter for the ptl genes of *Bordetella pertussis*, which encode proteins essential for secretion of pertussis toxin. Infect Immun *63*, 3227-3230.
Kubista, M., Andrade, J.M., Bengtsson, M., Forootan, A., Jonak, J., Lind, K., Sindelka, R., Sjoback, R., Sjogreen, B., Strombom, L., *et al.* (2006). The real-time polymerase chain reaction. Mol Aspects Med *27*, 95-125.
Kuo, P.C., Schroeder, R.A., and Bartlett, S.T. (1997). Endotoxin-mediated synthesis of nitric oxide is dependent on Gq protein signal transduction. Surgery *122*, 394-402; discussion 402-393.
Kurushima, J., Kuwae, A., and Abe, A. (2012). The type III secreted protein BspR regulates the virulence genes in *Bordetella bronchiseptica*. PLoS One *7*, e38925.
la Sala, A., He, J., Laricchia-Robbio, L., Gorini, S., Iwasaki, A., Braun, M., Yap, G.S., Sher, A., Ozato, K., and Kelsall, B. (2009). Cholera toxin inhibits IL-12 production and CD8alpha+ dendritic cell differentiation by cAMP-mediated inhibition of IRF8 function. J Exp Med *206*, 1227-1235.
Ladant, D. (1988). Interaction of *Bordetella pertussis* adenylate cyclase with calmodulin. Identification of two separated calmodulin-binding domains. J Biol Chem *263*, 2612-2618.

Ladant, D., Michelson, S., Sarfati, R., Gilles, A.M., Predeleanu, R., and Barzu, O. (1989). Characterization of the calmodulin-binding and of the catalytic domains of *Bordetella pertussis* adenylate cyclase. J Biol Chem *264*, 4015-4020.
Ladant, D., and Ullmann, A. (1999). *Bordatella pertussis* adenylate cyclase: a toxin with multiple talents. Trends Microbiol *7*, 172-176.
Lally, E.T., Kieba, I.R., Sato, A., Green, C.L., Rosenbloom, J., Korostoff, J., Wang, J.F., Shenker, B.J., Ortlepp, S., Robinson, M.K., *et al.* (1997). RTX toxins recognize a beta2 integrin on the surface of human target cells. J Biol Chem *272*, 30463-30469.
Lamberti, Y., Gorgojo, J., Massillo, C., and Rodriguez, M.E. (2013). *Bordetella pertussis* entry into respiratory epithelial cells and intracellular survival. Pathog Dis *69*, 194-204.
Lamberti, Y.A., Hayes, J.A., Perez Vidakovics, M.L., Harvill, E.T., and Rodriguez, M.E. (2010). Intracellular trafficking of *Bordetella pertussis* in human macrophages. Infect Immun *78*, 907-913.
Lane, C., Knight, D., Burgess, S., Franklin, P., Horak, F., Legg, J., Moeller, A., and Stick, S. (2004). Epithelial inducible nitric oxide synthase activity is the major determinant of nitric oxide concentration in exhaled breath. Thorax *59*, 757-760.
Laoide, B.M., and Ullmann, A. (1990). Virulence dependent and independent regulation of the *Bordetella pertussis* cya operon. EMBO J *9*, 999-1005.
Lapouge, K., Smith, S.J., Groemping, Y., and Rittinger, K. (2002). Architecture of the p40-p47-p67phox complex in the resting state of the NADPH oxidase. A central role for p67phox. J Biol Chem *277*, 10121-10128.
Lee, S.H., Nishino, M., Mazumdar, T., Garcia, G.E., Galfione, M., Lee, F.L., Lee, C.L., Liang, A., Kim, J., Feng, L., *et al.* (2005a). 16-kDa prolactin down-regulates inducible nitric oxide synthase expression through inhibition of the signal transducer and activator of transcription 1/IFN regulatory factor-1 pathway. Cancer Res *65*, 7984-7992.
Lee, S.J., Gray, M.C., Zu, K., and Hewlett, E.L. (2005b). Oligomeric behavior of *Bordetella pertussis* adenylate cyclase toxin in solution. Arch Biochem Biophys *438*, 80-87.
Lee, S.M., Kim, E.J., Suk, K., and Lee, W.H. (2011). Synthetic peptides containing ITIM-like sequences of IREM-1 inhibit BAFF-mediated regulation of interleukin-8 expression and phagocytosis through SHP-1 and/or PI3K. Immunology *134*, 224-233.
Letoffe, S., Delepelaire, P., and Wandersman, C. (1996). Protein secretion in gram-negative bacteria: assembly of the three components of ABC protein-mediated exporters is ordered and promoted by substrate binding. EMBO J *15*, 5804-5811.
Li, J., Clinkenbeard, K.D., and Ritchey, J.W. (1999). Bovine CD18 identified as a species specific receptor for *Pasteurella haemolytica* leukotoxin. Vet Microbiol *67*, 91-97.
Linker, K., Pautz, A., Fechir, M., Hubrich, T., Greeve, J., and Kleinert, H. (2005). Involvement of KSRP in the post-transcriptional regulation of human iNOS expression-complex interplay of KSRP with TTP and HuR. Nucleic Acids Res *33*, 4813-4827.
Locht, C., Antoine, R., and Jacob-Dubuisson, F. (2001). *Bordetella pertussis*, molecular pathogenesis under multiple aspects. Curr Opin Microbiol *4*, 82-89.
Locht, C., Coutte, L., and Mielcarek, N. (2011). The ins and outs of pertussis toxin. FEBS J *278*, 4668-4682.
Lorsbach, R.B., Murphy, W.J., Lowenstein, C.J., Snyder, S.H., and Russell, S.W. (1993). Expression of the nitric oxide synthase gene in mouse macrophages activated

for tumor cell killing. Molecular basis for the synergy between interferon-gamma and lipopolysaccharide. J Biol Chem *268*, 1908-1913.
Lu, D.J., Takai, A., Leto, T.L., and Grinstein, S. (1992). Modulation of neutrophil activation by okadaic acid, a protein phosphatase inhibitor. Am J Physiol *262*, C39-49.
Luo, M., Jones, S.M., Phare, S.M., Coffey, M.J., Peters-Golden, M., and Brock, T.G. (2004). Protein kinase A inhibits leukotriene synthesis by phosphorylation of 5-lipoxygenase on serine 523. J Biol Chem *279*, 41512-41520.
Macdonald-Fyall, J., Xing, D., Corbel, M., Baillie, S., Parton, R., and Coote, J. (2004). Adjuvanticity of native and detoxified adenylate cyclase toxin of *Bordetella pertussis* towards co-administered antigens. Vaccine *22*, 4270-4281.
Mackman, N., Baker, K., Gray, L., Haigh, R., Nicaud, J.M., and Holland, I.B. (1987). Release of a chimeric protein into the medium from *Escherichia coli* using the C-terminal secretion signal of haemolysin. EMBO J *6*, 2835-2841.
MacMicking, J., Xie, Q.W., and Nathan, C. (1997). Nitric oxide and macrophage function. Annu Rev Immunol *15*, 323-350.
Magalhaes, J.G., Philpott, D.J., Nahori, M.A., Jehanno, M., Fritz, J., Le Bourhis, L., Viala, J., Hugot, J.P., Giovannini, M., Bertin, J., *et al.* (2005). Murine Nod1 but not its human orthologue mediates innate immune detection of tracheal cytotoxin. EMBO Rep *6*, 1201-1207.
Makranz, C., Cohen, G., Reichert, F., Kodama, T., and Rotshenker, S. (2006). cAMP cascade (PKA, Epac, adenylyl cyclase, Gi, and phosphodiesterases) regulates myelin phagocytosis mediated by complement receptor-3 and scavenger receptor-AI/II in microglia and macrophages. Glia *53*, 441-448.
Mandell, G.L., and Hook, E.W. (1969). Leukocyte bactericidal activity in chronic granulomatous disease: correlation of bacterial hydrogen peroxide production and susceptibility to intracellular killing. J Bacteriol *100*, 531-532.
Marletta, M.A., Yoon, P.S., Iyengar, R., Leaf, C.D., and Wishnok, J.S. (1988). Macrophage oxidation of L-arginine to nitrite and nitrate: nitric oxide is an intermediate. Biochemistry *27*, 8706-8711.
Marr, N., Luu, R.A., and Fernandez, R.C. (2007). *Bordetella pertussis* binds human C1 esterase inhibitor during the virulent phase, to evade complement-mediated killing. J Infect Dis *195*, 585-588.
Marr, N., Shah, N.R., Lee, R., Kim, E.J., and Fernandez, R.C. (2011). *Bordetella pertussis* autotransporter Vag8 binds human C1 esterase inhibitor and confers serum resistance. PLoS One *6*, e20585.
Masin, J., Basler, M., Knapp, O., El-Azami-El-Idrissi, M., Maier, E., Konopasek, I., Benz, R., Leclerc, C., and Sebo, P. (2005). Acylation of lysine 860 allows tight binding and cytotoxicity of *Bordetella adenylate* cyclase on CD11b-expressing cells. Biochemistry *44*, 12759-12766.
Masin, J., Fiser, R., Linhartova, I., Osicka, R., Bumba, L., Hewlett, E.L., Benz, R., and Sebo, P. (2013). Differences in purinergic amplification of osmotic cell lysis by the pore-forming RTX toxins *Bordetella pertussis* CyaA and *Actinobacillus pleuropneumoniae* ApxIA: the role of pore size. Infect Immun *81*, 4571-4582.
Masin, J., Konopasek, I., Svobodova, J., and Sebo, P. (2004). Different structural requirements for adenylate cyclase toxin interactions with erythrocyte and liposome membranes. Biochim Biophys Acta *1660*, 144-154.
Massenet, C., Chenavas, S., Cohen-Addad, C., Dagher, M.C., Brandolin, G., Pebay-Peyroula, E., and Fieschi, F. (2005). Effects of p47phox C terminus phosphorylations

on binding interactions with p40phox and p67phox. Structural and functional comparison of p40phox and p67phox SH3 domains. J Biol Chem *280*, 13752-13761.
Masure, H.R., Au, D.C., Gross, M.K., Donovan, M.G., and Storm, D.R. (1990). Secretion of the *Bordetella pertussis* adenylate cyclase from Escherichia coli containing the hemolysin operon. Biochemistry *29*, 140-145.
Mattoo, S., and Cherry, J.D. (2005). Molecular pathogenesis, epidemiology, and clinical manifestations of respiratory infections due to *Bordetella pertussis* and other *Bordetella* subspecies. Clin Microbiol Rev *18*, 326-382.
Mattoo, S., Miller, J.F., and Cotter, P.A. (2000). Role of *Bordetella bronchiseptica* fimbriae in tracheal colonization and development of a humoral immune response. Infect Immun *68*, 2024-2033.
Mayer, A.K., and Dalpke, A.H. (2007). Regulation of local immunity by airway epithelial cells. Arch Immunol Ther Exp (Warsz) *55*, 353-362.
McConnachie, G., Langeberg, L.K., and Scott, J.D. (2006). AKAP signaling complexes: getting to the heart of the matter. Trends Mol Med *12*, 317-323.
Medhekar, B., Shrivastava, R., Mattoo, S., Gingery, M., and Miller, J.F. (2009). *Bordetella* Bsp22 forms a filamentous type III secretion system tip complex and is immunoprotective in vitro and in vivo. Mol Microbiol *71*, 492-504.
Meijles, D.N., Fan, L.M., Howlin, B.J., and Li, J.M. (2014). Molecular insights of p47phox phosphorylation dynamics in the regulation of NADPH oxidase activation and superoxide production. J Biol Chem *289*, 22759-22770.
Melvin, J.A., Scheller, E.V., Miller, J.F., and Cotter, P.A. (2014). *Bordetella pertussis* pathogenesis: current and future challenges. Nat Rev Microbiol *12*, 274-288.
Meri, T., Amdahl, H., Lehtinen, M.J., Hyvarinen, S., McDowell, J.V., Bhattacharjee, A., Meri, S., Marconi, R., Goldman, A., and Jokiranta, T.S. (2013). Microbes bind complement inhibitor factor H via a common site. PLoS Pathog *9*, e1003308.
Messmer, U.K., and Brune, B. (1994). Modulation of inducible nitric oxide synthase in RINm5F cells. Cell Signal *6*, 17-24.
Mittal, M., Siddiqui, M.R., Tran, K., Reddy, S.P., and Malik, A.B. (2014). Reactive oxygen species in inflammation and tissue injury. Antioxid Redox Signal *20*, 1126-1167.
Mizuno, K., Tagawa, Y., Mitomo, K., Watanabe, N., Katagiri, T., Ogimoto, M., and Yakura, H. (2002). Src homology region 2 domain-containing phosphatase 1 positively regulates B cell receptor-induced apoptosis by modulating association of B cell linker protein with Nck and activation of c-Jun NH2-terminal kinase. J Immunol *169*, 778-786.
Mobberley-Schuman, P.S., Connelly, B., and Weiss, A.A. (2003). Phagocytosis of *Bordetella pertussis* incubated with convalescent serum. J Infect Dis *187*, 1646-1653.
Mooi, F.R., Jansen, W.H., Brunings, H., Gielen, H., van der Heide, H.G., Walvoort, H.C., and Guinee, P.A. (1992). Construction and analysis of *Bordetella pertussis* mutants defective in the production of fimbriae. Microb Pathog *12*, 127-135.
Morova, J., Osicka, R., Masin, J., and Sebo, P. (2008). RTX cytotoxins recognize beta2 integrin receptors through N-linked oligosaccharides. Proc Natl Acad Sci U S A *105*, 5355-5360.
Morse, S.I., and Morse, J.H. (1976). Isolation and properties of the leukocytosis- and lymphocytosis-promoting factor of *Bordetella pertussis*. J Exp Med *143*, 1483-1502.
Moskwa, P., Dagher, M.C., Paclet, M.H., Morel, F., and Ligeti, E. (2002). Participation of Rac GTPase activating proteins in the deactivation of the phagocytic NADPH oxidase. Biochemistry *41*, 10710-10716.

Mugoni, V., and Santoro, M.M. (2013). Manipulating Redox Signaling to Block Tumor Angiogenesis.
Munier, H., Bouhss, A., Krin, E., Danchin, A., Gilles, A.M., Glaser, P., and Barzu, O. (1992). The role of histidine 63 in the catalytic mechanism of *Bordetella pertussis* adenylate cyclase. J Biol Chem *267*, 9816-9820.
Murray, A.J. (2008). Pharmacological PKA inhibition: all may not be what it seems. Sci Signal *1*, re4.
Musial, A., and Eissa, N.T. (2001). Inducible nitric-oxide synthase is regulated by the proteasome degradation pathway. J Biol Chem *276*, 24268-24273.
Nagamatsu, K., Kuwae, A., Konaka, T., Nagai, S., Yoshida, S., Eguchi, M., Watanabe, M., Mimuro, H., Koyasu, S., and Abe, A. (2009). *Bordetella* evades the host immune system by inducing IL-10 through a type III effector, BopN. J Exp Med *206*, 3073-3088.
Nakai, T., Sawata, A., and Kume, K. (1985). Intracellular locations of dermonecrotic toxins in *Pasteurella multocida* and in *Bordetella bronchiseptica*. Am J Vet Res *46*, 870-874.
Nakayama, H., Ogawa, H., Takamori, K., and Iwabuchi, K. (2013). GSL-enriched membrane microdomains in innate immune responses. Arch Immunol Ther Exp (Warsz) *61*, 217-228.
Nambu, M., Morita, M., Watanabe, H., Uenoyama, Y., Kim, K.M., Tanaka, M., Iwai, Y., Kimata, H., Mayumi, M., and Mikawa, H. (1989). Regulation of Fc gamma receptor expression and phagocytosis of a human monoblast cell line U937. Participation of cAMP and protein kinase C in the effects of IFN-gamma and phorbol ester. J Immunol *143*, 4158-4165.
Nandan, D., Lo, R., and Reiner, N.E. (1999). Activation of phosphotyrosine phosphatase activity attenuates mitogen-activated protein kinase signaling and inhibits c-FOS and nitric oxide synthase expression in macrophages infected with *Leishmania donovani*. Infect Immun *67*, 4055-4063.
Nixon, J.B., and McPhail, L.C. (1999). Protein kinase C (PKC) isoforms translocate to Triton-insoluble fractions in stimulated human neutrophils: correlation of conventional PKC with activation of NADPH oxidase. J Immunol *163*, 4574-4582.
Njamkepo, E., Pinot, F., Francois, D., Guiso, N., Polla, B.S., and Bachelet, M. (2000). Adaptive responses of human monocytes infected by *Bordetella pertussis*: the role of adenylate cyclase hemolysin. J Cell Physiol *183*, 91-99.
Noda, T., and Amano, F. (1997). Differences in nitric oxide synthase activity in a macrophage-like cell line, RAW264.7 cells, treated with lipopolysaccharide (LPS) in the presence or absence of interferon-gamma (IFN-gamma): possible heterogeneity of iNOS activity. J Biochem *121*, 38-46.
Nokta, M.A., and Pollard, R.B. (1992). Human immunodeficiency virus replication: modulation by cellular levels of cAMP. AIDS Res Hum Retroviruses *8*, 1255-1261.
Norton, C.E., Broughton, B.R., Jernigan, N.L., Walker, B.R., and Resta, T.C. (2013). Enhanced depolarization-induced pulmonary vasoconstriction following chronic hypoxia requires EGFR-dependent activation of NAD(P)H oxidase 2. Antioxid Redox Signal *18*, 1777-1788.
O'Dorisio, M.S., Vandenbark, G.R., and LoBuglio, A.F. (1979). Human monocyte killing of *Staphylococcus aureus*: modulation by agonists of cyclic adenosine 3',5'-monophosphate and cyclic guanosine 3',5'-monophosphate. Infect Immun *26*, 604-610.

Ohnishi, H., Miyake, M., Kamitani, S., and Horiguchi, Y. (2008). The morphological changes in cultured cells caused by *Bordetella pertussis* adenylate cyclase toxin. FEMS Microbiol Lett *279*, 174-179.
Omsland, A., Miranda, K.M., Friedman, R.L., and Boitano, S. (2008). *Bordetella bronchiseptica* responses to physiological reactive nitrogen and oxygen stresses. FEMS Microbiol Lett *284*, 92-101.
Osicka, R., Osickova, A., Basar, T., Guermonprez, P., Rojas, M., Leclerc, C., and Sebo, P. (2000). Delivery of CD8(+) T-cell epitopes into major histocompatibility complex class I antigen presentation pathway by *Bordetella pertussis* adenylate cyclase: delineation of cell invasive structures and permissive insertion sites. Infect Immun *68*, 247-256.
Osickova, A., Masin, J., Fayolle, C., Krusek, J., Basler, M., Pospisilova, E., Leclerc, C., Osicka, R., and Sebo, P. (2010). Adenylate cyclase toxin translocates across target cell membrane without forming a pore. Mol Microbiol *75*, 1550-1562.
Osickova, A., Osicka, R., Maier, E., Benz, R., and Sebo, P. (1999). An amphipathic alpha-helix including glutamates 509 and 516 is crucial for membrane translocation of adenylate cyclase toxin and modulates formation and cation selectivity of its membrane channels. J Biol Chem *274*, 37644-37650.
Otero, A.S., Yi, X.B., Gray, M.C., Szabo, G., and Hewlett, E.L. (1995). Membrane depolarization prevents cell invasion by *Bordetella pertussis* adenylate cyclase toxin. J Biol Chem *270*, 9695-9697.
Paccani, S.R., Dal Molin, F., Benagiano, M., Ladant, D., D'Elios, M.M., Montecucco, C., and Baldari, C.T. (2008). Suppression of T-lymphocyte activation and chemotaxis by the adenylate cyclase toxin of *Bordetella pertussis*. Infect Immun *76*, 2822-2832.
Paccani, S.R., Finetti, F., Davi, M., Patrussi, L., D'Elios, M.M., Ladant, D., and Baldari, C.T. (2011). The *Bordetella pertussis* adenylate cyclase toxin binds to T cells via LFA-1 and induces its disengagement from the immune synapse. J Exp Med *208*, 1317-1330.
Paddock, C.D., Sanden, G.N., Cherry, J.D., Gal, A.A., Langston, C., Tatti, K.M., Wu, K.H., Goldsmith, C.S., Greer, P.W., Montague, J.L., *et al.* (2008). Pathology and pathogenesis of fatal *Bordetella pertussis* infection in infants. Clin Infect Dis *47*, 328-338.
Pang, L., and Hoult, J.R. (1997). Repression of inducible nitric oxide synthase and cyclooxygenase-2 by prostaglandin E2 and other cyclic AMP stimulants in J774 macrophages. Biochem Pharmacol *53*, 493-500.
Park, J., Zhang, Y., Buboltz, A.M., Zhang, X., Schuster, S.C., Ahuja, U., Liu, M., Miller, J.F., Sebaihia, M., Bentley, S.D., *et al.* (2012). Comparative genomics of the classical *Bordetella* subspecies: the evolution and exchange of virulence-associated diversity amongst closely related pathogens. BMC Genomics *13*, 545.
Park, J.W., Benna, J.E., Scott, K.E., Christensen, B.L., Chanock, S.J., and Babior, B.M. (1994). Isolation of a complex of respiratory burst oxidase components from resting neutrophil cytosol. Biochemistry *33*, 2907-2911.
Park, J.W., Ma, M., Ruedi, J.M., Smith, R.M., and Babior, B.M. (1992). The cytosolic components of the respiratory burst oxidase exist as a M(r) approximately 240,000 complex that acquires a membrane-binding site during activation of the oxidase in a cell-free system. J Biol Chem *267*, 17327-17332.
Parkhill, J., Sebaihia, M., Preston, A., Murphy, L.D., Thomson, N., Harris, D.E., Holden, M.T., Churcher, C.M., Bentley, S.D., Mungall, K.L., *et al.* (2003).

Comparative analysis of the genome sequences of *Bordetella pertussis*, *Bordetella parapertussis* and *Bordetella bronchiseptica*. Nat Genet *35*, 32-40.
Pautz, A., Art, J., Hahn, S., Nowag, S., Voss, C., and Kleinert, H. (2010). Regulation of the expression of inducible nitric oxide synthase. Nitric Oxide *23*, 75-93.
Pawloski, L.C., Queenan, A.M., Cassiday, P.K., Lynch, A.S., Harrison, M.J., Shang, W., Williams, M.M., Bowden, K.E., Burgos-Rivera, B., Qin, X., *et al.* (2014). Prevalence and molecular characterization of pertactin-deficient *Bordetella pertussis* in the United States. Clin Vaccine Immunol *21*, 119-125.
Pearson, R.D., Symes, P., Conboy, M., Weiss, A.A., and Hewlett, E.L. (1987). Inhibition of monocyte oxidative responses by *Bordetella pertussis* adenylate cyclase toxin. J Immunol *139*, 2749-2754.
Pedroni, P., Riboli, B., de Ferra, F., Grandi, G., Toma, S., Arico, B., and Rappuoli, R. (1988). Cloning of a novel pilin-like gene from *Bordetella pertussis*: homology to the fim2 gene. Mol Microbiol *2*, 539-543.
Pellegrino, M.J., and Stork, P.J. (2006). Sustained activation of extracellular signal-regulated kinase by nerve growth factor regulates c-fos protein stabilization and transactivation in PC12 cells. J Neurochem *99*, 1480-1493.
Perisic, O., Wilson, M.I., Karathanassis, D., Bravo, J., Pacold, M.E., Ellson, C.D., Hawkins, P.T., Stephens, L., and Williams, R.L. (2004). The role of phosphoinositides and phosphorylation in regulation of NADPH oxidase. Adv Enzyme Regul *44*, 279-298.
Perkins, D.J., Gray, M.C., Hewlett, E.L., and Vogel, S.N. (2007). *Bordetella pertussis* adenylate cyclase toxin (ACT) induces cyclooxygenase-2 (COX-2) in murine macrophages and is facilitated by ACT interaction with CD11b/CD18 (Mac-1). Mol Microbiol *66*, 1003-1015.
Peters-Golden, M. (2009). Putting on the brakes: cyclic AMP as a multipronged controller of macrophage function. Sci Signal *2*, pe37.
Porter, J.F., Connor, K., and Donachie, W. (1994). Isolation and characterization of *Bordetella parapertussis*-like bacteria from ovine lungs. Microbiology *140 (Pt 2)*, 255-261.
Porter, J.F., Parton, R., and Wardlaw, A.C. (1991). Growth and survival of *Bordetella bronchiseptica* in natural waters and in buffered saline without added nutrients. Appl Environ Microbiol *57*, 1202-1206.
Potter, A.J., Kidd, S.P., Edwards, J.L., Falsetta, M.L., Apicella, M.A., Jennings, M.P., and McEwan, A.G. (2009). Thioredoxin reductase is essential for protection of *Neisseria gonorrhoeae* against killing by nitric oxide and for bacterial growth during interaction with cervical epithelial cells. J Infect Dis *199*, 227-235.
Powthongchin, B., and Angsuthanasombat, C. (2009). Effects on haemolytic activity of single proline substitutions in the *Bordetella pertussis* CyaA pore-forming fragment. Arch Microbiol *191*, 1-9.
Preston, A., Parkhill, J., and Maskell, D.J. (2004). The *Bordetellae*: lessons from genomics. Nat Rev Microbiol *2*, 379-390.
Pryzwansky, K.B., Kidao, S., and Merricks, E.P. (1998). Compartmentalization of PDE-4 and cAMP-dependent protein kinase in neutrophils and macrophages during phagocytosis. Cell Biochem Biophys *28*, 251-275.
Qi, X.F., Kim, D.H., Yoon, Y.S., Li, J.H., Song, S.B., Jin, D., Huang, X.Z., Teng, Y.C., and Lee, K.J. (2009). The adenylyl cyclase-cAMP system suppresses TARC/CCL17 and MDC/CCL22 production through p38 MAPK and NF-kappaB in HaCaT keratinocytes. Mol Immunol *46*, 1925-1934.

Quintin, J., Cheng, S.C., van der Meer, J.W., and Netea, M.G. (2014). Innate immune memory: towards a better understanding of host defense mechanisms. Curr Opin Immunol *29*, 1-7.
Rangel Moreno, J., Estrada Garcia, I., De La Luz Garcia Hernandez, M., Aguilar Leon, D., Marquez, R., and Hernandez Pando, R. (2002). The role of prostaglandin E2 in the immunopathogenesis of experimental pulmonary tuberculosis. Immunology *106*, 257-266.
Rehmann, H., Schwede, F., Doskeland, S.O., Wittinghofer, A., and Bos, J.L. (2003). Ligand-mediated activation of the cAMP-responsive guanine nucleotide exchange factor Epac. J Biol Chem *278*, 38548-38556.
Rescigno, M., Martino, M., Sutherland, C.L., Gold, M.R., and Ricciardi-Castagnoli, P. (1998). Dendritic cell survival and maturation are regulated by different signaling pathways. J Exp Med *188*, 2175-2180.
Rhee, S.H., Jones, B.W., Toshchakov, V., Vogel, S.N., and Fenton, M.J. (2003). Toll-like receptors 2 and 4 activate STAT1 serine phosphorylation by distinct mechanisms in macrophages. J Biol Chem *278*, 22506-22512.
Rhodes, C.R., Gray, M.C., Watson, J.M., Muratore, T.L., Kim, S.B., Hewlett, E.L., and Grisham, C.M. (2001). Structural consequences of divalent metal binding by the adenylyl cyclase toxin of *Bordetella pertussis*. Arch Biochem Biophys *395*, 169-176.
Rogel, A., and Hanski, E. (1992). Distinct steps in the penetration of adenylate cyclase toxin of *Bordetella pertussis* into sheep erythrocytes. Translocation of the toxin across the membrane. J Biol Chem *267*, 22599-22605.
Rogel, A., Meller, R., and Hanski, E. (1991). Adenylate cyclase toxin from *Bordetella pertussis*. The relationship between induction of cAMP and hemolysis. J Biol Chem *266*, 3154-3161.
Rocha, G., Soares, P., Soares, H., Pissarra, S., and Guimaraes, H. (2015). Pertussis in the Newborn: certainties and uncertainties in 2014. Paediatr Respir Rev *16*, 112-118.
Rose, T., Sebo, P., Bellalou, J., and Ladant, D. (1995). Interaction of calcium with *Bordetella pertussis* adenylate cyclase toxin. Characterization of multiple calcium-binding sites and calcium-induced conformational changes. J Biol Chem *270*, 26370-26376.
Ross, P.J., Lavelle, E.C., Mills, K.H., and Boyd, A.P. (2004). Adenylate cyclase toxin from *Bordetella pertussis* synergizes with lipopolysaccharide to promote innate interleukin-10 production and enhances the induction of Th2 and regulatory T cells. Infect Immun *72*, 1568-1579.
Rossi Paccani, S., Benagiano, M., Capitani, N., Zornetta, I., Ladant, D., Montecucco, C., D'Elios, M.M., and Baldari, C.T. (2009). The adenylate cyclase toxins of *Bacillus anthracis* and *Bordetella pertussis* promote Th2 cell development by shaping T cell antigen receptor signaling. PLoS Pathog *5*, e1000325.
Rotfeld, H., Hillman, P., Ickowicz, D., and Breitbart, H. (2014). PKA and CaMKII mediate PI3K activation in bovine sperm by inhibition of the PKC/PP1 cascade. Reproduction *147*, 347-356.
Rowlands, H.E., Goldman, A.P., Harrington, K., Karimova, A., Brierley, J., Cross, N., Skellett, S., and Peters, M.J. (2010). Impact of rapid leukodepletion on the outcome of severe clinical pertussis in young infants. Pediatrics *126*, e816-827.
Sakamoto, H., Bellalou, J., Sebo, P., and Ladant, D. (1992). *Bordetella pertussis* adenylate cyclase toxin. Structural and functional independence of the catalytic and hemolytic activities. J Biol Chem *267*, 13598-13602.
Sato, K., Nagayama, H., Tadokoro, K., Juji, T., and Takahashi, T.A. (1999). Extracellular signal-regulated kinase, stress-activated protein kinase/c-Jun N-

terminal kinase, and p38mapk are involved in IL-10-mediated selective repression of TNF-alpha-induced activation and maturation of human peripheral blood monocyte-derived dendritic cells. J Immunol *162*, 3865-3872.
Satriano, J. (2004). Arginine pathways and the inflammatory response: interregulation of nitric oxide and polyamines: review article. Amino Acids *26*, 321-329.
Sawal, M., Cohen, M., Irazuzta, J.E., Kumar, R., Kirton, C., Brundler, M.A., Evans, C.A., Wilson, J.A., Raffeeq, P., Azaz, A., *et al.* (2009). Fulminant pertussis: a multi-center study with new insights into the clinico-pathological mechanisms. Pediatr Pulmonol *44*, 970-980.
Sebo, P., and Ladant, D. (1993). Repeat sequences in the *Bordetella pertussis* adenylate cyclase toxin can be recognized as alternative carboxy-proximal secretion signals by the Escherichia coli alpha-haemolysin translocator. Mol Microbiol *9*, 999-1009.
Sebo, P., Osicka, R., and Masin, J. (2014). Adenylate cyclase toxin-hemolysin relevance for pertussis vaccines. Expert Rev Vaccines *13*, 1215-1227.
Seger, R., and Krebs, E.G. (1995). The MAPK signaling cascade. FASEB J *9*, 726-735.
Serezani, C.H., Ballinger, M.N., Aronoff, D.M., and Peters-Golden, M. (2008). Cyclic AMP: master regulator of innate immune cell function. Am J Respir Cell Mol Biol *39*, 127-132.
Serezani, C.H., Chung, J., Ballinger, M.N., Moore, B.B., Aronoff, D.M., and Peters-Golden, M. (2007). Prostaglandin E2 suppresses bacterial killing in alveolar macrophages by inhibiting NADPH oxidase. Am J Respir Cell Mol Biol *37*, 562-570.
Shen, B., Kwan, H.Y., Ma, X., Wong, C.O., Du, J., Huang, Y., and Yao, X. (2011). cAMP activates TRPC6 channels via the phosphatidylinositol 3-kinase (PI3K)-protein kinase B (PKB)-mitogen-activated protein kinase kinase (MEK)-ERK1/2 signaling pathway. J Biol Chem *286*, 19439-19445.
Shen, Y., Zhukovskaya, N.L., Zimmer, M.I., Soelaiman, S., Bergson, P., Wang, C.R., Gibbs, C.S., and Tang, W.J. (2004). Selective inhibition of anthrax edema factor by adefovir, a drug for chronic hepatitis B virus infection. Proc Natl Acad Sci U S A *101*, 3242-3247.
Schaeffer, L.M., and Weiss, A.A. (2001). Pertussis toxin and lipopolysaccharide influence phagocytosis of *Bordetella pertussis* by human monocytes. Infect Immun *69*, 7635-7641.
Scheffzek, K., Ahmadian, M.R., Kabsch, W., Wiesmuller, L., Lautwein, A., Schmitz, F., and Wittinghofer, A. (1997). The Ras-RasGAP complex: structural basis for GTPase activation and its loss in oncogenic Ras mutants. Science *277*, 333-338.
Schleimer, R.P., Kato, A., Kern, R., Kuperman, D., and Avila, P.C. (2007). Epithelium: at the interface of innate and adaptive immune responses. J Allergy Clin Immunol *120*, 1279-1284.
Schmidt, G., Goehring, U.M., Schirmer, J., Lerm, M., and Aktories, K. (1999). Identification of the C-terminal part of *Bordetella* dermonecrotic toxin as a transglutaminase for rho GTPases. J Biol Chem *274*, 31875-31881.
Schuler, D., Lubker, C., Lushington, G.H., Tang, W.J., Shen, Y., Richter, M., and Seifert, R. (2012). Interactions of *Bordetella pertussis* adenylyl cyclase toxin CyaA with calmodulin mutants and calmodulin antagonists: comparison with membranous adenylyl cyclase I. Biochem Pharmacol *83*, 839-848.

Siciliano, N.A., Skinner, J.A., and Yuk, M.H. (2006). *Bordetella bronchiseptica* modulates macrophage phenotype leading to the inhibition of CD4+ T cell proliferation and the initiation of a Th17 immune response. J Immunol *177*, 7131-7138.
Skinner, J.A., Reissinger, A., Shen, H., and Yuk, M.H. (2004). *Bordetella* type III secretion and adenylate cyclase toxin synergize to drive dendritic cells into a semimature state. J Immunol *173*, 1934-1940.
Sloan, G.P., Love, C.F., Sukumar, N., Mishra, M., and Deora, R. (2007). The *Bordetella* Bps polysaccharide is critical for biofilm development in the mouse respiratory tract. J Bacteriol *189*, 8270-8276.
Smidkova, M., Dvorakova, A., Tloust'ova, E., Cesnek, M., Janeba, Z., and Mertlikova-Kaiserova, H. (2014). Amidate prodrugs of 9-[2-(phosphonomethoxy)ethyl]adenine as inhibitors of adenylate cyclase toxin from *Bordetella pertussis*. Antimicrob Agents Chemother *58*, 664-671.
Soane, M.C., Jackson, A., Maskell, D., Allen, A., Keig, P., Dewar, A., Dougan, G., and Wilson, R. (2000). Interaction of *Bordetella pertussis* with human respiratory mucosa in vitro. Respir Med *94*, 791-799.
Soehnlein, O., and Lindbom, L. (2010). Phagocyte partnership during the onset and resolution of inflammation. Nat Rev Immunol *10*, 427-439.
Soelaiman, S., Wei, B.Q., Bergson, P., Lee, Y.S., Shen, Y., Mrksich, M., Shoichet, B.K., and Tang, W.J. (2003). Structure-based inhibitor discovery against adenylyl cyclase toxins from pathogenic bacteria that cause anthrax and whooping cough. J Biol Chem *278*, 25990-25997.
Someya, A., Nunoi, H., Hasebe, T., and Nagaoka, I. (1999). Phosphorylation of p40-phox during activation of neutrophil NADPH oxidase. J Leukoc Biol *66*, 851-857.
Spangrude, G.J., Sacchi, F., Hill, H.R., Van Epps, D.E., and Daynes, R.A. (1985). Inhibition of lymphocyte and neutrophil chemotaxis by pertussis toxin. J Immunol *135*, 4135-4143.
Spensieri, F., Fedele, G., Fazio, C., Nasso, M., Stefanelli, P., Mastrantonio, P., and Ausiello, C.M. (2006). *Bordetella pertussis* inhibition of interleukin-12 (IL-12) p70 in human monocyte-derived dendritic cells blocks IL-12 p35 through adenylate cyclase toxin-dependent cyclic AMP induction. Infect Immun *74*, 2831-2838.
Stadtmann, A., and Zarbock, A. (2012). CXCR2: From Bench to Bedside. Front Immunol *3*, 263.
Stainer, D.W., and Scholte, M.J. (1970). A simple chemically defined medium for the production of phase I *Bordetella pertussis*. J Gen Microbiol *63*, 211-220.
Stein, P.E., Boodhoo, A., Armstrong, G.D., Cockle, S.A., Klein, M.H., and Read, R.J. (1994a). The crystal structure of pertussis toxin. Structure *2*, 45-57.
Stein, P.E., Boodhoo, A., Armstrong, G.D., Heerze, L.D., Cockle, S.A., Klein, M.H., and Read, R.J. (1994b). Structure of a pertussis toxin-sugar complex as a model for receptor binding. Nat Struct Biol *1*, 591-596.
Subrini, O., Sotomayor-Perez, A.C., Hessel, A., Spiaczka-Karst, J., Selwa, E., Sapay, N., Veneziano, R., Pansieri, J., Chopineau, J., Ladant, D., *et al.* (2013). Characterization of a membrane-active peptide from the *Bordetella pertussis* CyaA toxin. J Biol Chem *288*, 32585-32598.
Sugita, S., Baxter, D.A., and Byrne, J.H. (1994). cAMP-independent effects of 8-(4-parachlorophenylthio)-cyclic AMP on spike duration and membrane currents in pleural sensory neurons of Aplysia. J Neurophysiol *72*, 1250-1259.

Szabo, G., Gray, M.C., and Hewlett, E.L. (1994). Adenylate cyclase toxin from *Bordetella pertussis* produces ion conductance across artificial lipid bilayers in a calcium- and polarity-dependent manner. J Biol Chem *269*, 22496-22499.
Tai, Z., Lin, Y., He, Y., Huang, J., Guo, J., Yang, L., Zhang, G., and Wang, F. (2014). Luteolin sensitizes the antiproliferative effect of interferon alpha/beta by activation of Janus kinase/signal transducer and activator of transcription pathway signaling through protein kinase A-mediated inhibition of protein tyrosine phosphatase SHP-2 in cancer cells. Cell Signal *26*, 619-628.
Thanabalu, T., Koronakis, E., Hughes, C., and Koronakis, V. (1998). Substrate-induced assembly of a contiguous channel for protein export from *E.coli*: reversible bridging of an inner-membrane translocase to an outer membrane exit pore. EMBO J *17*, 6487-6496.
Thomas, S., Holland, I.B., and Schmitt, L. (2014). The Type 1 secretion pathway - the hemolysin system and beyond. Biochim Biophys Acta *1843*, 1629-1641.
Tohyama, Y., and Yamamura, H. (2009). Protein tyrosine kinase, syk: a key player in phagocytic cells. J Biochem *145*, 267-273.
Tsukamoto, K., Hazeki, K., Hoshi, M., Nigorikawa, K., Inoue, N., Sasaki, T., and Hazeki, O. (2008). Critical roles of the p110 beta subtype of phosphoinositide 3-kinase in lipopolysaccharide-induced Akt activation and negative regulation of nitrite production in RAW 264.7 cells. J Immunol *180*, 2054-2061.
Tsunawaki, S., and Yoshikawa, K. (2000). Relationships of p40(phox) with p67(phox) in the activation and expression of the human respiratory burst NADPH oxidase. J Biochem *128*, 777-783.
Uhl, M.A., and Miller, J.F. (1994). Autophosphorylation and phosphotransfer in the *Bordetella pertussis* BvgAS signal transduction cascade. Proc Natl Acad Sci U S A *91*, 1163-1167.
Uhl, M.A., and Miller, J.F. (1996). Integration of multiple domains in a two-component sensor protein: the *Bordetella pertussis* BvgAS phosphorelay. EMBO J *15*, 1028-1036.
Valsecchi, F., Konrad, C., and Manfredi, G. (2014). Role of soluble adenylyl cyclase in mitochondria. Biochim Biophys Acta *1842*, 2555-2560.
van der Pouw Kraan, T.C., Boeije, L.C., Smeenk, R.J., Wijdenes, J., and Aarden, L.A. (1995). Prostaglandin-E2 is a potent inhibitor of human interleukin 12 production. J Exp Med *181*, 775-779.
van der Zee, A., Mooi, F., Van Embden, J., and Musser, J. (1997). Molecular evolution and host adaptation of *Bordetella* spp.: phylogenetic analysis using multilocus enzyme electrophoresis and typing with three insertion sequences. J Bacteriol *179*, 6609-6617.
Van Strijp, J.A., Russell, D.G., Tuomanen, E., Brown, E.J., and Wright, S.D. (1993). Ligand specificity of purified complement receptor type three (CD11b/CD18, alpha m beta 2, Mac-1). Indirect effects of an Arg-Gly-Asp (RGD) sequence. J Immunol *151*, 3324-3336.
Veal-Carr, W.L., and Stibitz, S. (2005). Demonstration of differential virulence gene promoter activation in vivo in *Bordetella pertussis* using RIVET. Mol Microbiol *55*, 788-798.
Vetter, I.R., and Wittinghofer, A. (2001). The guanine nucleotide-binding switch in three dimensions. Science *294*, 1299-1304.
Vignais, P.V. (2002). The superoxide-generating NADPH oxidase: structural aspects and activation mechanism. Cell Mol Life Sci *59*, 1428-1459.

Villarino Romero, R., Bibova, I., Cerny, O., Vecerek, B., Wald, T., Benada, O., Zavadilova, J., Osicka, R., and Sebo, P. (2013). The *Bordetella pertussis* type III secretion system tip complex protein Bsp22 is not a protective antigen and fails to elicit serum antibody responses during infection of humans and mice. Infect Immun *81*, 2761-2767.
Villarino Romero, R., Osicka, R., and Sebo, P. (2014). Filamentous hemagglutinin of *Bordetella pertussis*: a key adhesin with immunomodulatory properties? Future Microbiol *9*, 1339-1360.
Vojtova-Vodolanova, J., Basler, M., Osicka, R., Knapp, O., Maier, E., Cerny, J., Benada, O., Benz, R., and Sebo, P. (2009). Oligomerization is involved in pore formation by *Bordetella* adenylate cyclase toxin. FASEB J *23*, 2831-2843.
Vojtova, J., Kamanova, J., and Sebo, P. (2006). *Bordetella* adenylate cyclase toxin: a swift saboteur of host defense. Curr Opin Microbiol *9*, 69-75.
Wald, T., Petry-Podgorska, I., Fiser, R., Matousek, T., Dedina, J., Osicka, R., Sebo, P., and Masin, J. (2014). Quantification of potassium levels in cells treated with *Bordetella* adenylate cyclase toxin. Anal Biochem *450*, 57-62.
Wang, H., Jiang, Y., Shi, D., Quilliam, L.A., Chrzanowska-Wodnicka, M., Wittchen, E.S., Li, D.Y., and Hartnett, M.E. (2014). Activation of Rap1 inhibits NADPH oxidase-dependent ROS generation in retinal pigment epithelium and reduces choroidal neovascularization. FASEB J *28*, 265-274.
Wang, L., Liu, F., and Adamo, M.L. (2001). Cyclic AMP inhibits extracellular signal-regulated kinase and phosphatidylinositol 3-kinase/Akt pathways by inhibiting Rap1. J Biol Chem *276*, 37242-37249.
Wang, X., and Maynard, J.A. (2014). The *Bordetella* Adenylate Cyclase Toxin RTX Domain is Immunodominant and Elicits Neutralizing Antibodies. J Biol Chem.
Warfel, J.M., Beren, J., Kelly, V.K., Lee, G., and Merkel, T.J. (2012a). Nonhuman primate model of pertussis. Infect Immun *80*, 1530-1536.
Warfel, J.M., Beren, J., and Merkel, T.J. (2012b). Airborne transmission of *Bordetella pertussis*. J Infect Dis *206*, 902-906.
Weber, C., Boursaux-Eude, C., Coralie, G., Caro, V., and Guiso, N. (2001). Polymorphism of *Bordetella pertussis* isolates circulating for the last 10 years in France, where a single effective whole-cell vaccine has been used for more than 30 years. J Clin Microbiol *39*, 4396-4403.
Weingart, C.L., Mobberley-Schuman, P.S., Hewlett, E.L., Gray, M.C., and Weiss, A.A. (2000). Neutralizing antibodies to adenylate cyclase toxin promote phagocytosis of *Bordetella pertussis* by human neutrophils. Infect Immun *68*, 7152-7155.
Weischenfeldt, J., and Porse, B. (2008). Bone Marrow-Derived Macrophages (BMM): Isolation and Applications. CSH Protoc *2008*, pdb prot5080.
Weiss, A.A., Hewlett, E.L., Myers, G.A., and Falkow, S. (1984). Pertussis toxin and extracytoplasmic adenylate cyclase as virulence factors of *Bordetella pertussis*. J Infect Dis *150*, 219-222.
Weisz, A., Oguchi, S., Cicatiello, L., and Esumi, H. (1994). Dual mechanism for the control of inducible-type NO synthase gene expression in macrophages during activation by interferon-gamma and bacterial lipopolysaccharide. Transcriptional and post-transcriptional regulation. J Biol Chem *269*, 8324-8333.
Westrop, G.D., Campbell, G., Kazi, Y., Billcliffe, B., Coote, J.G., Parton, R., Freer, J.H., and Edwards, J.G. (1994). A new assay for the invasive adenylate cyclase toxin of *Bordetella pertussis* based on its morphological effects on the fibronectin-stimulated spreading of BHK21 cells. Microbiology *140 (Pt 2)*, 245-253.

Wiles, T.J., Dhakal, B.K., Eto, D.S., and Mulvey, M.A. (2008). Inactivation of host Akt/protein kinase B signaling by bacterial pore-forming toxins. Mol Biol Cell *19*, 1427-1438.
Willems, R., Paul, A., van der Heide, H.G., ter Avest, A.R., and Mooi, F.R. (1990). Fimbrial phase variation in *Bordetella pertussis*: a novel mechanism for transcriptional regulation. EMBO J *9*, 2803-2809.
Willems, R.J., van der Heide, H.G., and Mooi, F.R. (1992). Characterization of a *Bordetella pertussis* fimbrial gene cluster which is located directly downstream of the filamentous haemagglutinin gene. Mol Microbiol *6*, 2661-2671.
Wirth, J.J., and Kierszenbaum, F. (1984). Macrophage mediation of the inhibitory effects of elevated intracellular levels of adenosine-3':5' cyclic monophosphate (cAMP) on macrophage-Trypanosoma cruzi association. Int J Parasitol *14*, 401-404.
Worthington, Z.E., and Carbonetti, N.H. (2007). Evading the proteasome: absence of lysine residues contributes to pertussis toxin activity by evasion of proteasome degradation. Infect Immun *75*, 2946-2953.
Xie, Q.W., Whisnant, R., and Nathan, C. (1993). Promoter of the mouse gene encoding calcium-independent nitric oxide synthase confers inducibility by interferon gamma and bacterial lipopolysaccharide. J Exp Med *177*, 1779-1784.
Xu, X.J., Reichner, J.S., Mastrofrancesco, B., Henry, W.L., Jr., and Albina, J.E. (2008). Prostaglandin E2 suppresses lipopolysaccharide-stimulated IFN-beta production. J Immunol *180*, 2125-2131.
Yue, C., Dodge, K.L., Weber, G., and Sanborn, B.M. (1998). Phosphorylation of serine 1105 by protein kinase A inhibits phospholipase Cbeta3 stimulation by Galphaq. J Biol Chem *273*, 18023-18027.
Zaretzky, F.R., Gray, M.C., and Hewlett, E.L. (2002). Mechanism of association of adenylate cyclase toxin with the surface of *Bordetella pertussis*: a role for toxin-filamentous haemagglutinin interaction. Mol Microbiol *45*, 1589-1598.
Zentella de Pina, M., Vazquez-Meza, H., Agundis, C., Pereyra, M.A., Pardo, J.P., Villalobos-Molina, R., and Pina, E. (2007). Inhibition of cAMP-dependent protein kinase A: a novel cyclo-oxygenase-independent effect of non-steroidal anti-inflammatory drugs in adipocytes. Auton Autacoid Pharmacol *27*, 85-92.
Zhang, J., Somani, A.K., and Siminovitch, K.A. (2000). Roles of the SHP-1 tyrosine phosphatase in the negative regulation of cell signalling. Semin Immunol *12*, 361-378.
Zhao, C., Zhang, H., Wong, W.C., Sem, X., Han, H., Ong, S.M., Tan, Y.C., Yeap, W.H., Gan, C.S., Ng, K.Q., *et al.* (2009). Identification of novel functional differences in monocyte subsets using proteomic and transcriptomic methods. J Proteome Res *8*, 4028-4038.
Ziolo, K.J., Jeong, H.G., Kwak, J.S., Yang, S., Lavker, R.M., and Satchell, K.J. (2014). *Vibrio vulnificus* biotype 3 multifunctional autoprocessing RTX toxin is an adenylate cyclase toxin essential for virulence in mice. Infect Immun *82*, 2148-2157.